NASA/CR-2010-216842

N+2 Supersonic Concept Development and Systems Integration

Harry R. Welge, John Bonet, Todd Magee, Daniel Chen, Steve Hollowell, Aaron Kutzmann, Alan Mortlock, and Josh Stengle
Boeing Research & Technology, Huntington Beach, California

Chet Nelson, Eric Adamson, Steve Baughcum, Robert T. Britt, and Gregory Miller
Boeing Commercial Airplanes, Seattle, Washington

Jimmy Tai
Georgia Institute of Technology, Atlanta, Georgia

August 2010

NASA STI Program . . . in Profile

Since its founding, NASA has been dedicated to the advancement of aeronautics and space science. The NASA scientific and technical information (STI) program plays a key part in helping NASA maintain this important role.

The NASA STI program operates under the auspices of the Agency Chief Information Officer. It collects, organizes, provides for archiving, and disseminates NASA's STI. The NASA STI program provides access to the NASA Aeronautics and Space Database and its public interface, the NASA Technical Report Server, thus providing one of the largest collections of aeronautical and space science STI in the world. Results are published in both non-NASA channels and by NASA in the NASA STI Report Series, which includes the following report types:

- TECHNICAL PUBLICATION. Reports of completed research or a major significant phase of research that present the results of NASA programs and include extensive data or theoretical analysis. Includes compilations of significant scientific and technical data and information deemed to be of continuing reference value. NASA counterpart of peer-reviewed formal professional papers, but having less stringent limitations on manuscript length and extent of graphic presentations.

- TECHNICAL MEMORANDUM. Scientific and technical findings that are preliminary or of specialized interest, e.g., quick release reports, working papers, and bibliographies that contain minimal annotation. Does not contain extensive analysis.

- CONTRACTOR REPORT. Scientific and technical findings by NASA-sponsored contractors and grantees.

- CONFERENCE PUBLICATION. Collected papers from scientific and technical conferences, symposia, seminars, or other meetings sponsored or co-sponsored by NASA.

- SPECIAL PUBLICATION. Scientific, technical, or historical information from NASA programs, projects, and missions, often concerned with subjects having substantial public interest.

- TECHNICAL TRANSLATION. English-language translations of foreign scientific and technical material pertinent to NASA's mission.

Specialized services also include creating custom thesauri, building customized databases, and organizing and publishing research results.

For more information about the NASA STI program, see the following:

- Access the NASA STI program home page at *http://www.sti.nasa.gov*

- E-mail your question via the Internet to help@sti.nasa.gov

- Fax your question to the NASA STI Help Desk at 443-757-5803

- Phone the NASA STI Help Desk at 443-757-5802

- Write to:
  NASA STI Help Desk
  NASA Center for AeroSpace Information
  7115 Standard Drive
  Hanover, MD 21076-1320

NASA/CR-2010-216842

N+2 Supersonic Concept Development and Systems Integration

Harry R. Welge, John Bonet, Todd Magee, Daniel Chen, Steve Hollowell, Aaron Kutzmann, Alan Mortlock, and Josh Stengle
Boeing Research & Technology, Huntington Beach, California

Chet Nelson, Eric Adamson, Steve Baughcum, Robert T. Britt, and Gregory Miller
Boeing Commercial Airplanes, Seattle, Washington

Jimmy Tai
Georgia Institute of Technology, Atlanta, Georgia

National Aeronautics and
Space Administration

Langley Research Center
Hampton, Virginia 23681-2199

Prepared for Langley Research Center
under Contract NNL08AA16B

August 2010

Available from:

NASA Center for AeroSpace Information
7115 Standard Drive
Hanover, MD 21076-1320
443-757-5802

Table of Contents

Submitted to NASA LaRC:

Lori Ozoroski, Technical Monitor
Peter Coen, NASA Principal Investigator

Program Management:

Toni Antani BR&T Peter Radloff BCA

Principal Investigator: Bob Welge

Co-Investigators:

John Bonet Todd Magee Chet Nelson

Report Authors:

Eric Adamson	Steve Baughcum	John Bonet	Robert T. Britt
Daniel Chen	Steve Hollowell	Aaron Kutzmann	Todd Magee
Greg Miller	Alan Mortlock	Chet Nelson	Josh Stengle
Jimmy Tai, GaTech	Bob Welge		

Technical contributors in addition to authors:

Acoustics:
Kevin Elmer

Aerodynamics:

Alicia Bidwell	Dave Bruns	Peter Camacho
Andy Grothues	Brandon Huelman	David Hyde
Geojoe Kuruvila	Eric Unger	

Configuration:
Kevin Lutke Greg Oakes Tom Smith

Propulsion:

Boeing
Edward Lawson Kurt Acheson Wesley Moore Kimberly P. Nguyen

Georgia Institute of Technology
Russell Denney Christopher Perullo Jonathan Sands

Pratt & Whitney
Joseph B. Staubach Naushir Bala Peter Robinson Doug Stetson

Rolls-Royce Liberty Works
Joshua Clough Andrew Barlow Jerry Brines Robert Duge

Structures/Materials:
Tom Tsotsis

Weights:
Tony Gonzales Paul Miller Brandin Northrop

0.0 Abstract

Supersonic airplanes for two generations into the future (N+2, 2020-2025 EIS) were designed: the 100 passenger 765-072B, and the 30 passenger 765-076E. Both achieve a trans-Atlantic range of about 4000nm. The larger 765-072B meets fuel burn and emissions goals forecast for the 2025 time-frame, and the smaller 765-076E improves the boom and confidence in utilization that accompanies lower seat count. The boom level of both airplanes was reduced until balanced with performance. The final configuration product is two "realistic", non-proprietary future airplane designs, described in sufficient detail for subsequent multi-disciplinary design and optimization, with emphasis on the smaller 765-076E because of its lower boom characteristics. In addition IGES CAD files of the OML lofts of the two example configurations, a non-proprietary parametric engine model, and a first-cycle Finite Element Model are also provided for use in future multi-disciplinary analysis, optimization, and technology evaluation studies.

0.1 Executive Summary

This report summarizes the work, the findings, and the contract deliverables by Boeing to NASA LaRC under NRA Subtask A.4.7.1 of Contract NNL08AA16B, Order NNL08AA35T.

.

A. Fundamental Aeronautics Research Program.
A.4 Supersonics.
A.4.7 Systems Integration, Assessment and Validation.
A.4.7.1 Supersonic Concept Development and Systems Studies.

Work under the contract helped reveal some of the key system-level integration challenges for supersonic cruise commercial aircraft. It involved many variations of several innovative and highly integrated configurations that applied advanced technologies appropriate for the N+2 years 2020 to 2025 (Entry Into Service target). Two of the most promising configurations; a larger 100 passenger, high efficiency airplane and a smaller 30 passenger, low boom airplane, were selected for more detailed assessment and design. From those, the smaller low boom airplane was chosen to provide a vehicle for an even more thorough assessment and more detailed design of a non-proprietary, small, supersonic airliner for delivery to NASA. It is accompanied by a substantive description of a viable airplane configuration for exercising alternative design and analysis methods.

Figure 0.1.1 outlines the overall process followed in the course of arriving at the final configuration. The first step was arriving at an achievable set of reference vehicle requirements that could lead to an economically and environmentally viable supersonic airliner in the specified time frame. That was followed by sizing various airframe and engine combinations to meet those requirements. Subsequent analysis and design of many other configuration and technology options, both by individual expert and by automated Multi-Disciplinary Analysis (MDA) and Multi-Disciplinary Optimization (MDO), investigated several different aspects of integrated airframe, engine, payload and mission parameters. Once a final configuration was selected, CFD design was used to benchmark the currently achievable cruise performance relative to that projected based on Linear Theory design, and to explore whether achieving those levels demanded significant modification. A FEM structural sizing and one iteration of re-design was performed to help guide future structural design and identify structures related development and technology gaps. A higher fidelity MDA; including a highly effective, response-surface based, and non-proprietary engine design capability from the Georgia Institute of Technology; was employed in an integrated study to balance engine noise at takeoff with overall performance. A complete description, analysis results and geometric definition of the final airplane is provided to NASA within this report and separate files.

The optimized 100 and 30 passenger airplanes and their many relatives that were part of this study provide evidence that the achievement of very low boom levels and maximizing fuel mileage efficiency are mutually exclusive objectives for optimized airplanes of the N+2 generation. However, hypothetically, the two representative configurations chosen could be equally viable N+2 concepts, provided that “express” supersonic over land service with higher ticket surcharges provided sufficient economic and social value to the airlines and customers relative to a larger airliner that only operates at full speed over water. This is especially true if the impact of the higher fuel burn per seat of the smaller vehicle could be offset by improvements in low-NOx combustor technology and the use of carbon-neutral bio-fuels.

Other key results of the study are that designs resulting from Linear Theory, at least those to which Linear Theory readily applies, are reasonably good predictors of the performance achievable after design by CFD helps to realize the details. Also it is believed that linear-based solutions can be successfully used to establish the low-boom potential “goal” of most configurations. Analysis of the jet velocity characteristics of the final -076E concept with an optimized engine cycle indicated that it should be possible for such a configuration to achieve the minimum community noise standard of 15dB cumulative reduction relative to “Stage 3/Chapter 3”. The -15 EPNdB cumulative delta could be achieved using a thrust derate scheme without resorting to complex mixer-ejector nozzles like those developed under the HSR program in the

1990's. If the required noise stringency moves toward 18-20dB cumulative reduction, a low noise inlet concept and some type of low-impact suppressor nozzle are likely required technologies. Finally, improvements to boom will demand, to an even greater extent than improvements to basic performance, aggressive structures, materials, and controls technology.

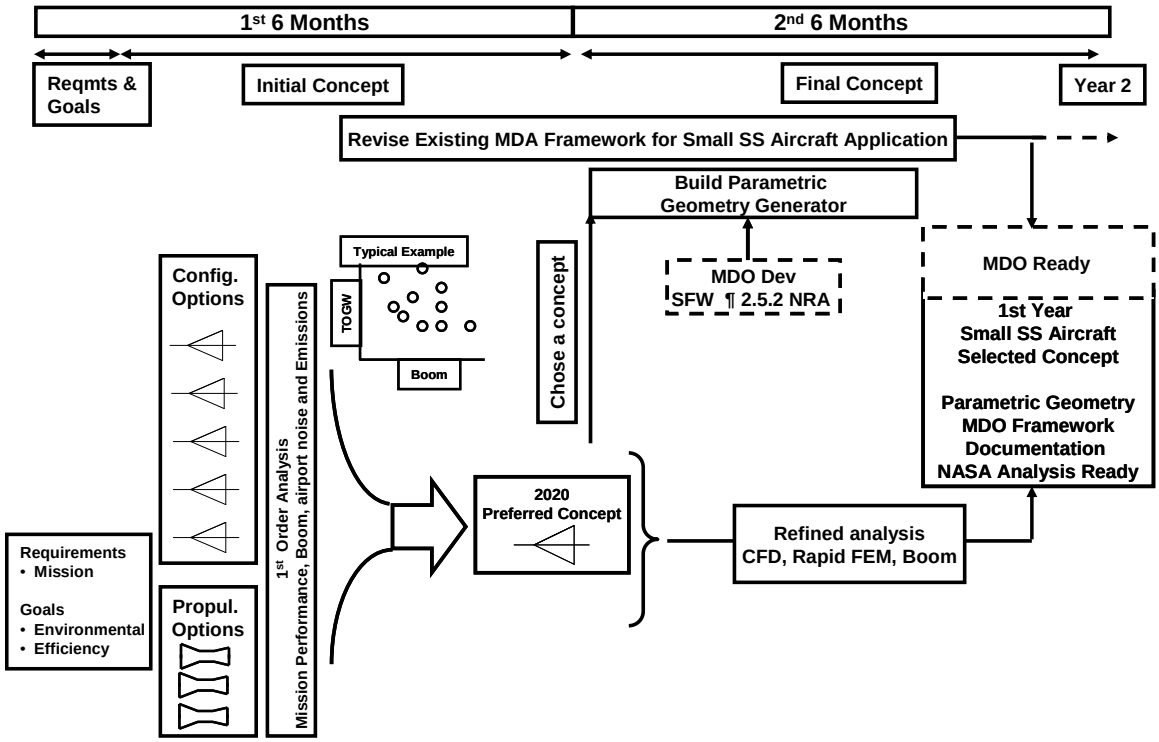

Figure 0.1.1 Roadmap to accomplish the goals and requirements of the NRA task A.4.7.1.

1.0 Market Study and Goals

The present N+2 study is to represent supersonic airliner concepts that, hypothetically, if market and regulatory conditions were favorable, could enter passenger service as early as the year 2020-2025. A part of the study is to forecast these conditions, and to construct the requirements and objectives that will guide the airplane design.

1.1 Timing

Developmental and certification flow-times for recent new airplane programs suggest that roughly 5 to 8 years of dedicated research and development would be required to achieve appropriate technology levels. Accordingly, the several Supersonic Business Jet (SSBJ) development programs that have been appearing in the press for several years represent N+1 level technologies, while the last of the large Mach 2.4 High Speed Civil Transports of the NASA HSR program of the 1990's would represent technologies somewhere between the NASA N+2 and N+3 levels. The Entry Into Service (EIS) date of the present N+2 falls between the EIS assumed for these other existing studies.

1.2 General Market & Regulation Forecast

The viability of any future supersonic airplane will depend on its ability to deliver sufficient economic value to its passengers, operators and manufacturers while meeting safety, environmental, and operational requirements. These will be accompanied by a wide variety of subjective judgments about capabilities and requirements (e.g. a 100% consensus on acceptable boom level might never be achieved, despite any official ruling), and the essential value of speed.

During the lifetime of the Concorde, market demand for speed was apparent. Due to premium fares, the two operating airlines were able to operate profitably on selected routes in the end, although the direct economic returns to its manufacturers were limited. Since the retirement of Concorde in 2003, there are no longer any large differences between airliner speeds, and there are few differences between services offered to high-yield travelers. But, the disruption in air travel following September 11, 2001 was followed by increasing demand from travelers willing to pay a premium price to shorten travel time by flying business jets, and an overall trend of increasing delivery of new business jets, as shown in Figure 1.2.1. It was more evidence of a continued demand for improved service and speed. The present economic downturn has curtailed overall travel and business travel, but projections are for a gradual return to the long-term, pre-recession trends, with some variation due to shifts in the energy and investment sectors. That trend includes increasing numbers of travelers willing to pay premium fares to save time. Recent air travel statistics also indicate that premium fares are paid by about 10% of travelers on scheduled international airlines, and Figure 1.2.2 shows a trend of slow, continuous growth in overall premium ticket volume. At some point in the future, a critical mass of high value, time-sensitive travelers would likely be sufficient to support at least a limited civil supersonic fleet in at least some markets. Initially, this projected demand for faster travel might be satisfied by supersonic business jets. Eventually, if the trend continues, supersonic airliners of 30 to 100+ passengers may become viable. But an important lesson from Concorde is that, even if market demand in 2020-2025 were theoretically sufficient to support a fleet of supersonic airliners, directly replacing the Concorde without incorporating significant advancements in fuel efficiency, noise and reliability would clearly be a business disaster, and environmentally irresponsible.

Some compromise in cabin comfort for supersonic speed would likely be economically sustainable because flight times would be shorter. The highest density and lowest acceptable level of comfort would probably be the present-day coach class interior of a medium range single aisle airplane, but a typical interior of a supersonic airplane would likely be similar to the business class configurations of subsonic airliners already familiar to the anticipated community of travelers.

An economic goal for the large HSCT airplanes was to fly profitably with a ticket surcharge of less than 20% above premium subsonic prices for supersonic airplanes introduced 10 years in the future, and 10% for airplanes introduced 20 years in the future. N+2 airplanes have neither the development time, nor the efficiency per seat , due mainly to their smaller size and seating capacity, so those are probably not realistic goals for N+2. But they are representative of the strong pressure to keep operating and ownership costs low; costs that will inevitably be compared to the best subsonic aircraft of the same generation.

Another important lesson from Concorde, and from subsonic 1st class and other premium fare service—particularly the all 1st or all business class cabin arrangements--is that matching demand with supply is crucial for achieving favorable economics. The number of markets that could support supersonic service, the size of a viable supersonic fleet, and the number of seats within a supersonic airliner would all be limited. Airplanes between 30 and 100 passengers are assumed for N+2; larger than an SSBJ to improve the fuel mileage per seat, but not as large as the 250 to 300 passenger HSR/HSCT airplanes that might be more difficult to fill regularly.

Environmental acceptability will likely be the most important requirement to meet, as it was for the HSCT/HSR program of the 1990's, i.e.

- No significant impact on stratospheric ozone.
- Compliance with then-year airport and community noise standards.
- No environmental damage from sonic booms.
- Compliance with all then-year requirements for low and high altitude aircraft engine emissions (including airport NOx & CO_2).

At both high and low altitude, lower emissions are historically achieved through basic aerodynamic and propulsion efficiency and lower weight, and those are good for basic performance as well. Improved combustor design will have the largest effect on reducing NOx. But, the susceptibility of the stratospheric ozone to NOx released at high altitude introduces cruise altitude as another factor that must be considered. Recent studies by Baughcum (Ref 1) and Wuebbles (Ref 2) show that the impact on ozone increases with increasing altitude, and that the impact varies linearly with total NOx emitted. These results update similar studies during the HSR Program (Ref 3 and Ref 4), taking advantage of recent advances in atmospheric knowledge and modeling capabilities. One significant result in the IPCC aviation assessment (Ref 4) was that the water vapor emissions from the HSCT (Mach 2.4) could accumulate in the stratosphere and be more important than the HSCT's CO_2 emissions in terms of climate impact. It is likely that emissions would dictate a lower cruise altitude than was assumed during the HSR Program, and most likely below the altitude that would minimize fuel burn alone. A balance must be struck between the total emissions and the susceptibility of the atmosphere. Lower cruise altitudes could also favor lower cruise Mach numbers, easier emergency descent certification, and engine cycle parameters that better match requirements for reduced takeoff noise.

Airframe and engine noise must be addressed through a balanced combination of engine and configuration features. Light weight, low wing loading, high lift-to-drag ratio (L/D) at low speed, and high bypass ratio engines are important characteristics that should help noise. But pursuing them exclusively could adversely affect cruise efficiency, so proper, cycled trades are necessary to realize a balanced compromise between features favorable for noise and their impact on cruise performance. And other details, like clean arrangements of high lift devices to reduce airframe noise, might also come with a weight or cruise drag penalty, and must be assessed before assuming them. During HSCT, the airport noise requirements for 10 years in the future were Stage III -1 EPNdB sideline, -5 cutback and -1 approach. At 20 years, the forecast was for -4 to -6 sideline, -8 to -10 cutback, and -5 to -6 approach. For N+2 the noise goal was set to an overall -15 EPNdB, with -3 sideline, -7 cutback and -5 approach. Figure 1.2.3 points to an increasing number of airports setting increasingly stringent noise restrictions beyond the FAR 36 requirements, so noise appears to be a subject of growing importance and awareness to regulators and the population.

Some progress in engine noise suppression technology has been demonstrated, as shown in Figure 1.2.4, but forecasts from the HSCT/HSR Program for the present day have not been met. A part of the shortfall can be attributed to a focus on much larger bypass ratio subsonic engines, and minimal investment in supersonic technologies. It exposes an area of risk where development is required.

It is critical to achieve an "acceptable" level of sonic boom, but this will almost certainly come at some cost in efficiency of the airplane. Concepts for boom reduction and boom shaping generally demand slender, lightly loaded, and uniquely tailored airframes that are not as efficient structurally or aerodynamically as an unconstrained design. Cruise efficiency already argues for relatively thin lifting surfaces and slender bodies with challenging Aero- Propulsion- Servo- Elastic (APSE) characteristics, and low boom concepts add to that challenge. It will demand material, structural mode control, and flight stability & control capabilities beyond those already assumed for keeping weight and drag low on an airplane optimized for performance. Avoiding boom by selectively flying at or below "threshold Mach" sacrifices some of the speed advantage, and would somewhat compromise the cruise efficiency if the airplane were to be designed for a wide range of cruise speeds. Aggressive strategies for boom are constrained by their impact on performance, and on the risk that technical solutions would not be available in the N+2 time frame.

The advantages of twin engine configurations for all but the largest subsonic airplanes--reduced acquisition and maintenance costs, fuel efficiency and structural efficiency of the installation--are assumed to apply to supersonic configurations as well. Twin engines are assumed for the N+2 airplanes, setting these airplanes apart from Concorde and the larger 4 engine configurations of HSR/HSCT.

Seating density and weight of passenger accommodations in most 1st class cabins today result in about 3 times the fuel per seat as coach class due to inefficiencies of reduced scale, and typical business jets burn roughly twice the fuel per passenger as airliners. This is illustrated in Figure 1.2.5. So premium fare service in a supersonic airplane could be offered without extremely tight interior arrangements while still comparing favorably with subsonic economics from the operator's perspective. But public scrutiny of fuel consumed by air travel has been growing, and will likely continue to grow, so a supersonic N+2 airplane should avoid being a major outlier in fuel use or associated emissions. An achievable N+2 target of about 20% reduction in fuel burn per passenger per nautical mile over current business jets and 33% reduction from Concorde (and even better in more typical mixed-Mach operation) is identified in Figure 1.2.5.

Similar fuel burn data versus passenger count in Figure 1.2.6 depicts how the 100 passenger N+2 supersonic fuel burn target was chosen using a curve fit to be 0.29 lb fuel per passenger mile. Figure 1.2.7 demonstrates that the resulting range varies significantly, depending on the payload and configuration. Trans Atlantic range is assumed essential for capturing high-density markets that support premium fares and involving time-sensitive travel, and for showcasing the advantage of speed. 4000nmi will be the range required for the N+2 airplanes.

We assume that some fuel--petroleum, bio, other synthetic or some blend--with roughly equivalent heating value to present jet fuel will be available throughout the operational lifetime of an N+2 airplane. But fuel cost will continue to rise, emphasizing fuel efficiency as an essential part of keeping the airplanes economically viable.

Safety will not be compromised, and certain lessons since the original HSR/HSCT have raised the awareness of designers and regulators to issues that must be addressed during the design. A sample is included in Table 1.2.1, showing how the N+2 airplanes will require additional features and design effort.

An initial step to an operational supersonic airliner might necessarily be a SSBJ that paves the technical and regulatory path to a safe, economical, and certifiable airplane. A smaller predecessor would not only provide lessons, but also set in place some regulations, and, more importantly, help establish the framework within which regulations would be set.

1.3 Initial Market/Design Requirements & Objectives

The full list of Market/Design Requirements & Objectives (M/DR&O) for a 30 passenger airplane is attached in Table 1.3.1, and for a 100 passenger airplane in Table 1.3.2. Some key points for are the following:

- 1.6-1.8 cruise Mach. Low enough to enhance engine durability, BPR for takeoff & approach noise, restricted cruise altitude, ordinary temperature structural materials. High enough to offer significantly shorter flight times.
- 55,000ft cruise altitude, or lower, for emissions & simpler cabin certification.
- 0.95 or lower cruise Mach below 39,000ft for ATC margins.
- No supersonic speeds below 41,000ft for ATC margins.
- Supersonic fuel burn less than 0.3 lb/pax/nmi, for economics and emissions on the 100 passenger airplane.
- Sonic boom as low a practical, less than Concorde over water, and possibly "boomless" flight at "threshold Mach" or lower over land.

Table 1.2.1 Areas of safety and certification that have received additional attention in recent years.

CONCERN	CAUSE	IMPACTS
Takeoff / approach speeds	Over-run incidents	Downward pressure on speeds, increased training
Tire burst, tread loss	Concorde et al	Tire design, size, pressure, speed limits
Engine/ systems FOD damage potential	Concorde	Stricter FOD protection
Fire protection	Flight 800 et al	Tank inerting, fire bottles
Engine rotor/ fan burst	Several incidents	Increased systems shielding, cabin decompression
High altitude decompression	Payne Stewart crash, "Shoe bomber" incident	Increased scrutiny of decompression/ emerg. descent
Handling qualities after systems failures	Trends toward lower time pilots, design for more benign failure modes	Systems redundancy, FBW backup modes, aeroelastic effectiveness losses, Vappr
Fuel dumping health/safety environmental impact	Trend away from allowing dumping of large fuel loads	Max landing weight fraction, Max. approach speed limits
Emergency egress	Concern over ease of exit on new (A380, SC, BWB)	Door/hatch sizes, slide size/ location/ distance restrictions
Minimum altitude for high speed flight	Air traffic control, traffic growth	.85 Mach below 37,000 ft .90 Mach 39,000 ft and above Supersonic 41,000 ft and above
Gear break-away and fuel containment	Several incidents	Fuel locations, bladders, tank reinforcements

Table 1.3.1 Reference Market/Design Requirements and Objectives for 30 pass. low boom airplane.

	Description	Item	Reqirement	Objective	Comment
1	EIS	EIS	2025	2020	
2	Type Cert	Type Cert	FAR Pt 25		
3	Op Cert	Op Cert	FAR Pt 135		
4	Cruise Speed	Cruise Mach	1.6	1.8	
	Initial Subsonic Cruise Altitude Capability (M=.95)	ISCAC	39,000 ft	50,000 ft	
	Initial Supersonic Accel Altitude Capability	ISCAAC	41,000 ft	45,000 ft	
5	Initial Maximum Cruise Mach Altitude Capability	ICAC	45,000 ft	50,000 ft	
6	Maximum Altitude	MAC	55,000 ft	53,000 ft	emissions & decompression
7	Time and Distance to Climb	Time (ISA+ 10 deg C, MTOW)	<= 40 min to 45,000 ft	<= 25 min to 50,000 ft	
8	Payload/Range	Range	4000 nm	6000 nmi @ M1.6	
		Mission Payload	30pax	45pax	210lb/pax + 9,000lb cargo
		ETOPS	120 min		
9	Takeoff Field Length	Balanced TOFL	10000 ft	9000 ft	SL/86 deg @ MTOW
10	Landing Field Length		7000 ft	6000 ft	SL/86 deg @ MLW
11	Approach Speed	Vapp @ MLW	160 kt	150 kt	
12	Takeoff Weight	MTOW	180,000lb		
13	Max Zero Fuel Weight	MZFW	Basic OEW+ payload		
14	Max Landing Weight	MLW	MZFW + FAR reserves		
15	Environmental	fuel consumpton	best achievable	best achievable	proportional to CO2, NOx & water vapor emissions
		Steady over land boom in corridor	0.8psf	0.5psf	
		Steady over land boom unrestricted	0.35psf	0.25psf	
		Steady over water boom	2psf	1.5psf	
		Community Noise	Ch 4 minus 10 EPNdB	Ch 4 minus 14 EPNdB	
		Ramp Noise	<= 82 dBA @ service locations	<= 80 dBA	
		Interior Noise	<= 90 dBA	<= 80 dBA	
16	Longitudinal CG	Design CG Limits	Available aero limits		
17	Flight Operations Balance	Pasenger seating limitations	None		
		Fwd CG limit	MZFW CG + fwd OEW variation		
		Aft CG Limit	OEW CG + aft OEW variation		
18	Ground Operations Balance	Static: Tip up	unlimited passenge movement		
19	Taxi Ride Comfort	Ride Smoothness	No worse than 737NG		
20	Turning Radius	Turning Radius	ICAO Class B	ICAO Class C	
21	Airframe Design Life	Airframe Design Life	20K hrs/10,000 cycles/20 yrs	30K hrs/15,000 cycles/25 yrs	
22	Cabin	Passengers	30, dual class bus. + econ.		
		Width	2-3 AB bus. class		
		Seat Bottom	18"	20" bus / 18" econ	Data from Payloads
		Aisle	16"	21" bus / 19" econ	
		Seat Pitch	40" bus / 30" econ	40" bus / 32" econ	
		Galley Carts	4		
		Cargo load	9,000 lb		
		Cargo volume	900ft^3		
		Pressure Altitude	6000 ft		
		Flight Crew	2	2	
		Cabin Attendant	Per regs		
23	Engines	Number	4		
		Min Supercruise TBO	2500 hrs	3500 hrs	
		Failures	Meet FAA Adv Circ 10 128A		
24	Fuel System	Fuel type	ASTM 1655 Jet A, A-1, JP-4, E7		
		Active CG management	Fuel transfer system		
25	Landing Gear	Runway loading	ICAO Class B		
26	Door Sill Height	Door Sill Height	Between 10ft & 20ft		
27	Auxiliary Power	APU	120 kVA		Scaled from 787
28	Electrical Power	Electrical power required	300 kVA VFG		Scaled from 787
29	Flight Deck	Pilot training reqd	Similar to conventional airliner		
30	Flight Controls	Control philosophy	FBW		
31	Gear Breakaway		Prevent damage to primary structure and breech of fuel tanks.		
32	Foreign Object Injestion		No worse than 737NG.		
33	Fuel Inerting		Required.		
34	Engine containment		Critical systems and structure within burst zone must be redundant and separated.		
35	Control Authority with Failed systems		Single failures will be surviable.		
36	Passenger Cabin egress		Door number & proximity to meet FAR Part 25		

Table 1.3.2 Reference Market/Design Requirements and Objectives for 100 passenger high efficiency airplane.

	Description	Item	Reqirement	Objective	Comment
1	EIS	EIS	2025	2020	
2	Type Cert	Type Cert	FAR Pt 25		
3	Op Cert	Op Cert	FAR Pt 135		
4	Cruise Speed	Cruise Mach	1.6	2.0	
	Initial Subsonic Cruise Altitude Capability (M=.95)	ISCAC	39,000 ft	50,000 ft	
	Initial Supersonic Accel Altitude Capability	ISCAAC	41,000 ft	45,000 ft	
5	Initial Maximum Cruise Mach Altitude Capability	ICAC	45,000 ft	50,000 ft	
6	Maximum Altitude	MAC	55,000 ft	53,000 ft	emissions & decompression
7	Time and Distance to Climb	Time (ISA+ 10 deg C, MTOW)	<= 40 min to 45,000 ft	<= 25 min to 50,000 ft	
8	Payload/Range	Range	4000 nm	6000 nmi @ M1.6	
		Mission Payload	100pax	100pax	210lb/pax + 9,000lb cargo
		ETOPS	120 min		
9	Takeoff Field Length	Balanced TOFL	10000 ft	9000 ft	SL/86 deg @ MTOW
10	Landing Field Length		7000 ft	6000 ft	SL/86 deg @ MLW
11	Approach Speed	Vapp @ MLW	160 kt	150 kt	
12	Takeoff Weight	MTOW	300,000lb		
13	Max Zero Fuel Weight	MZFW	Basic OEW+ payload		
14	Max Landing Weight	MLW	MZFW + FAR reserves		
15	Environmental	fuel consumpton	<= 0.35lb/nmi/pax	<= 0.30 lb/nmi/pax	proportional to CO2, NOx & water vapor emissions
		Steady over land boom in corridor	0.8psf	0.5psf	
		Steady over land boom unrestricted	0.35psf	0.25psf	
		Steady over water boom	2psf	1.5psf	
		Community Noise	Ch 4 minus 10 EPNdB	Ch 4 minus 14 EPNdB	
		Ramp Noise	<= 82 dBA @ service locations	<= 80 dBA	
		Interior Noise	<= 90 dBA	<= 80 dBA	
16	Longitudinal CG	Design CG Limits	Available aero limits		
17	Flight Operations Balance	Pasenger seating limitations	None		
		Fwd CG limit	MZFW CG + fwd OEW variation		
		Aft CG Limit	OEW CG + aft OEW variation		
18	Ground Operations Balance	Static: Tip up	unlimited passenge movement		
19	Taxi Ride Comfort	Ride Smoothness	No worse than 737NG		
20	Turning Radius	Turning Radius	ICAO Class B	ICAO Class C	
21	Airframe Design Life	Airframe Design Life	20K hrs/10,000 cycles/20 yrs	30K hrs/15,000 cycles/25 yrs	
22	Cabin	Passengers	100, dual class bus. + econ.		
		Width	4 AB bus. class		
		Seat Bottom	18"	20" bus / 18" econ	Data from Payloads
		Aisle	16"	21" bus / 19" econ	
		Seat Pitch	40" bus / 30" econ	40" bus / 32" econ	
		Galley Carts	4		
		Cargo load	15,000 lb		
		Cargo volume	1,500ft^3		
		Pressure Altitude	6000 ft		
		Flight Crew	2	2	
		Cabin Attendant	Per regs		
23	Engines	Number	4		
		Min Supercruise TBO	2500 hrs	3500 hrs	
		Failures	Meet FAA Adv Circ 10 128A		
24	Fuel System	Fuel type	ASTM 1655 Jet A, A-1, JP-4, E7		
		Active CG management	Fuel transfer system		
25	Landing Gear	Runway loading	ICAO Class B		
26	Door Sill Height	Door Sill Height	Between 10ft & 20ft		
27	Auxiliary Power	APU	200 kVA		Scaled from 787
28	Electrical Power	Electrical power required	500 kVA VFG		Scaled from 787
29	Flight Deck	Pilot training reqd	Similar to conventional airliner		
30	Flight Controls	Control philosophy	FBW		
31	Gear Breakaway		Prevent damage to primary structure and breech of fuel tanks.		
32	Foreign Object Injestion		No worse than 737NG.		
33	Fuel Inerting		Required.		
34	Engine containment		Critical systems and structure within burst zone must be redundant and separated.		
35	Control Authority with Failed systems		Single failures will be surviable.		
36	Passenger Cabin egress		Door number & proximity to meet FAR Part 25		

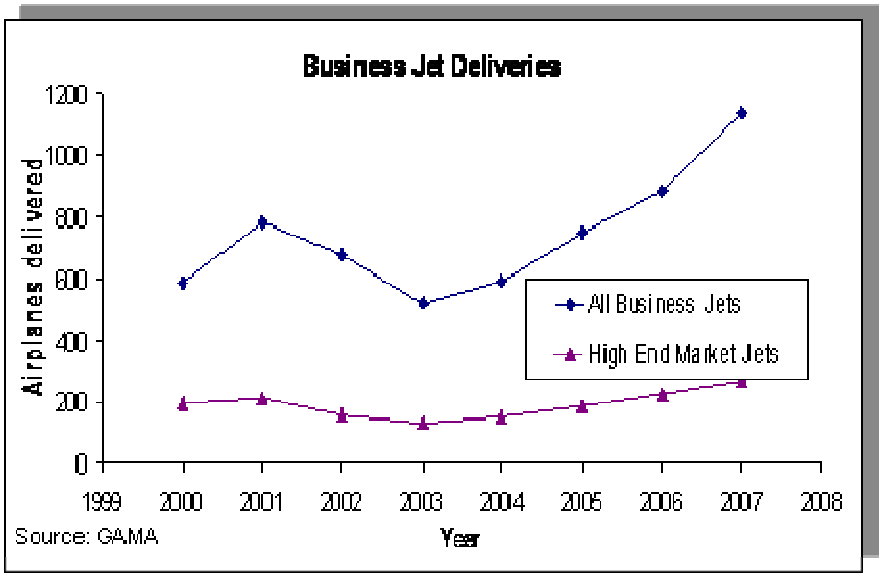

Figure 1.2.1 Trends in new business jet deliveries.

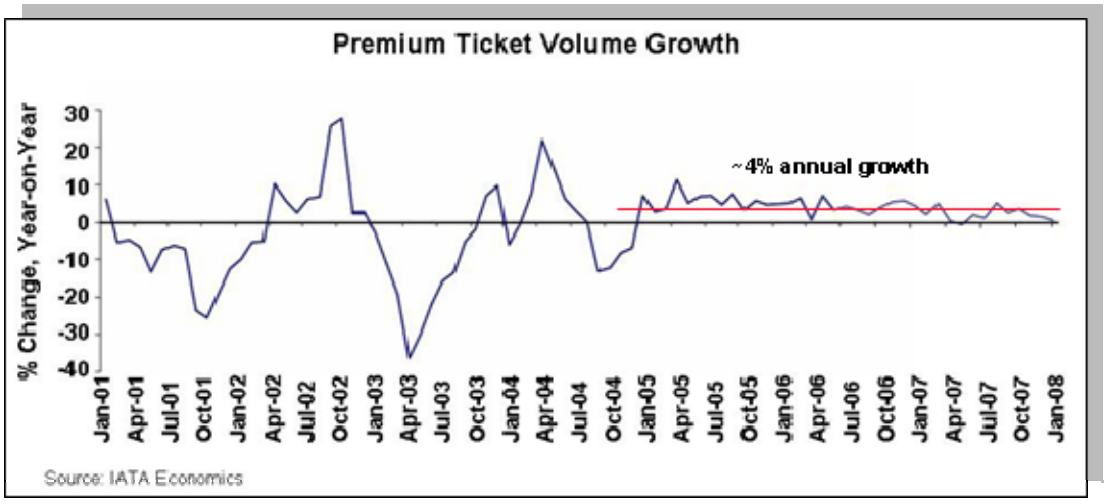

Figure 1.2.2. Trend in premium ticket volume.

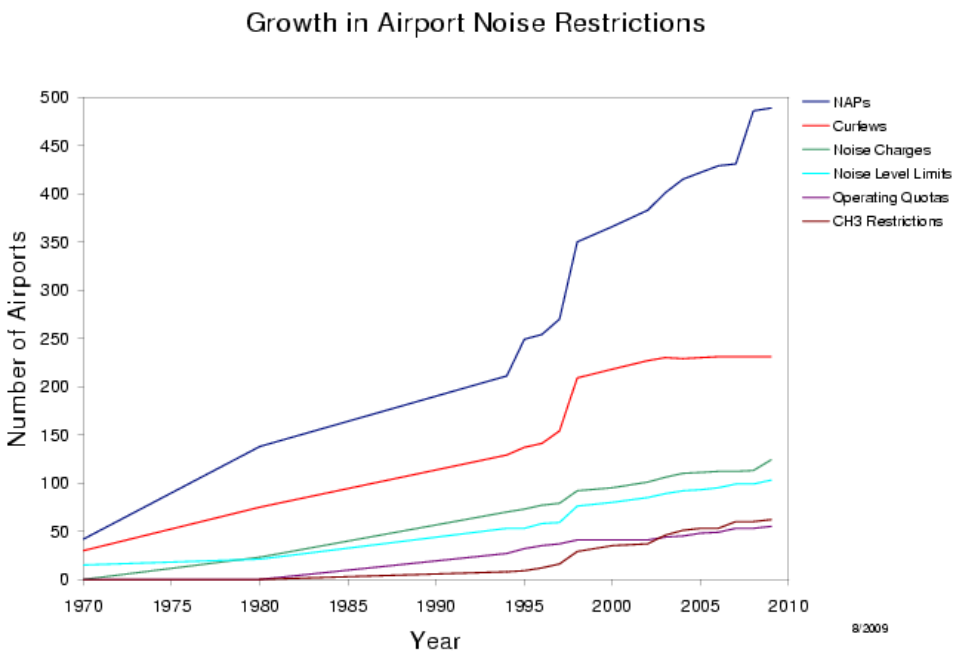

Figure 1.2.3 Increasing numbers of airports setting noise restrictions more stringent than FAR36. NAP means Noise Abatement Procedures are in effect. Airport data compiled by Boeing Noise Engineering, Community Noise.

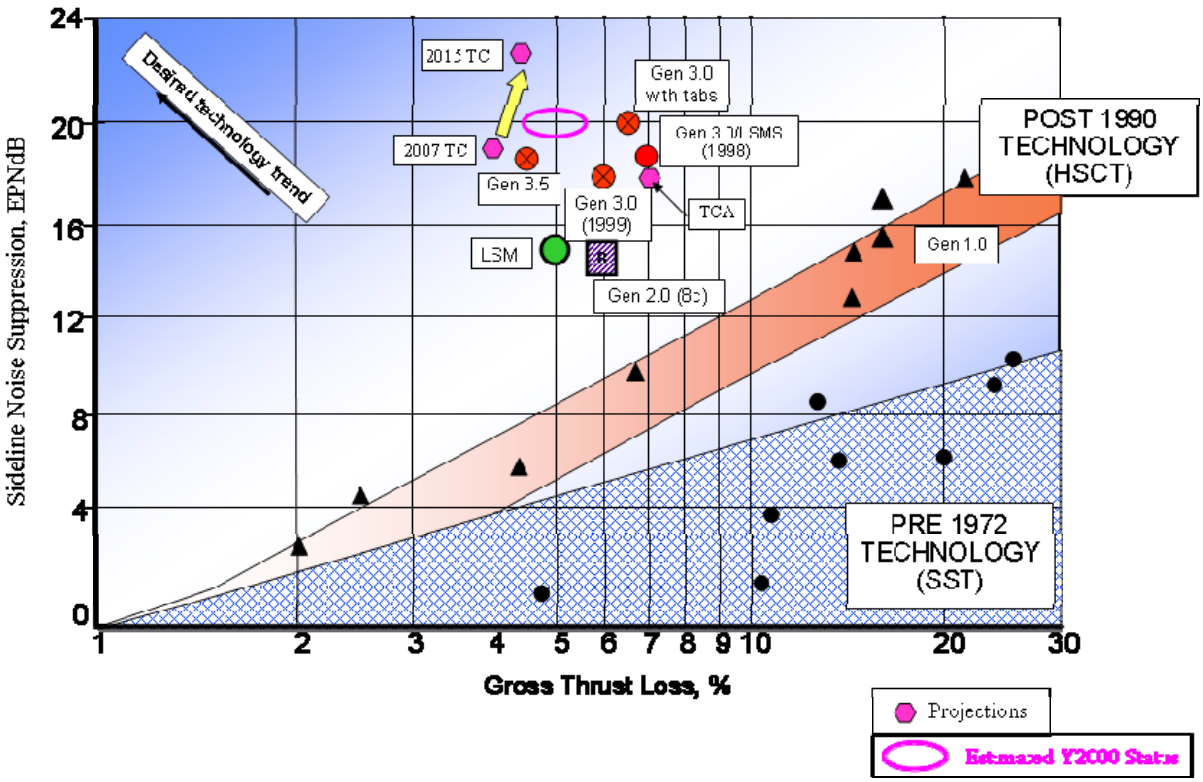

Figure 1.2.4 HSCT noise suppression, demonstrated (solid black symbols) and projected.

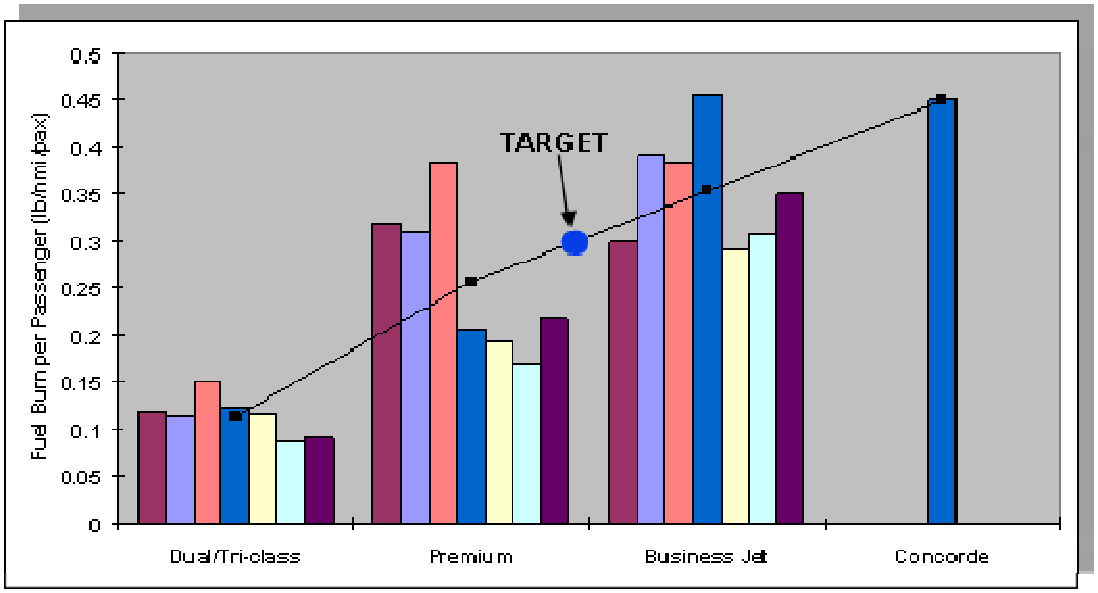

Figure 1.2.5 Fuel burn per passenger for several types of airplanes.

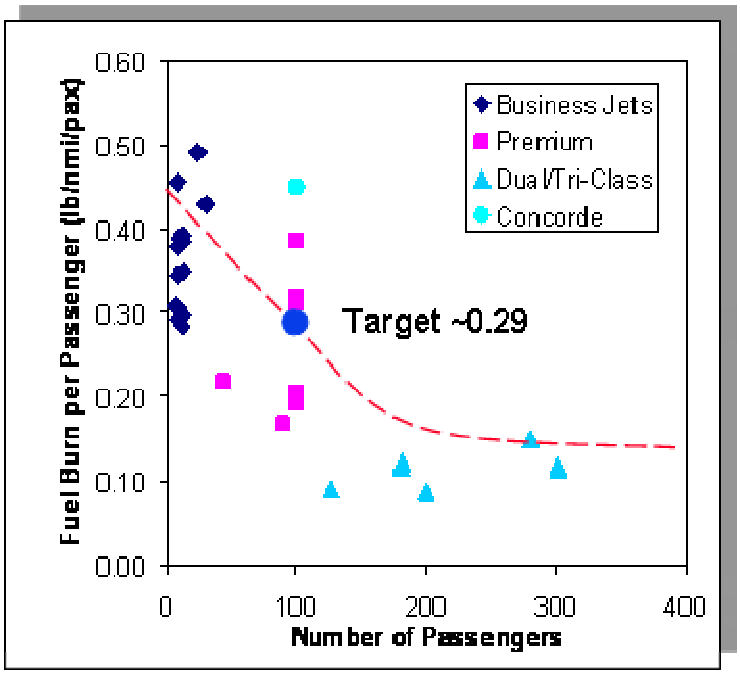

Figure 1.2.6 Fuel burn versus passengers for various types of airplanes.

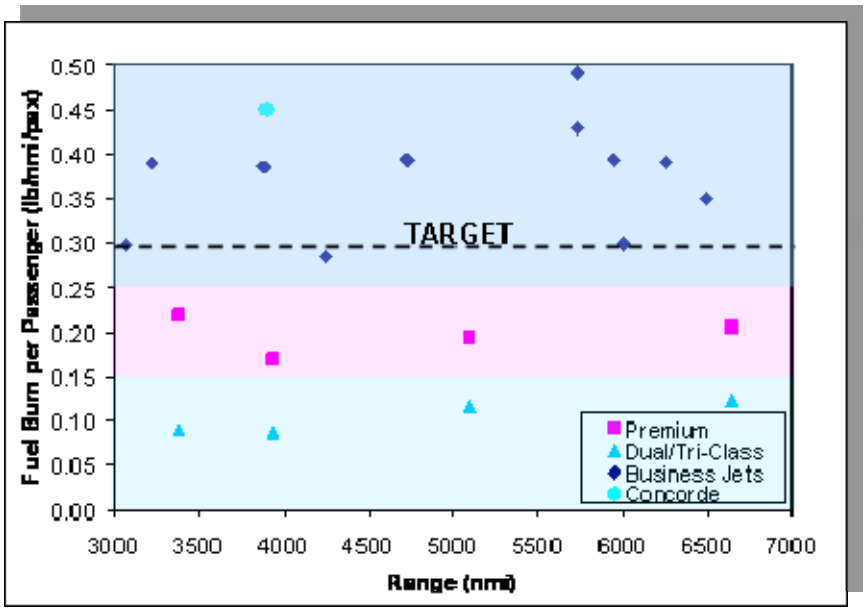

Figure 1.2.7 Fuel burn versus range for various types of airplanes. Different and unspecified payload accounts for much of the wide variation in range.

2.0 Concept Development

Overview

Results of the Market Study served in all subsequent concept development activity to set requirements and help evaluate trades. Their influence will appear directly or implicitly throughout this document.

The overall scale of a 100 passenger N+2 airplane falls between the larger HSR/HSCT and smaller SSBJ, as shown in Figure 2.0.1, with no overlap with either. Little direct comparison to previous work will be possible without relying on basic scaling, and few of the detailed configuration analyses (e.g. addressing APSE, planform optimization, engine-airframe matching, etc.) from the other projects will be directly applicable. As a result, the N+2 work will necessarily include additional studies, and areas of risk that might have already been covered in the other programs. Figure 2.0.2 provides a notional view of how aggressive payload, range and boom targets have the potential to leave no feasible territory. Requirements and goals will likely need to evolve in order to produce an airplane for N+2.

Some enabling technologies have matured significantly since HSCT/HSR, and are now on production airplanes. For example, the 787 has an "all composite" structure, nozzle chevrons and improved inlet noise treatment. Active maneuver/gust load alleviation systems, flight deck technology (including EVS/SVS/XVS), adaptable FBW/mixed function control surfaces, and the efficiency of turbo-machinery have all advanced. And designers enjoy improvements to CFD, FEM and optimization tools; better aerodynamic testing methods and instrumentation; and improved aeroelastics tools and methods. But development of most technologies specific to supersonics has slowed significantly or stagnated since the end of HSR, and in some cases HSCT ideas and lessons have been lost. SSBJ and related R&D have carried a few technologies forward, but, as a sign of things to come, many old lessens had to be re-learned. In general, the final HSCT configurations are actually 4-7 years advanced from the N+2 time-frame.

The first steps in the present work toward an N+2 airplane began with a "level 0" analysis to establish a notional "green" Concorde, with about 75% of the TOGW while carrying 50 first class or 100 dual class passengers. The engine was selected from a matrix of available study engines by installing them on scaled versions of two of the best final HSR configurations at constant wing loading and thrust loading. A preliminary configuration was assembled from promising features and sized. A 30 passenger candidate was also developed, starting with existing Boeing and NASA trade-study results, to provide an alternative with lower boom. Both the large and small configurations were developed further using a combination of interactive and automated design methods.

2.1 Initial Concepts

The initial sizing study began with two concepts derived from airplanes of the NASA HSR/HSCT Program. One was the 765-070A (figure 2.1.1) based on the 1080-2015 configuration, or "2015-TC". The other was the 765-071B (figure 2.1.2) based on the 1080-2154 configuration, or "2154 HISCAT" that promised lower noise and increased structural stiffness near the engines. The red dashed lines in Figure 2.1.1 suggest an aft deck that might provide a similar increase in stiffness for the 765-070A, and will appear subsequently on the 765-072B discussed below.

The Boeing performance sizing code ASAP was used to size thrust and area at 1.8 Mach with 47 passengers and fixed 300,000lb TOGW to meet the fuel burn target of 0.3 lb fuel per passenger-mile on a long range mission. The sizing was repeated for several Boeing proprietary study engines, and it was the Boeing Study Engine 2, or "BSE-2", engine that proved most favorable. Figures 2.1.3 and 2.1.4 are representative sizing charts showing the results for one of the engines. These sizing results led to configurations that were essentially 76% scale versions of the originals.

Compared to the HSCT engines, these BSE-2 engines have higher bypass ratio and lower fan pressure ratio appropriate for lower cruise Mach. That should improve both subsonic and supersonic SFC, and takeoff & approach noise should also improve. With lower nozzle pressure ratio and jet velocity, nozzles are expected to be lighter, simpler, and less expensive to maintain. But being twin engine airplanes, these N+2 concepts will demand higher thrust-to-weight ratio for engine-out performance than the quad HSR/HSCT airplanes. Regulatory restrictions for traffic and boom would also argue for higher thrust-to-weight, despite any engine differences, because less efficient profiles of speed vs. altitude are expected for N+2 airplanes than were assumed during HSR/HSCT. Higher bypass ratio and thrust-to-weight both mean larger nacelles, as shown in figure 2.1.5, so drag and weight—including some for the likely additional aft deck area to stiffen the engine support structure--will offset some of the gain. And while the inlet flow path feeding a single engine will be simpler, the inlet will be longer for acoustic treatment to address increased fan noise, for variable geometry for takeoff and transonic airflow control, and for FOD shielding.

Varying passenger count (i.e. changing the weight of passengers and their accommodation in proportion) and cruise Mach, Figure 2.1.6 shows the range that the 765-071B could fly if TOGW were fixed at 300,000lb. Cruising at high subsonic Mach number for part of a mission could extend range, providing some compensation for the lost speed. But choosing to slow to Mach 1.2 would cost both speed and range, indicating that the advantage of possibly flying at "threshold Mach" to avoid boom must be weighed against the penalty in performance. The value of speed has not been formulated, so it is not clear whether that would be a favorable trade. Figure 2.1.6 also illustrates how range and passenger count trade. Clearly there is a cost in range for hauling more passengers and less fuel, but seat-mile economics generally favor more passengers, so the best design will just meet the required range.

The result of sizing the wing area, thrust and fuel load of the 765-071B with 100 passengers at Mach 1.8 for various different ranges is shown in Figures 2.1.7. It demonstrates that an N+2 configuration can achieve the CO_2 emissions goal of 0.9 lb/pax/nmi and the fuel consumption goal of 0.30 lb/pax/nmi with a 300,000lb airplane flying a 4000nmi mission. Similar sizing was performed assuming 25, 50 and 75 passengers, and demonstrates that the per-passenger economics clearly favor the largest passenger counts. Arguing for lower (or not any higher than 100) passengers are the practical lessons from the Concorde and ordinary first class service--that an airline might have difficulty keeping load factors high on flights with a premium price. Figure 2.1.7 also includes the result for flying each of those sized airplanes at other Mach numbers, and it reiterates the message of Figure 2.1.6, that flying at high subsonic speed improves performance, but that the low supersonic speed of 1.2 Mach is detrimental.

Compared to the 1080-2154 HISCAT at Mach 2.4, the 765-071B had 13% lower (worse) cruise L/D and 17% lower (better) SFC. The main contributors to lower L/D were the lower Reynolds number and increased relative excrescence that comes with a smaller airplane, larger nacelles to house larger engines, longer inlets, lower aero technology projections assuming fewer opportunities on the N+2 configurations and less optimism regarding stability augmentation and structural mode control systems. The gain in SFC is primarily from the reduced Mach and higher bypass, and with that comes a favorable reduction in noise.

A more complete description of the 765-070A is in figures 2.1.8 through 2.1.12, and of the 765-071B in figures 2.1.12 through 2.1.16. Comparing some of the data listed in figures 2.1.9 and 2.1.14, the 765-071B has a slightly higher cruise L/D of 8.73 and lower fuel burn of 0.280lb/pax/nmi compared to to 8.59 and 0.288lb/pax/nmi for the 765-070A, so it is a slightly more efficient airplane.

Interior arrangements in Figures 2.1.11 and 2.1.16, configured by Boeing Payloads Engineering, demonstrate that dual class arrangements of 100 seats are feasible within each cabin. The 765-070A has a longer and narrower single aisle arrangement that loads closer to the overall airplane CG. The wider and shorter cabin of the 765-071B just allows dual aisles, affording some structural advantage from this and from eliminating a pair of doors, but with some disadvantage of narrowing rapidly near the structural joint to the wing box.

The weights summaries in Figures 2.1.10 and 2.1.15 illustrate that some structural weight in the wing and fuselage swap between the two configurations (i.e. the 765-070A has a smaller and lighter wing but heavier body), but the 765-071B has 2,850lb greater overall structural weight, primarily because of the

larger and heavier wing that is not completely compensated by the lighter body. Some of that difference would disappear if a more prominent aft deck were added to the 765-070A to stiffen it comparably. The 765-071B has 1,600lb less weight associated with passenger accommodations (partly from eliminating the pair of doors), and is less than 1% heavier in overall OEW.

Figures 2.1.12 and 2.1.17 tell that the boom of the 765-071B at 103.72 PLdB is better than the 765-070A at 109.16 PLdB, but with little margin to meet future over-water regulation. Neither airplane would likely be allowed to fly near population at cruise Mach. So, while these two airplanes meet the cruise performance and emissions goals, they do not meet the goal for boom. To pursue boom, two paths were followed. One was to configure a 100 passenger derivative of these two airplanes that incorporates their favorable features with an emphasis on promising avenues for reducing boom. That became the 765-072B that will be described in section 2.2. The other approach was to configure a smaller airplane that sacrifices some of the payload and fuel efficiency, but would allow significant boom reduction. That became the 30 passenger 765-076E described in section 2.3.

2.2 100 Passenger High Performance Transport

After demonstrating with the 765-070A and 765-071B concept airplanes that the performance targets for N+2 were feasible, the 765-072 was assembled using them as a guide, but with some emphasis on features that would assist in integrating an airplane with lower or "softened" boom. It was initially constructed and analyzed interactively within the Boeing MTA conceptual design tool, and several cycles of interactive design led to the 765-072B configuration. A python-based MDA was also employed using brute force runs of thousands of cases, single-objective MDO, and multi-objective (Pareto) optimization. Some of these studies and their results will follow. Analysis and design at higher fidelity was accomplished with the ModelCenter-based MDA and MDO.

2.2.1 Initial Trade Studies

Initial trade studies employed a combination of interactive and automated design. The Boeing Multi-disciplinary Trade and Analysis (MTA) tool provided the interactive capability. It is an Excel interface to configuration definition and Level 0-1 analysis tools. It enables ad hoc programming to enforce the relationships unique to a study (e.g. a particular parametrization of a planform); and a push-button interface (inputs, execution & outputs) to the analysis tools ANLZ, NFWD, SKFR, T080, DragJ, MDboom/MDplot, Zephyrus/Loudboom, a SEEB boom worksheet, QWICKO, and a mission performance simulator. Typical studies involved varying either geometry or the F-function, and letting the drag, boom PLdB, or closeness to target (e.g. target F-function when varying geometry, or target geometry when varying F-function) guide next steps. Success depended critically on the creativity and insight of the designer, but allowed broad flexibility in configuration options and design methods.

Automated study and MDO of the initial concepts were with a multi-disciplinary analysis tool built as a python-scripted interface to the same aerodynamics, drag and boom analysis tools. It allowed one-off runs, brute-force sampling of design space, or optimization under the direction of Design Explorer. It could be driven either through parametrized geometry, or through parametrized F-function. Typical objectives were L/D (at single Mach or weighted sum), boom PLdB (overall, forward, or aft), and overall body volume--a surrogate for volume of the passenger cabin, baggage, cockpit, some fuel, systems, and gear wells. While not as flexible as the interactive MTA tool because it demands an explicit statement of any new configuration or design approach, this automated tool facilitated numerical optimization and massive sampling of the parametrized design space.

Promising candidates from either design approach were fitted with an interior arrangement by Boeing Payloads Engineering according to industry standards for airliners and regional jets. These airplanes also received a more thorough weights and performance assessment, including an attempt to re-size the wing

and engine using ASAP. And each was cycled through both the interactive and the automated tools as a safeguard against spurious results unique to one of the methods.

Higher fidelity analysis and design was accomplished using an MDA assembled in ModelCenter. A parametric geometry generator fed a series of the same linearized aerodynamics tools, followed by NPSS, CART3D, CASES, and QWICKO. The usage of NPSS pre-dated the full capability employed subsequently on the 765-076E, but took advantage of some of the preliminary design-space surveys and response surface information about the engines produced by Georgia Tech.

Early work was focused on selecting appropriate objectives and design variables for subsequent optimizations. Figure 2.2.1.1 shows an example, where the Mach number used within T080 for constrained minimum wave drag was either fixed at the cruise Mach number of 1.8 or free to be any value between 1.1 and 2.0. The initially surprising result that design Mach numbers other than cruise could lead to better L/D illuminates the unsurprising conclusion that minimizing volume wave drag does not minimize overall drag (volume wave + lift induced wave + skin friction + interference). The design Mach within T080 became a variable in subsequent optimizations.

Another preliminary study explored the effect of considering L/D evaluated at the transonic thrust pinch (typically Mach 1.1) in the L/D objective. Studies of the 765-072A using ASAP revealed that L/D at the thrust pinch had about 50% greater impact on the cycled airplane than L/D at cruise. The effect that Mach at which to evaluate L/D had on optimization was demonstrated using 2-objective Pareto optimizations, with one objective to maximize the body volume, and the other to alternatively maximize the L/D at cruise, the L/D at pinch and a weighted sum of 40% cruise and 60% pinch. Results in Figure 2.2.1.2 show that maximizing L/D at cruise alone leads to a substantially lower L/D at pinch than if L/D at pinch alone were maximized, and vice a verse. It also reveals that including the L/D at pinch produces the same result whether the L/D at cruise is included or not. Subsequent optimizations used the weighted sum. And whenever planform trades included span, a third component, the L/D at subsonic Mach 0.95, was added to the weighted sum to ensure that it would influence the objective.

Optimum body cross-section for the fixed wing planform of the 765-072A was investigated using a 2-objective Pareto optimization to maximize L/D and overall body volume using body variables, resulting in an estimate of the best L/D available for any given body volume. Data of this type was essential for configuration trades involving the body because, lacking a carefully arranged interior for each candidate, it was not yet obvious which would hold the required 100 passengers. And no more than 100, since excess volume would clearly impact L/D, as demonstrated in both Figures 2.2.1.2 and 2.2.1.3. But achieving the highest L/D depended, in part, on how much area ruling could be accomplished in the aft fuselage. Consequently, configurations on the Pareto frontier had unacceptably narrow bodies at the wing spar, where the critical structural joint between wing and fuselage occurs. So optimization was repeated with the body constrained to be at least some minimum depth at a location near the wing spar, and that location was varied to produce the family of curves in Figure 2.2.1.3. They show the cost in L/D for increasing the fuselage depth near the spar. Figure 2.2.1.4 shows examples of the resulting optimal area distributions for fixed overall body volume of 14,000 cubic feet, revealing that the aft fuselage depth could be doubled (green vs. red) at a cost of about 1% in L/D. The corresponding structural advantage is at least a weight savings, but potentially salvages an otherwise infeasible structural arrangement. It also moves the passenger load aft, closer to the overall CG. Results from this study helped establish the overall volume of the body and aft body shape on the 765-072B.

A study of the outboard wing sweep and span revealed that supersonic L/D at this level of analysis is not very sensitive to planform, and that subsonic L/D is predictably sensitive to span through induced drag. A more comprehensive figure of merit that credits the subsonic segments of the mission would respond to these variables, but static and dynamic structural and control issues argue against any changes in sweep or span toward improving L/D. The results were the same whether simply varying sweep and span (i.e. nothing else varied except for the T080 minimum wave drag fuselage design through fixed constraint points), or optimizing and letting all the body variables free.

The effect of sweep and span on boom PLdB was also both modest and accompanied by adverse consequences for the structure. Results for a simple parameter variation (i.e. without optimization) are shown in Figure 2.2.1.5, depicting a range of variation in boom PLdB no greater than what could be achieved by modest variation of the body cross-section. It is likely that simultaneously designing the planform and body to minimize boom would result in practically the same level, and exploiting any small advantage offered at this level of analysis by a particular span and sweep would probably require higher fidelity tools.

The effect of altitude and Mach number on boom PLdB is shown in Figure 2.2.1.6 for the 765-072A cruising at 270,000lb. Unfortunately, boom PLdB appears to be maximized at the chosen cruise Mach of 1.8, although it is not clear that any general conclusion can be drawn from this particular case. The sudden change in the trends near 55,000ft is explained in Figure 2.2.1.7, where the double shocks in the front coalesce before reaching the ground. It is not surprising that cruise altitude can affect the ground signature this way, but it demonstrates one of the many challenges to achieving desired boom characteristics.

A direct application of the multi-objective optimizer was to use 3-objective Pareto optimization to trade L/D, body volume and boom. L/D was typically either the weighted sum of 40% cruise plus 60% pinch, or 32% cruise plus 48% pinch plus 20% subsonic. Figure 2.2.1.8 shows two dimensions—volume and L/D—from such a 3-objective optimization, and included on it are results from the corresponding 2-objective optimization in those same two dimensions. The agreement between the two results at the volume-L/D frontier is excellent, lending confidence in 3-objective results. In Figure 2.2.1.9 all three dimensions are portrayed, along with contours of constant PLdB that help illustrate a steep trade in PLdB near the volume-L/D frontier. And scatter in the PLdB values for the 2-objective results is more evidence that only a small price in L/D or volume would have to be paid to lower boom PLdB measurably. Away from the volume-L/D frontier, the trends are more gradual but consistent--PLdB gets worse when L/D or volume increase. These trends are made clear in figures 2.2.1.10a & b, showing orthogonal views of the three-dimensional data, with iso-curves of the parameter normal to each plot.

An allied dataset optimizing the same 3 objectives, but with more design degrees of freedom at the nose and aft end of the body, is shown in Figure 2.2.1.11. As expected, the additional freedom leads to better values of the objectives, but the interesting result shown here is evidence that the aft part of the boom is the dominant contributor to overall PLdB. The forward and aft components of the boom PLdB were estimated starting with the whole ground pressure signal that MDboom predicts, then discarding half of it, and then analyzing in MDplot in the usual way, as if it were the whole ground pressure signal. Either a falling or rising hyperbolic tangent step of the form (1-tanh(x))/2 was used to clip the forward or aft parts of the pressure signal smoothly to minimize any spurious content. The centers of the tanh() steps were aligned with the centroid of pressure fluctuations, and the width (i.e. reciprocal of the scale of the argument) was set to 10ft. This forward-aft decomposition of the boom PLdB provides some opportunity for the optimizer to discover and exploit some direct relationships between geometry and boom. In some later studies when one end of the boom was consistently dominant (typically the aft end, but not always), minimizing PLdB for that end alone was an objective. Just as in Figures 2.2.1.8 through 2.2.1.10, these data also indicate that overall PLdB gets worse when either L/D or volume increase, although plotting all the data together in Figure 2.2.1.11 masks these individual trends.

At the conclusion of these and several cycles of interactive design using the Boeing MTA tool, the 765-072B configuration emerged, shown in Figure 2.2.1.12. Its fuel efficiency was promising, and additional design and analysis was performed at higher fidelity using the ModelCenter-based MDA/O, as described below. An important general result from these and several other similar optimization studies on 100 passenger airplanes was that the design space afforded little opportunity to improve boom without sacrificing performance and demanding development beyond the N+2 level. That result was reinforced with the manual development of 765-078A & B, using the MTA tool, described in Section 2.2.10.

2.2.2 Trade Space Studies Using MDAO Model of the 072B Concept

To provide a comprehensive analysis of the 765-072B, and to gain confidence in the decision to accept it as the 100 passenger candidate, a higher fidelity analysis and engine matching effort was performed. It involved a more detailed series of system level trades on 072 and 070 type concepts. In order to capture the interactions between the various analysis disciplines (geometry, aero, weights, propulsion, mission performance, takeoff performance), an in-house MDAO model was used. (This MDAO model is described in Appendix 2).

Two MDAO models for the 072B and 070 (2015-TC) type aircraft were developed. The following trade approach was followed:

- Species trade using both MDAO models
- System level trades using the best species MDAO model
    - Number of passengers
    - Cruise Mach
    - Cruise Range
    - Engine cycle (from 6 preselected cycles)

For all the trades, a supersonic non-stop mission profile was used to determine the performance of the concepts. This mission profile, shown in Figure 2.2.2.1A and 1B, is parameterized to allow for variations in cruise range and Mach number.

For the species trade, the 765-070 type and 765-072B type species were compared and the best species was selected for the remaining trades.

For the engine cycle trades, a series of six candidate engines cycles, three from P&W and three from RR, were evaluated. These were provided to the MDAO model in the form of installed thrust and fuel flow tables for a reference thrust. In deciding how to choose the engine cycles for the system level assessment, the design team believed that jet noise and engine diameter would be two competing characteristics. Jet noise was expected to be the dominant noise component, so jet velocity (Vj) served as a surrogate for propulsion noise. It was generally understood that we wanted a low diameter engine for best supersonic aerodynamic performance and we wanted a low Vj to minimize the jet noise. However, because of the fundamental physics of turbine engines, minimizing Vj results in a large diameter engine, and vice versa. Therefore, Georgia Tech prepared three engine cycles for each of the engine company's proposed technology level representing a range of diameter and Vj. These engines are designated

- Low Diameter #1 and #2,
- Low Vj #1 and #2, and
- Compromise #1 and #2

for the purposes of the trade studies. Trade studies selecting the Compromise Engine # 1 for the other trades discussed below is given in Section 2.2.8.

For each of the trade study points, the concept was "optimized" to maximize the Figure of Merit (FOM) of PAX*nmi/lbs of fuel by varying the wing area and engine size (reference thrust). When the wing area is scaled, the MDAO model recalculates all the aerodynamics, weights, and resulting performance. When the reference thrust is scaled, the MDAO model changes engine size/weight, along with the thrust and fuel flow tables. When the engine size changes the nacelle will also change. So the aerodynamics must be recalculated. All of these will affect the performance. The optimum aircraft must meet the following constraints.

- Greater than 300 fpm rate of climb (ROC) anywhere in the mission
- Less than 10,000 ft balanced field length (with engine failure)
- Sufficient fuel volume in the wing (desired) or wing and fuselage (required)
- Less than 78 psf wing loading (W/S)

The wing loading constraint was selected based on historical data which indicated that keeping it below 78 psf would result in an approach speed below 155 kts at typical maximum landing weight, and Initial Cruise Altitude Capability (ICAC) unrestricted by buffet boundary at subsonic and supersonic Mach. The results of a two variable optimization can be depicted graphically with all the constraints in a carpet plot or thumb

print. Graphical results are easy to comprehend and give insight into what constraints are driving the optimum design and what alternatives the design space allows.

Following the trades, a preferred concept was selected and a fairly simple multi-disciplinary optimization (MDO) was conducted to demonstrate the parametric capability of the MDAO model. At the time the trade studies were conducted, the aerodynamics, propulsion, and performance analyses in the MDAO model were still being validated. This exercise was completed after the trades and the performance of the preferred concept received minor updates. The changes to the model as a result of the validation did not affect the relative trade study results or the conclusions.

2.2.3 Species Trade

The 765-070 type and 765-072B type species were compared in the species trade. For the purposes of performance assessment, the primary difference in these two concepts will be in the cruise aerodynamics. Figure 2.2.3.1 shows a comparison of the lift over drag (L/D) ratios for these two concepts. The -070 has approximately a 5% lower maximum L/D and the differences increase slightly with increasing lift coefficient (C_L). The aerodynamic differences are caused primarily by the horizontal tail on the -070, as well as small differences in wing sweep, thickness, and aspect ratio.

In a separate analysis, the Boeing team determined that the airport noise requirements (10-20 EPNdB below Stage 3) had a high probability of being met without a noise suppressor on the nozzle if the Vj could be kept at or below 1100 fps. During the prescreening performance runs, we observed that none of the six candidate engines could achieve 1100 fps Vj at maximum takeoff power. We also observed that, in general, the engines were sized to get through the transonic pinch point without diving the aircraft or using afterburners. In doing this, they had excess thrust for takeoff. This meant that the engines could be throttled back (or derated) for takeoff as a means to reduce the Vj. Figure 2.2.3.2 depicts how this works. For this example, an aircraft with the engine sized for transonic ROC > 300 fpm could achieve a balanced field length of ~ 5500 ft using 100% power (blue line). At 100% power the engine would have a Vj of 1530 fps (magenta line). By reducing the power to 60%, the same aircraft achieves a 10,000 ft balanced field length. At 60% power the Vj is approximately 1200 fps. However, for engine-out performance, the FAR allows the thrust to be increased by 10% and does not require that the noise requirements be met. This means that for meeting the noise requirements we can use the jet velocity for an all-engine takeoff at 10% lower thrust. The resulting Vj is 1100 fps, meeting the goal for the study. Simple constant derate is assumed in this study, recognizing that Takeoff Field Length or noise could be reduced through a fully optimized thrust lapse starting with full thrust a brake release, as in the "PLR" system during HSCT.

Figure 2.2.3.3 takes this concept a step further. In this example, the engine sized for transonic ROC, meets the 10,000 ft balanced field distance at 77% power. At that power setting, even accounting for the 10% FAR thrust increase, it will not meet the 1100 fps Vj goal. So the thrust must be increased (blue dotted line) until it does meet the 1100 fps goal. This will occur when the engine has enough thrust to meet the 10,000 ft balanced field length at 66% power. The carpet plots shown for the trades will be using a 10,000 ft balanced field distance constraint for a partial power takeoff which meets the 1100 fps Vj goal.

Figure 2.2.3.4 shows the carpet plot for the 100 passenger 072B species with Compromise #1 engine. Each of the points in this plot meet a Mach 1.6 cruise and a 4000 nm range. The objective is to maximize FOM. The carpet is plotting thrust from 45,000 to 80,000 lbs and wing area from 3000 to 5000 ft^2. The blue line shows the 300 fpm ROC constraint. The red line shows that meeting the 10,000 ft balanced field distance with the engine de-rated (throttled) to meet 1100 fps Vj is more constraining than ROC. The orange line shows the 78 psf W/S constraint and the green line shows the wing fuel volume constraint. The cross-hatched side of the constraint lines shows the infeasible portion of the design space. The point where the balanced field distance and W/S constraints cross represents the maximum FOM concept that meets all of the constraints. This optimum concept has a FOM of 3.7, which is better than the project goal of 3. It has a wing area of 4600 ft^2 and a thrust of 55,000 lbs. If we were to relax the derated balanced field constraint then the optimum concept would move up the the intersection of the ROC and W/S constraints and the FOM would increase to 3.8.

Figure 2.2.3.5 shows a similar carpet plot for the 100 passenger -070 species with Compromise #1 engine meeting a Mach 1.6 cruise and 4000 nm range. Thrust and wing area were selected to vary the same as the -072B and the FOM was plotted at the same scale as it was for the -072B to depict the fact that the design space for the -070 species collapses down to a lower FOM than the -072B species. As before, the optimum design which meets all the constraints occurs at the intersection of the balanced field distance and W/S constraints. This concept has an FOM of 3.36, a wing area of 4550 ft2 and a thrust of 59,500 lbs. The increased thrust required was due to the higher drag depicted in Figure 2.2.3.1 shown previously.

The species trade results are summarized in Figure 2.2.3.6. This figure shows that the -072B species has higher FOM, lower takeoff gross weight (TOGW) and lower thrust per engine.

The conclusion of this trade is that the -072B species is the preferred species for the rest of the trades.

2.2.4 Number of Passengers Trade

The -072B species was laid out with a 100 passenger configuration. The passenger trade additionally considered concepts with 50 and 25 passengers. For this trade, the Compromise #1 engine was used. Initially the cruise Mach was set at 1.6 and the range was set at 4000 nm. Later, the combined trade will look at varying Mach and range, along with the number of passengers. In order to conduct the passenger trade, 25 and 50 passenger fuselages had to be manually laid out. The fuselage cross-section constraints for two (blue), three (red), and four (gold) abreast seating is shown in Figure 2.2.4.1. These cross-sections were combined into seating cylinders for new 25 and 50 passenger fuselages, as shown in Figure 2.2.4.2. The goal was to keep a constant overall fineness ratio and the resulting overall lengths are shown in the figure. The fuselage constraints for each of these three passenger layouts were coded into the MDAO model, so that the user merely had to select 25, 50, or 100 passengers and the model would automatically reconfigure the fuselage.

Figure 2.2.3.4 from the previous species trade shows the carpet plot for the 100 passenger 072B, having an FOM of 3.7. Figure 2.2.4.3 and 4 show the carpet plots for the 50 and 25 passenger 072B concepts, respectively. On the 50 passenger concept the constraints for ROC and balanced field distance lie almost on top of each other, but the ROC is slightly more constraining. So the optimum concept occurs at the intersection of the W/S and ROC constraints. This concept has an FOM of 2.3. On the 25 passenger concept, the balanced field distance and the ROC constraints cross at a wing area of approximately 3300 ft^2. At the intersection of the W/S constraint, the balanced field distance is more constraining. The green line in Figure 2.2.4.4 shows that the 25 passenger concept does not have sufficient wing volume for fuel. Therefore, some of the fuel is placed in the fuselage (below the passenger compartment). The orange line shows the limit for the combination of wing and fuselage fuel volume. The resulting FOM for 25 passenger concept is 1.3. Figure 2.2.4.5 shows a summary of the passenger trade results. As expected, the FOM significantly improves with increasing passenger count. The 100 passenger concept has almost three times the FOM of the 25 passenger concept. Since the larger number of passengers results in a larger aircraft, the TOGW and thrust per engine also increase with the number of passengers.

2.2.5 Cruise Mach Trade

The Mach trade will use the -072B concept with the Compromise #1 engine, initially the 100 passenger concept with a 4000 nm range will be compared. Later the Mach number will be combined with variations in number of passengers and range. Figure 2.2.3.4 from the species trade shows the carpet plot for the Mach 1.6 072B, having an FOM of 3.7. Figures 2.2.5.1 and 2 show carpet plots for Mach 1.8 and 2.0, respectively. For Mach 1.8 the intersection of the balanced field distance and wing loading constraints defines the optimum aircraft with an FOM of 3.55. The Mach 2.0 concept is constrained by the intersection of the W/S and ROC constraints with an FOM of 2.55. The carpet plot in this figure was flipped for clarity in displaying the constraints. Figure 2.2.5.3 shows a summary of the Mach trade results. There is very

little difference (~4%) between the Mach 1.6 and 1.8 cruise points. On the other hand, cruising at Mach 2 significantly degrades the FOM (~30%) versus Mach 1.6. Since reduced travel time is a principal motive behind these supersonic airliner studies, there are other figures of merit, such as productivity (block time) or passenger preference that would favor selecting the Mach 1.8 cruise speed. While this particular engine cycle and airframe shape shows the Mach 1.6 to have the best FOM, there may be other engine/airframe combinations that will give a slight edge to Mach 1.8.

2.2.6 Range Trade

The Range trade will use the -072B concept with the Compromise #1 engine, initially the 100 passenger concept with a Mach 1.6 cruise will be compared. Later the range will be combined with variations in number of passengers and Mach number. Figure 2.2.3.4 shown previously from the species trade shows the carpet plot for the 4000 nm 072B, having an FOM of 3.7. Figures 2.2.6.1 and 2 show carpet plots for 5000 nm and 6000 nm, respectively. The optimum concept for the 5000 nm range occurs at the intersection of the W/S and balanced field constraints, with an FOM of 2.95. The 6000 nm concept is not really feasible. None of the points meet either the wing loading or derated balanced field constraints. In an effort to find a feasible solution, additional points were run at larger thrust and wing area. Various analyses failed to converge at these excessively large wing areas and thrust, so it was not possible to find a feasible solution without changing the configuration or planform, or sacrificing other parameters. If the W/S and balanced field constraints are ignored, the resulting FOM is 2.55. Figure 2.2.6.3 shows a summary of the range trade. Only the 4000 nm range results in an FOM above the project goal of 3.

2.2.7 Combined Range, Mach, # Passengers Trade

Figure 2.2.7.1 shows a 27 point matrix (3 X 3 X 3) of the Range, # passengers, and Mach trades. To visualize the results, the FOM is plotted versus range and a separate curve is shown for each of 25, 50, and 100 passengers. Then a separate plot is shown for each cruise Mach (1.6, 1.8, 2.0). Starting at a cruise Mach of 2.0, none of the combinations of range and # passengers will reach the FOM goal of 3. Further, 6000 nm range is not feasible and the 5000 nm 100 passenger point does not meet the W/S constraint. Next, we see that the Mach 1.6 and 1.8 plots are very similar. None of the 6000 nm points meet the W/S constraint. Only one range/passenger combination exceeds the project FOM goal of 3. It is 4000 nm range and 100 passengers. So ignoring the boom for now, the recommended combination would be 4000 nm range, 100 passenger and either Mach 1.6 or 1.8 cruise.

2.2.8 Engine Cycle Trade, Fixed Engine Decks

The engine cycle trades were all run using a 100 passenger -072B species with a Mach 1.6 cruise and 4000 nm range. Six engine cycles were run (see Section 3). The six cycles and their corresponding carpet plots figures are shown below.

- Low Vj #1: Figure 2.2.8.1
- Low Vj #2: Figure 2.2.8.2
- Compromise #1: Figure 2.2.8.3
- Compromise #2: Figure 2.2.8.4
- Low Diameter #1: Figure 2.2.8.5
- Low Diameter #1: Figure 2.2.8.6

For the Low Vj #1 engine, the optimum point occurs at the intersection of the W/S and ROC constraints with a FOM of 4. The balanced field distance constraint does not show on the plot because all the points meet the constraint with a derate power of 79%. This engine starts out with the lowest Vj at 100% power, so we would expect the minimum amount of derate required to meet the 1100 fps Vj goal. For low Vj #2 engine, the optimum point which meets all the constraints occurs at the intersection of the balanced field and W/S constraints. It has an FOM of 3.21. The required derate power is 66% in order to meet the 1100 fps Vj. There is quite a bit of difference between the balanced field constraint and the ROC constraint for

this engine. If the balanced field constraint is ignored, then the FOM rises to 3.57. For Compromise #1 engine, the optimum point occurs at the intersection of the balanced field and W/S constraints. It has an FOM of 3.7. This is the same airframe/engine combination that was used for the Mach, range and passenger trades. The required derate power is 60% in order to meet the 1100 fps Vj. For the Compromise #2 engine, none of the points were able to meet the 10,000 ft balanced field distance with the required 54% derate power. Ignoring this constraint, the FOM would be 3.8. For the Low Diameter #1 engine, none of the points were able to meet the 10,000 ft balanced field distance with the required derate power. Ignoring the balanced field constraint, the FOM is 3.9. Finally, for the Low Diameter #2 engine, again none of the points were able to meet the 10,000 ft balanced field distance. Ignoring the balanced field constraint, the resulting FOM is 3.5.

Figure 2.2.8.7 summarizes the results of the engine cycle trade. The blue bars are for a non-derated takeoff and the number in the blue bar shows the Vj achieved. The maroon bars are for the derated takeoffs. Only three of the six cycles were able to achieve a 10,000 ft balanced field distance with the engine derated to an 1100 fps Vj. Based on FOM alone, the Low Vj #1 engine cycle would be the best, followed by the Compromise #1 and Low Vj #2. These three cycles all exceed the project FOM goal of 3 and meet all the constraints. The Compromise #1 engine, however, has the lowest thrust per engine. It was also the opinion of the team members that the Low Vj #1 engine cycle would be more difficult to integrate because of the large fan diameter. Therefore, Compromise #1 is the recommended engine cycle from this study. Subsequent improvements and errors fixed in the MDAO analysis changed the predicted performance level, but not the conclusions.

2.2.9 Trade Study Summary and Recommendations

Following these studies using the MDAO, improvements and corrections were made to the tool, changing the level of the answers (see Figure 2.2.9.1), but not the conclusions. The trade study results show that the -072B species is preferred over the 070 species based on FOM. Only the combination of 100 passengers and 4000 nm range were able to achieve the project FOM goal of 3. Either Mach 1.6 or 1.8 are acceptable for cruise and there is very little difference between their FOM, but with the (as yet un-quantified) value of speed arguing for faster. Finally, the Compromise # 1 cycle was selected for the purposes of producing a computer aided design (CAD) model of the 072B airplane, shown in Figure 2.2.9.2

2.2.10 Boom Reduction

The hopeful low boom successor to the two initial 100 passenger concept aircraft was to be the 765-072. But after several manual iterations and MDO studies, it became clear that the configuration afforded little opportunity to lower the boom significantly without substantially compromising the weight or drag, and adding development risk beyond the N+2 level. As a rough order of magnitude estimate, the goal was a 100 passenger airplane that has 35% lower fuel burn than Concorde, meets “Stage 5” noise criteria, and has less than 83 PLdB boom. Compared to the Concorde, it would need lower wing loading, greater span, a compound-sweep planform (possibly with variable sweep), moderate BPR engines with suppressor nozzles, very low NOx engines at low weight with commercial durability, 25% reduction in TOGW at 400nmi more range, 25-35% empty weight reduction, and a length of about 300ft. It requires light-weight, stiff and probably actively controlled structure with an effective structural l/d that exceeds that of any flying airplane, or even any HSR/HSCT designs, and represents technology beyond the N+2 time frame.

In light of the challenges, an attempt was made to soften the boom of the 765-072B using the 765-078 configurations. Both the A and B variants achieved lower boom through softening, but at the expense of performance, as they both exceeded the fuel burn requirement.

The 765-078 preserved many of the essential characteristics of the 765-072B. The overall length increased to 224ft, and some details of the body area distribution were free to change, but, as shown in Figure 2.2.10.1, some constraints were enforced to preserve the viability of the 100 passenger interior. One was to

preserve the width of the cockpit. Another was to ensure that the forward cabin and aft body cross-sectional areas remained large enough to hold a galley/lav, or 2-abreast seats, or APU and vertical tail tie-in; and that at least 14,200ft^3 total volume was preserved. A cruciform tail was added in an attempt to alter the aft lift signature, and the aspect ratio and sweep of the canard were raised to help drag. Wing planform was varied, but area was not allowed to change significantly.

The planform, lift distribution and body shape were designed using the Boeing MTA tool. The first step involved approximating the F-function of the 765-072B with a simplified model, then varying this simpler F-function iteratively to design a softened boom. The resulting F-function then became the target, and a first approximation to the airplane geometry that could produce it was calculated using the Abel transform. From that geometry began a series of geometric design iterations; where the resulting F-function, boom signature, PLdB and drag were monitored. The focus was on boom softening, with no particular attention paid to wave cancellation to lower the boom. Often the target F-function was re-examined and sometimes re-designed in light of results.

After several design cycles, two candidates with fairly good boom PLdB emerged, the 765-078A and 765-078B. Figure 2.2.10.2 shows the 765-078A in 3-view and its principal characteristics. Favorable boom reduction was achieved by creating a double shock in the forward part of the ground signature, and some subtle improvement in the aft, shown in Figure 2.2.10.3. MDboom and Zephyrus both report about the same boom level of 105 PLdB. That was clearly an improvement to the 109+ PLdB of the 765-072B, but it came at a cost of 11% higher fuel burn and 260nmi less range.

One more attempt to improve the boom was through softening the ground signature. The configuration was the 765-078B, and it is essentially the same at the 765-078A at the scale of the figure. Apparently minor modifications resulted in a significantly smoother front shock, and clipped aft shock on the ground, as shown in Figure 2.2.10.4. An even lower boom of less than 98 PLdB was achieved, but the penalty grew to 17% higher fuel burn and 410nmi range shortfall compared to the 765-072B.

The 765-078 A and B provided evidence that a penalty in performance can be expected for reducing the boom of an efficient cruise airplane. With the 765-072B just meeting the performance requirements, it appears that it can afford no further boom reduction.

2.3 Thirty (30) Passenger, Lower Boom Transport

The 765-076 model was introduced to study a smaller airplane with potential for substantially lower boom than the 100 passenger 765-072B, but accepting a loss in MTOGW and payload capacity, and with worse fuel burn and emissions per seat. It was initially sized to have a TOGW of 180,000lb with a similar wing loading and thrust loading as the 765-072B.

The E variant of the 765-076 is shown in figure 2.3.1. Overwing nacelles are to help achieve the lift and volume distributions required for low boom, but with some penalty in wave drag due to lift. Other benefits are some shielding of fan noise, and a significantly lower risk from runway, slush or tire FOD. Canard surfaces were omitted to avoid ingesting their vortices. V-tails assist with integrating the overwing nacelles, and theoretically add some (as yet unproven) virtual length to the lift distribution by their height above the wing, assuming a substantially aft CG for boom.

2.3.1 Trade Studies

The 765-076 matured into the E model through primarily manual iteration through the MTA tool. The approach began with analytical and optimization studies to arrive at a target F-function that produces reasonably good boom PLdB, then using the Abel transform to get a first approximation to the geometry that might produce it. Then the study proceeded much like the study of the 765-078, where geometry was varied toward matching the resulting F-function to the target. The target evolved according to the insight

gained by numerous boom analyses into the practical limits of using airplane geometry to control details of the realized F-function.

An early study of the 765-076 concept was an attempt to gage the potential for boom reduction while paying little attention to the penalty in performance. It began with an aft wing configuration scaled to 180,000lb MTOW. The python-based MDA was used with Design Explorer to minimize PLdB by varying the body cross-section distribution, wing span and outboard wing sweep. Figure 2.3.1.1 shows results from that study. L/D and overall body volume were constrained not to fall below values not far from the seed configuration. In figure a) the benefit of allowing overall length to vary is demonstrated, but, in this study the length was not independent of volume because the cabin cross-section was also roughly constrained to preserve space for constant seating capacity. Thus, longer airplanes had more total volume, so their boom suffered, despite the otherwise favorable effect of length on boom. When wing was fixed (red +) a small improvement was possible. But when the wing was free to change span and sweep, significantly lower boom was achieved. While initially promising, all of the configurations with better boom also had significantly higher span or sweep or both, assuring a penalty in weight (that was not assessed) and exaggerating the APSE challenges.

Another path of study was to drive a parametrized, constrained F-function with the optimizer to establish some off-body pressure targets that achieve good boom by various means (e.g. reduced overpressure, boom shaping, multiple shocks), as assessed by MDboom. A closed-form expression for the equivalent area distribution, derived in familiar form for a piece-wise linear F-function using the Abel transform, estimates the physical geometry and lift that could produce a similar off-body pressure distribution. Figure 2.3.1.2 shows a typical parametrized F-function. All points were free to vary in station and amplitude, but amplitudes were scaled collectively within each of the four groups shown to solve for the following four constraints on the equivalent, transformed geometry:

Overall lift must match weight, setting cross-section at aft end.
The slope of the aft end must match that of a typical supersonic airplane.
The maximum of the equivalent cross-section (lift plus volume), as fraction of aft cross-section.
Positive geometric volume at the aft end of lift.

Figure 2.3.1.3 makes those constraints in the transformed geometry apparent. Other constraints (e.g. overall equivalent volume or the station of the area maximum) and various combinations were also possible to satisfy explicitly.

Several optimizations were performed using Design explorer to drive toward minimum boom PLdB using this parametrized F-function formulation. In the cases that will be shown, the points defining the F-function were divided into three sets, and constraints on lift, slope of the equivalent geometry at the aft end, and overall volume of the equivalent body were met explicitly. The seed to each successive optimization was a promising point (typically the optimum) from a previous result. Bounds on the variables were successively adjusted to free any variables that had been up against them at the prior optimum. The data are shown in Figure 2.3.1.4. Figure 2.3.1.4a shows how PLdB was minimized by minimizing volume. It is not a surprising result, and re-iterates that basic parameters like volume (and lift, length) are the principal drivers of boom, so design of other details becomes something like an exercise in avoiding penalties from poor execution. The lower edge of the data spanning the plot represents an approximate Pareto frontier, providing an estimate of the minimum boom for any given volume. Figure 2.3.1.4b shows the forward and aft parts of the boom analyzed separately, and demonstrates that the forward part dominates. Two of the optimizations used a subset of the variables so that little would change in the aft boom, while attention would be focused on the forward boom.

The F-function of the two points with the lowest boom levels are shown in Figure 2.3.1.5. One surprising feature of the lowest, 82 PLdB case is the unusually small amplitude to the overpressure at the front. But, the other case has a more familiar “spike” in pressure (F-function), so it might not be an important feature. This method of driving the F-function provides no assurance that the corresponding pressure distribution could be realized in the signature of a real airplane, and the steep signals and large amplitude at the aft end of both of the curves in Figure 2.3.1.5 might, therefore, be spurious. Nevertheless, the ground signature, as

propagated from 50,000ft by MDboom, is plotted in figure 2.3.1.6. Surprisingly, the overpressure at the front of the lowest boom is substantially higher than the higher boom. But both have achieved a somewhat gradual initial shock, followed by a substantially more gradual rise to the maximum. The favorable aft boom levels measured in Figure 2.3.1.3 are evidently the result of fairly mild aft amplitude that relaxes essentially without a shock. That behavior is certainly favorable for boom, but probably spurious.

2.3.2 High Fidelity Analysis and Design.

Just prior to finally selecting the 765-076E, and while the more slender and lower boom 765-076F was still under consideration, TRANAIR design was used to trim the 765-076F, and to measure how much change from the Linear Theory design would be required to achieve the predicted performance. Four designs were attempted. The first allowed only wing and tail camber and twist to be free. The second added freedom of the aft body to the list. The third added the freedom of the nacelle shape to the list. And the final added the tail cant angle to the list, encompassing all the degrees of freedom. The resulting configuration from each design was also analyzed at Mach 0.95, and the third design at various tail angles to explore the effect of CG. Contours of local Mach number are shown in Figure 2.3.2.1 for the baseline before design and after the fourth design, the one with all degrees of freedom. With very little observable difference in local Mach distribution, an 11 count reduction in drag was achieved, bringing the designed case much closer to the predicted drag from Linear Theory.

The last three rows of Table 2.3.2.1 show the effect of CG on pressure drag, according to Tranair, on the third configuration designed by Tranair. Moving the CG aft costs drag for a trimmed airplane, opposite to conventional wisdom for ordinary subsonic airplanes, and perhaps adverse for minimizing boom. Carrying lift aft is typically good for boom, but apparently that comes at a price in drag.

To do an integrated performance analysis of the -076E, we needed a new species MDAO model. This model had more limited parametric capability than the -072B in order to keep the shaped boom signature characteristics. Specifically, the external shape of the vehicle was not allowed to scale. A non-parametric GEODUCK geometry model of the -076E was integrated into the same MDAO framework as the -076E model. The aero characteristics of the -076E were calculated with the same codes as the -072B. The only difference being that, since the geometry of the 076E was fixed, the fuselage volume distribution optimization to minimize wave drag was not done.

A point-of-departure engine cycle was needed for the NPSS non-proprietary engine cycle optimization (Section 3), and a proprietary BSE 04B cycle with a reference thrust of 33,000 lbs was used. This engine had a fan diameter of 66 inches. To meet the boom signature requirements, the TOGW was required to be 180,000 lbs or less. This meant that if the fuel required to meet a 4000 nm range caused the TOGW to exceed 180,000 lbs, then the range must be reduced until the TOGW was equal to 180,000 lbs. The initial performance runs showed that the thrust would have to be increased to 43,000 lbs to make it through the transonic pinch point. This level of thrust equates to a fan diameter of 75.4 inches with this BSE 04B engine cycle. Even with this extra thrust, the aircraft could not get through the pinch point with a 180,000 lb TOGW. So the fuel was removed until the aircraft achieved 300 fpm rate of climb capability at the transonic pinch point. This resulted in a TOGW of 171,800 lbs and a range of 3200 nm. The fan diameter of 75.4 inches was set as the point of departure for the non-proprietary engine cycle optimization in Section 3. Figure 2.3.2.2 shows a drawing of this configuration, and Figure 2.3.2.3 is the performance summary. The 765-076E is described in more detail in Section 4.

2.3.3 Boom Reduction.

With boom reduction a goal for the 30 passenger airplane, it was necessary to explore the potential. With that in mind, the 765-076F and G were configured with the same wing planform and engines but with significantly longer noses than the E. Cabin volume and overall volume were held nearly constant in an attempt to preserve the payload. The 765-076F configuration is shown in Figure 2.3.3.1, and the loft

compared to the 765-076E in shown in Figure 2.3.3.2. In addition to 20ft more of overall body length, nearly all of which was added to the nose, two streamlined volumes were added to the tips of the vertical. Their purpose is both as a housing and fairing for ballast for stabilizing the fin, and as an unproven technology for tailoring the boom. They have potential of either favorable wave cancellation, or of effectively lengthening the body by means of their height projected along the standard, forward leaning Mach cut for assessing boom. Perhaps the latter effect could only be favorable if the volume of the pods is offset by volume saved in the fins, themselves, but that is a possibility if the stabilizing effect of the pods were sufficient.

Figure 2.3.3.3 shows results from MDboom and Zephyrus at Mach 1.8 at 49,000ft and the same 162,000lb weight used to assess the 765-076E. 85 PLdB (the result from Zephyrus) might be achievable with the 765-076F. That is better than the 765-076E at 91 PLdB, but the advantage in boom comes with a penalty of 10% in both increased fuel burn and lost range. It also comes with additional APSE risk from the long, slender nose, and the additional overall weight cannot be accurately predicted without a more sophisticated and careful look at the loads and structural sizing. That weight would increase the penalty on efficiency and range, and decrease the benefit to boom.

Since adding 20ft was good for boom, adding more could be even better. The 765-076G was given an even longer nose in an attempt to find what length would be required to reach 70 PLdB. The result was an additional 30ft, to an overall length of over 200ft, or more than 30% longer than the 765-076E. Of course, all the disadvantages seen in the 765-076F are exaggerated, with about 14% higher fuel burn and less range than the 765-076E, and much greater risk of APSE issues; and all before assessing the impact of the certain increase in weight.

While the particular cases of the 765-076F and G might be too few to conclude that boom and drag would trade against one another, that conclusion can be drawn from the data in Figure 2.3.3.4. It shows results from a 2-dimensional Pareto optimization to minimize boom PLdB and maximize L/D, starting from the 765-076E. The body design variables are used, and cabin volume and overall body volume are constrained to be at least as much as the baseline. The results show that the 765-076E is near the Pareto frontier, and that, indeed, boom and drag will trade against one another on the frontier. While these results indicate some slack in the baseline, it is probably close enough to the frontier to justify leaving Linear Theory design for higher fidelity methods.

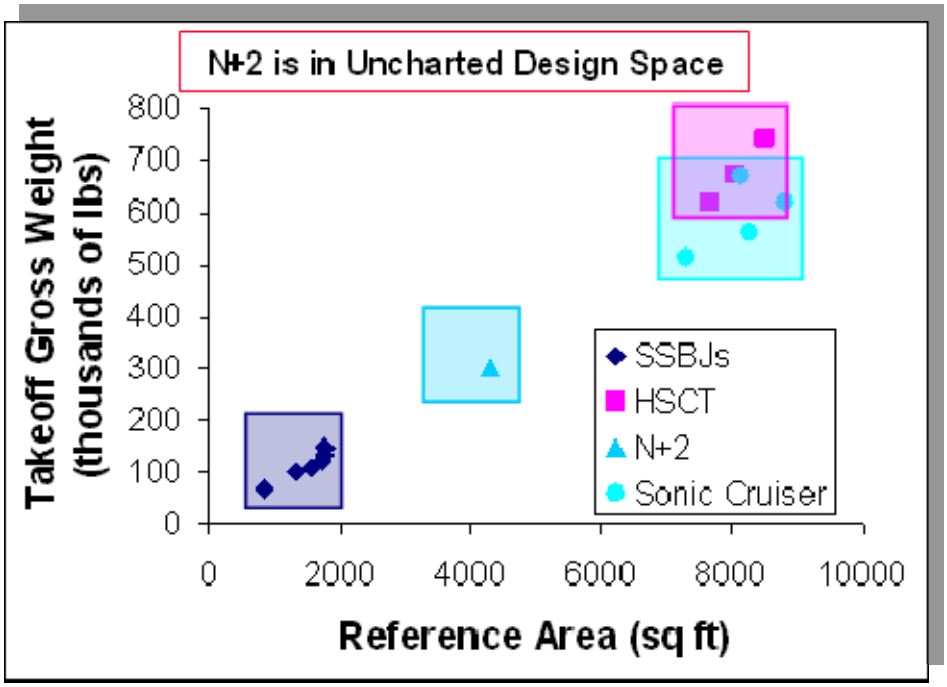

Figure 2.0.1 Size and weight of 100 passenger N+2 studies compared to other supersonic airplane studies.

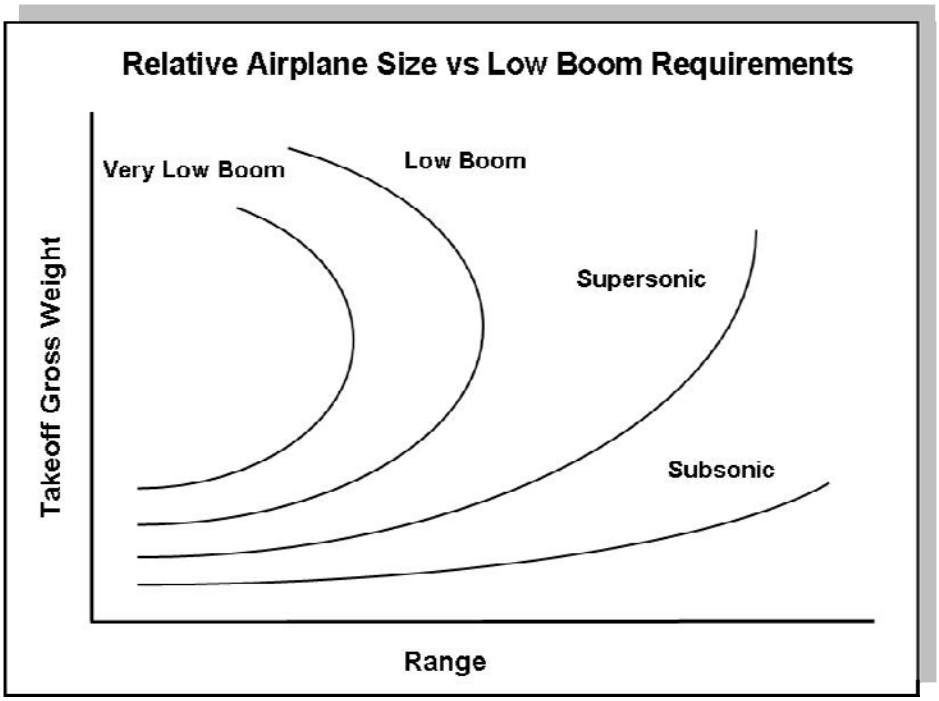

Figure 2.0.2. Notional TOGW required to meet range versus range for various different boom levels.

a. 76% 2015 OML

b. 765-070A OML

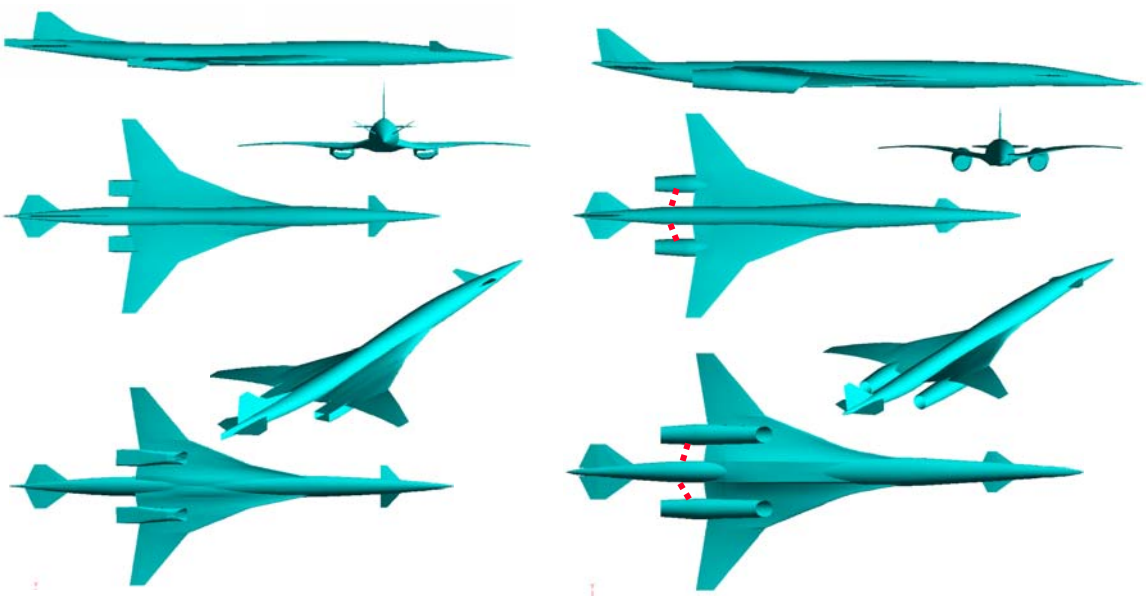

Figure 2.1.1 a. 76% scale "2015-TC". b. 765-070A external definition.

a. 76% 2154 OML

b. 765-071B OML

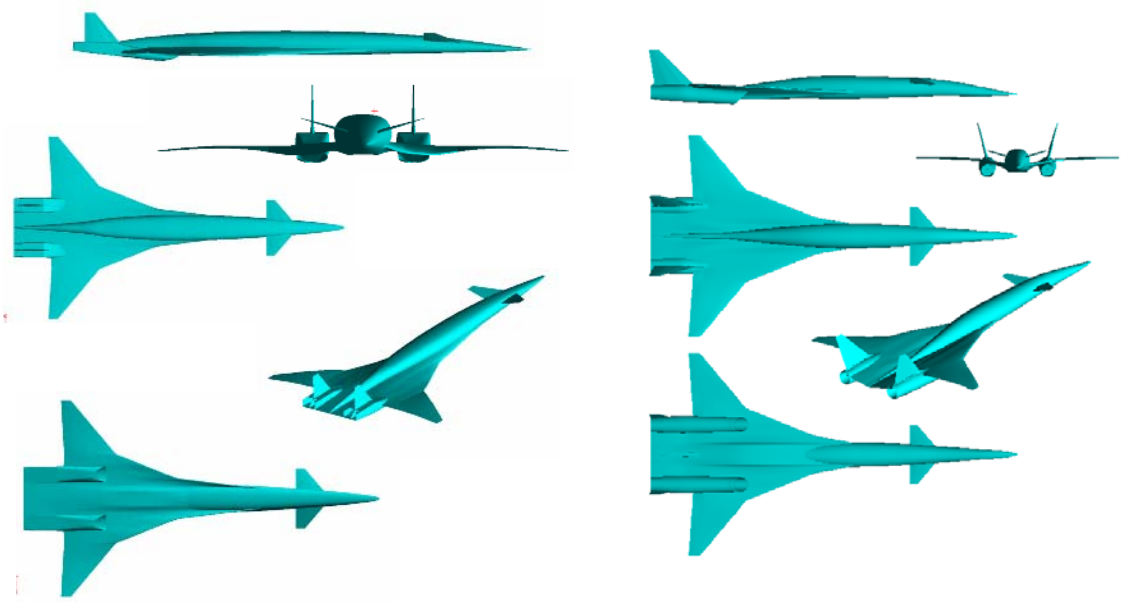

Figure 2.1.2 a. 76% "2154 HISCAT". b. 765-071B external definition.

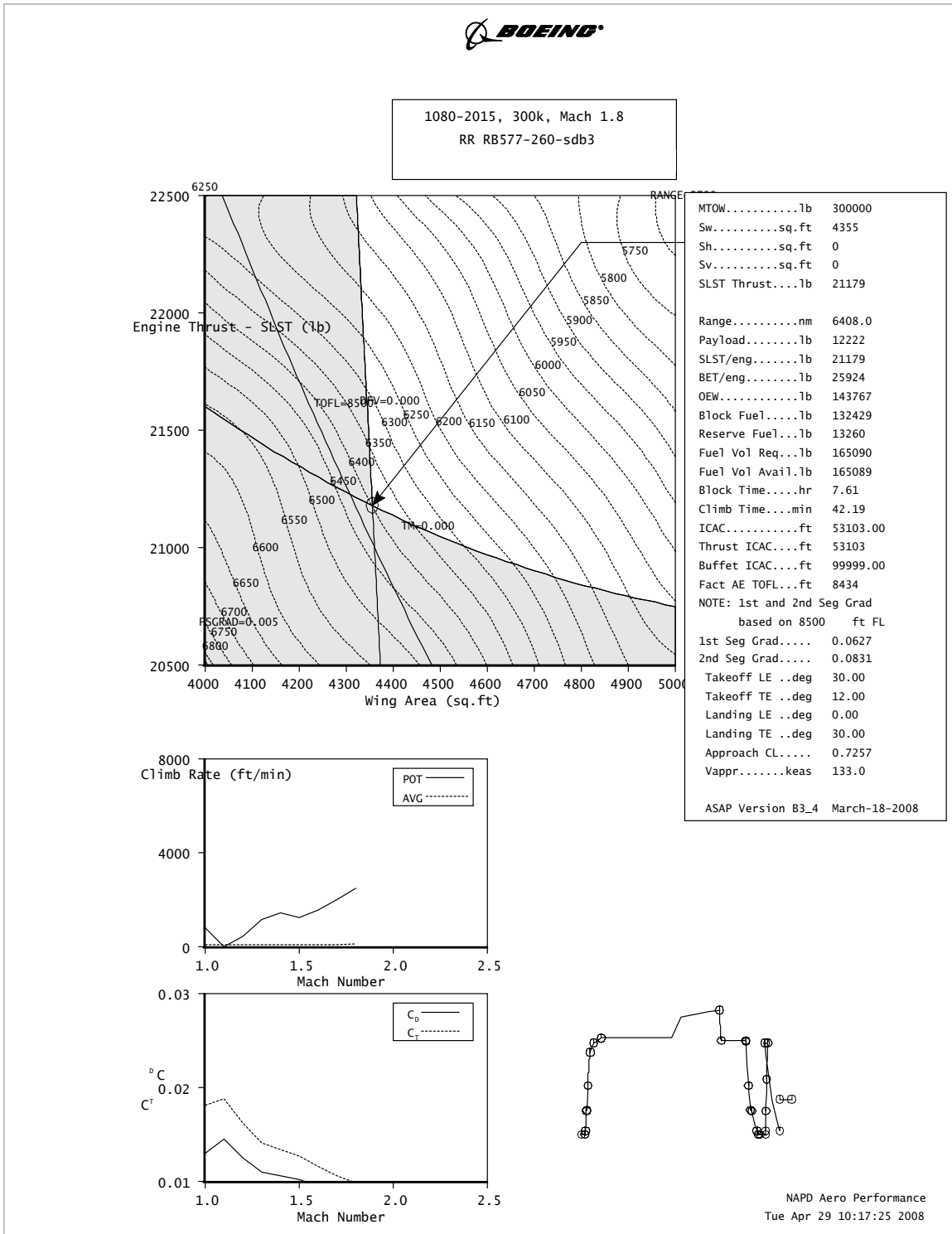

Figure 2.1.3 Level 0 sizing of 2015-TC.

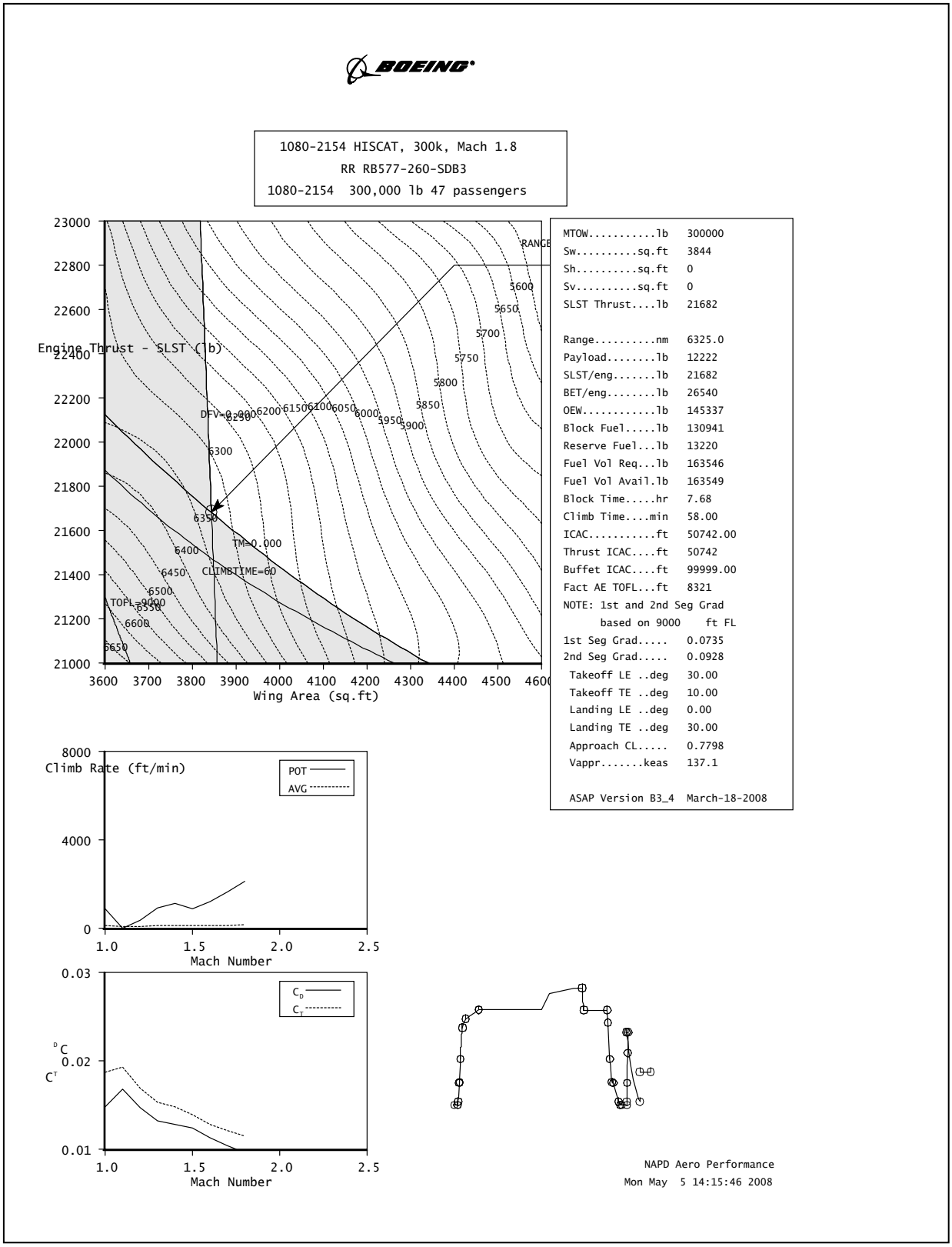

Figure 2.1.4 Level 0 sizing for 2154 HISCAT.

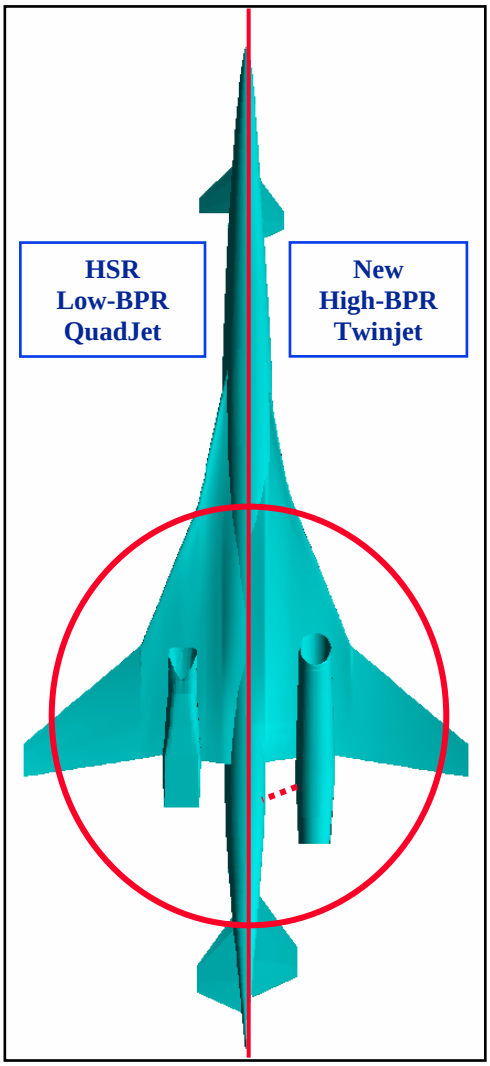

Figure 2.1.5 Engine integration differences between HSR/HSCT quad and 765-070A. Some aft deck area (dashed red line) is probably required for both strength and stiffness of the structure supporting the engine.

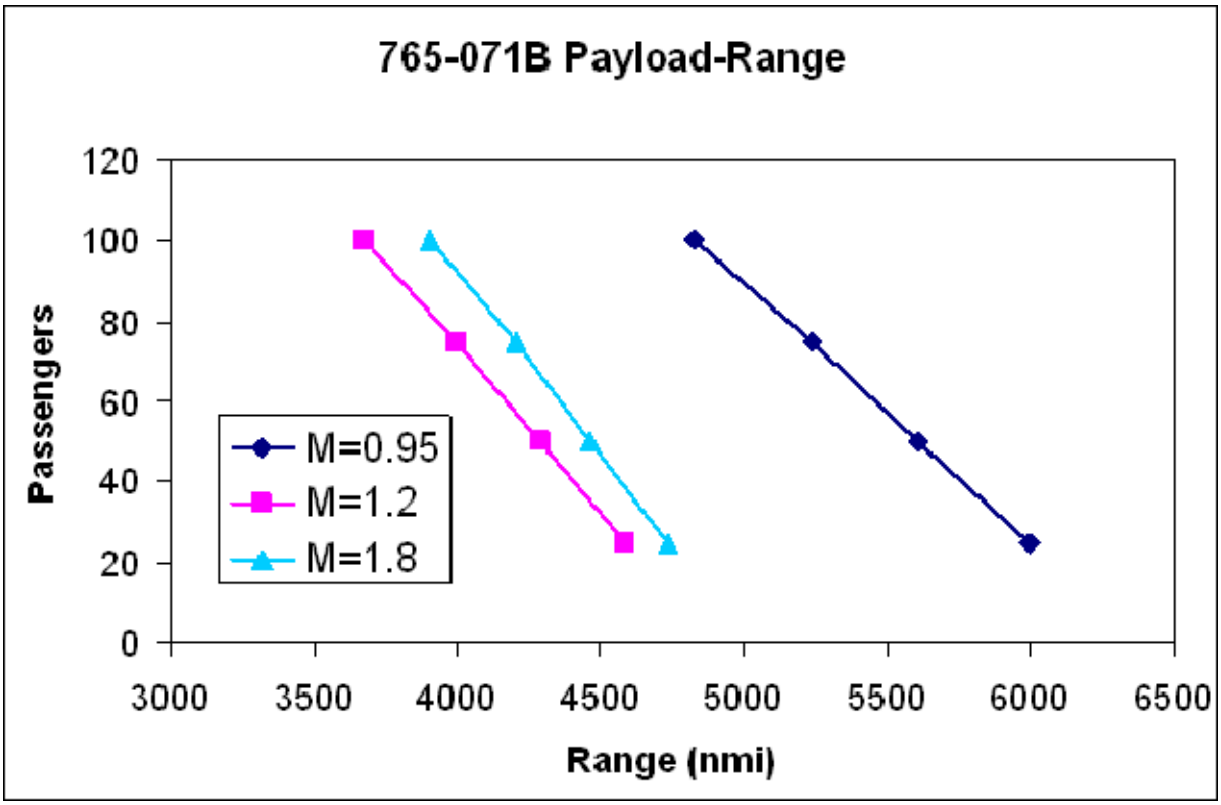

Figure 2.1.6 Maximum range of the 765-071B for various cruise Mach and passengers. Thrust and wing area sized at constant design weight of 300,000lb.

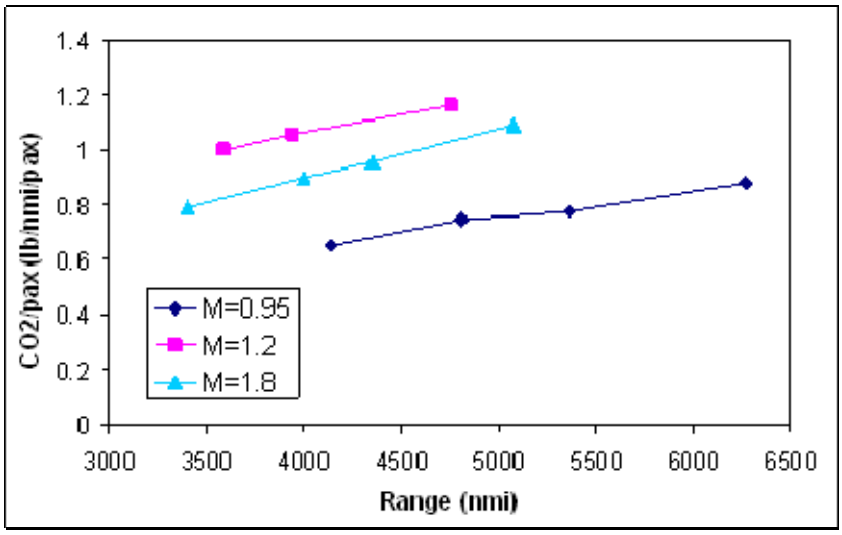

a)

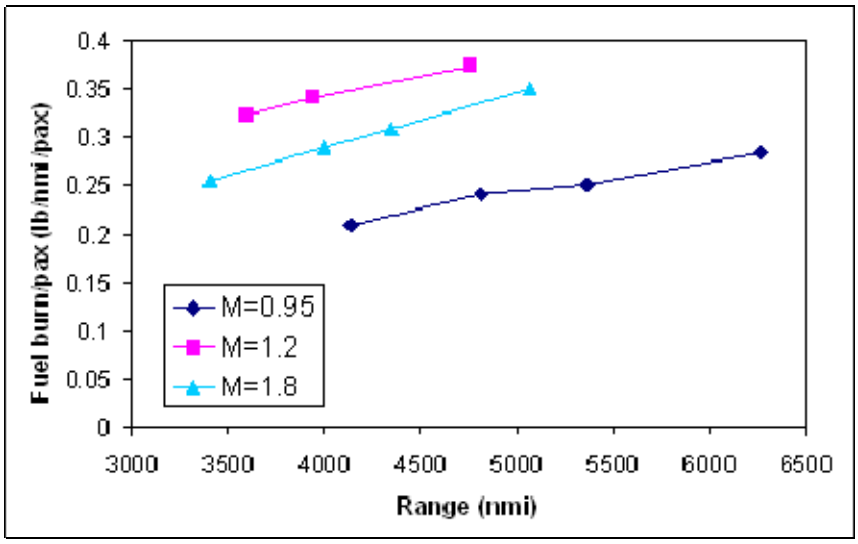

b)

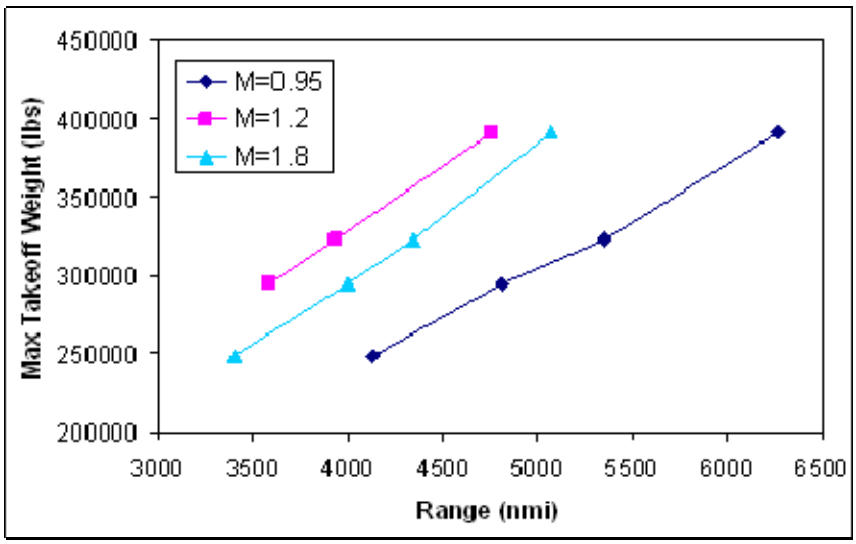

c)

Figure 2.1.7. a. CO_2, b. fuel burn, and c. MTOW for the 765-071 sized for particular range using wing area, thrust, and MTOW, for and 100 passenger payload.

Table 2.1.8 Characteristics data of 765-070A

model 765-070A	DATA TABLE (as drawn airplane)				
	Wing		Horizontal	Canard	Vertical
ITEM	ESDU	Total	Tail		Tail
Area to CL	4035.392	4403.4	323.92	110.90	208.32
Exposed			323.92	110.90	189.04
Reference	4035.392		323.92	110.90	189.04
Aspect Ratio	2.99	3.43	1.199	1.20	2.122
Taper Ratio	0.121812	-	0.283	1.199	0.235
LE Sweep angle		0.00	54.2	54.2	52.61
Dihedral, TE	12	55	0	0	0
T/C	0.024	0.024	0.035		0.000
Tail Volume		0.203	0.138	0.065	0.0891
Span , in	1317.84	903.808	236.49	138.37	169.93
Root Chord, In	786.1323	788.66	307.47	179.90	260.24
Tip Chord, in	95.76	56.000	87.01	50.91	61.23
M.A.C. IN	531.0202	746.643	217.77	127.42	181.27
X 1/4 mac	1713.044	1557.946	2629.15	463.05	2722.82
Y, Zmac	243.4895		80.108981	69.596	99.43
Tail Arm, IN.			916.10	1250.00	1009.7726

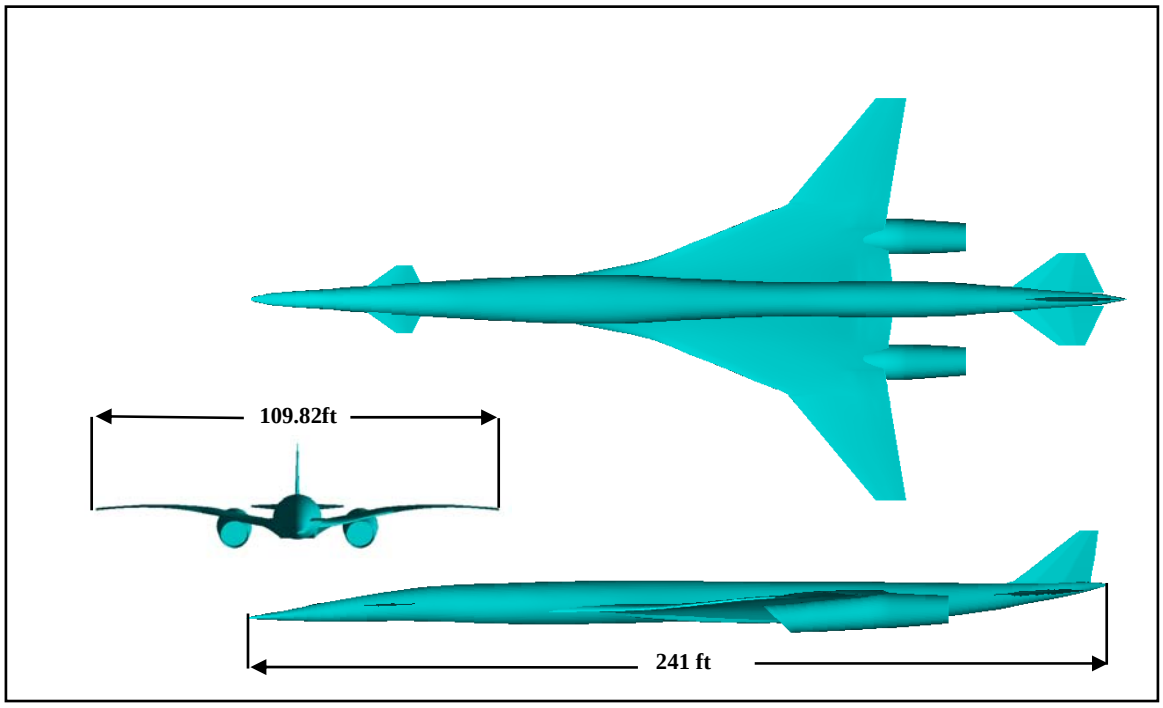

Figure 2.1.8 General arrangement of 765-070A.

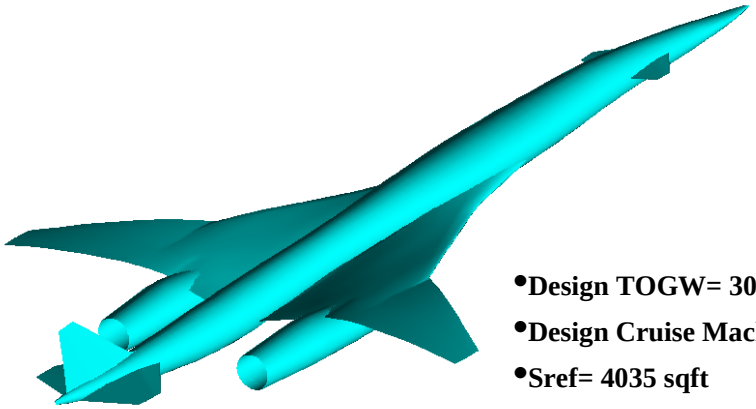

- **Design TOGW= 300,000 lbs**
- **Design Cruise Mach=1.8**
- **Sref= 4035 sqft**
- **Design Range (100-118 pass.)=4000 nmi**
- **Cruise L/D=8.59**
- **60K lb thrust class “BSE2” engine**
- **Fan diam. =84”**
- **HSCT-like LE, TE devices**
- **3-surface pitch control /trim/ ride qual.**
- **Fuel burn 0.288 lb/seat nmi @ 100 pass.**
  0.244 lb/seat nmi @ 118 pass.
  (=4 seat nmi /lb)

Figure 2.1.9 Features of 765-070A.

Table 2.1.10 Weights summary of 765-070A.

		Point Design 272,727 lb		Growth 300,000 lb	
FC	Description	Weight	CG	Weight	CG
01	Wing Structure	34210	1406	34660	1406
02	Horizontal Tail Struture	1840	2055	1880	2055
03	Vertical Tail Structure	1100	2756	1120	2756
04	Fuselage Structure	17280	1466	17500	1466
05	Main Landing Gear	7870	1705	8250	1705
07	Nose Landing Gear	870	679	940	679
08	Forebody Controls	650	2664	650	2664
	Structure Total	**63820**	**1504**	**65000**	**1504**
09	Inlet Structure and Systems	6020	1947	6020	1947
10	Cowling	2120	2104	2120	2104
11	Pylon/Strut	3260	2097	3260	2097
12	Engine	30920	2080	30920	2080
13	Nozzle	1620	2252	1620	2252
14	Installation (incl. fairings)	2200	2097	2200	2097
15	Engine Accessories, Controls, & Start System	200	2119	200	2119
	Propulsion Pod Total	**46340**	**2072**	**46340**	**2072**
23	Fuel System	4790	1755	4790	1755
24	APU/EPU	290	1025	290	1025
27	Instruments	1260	615	1260	615
28	Surface Controls	4440	2039	4500	2039
29	Hydraulic Power System	2250	1901	2250	1901
30	Pneumatic System	0	0	0	0
32	Electrical System	2520	1490	2520	1490
33	Electronics	880	1180	880	1180
34	Flight Provisions	760	350	760	350
35	Passenger Accomodations	12710	1471	12710	1471
37	Cargo Compartment	130	2313	130	2313
38	Emergency Equipment	600	1442	600	1442
39	Environmental Control Systems	1710	1871	1710	1871
40	Ice Protection	310	1585	310	1585
49	Exterior Markings	610	1715	610	1715
50	Load and Handling	0	0	0	0
55	Customer Options	0	0	0	0
	Systems & Fixed Equipment Total	**33260**	**1577**	**33320**	**1578**
	Manufacturer's Empty Weight (MEW)	**143420**	**1704**	**144660**	**1703**
97	Standard and Operational Items	5440	1492	5440	1492
	Operational Empty Weight (OEW)	**148860**	**1697**	**150100**	**1695**

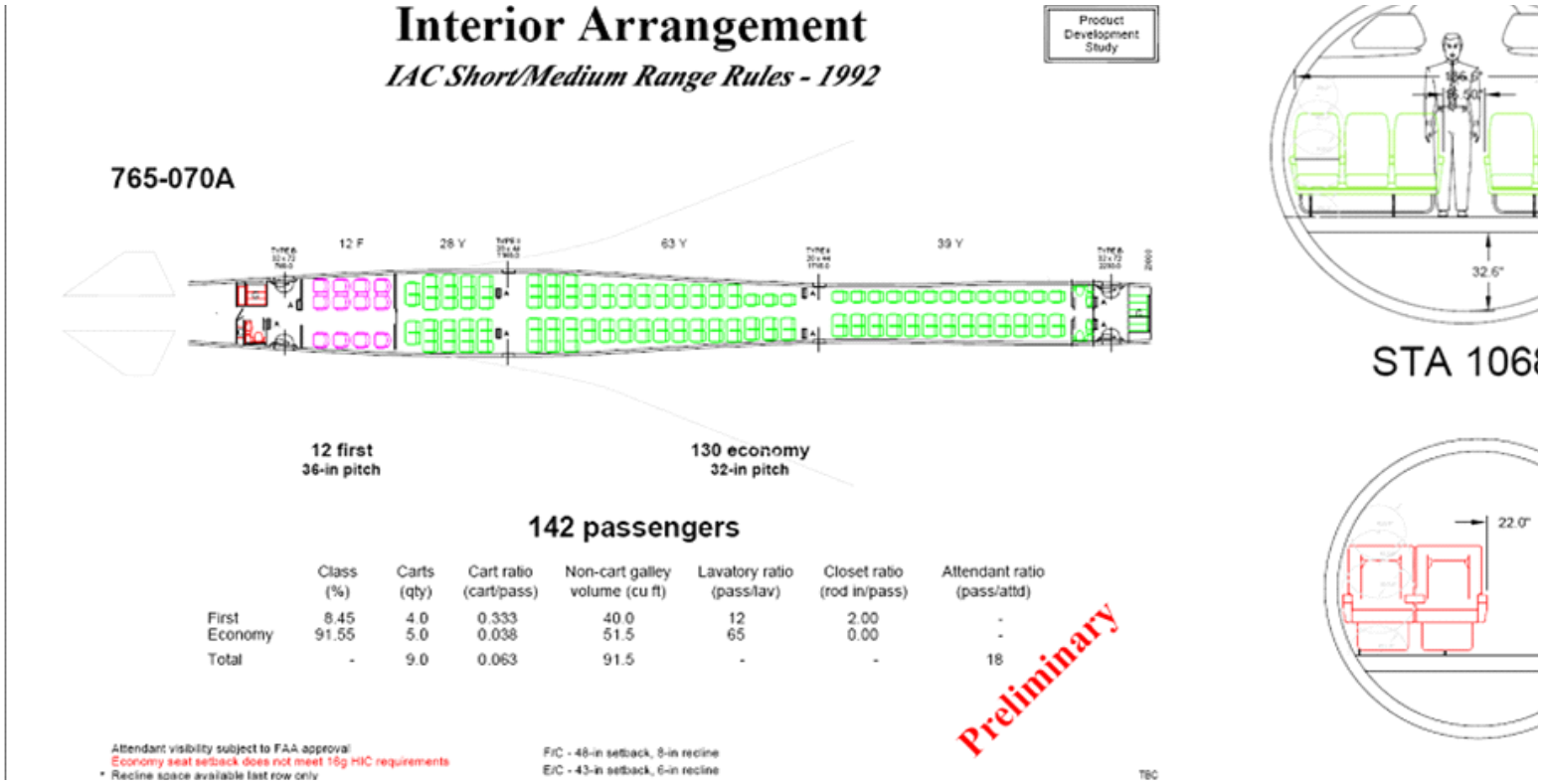

Figure 2.1.11 Interior arrangement of 765-070A.

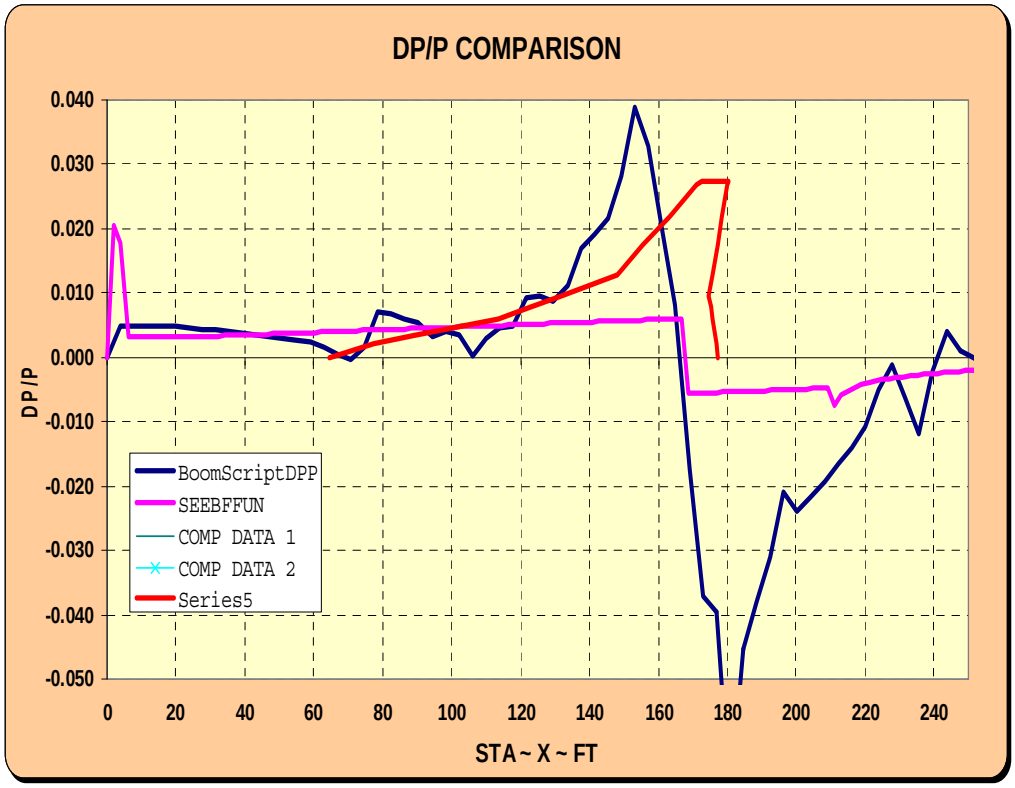
DP/P COMPARISON
0.040
0.030
0.020
0.010
0.000
-0.010
-0.020
-0.030
-0.040
-0.050
DP/P
BoomScriptDPP
SEEBFFUN
COMP DATA 1
COMP DATA 2
Series5
0
20
40
60
80
100
120
140
160
180
200
220
240
STA ~ X ~ FT

a)

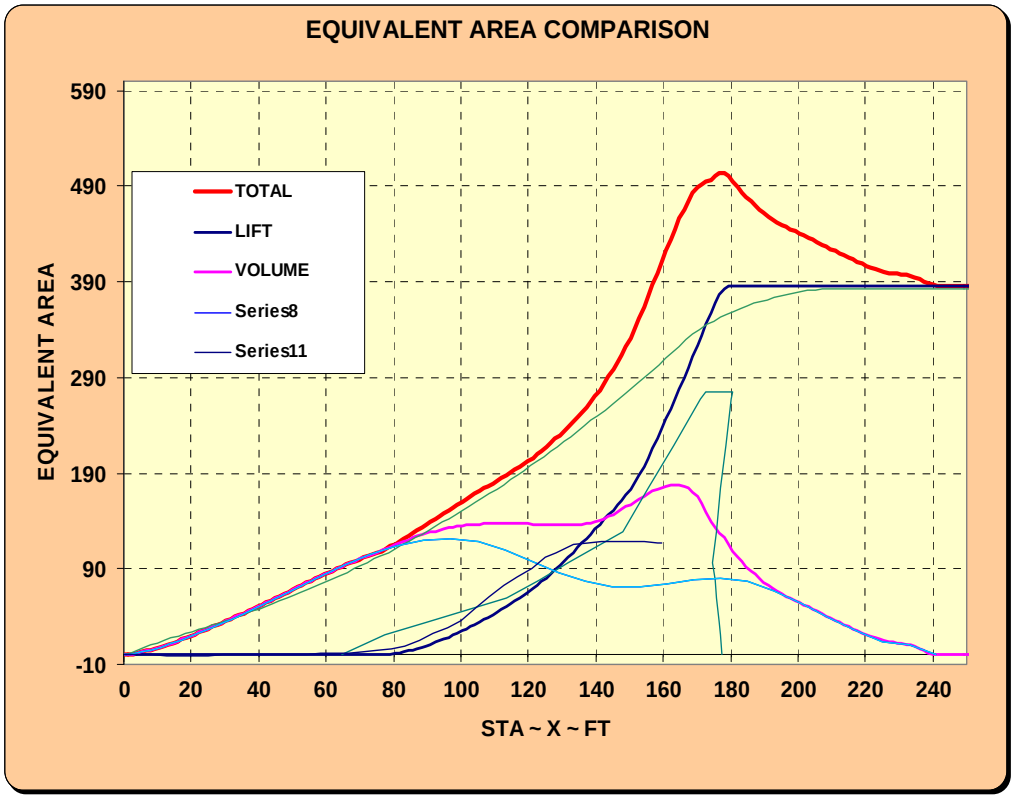
EQUIVALENT AREA COMPARISON
590
490
390
290
190
90
-10
EQUIVALENT AREA
TOTAL
LIFT
VOLUME
Series8
Series11
0
20
40
60
80
100
120
140
160
180
200
220
240
STA ~ X ~ FT

b)

c)

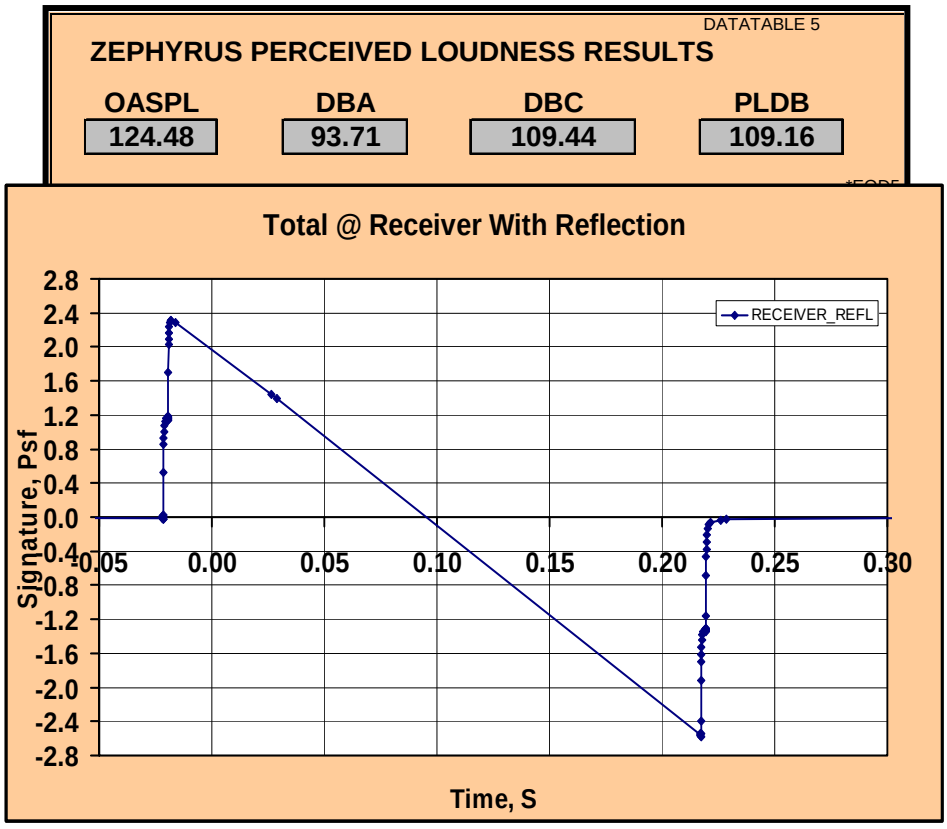

Figure 2.1.12 Boom summary of 765-070A, M1.6, 270,000lbs, 51,000ft, ~2.4 psf boom. a) Δp/p at 10 body lengths, b) equivalent area distribution, c) ground pressure signature and PLdB from Zephyrus.

Table 2.1.13 Characteristics data of 765-071B

model 765-071B	DATA TABLE (as drawn airplane)				
	Wing		Horizontal	Canard	Vertical
ITEM	ESDU	Total	Tail		Tail
Area to CL	4284.177	4699.1	254.40	136.98	664.42
Exposed			254.40	136.98	559.18
Reference	4284.177		254.40	136.98	559.18
Aspect Ratio	3.09	3.43	3.15	3.15	1.431
Taper Ratio	0.084754	-	0.25	3.150	0.229
LE Sweep angle		0.00	48	48	45.54
Dihedral, TE	12	62.928	0	0	14
T/C	0.024	0.024	0.000		0.000
Tail Volume		0.136	0.068	0.068	0.1316
Span , in	1381.753	903.808	339.70	249.27	240.01
Root Chord, In	823.1868	788.66	172.55	132.14	273.87
Tip Chord, in	69.768	56.000	43.14	26.13	62.73
M.A.C. IN	552.4253	761.020	120.78	90.97	190.38
X 1/4 mac	1809.845	1653.692	2446.45	640.50	2366.73
Y, Zmac	248.2853		330.44368	104.370	126.91
Tail Arm, IN.			636.61	1169.34	556.8896

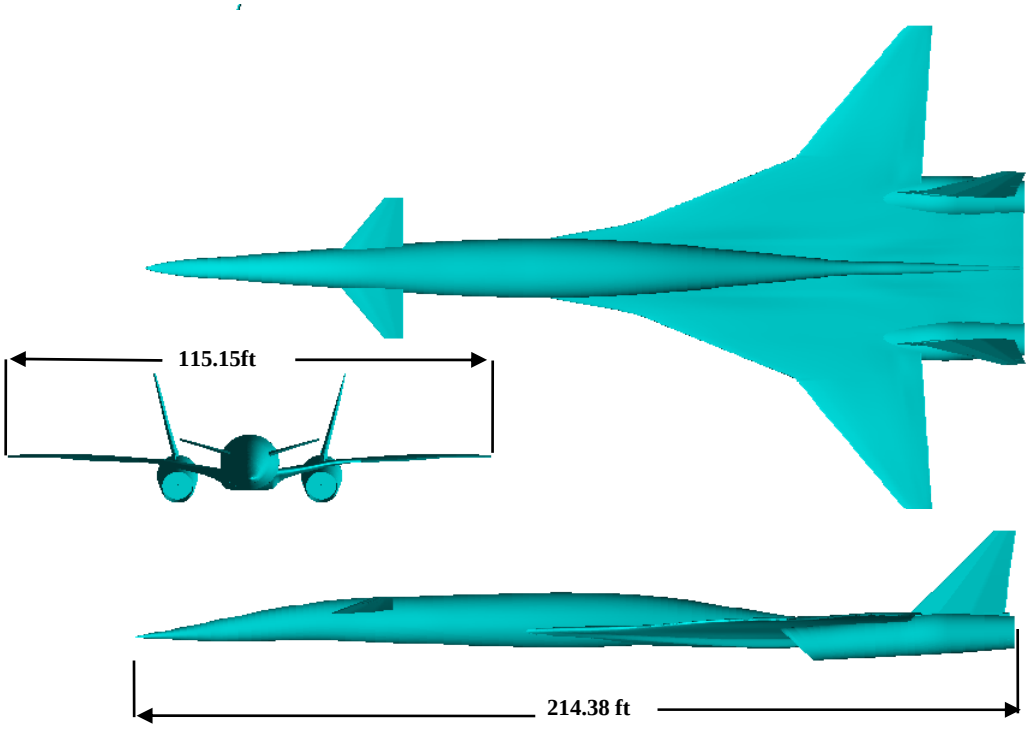

Figure 2.1.13 General arrangement of 765-071B.

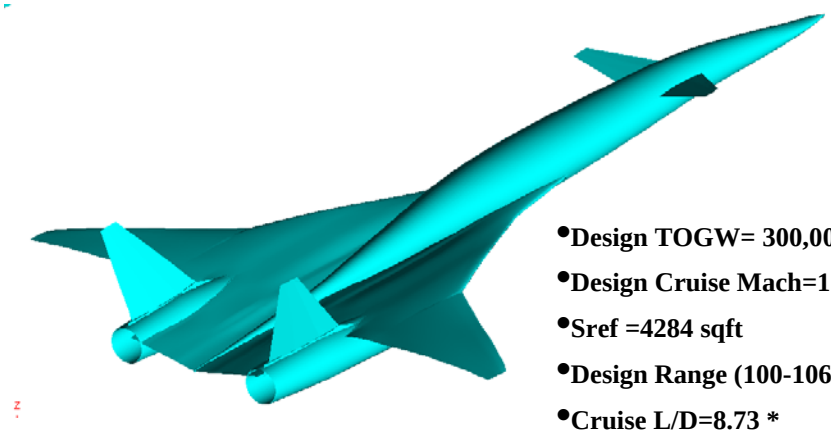

- **Design TOGW= 300,000 lbs**
- **Design Cruise Mach=1.8**
- **Sref =4284 sqft**
- **Design Range (100-106 pass.)= 4000 nmi**
- **Cruise L/D=8.73 ***
- **60K lb thrust class "BSE2" engine**
- **Fan diam. =84"**
- **HSCT-like LE, TE devices**
- **3-surface pitch control /trim/ ride qual.**
- **Fuel burn 0.28 lb/seat nmi @ 100 pass.**
  (= 3.6 seat nmi /lb)

***L/D=8.02 on -071A with lower-risk aft t/c**
but higher sized TOGW and boom level

Figure 2.1.14 Features of 765-071B.

Table 2.1.15 Weights summary of 765-071B.

		Point Design 272,727 lb		Growth 300,000 lb	
FC	Description	Weight	CG	Weight	CG
01	Wing Structure	37810	1590	38260	1590
02	Horizontal Tail Struture	1440	2416	1480	2416
03	Vertical Tail Structure	3240	2403	3260	2403
04	Fuselage Structure	14640	1328	14860	1328
05	Main Landing Gear	7870	1794	8250	1794
07	Nose Landing Gear	870	731	940	731
08	Forebody Controls	800	2457	800	2457
	Structure Total	**66670**	**1613**	**67850**	**1613**
09	Inlet Structure and Systems	6940	2083	6940	2083
10	Cowling	2120	2255	2120	2255
11	Pylon/Strut	3260	2248	3260	2248
12	Engine	30920	2231	30920	2231
13	Nozzle	1620	2403	1620	2403
14	Installation (incl. fairings)	2200	2248	2200	2248
15	Engine Accessories, Controls, & Start System	200	2270	200	2270
	Propulsion Pod Total	**47260**	**2218**	**47260**	**2218**
23	Fuel System	4650	1853	4650	1853
24	APU/EPU	290	1025	290	1025
27	Instruments	1260	540	1260	540
28	Surface Controls	3560	1798	3620	1798
29	Hydraulic Power System	2280	1992	2280	1992
30	Pneumatic System	0	0	0	0
32	Electrical System	2450	1380	2450	1380
33	Electronics	880	1115	880	1115
34	Flight Provisions	760	350	760	350
35	Passenger Accomodations	11140	1276	11140	1276
37	Cargo Compartment	130	1917	130	1917
38	Emergency Equipment	600	1249	600	1249
39	Environmental Control Systems	1680	1595	1680	1595
40	Ice Protection	310	1708	310	1708
49	Exterior Markings	590	1517	590	1517
50	Load and Handling	0	0	0	0
55	Customer Options	0	0	0	0
	Systems & Fixed Equipment Total	**30580**	**1455**	**30640**	**1455**
	Manufacturer's Empty Weight (MEW)	**144510**	**1778**	**145750**	**1776**
97	Standard and Operational Items	5440	1332	5440	1332
	Operational Empty Weight (OEW)	**149950**	**1761**	**151190**	**1760**

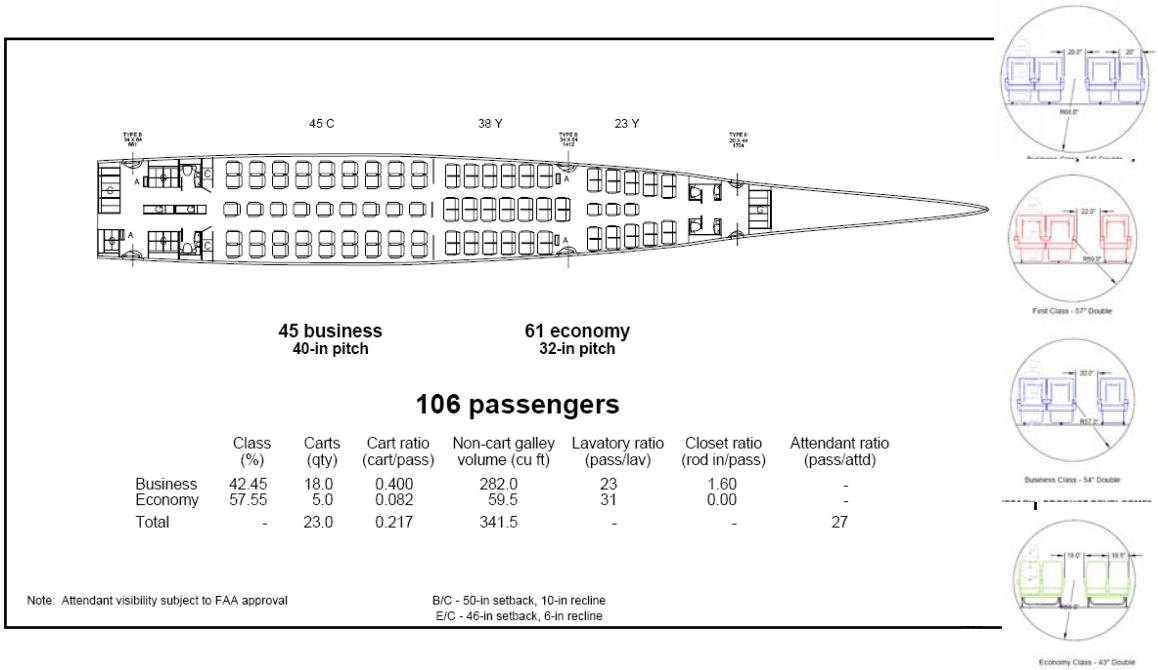

Figure 2.1.16 Interior arrangement of 765-071B.

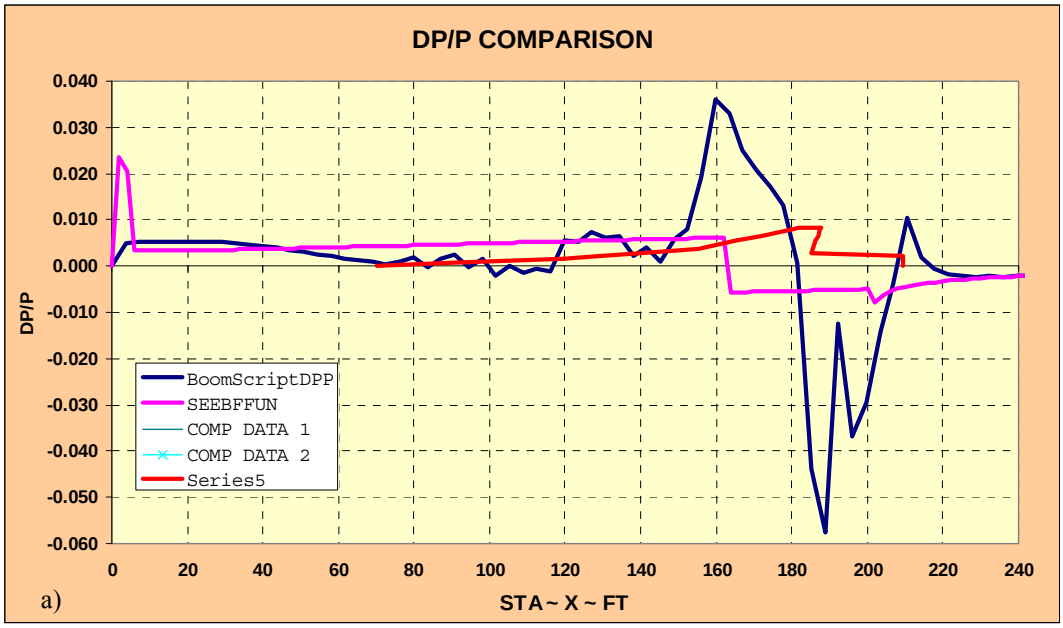
DP/P COMPARISON
0.040
0.030
0.020
0.010
0.000
-0.010
-0.020
-0.030
-0.040
-0.050
-0.060
DP/P
BoomScriptDPP
SEEBFFUN
COMP DATA 1
COMP DATA 2
Series5
0
20
40
60
80
100
120
140
160
180
200
220
240
STA ~ X ~ FT

a)

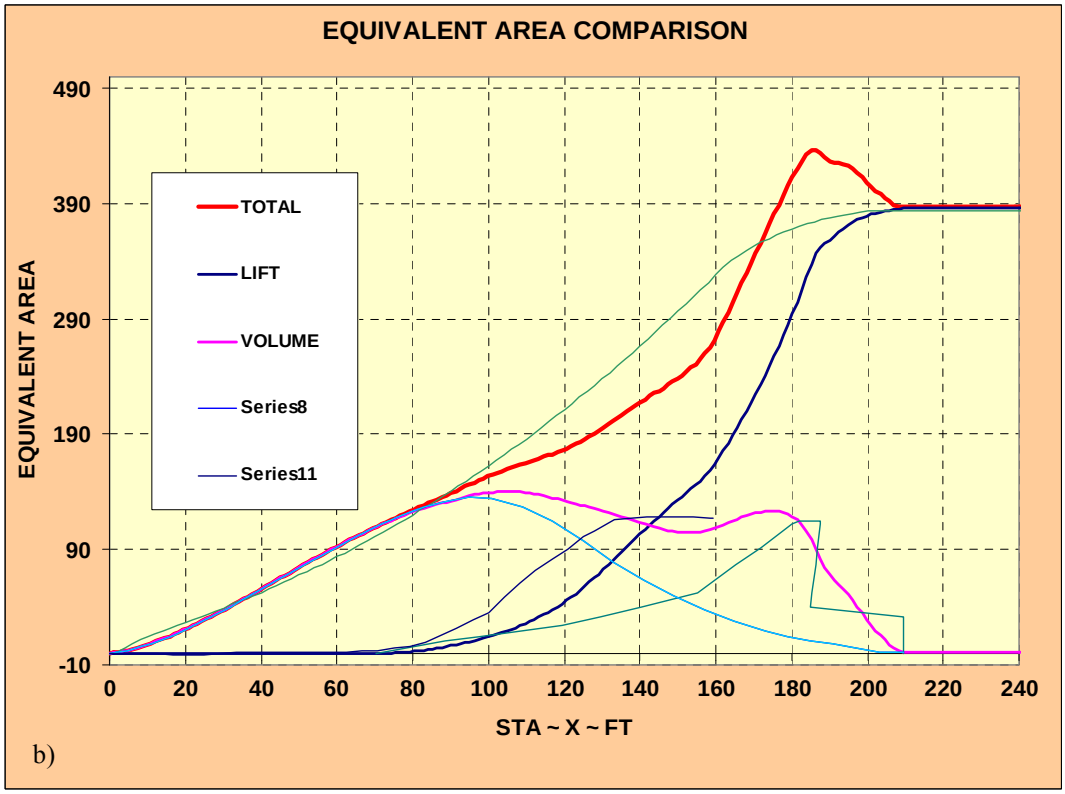
EQUIVALENT AREA COMPARISON
490
390
290
190
90
-10
EQUIVALENT AREA
TOTAL
LIFT
VOLUME
Series8
Series11
0
20
40
60
80
100
120
140
160
180
200
220
240
STA ~ X ~ FT

b)

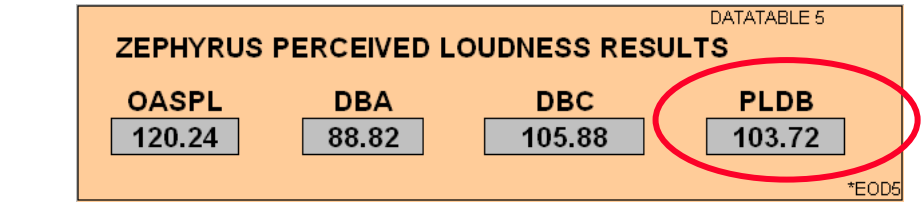

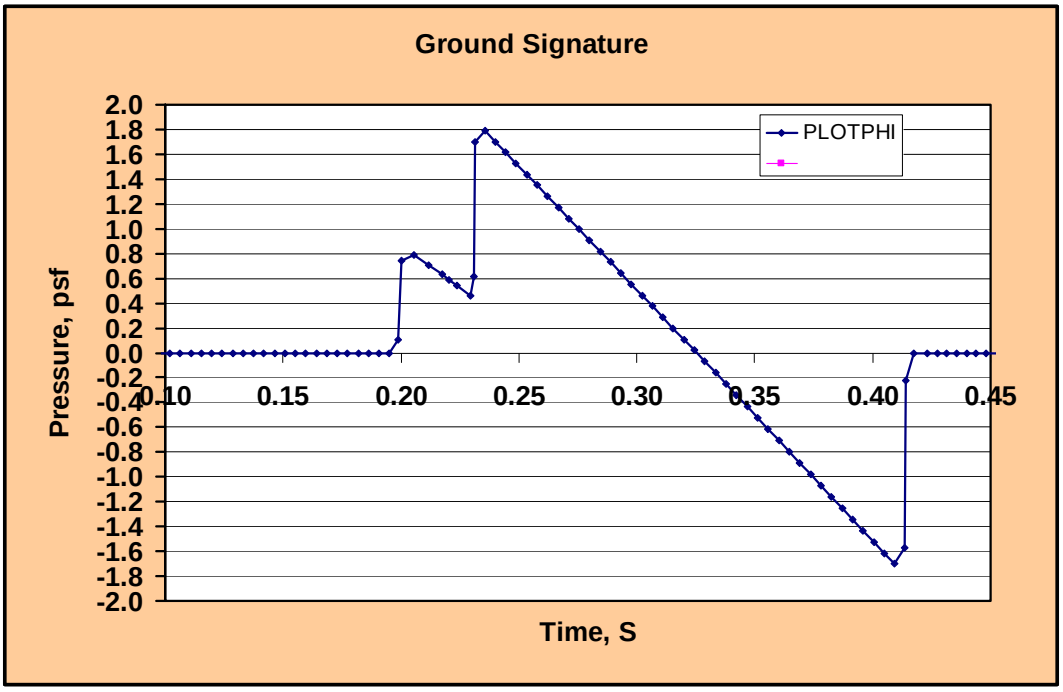

c)

Figure 2.1.17 Boom assessment of 765-071B at initial cruise M=1.6, 270,000lbs, 51,000 ft, ~1.7 psf boom. a) Δp/p at 10 body lengths, b) equivalent area distribution, c) ground signature and PLdB from Zephyrus.

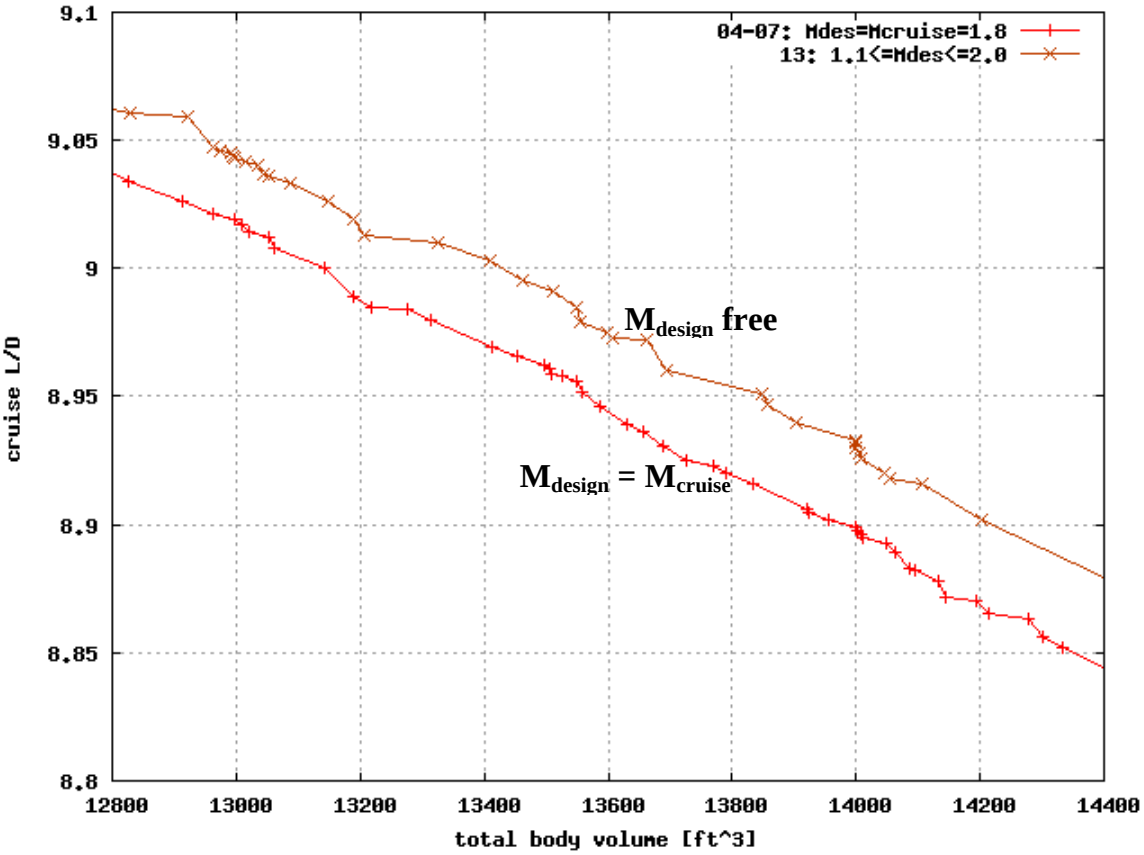

Figure 2.2.1.1 Pareto optima with the Mach number for T080 area-ruling (M_design) either fixed (red) or variable (brown). Optimization maximized cruise L/D and total body volume as objectives.

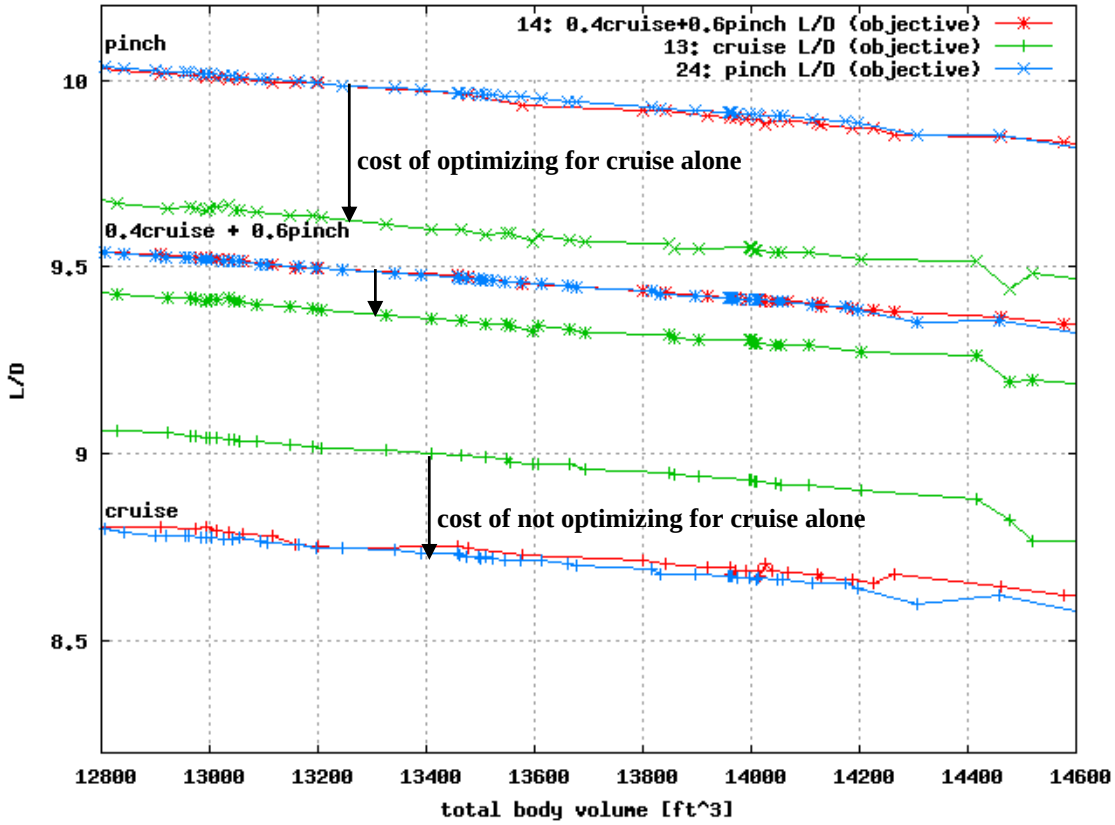

Figure 2.2.1.2. Pareto optima maximizing L/D and body volume. L/D alternatively at cruise (green), at the thrust pinch Mach 1.1 (blue), and a weighted sum (red) of cruise and pinch. It is important to consider the L/D at thrust pinch, and doing so will affect the L/D at cruise.

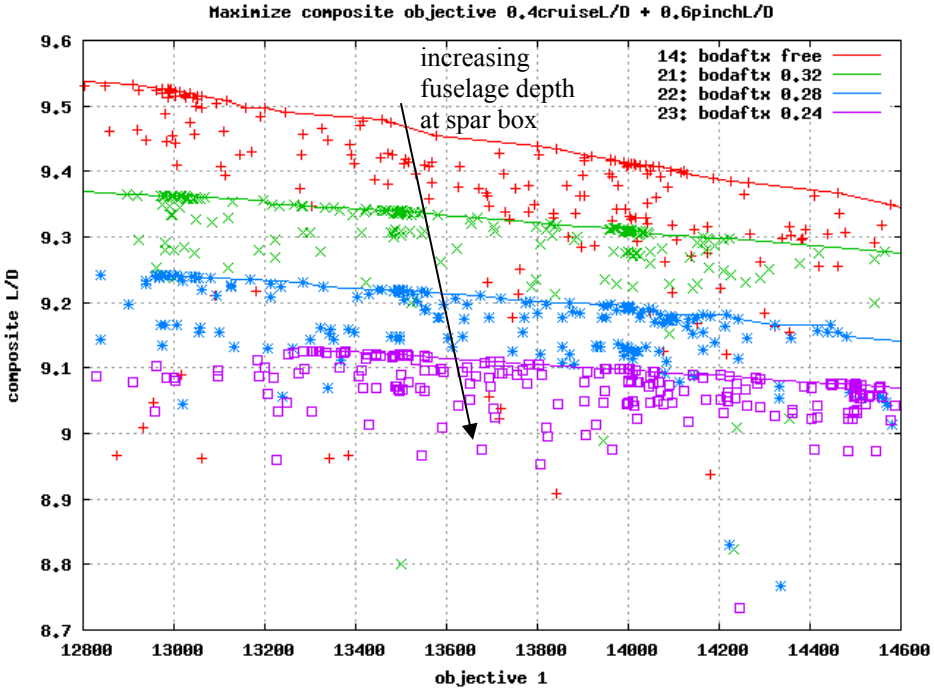

Figure 2.2.1.3. Pareto optima maximizing L/D and body volume for various depth of aft body at the wing box. Adding depth reduced L/D.

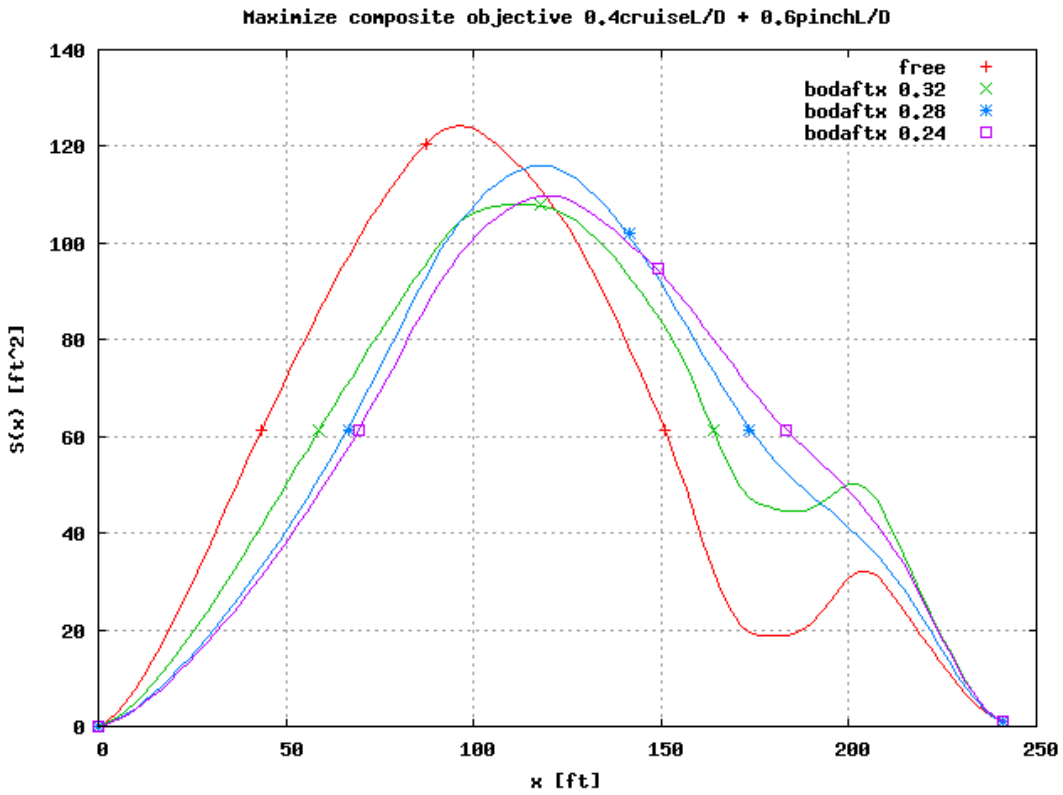

Figure 2.2.1.4 Body area distributions from increasing fuselage depth at the rear spar, for maximum L/D at fixed volume.

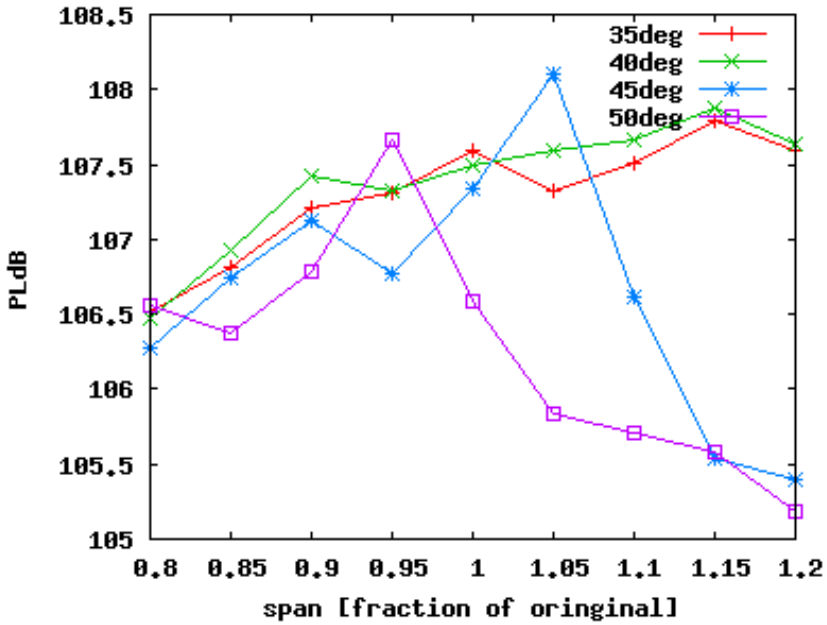

Figure 2.2.1.5 Effect of outboard wing span and sweep on boom PLdB. Only the outboard panel varied, but the span fraction represents the ratio of overall span to original overall span.

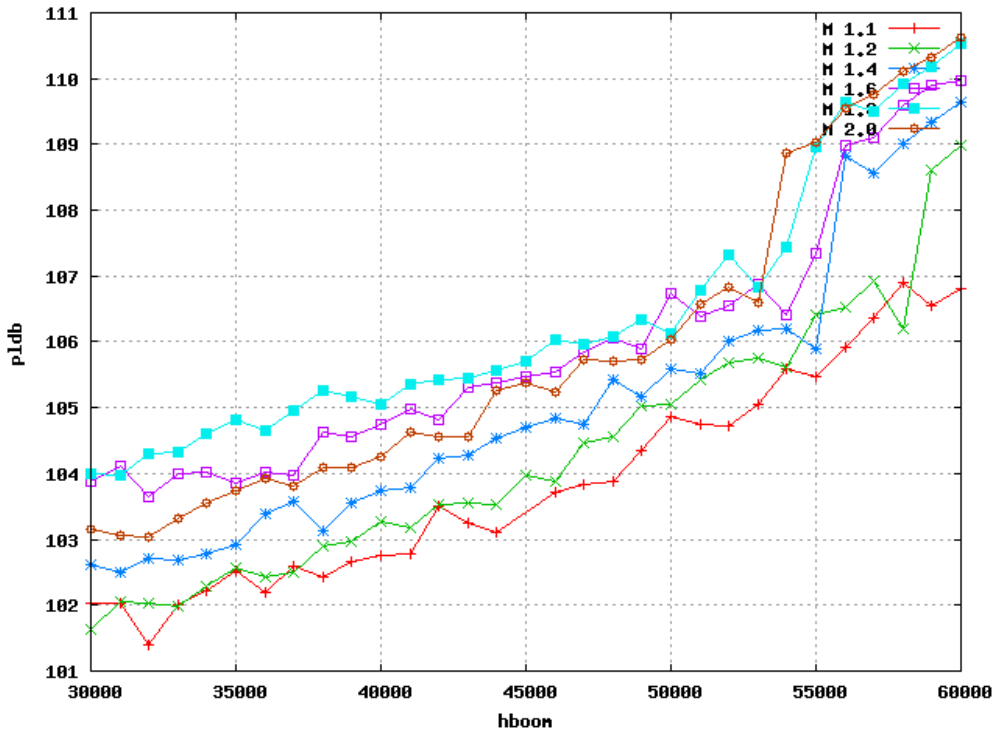

Figure 2.2.1.6 Effect of varying cruise altitude (ft) on boom PLdB for various Mach. Mach 1.8 is maximum. Jump near 55,000ft corresponds to coalescence of double shock.

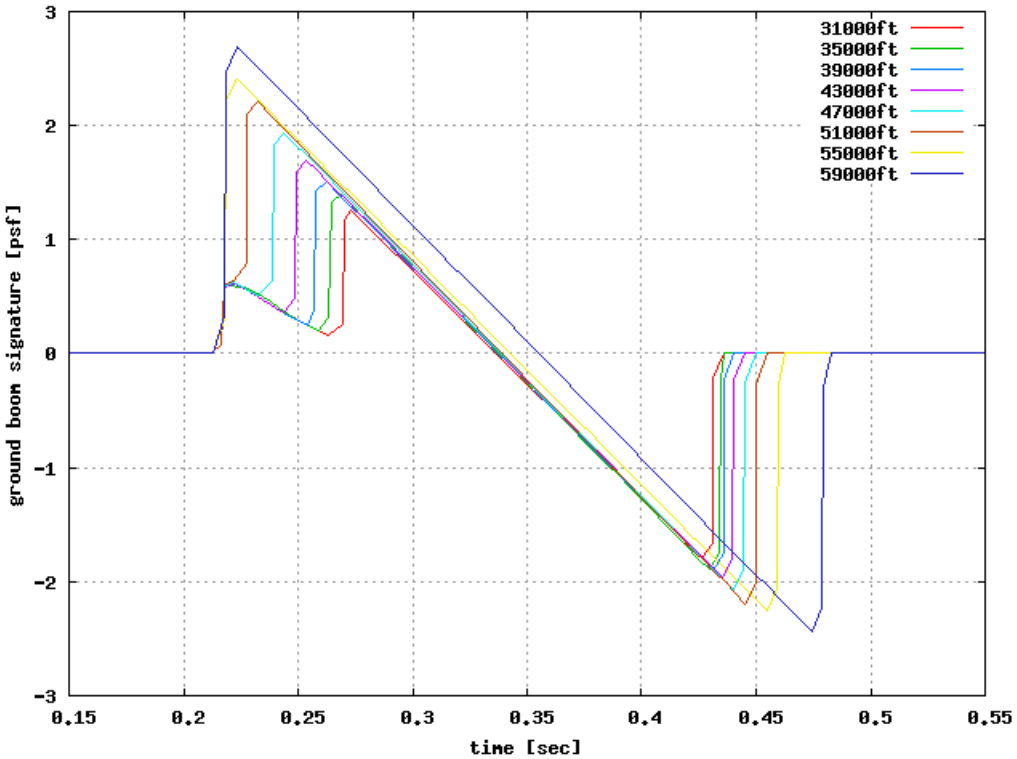

Figure 2.2.1.7 Effect of varying altitude on boom signature for Mach 1.8. Favorable double shock at the front coalesces and is lost for higher cruise altitude.

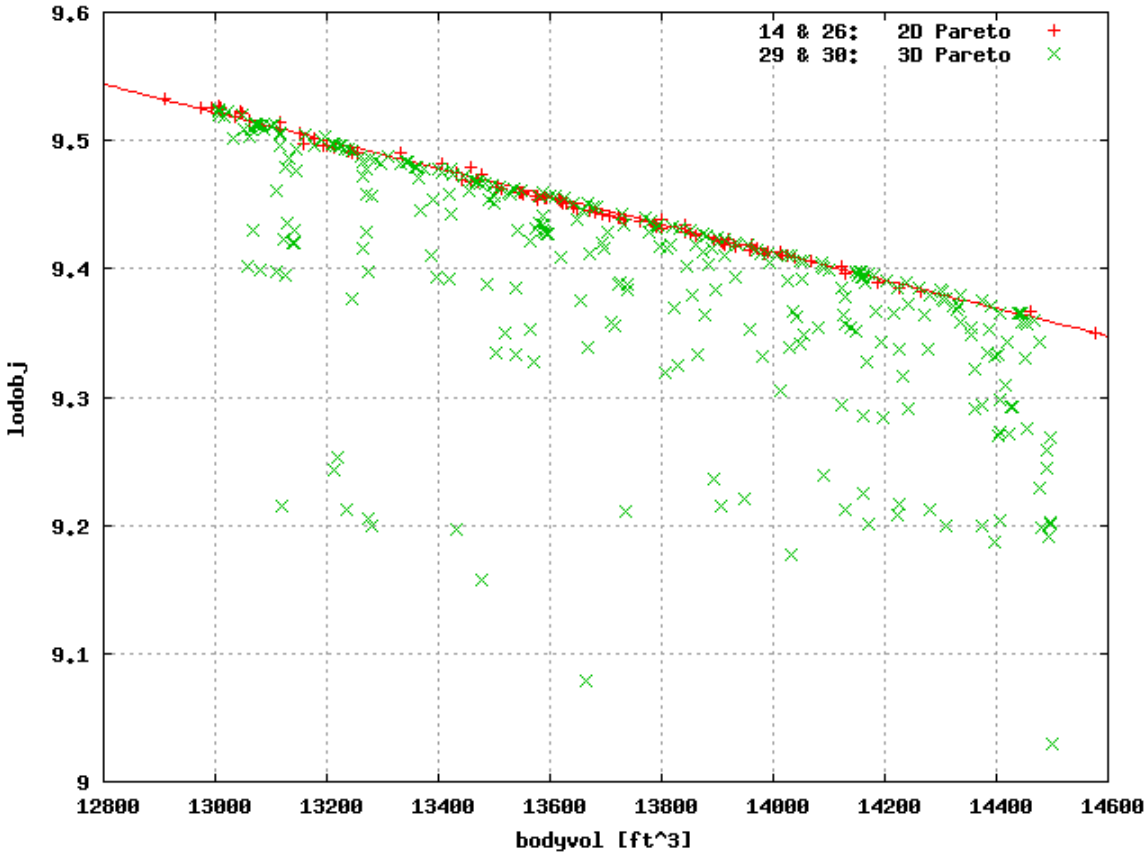

Figure 2.2.1.8 Pareto optima: (+) 2 objectives, maximize L/D & maximize volume; (x) 3 objectives, maximize L/D, maximize volume, minimize PLdB. The frontier of L/D & volume for each is essentially the same.

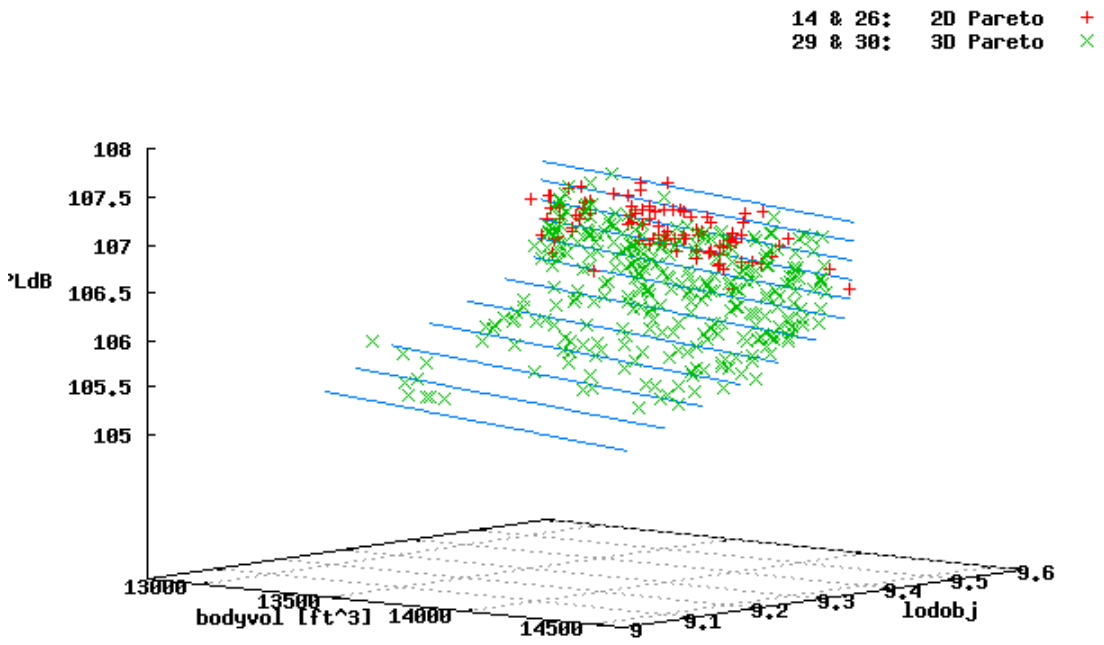

Figure 2.2.1.9 Pareto optima: (+) 2 objectives, maximize L/D & maximize volume with no influence of PLdB; (x) 3 objectives, includes minimizing PLdB. Lines are contours of constant PLdB (105.2 to 107.4 in steps of 0.2) of a best fit approximation to the data. 2-objective optima vary in PLdB, and 3-objective optima show that the cause is a steep trade in PLdB near the 2-objective L/D-volume frontier.

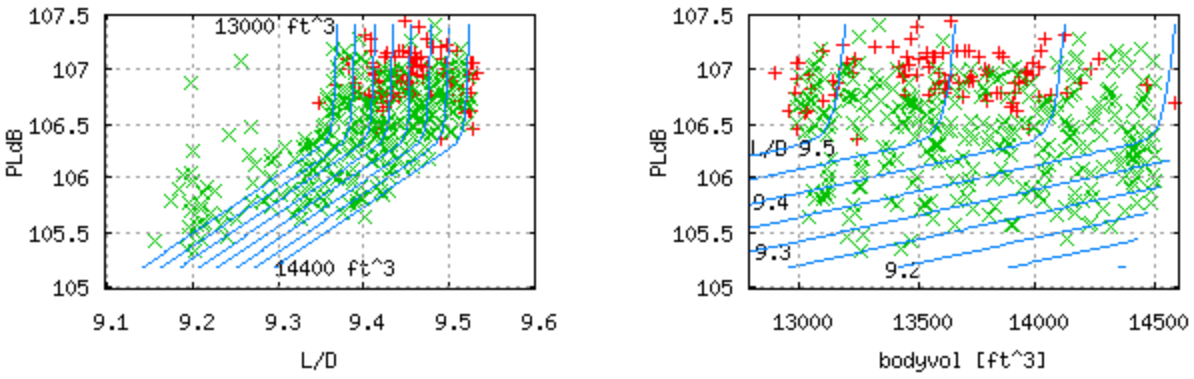

Figure 2.2.1.10 Pareto optima, maximizing volume & L/D while minimizing PLdB. Curves are cuts through best-fit surface of the Pareto frontier.

a)

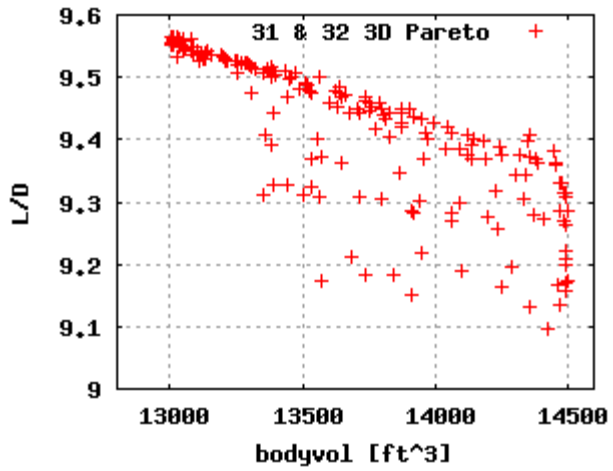

b)

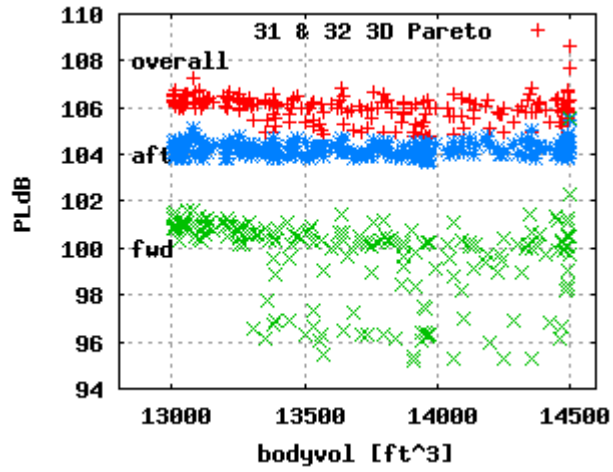

c)

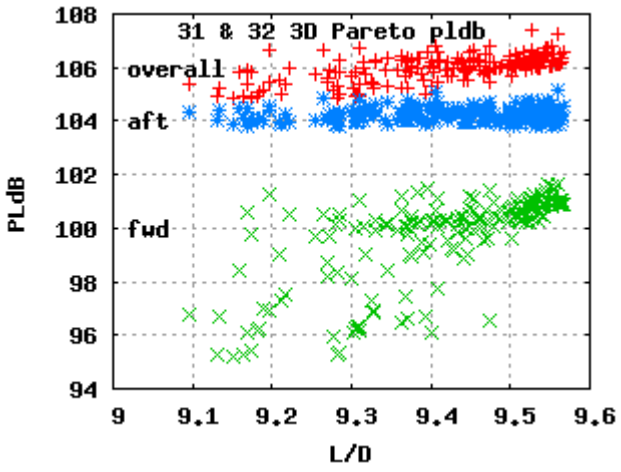

Figure 2.2.1.11a, b & c. Orthogonal views of 3-objective Pareto; maximize L/D, maximize bodyvol, minimize PLdB. Aft PLdB is the dominant contributor to overall PLdB. Additional degrees of freedom in forward and aft body result in a similar trade between L/D and volume at their frontier.

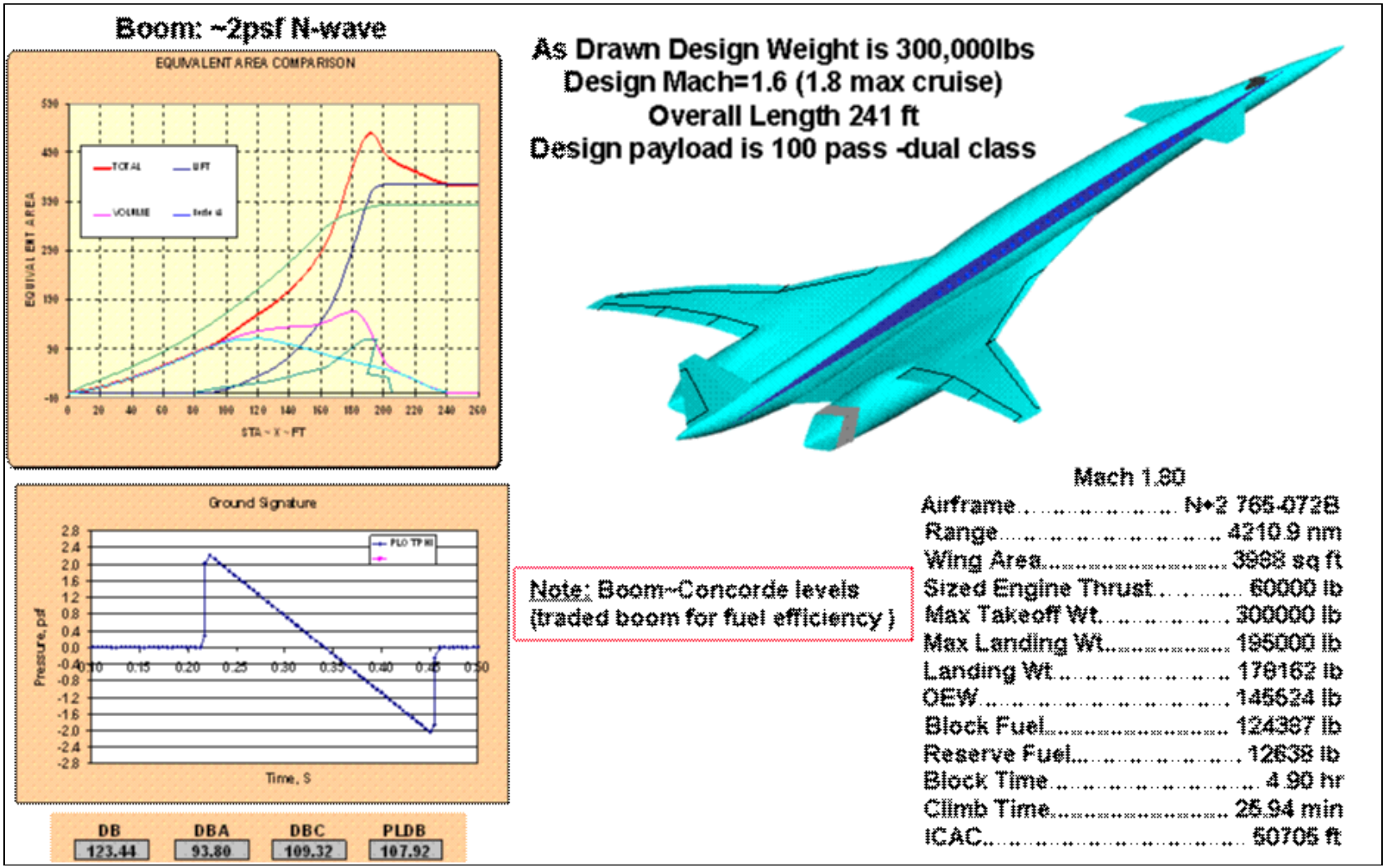

Figure 2.2.1.12 Initial N+2 Concept: 765-072B

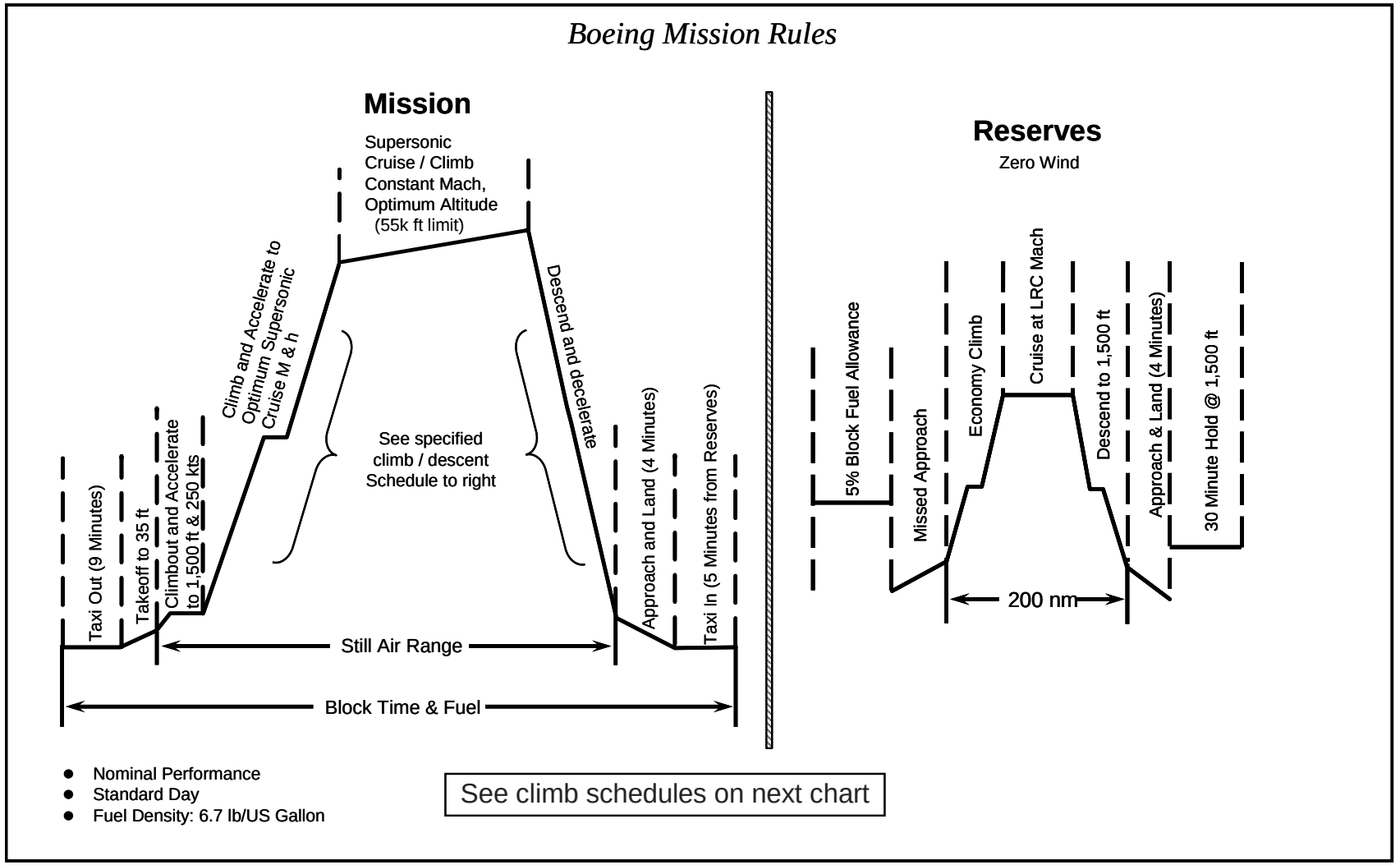

Figure 2.2.2.1A. Supersonic Non-Stop Mission Profile

Boeing Mission Rules

Climb / Descent Schedule

Mission Profile	ALTITUDE (FT)		MACH		Notes
	Initial	Final	Initial	Final	
CLIMB	1500	10000	0.39	0.45	Climb at 250 KCAS from 1500 ft to 10,000 ft
CLIMB	10000	10300	0.45	0.69	Accelerate to 375 KEAS at roughly constant altitude (10,300 ft)
CLIMB	10300	20774	0.69	0.85	Climb at constant 375 KEAS to Mach 0.85 (~20,800 ft altitude)
CLIMB	20774	35000	0.85	0.85	Climb at constant Mach 0.85 to 35,000 ft
CLIMB	35000	39000	0.85	0.95	Climb and accelerate to Mach 0.95 at 39,000 ft
CLIMB	39000	41000	0.95	M-crz	Climb and accelerate to Supersonic Cruise Mach (1.6 to 2.0) at 41,000 ft
CLIMB	41000	h-opt	M-crz	M-crz	Climb to optimum initial cruise altitude
					Climb/Cruise with 55,000 ft maximum altitude
DESCENT	53000	39000	M-crz	0.95	Descend & decelerate to Mach 0.95 @ 39,000 ft
DESCENT	39000	34960	0.95	0.85	Descend to Mach 0.85 and 273 KEAS (altitude ~ 35,000 ft)
DESCENT	34960	20774	0.85	0.85	Descend at Mach 0.85 and 375 KEAS (altitude ~20,800 ft)
DESCENT	20774	10300	0.85	0.69	Descend at constant 375 KEAS to ~10,300 ft
DESCENT	10300	10000	0.69	0.45	Decelerate to 250 KCAS at roughly constant altitude (10,000 ft)
DESCENT	10000	1500	0.45	0.39	Descend to 1500 ft at constant 250 KCAS

- Nominal Performance
- Standard Day
- Fuel Density: 6.7 lb/US Gallon

Figure 2.2.2.1B. Supersonic Non-Stop Mission Profile (con't)

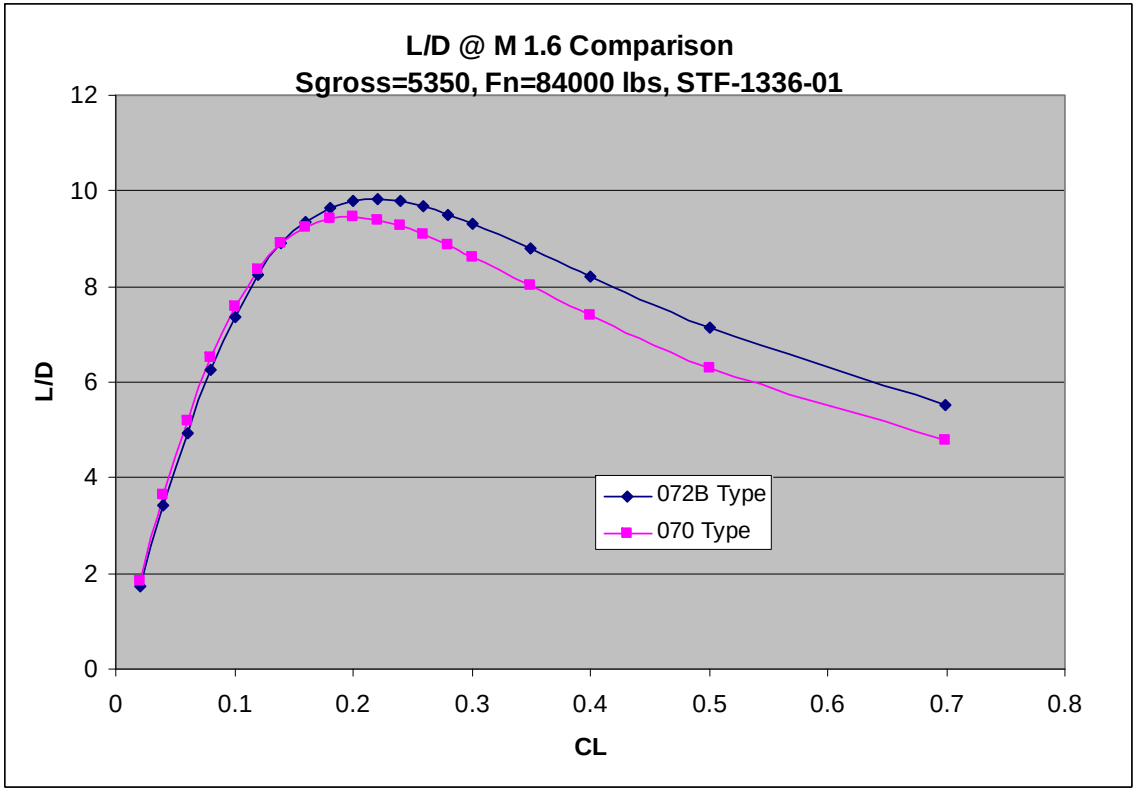

- Primary configuration differences
  - Horizontal tail on -070
  - Different planform (sweeps, thickness, aspect ratio)

Figure 2.2.3.1 Aerodynamic Differences between -070 and -072B Species

Case 1: Engine sized for performance also meets 10,000 ft takeoff at 1100 fps Vj

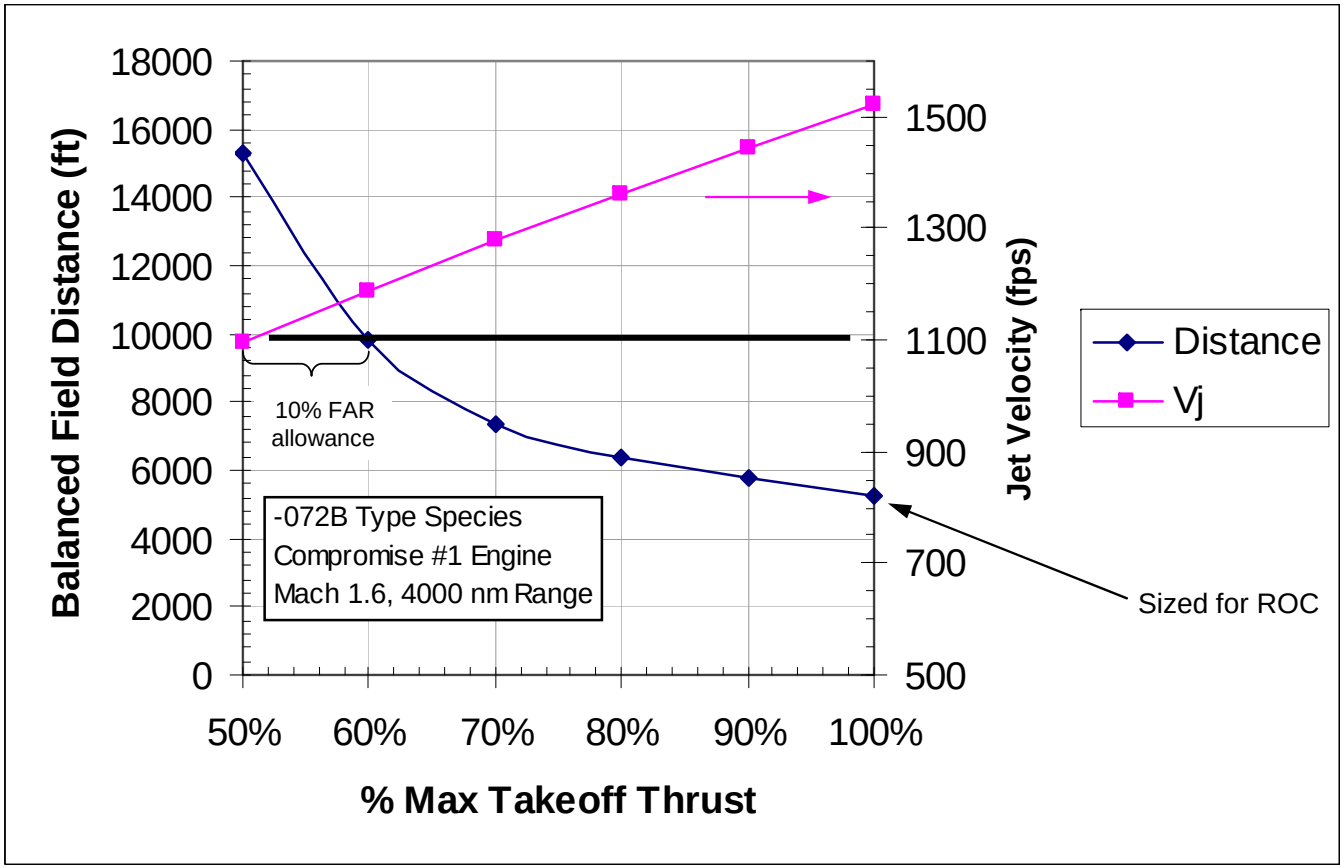

Figure 2.2.3.2 Partial Power Takeoff for 1100 fps Vj

Case 2: Engine must be sized up to meet 10,000 ft takeoff at 1100 fps Vj

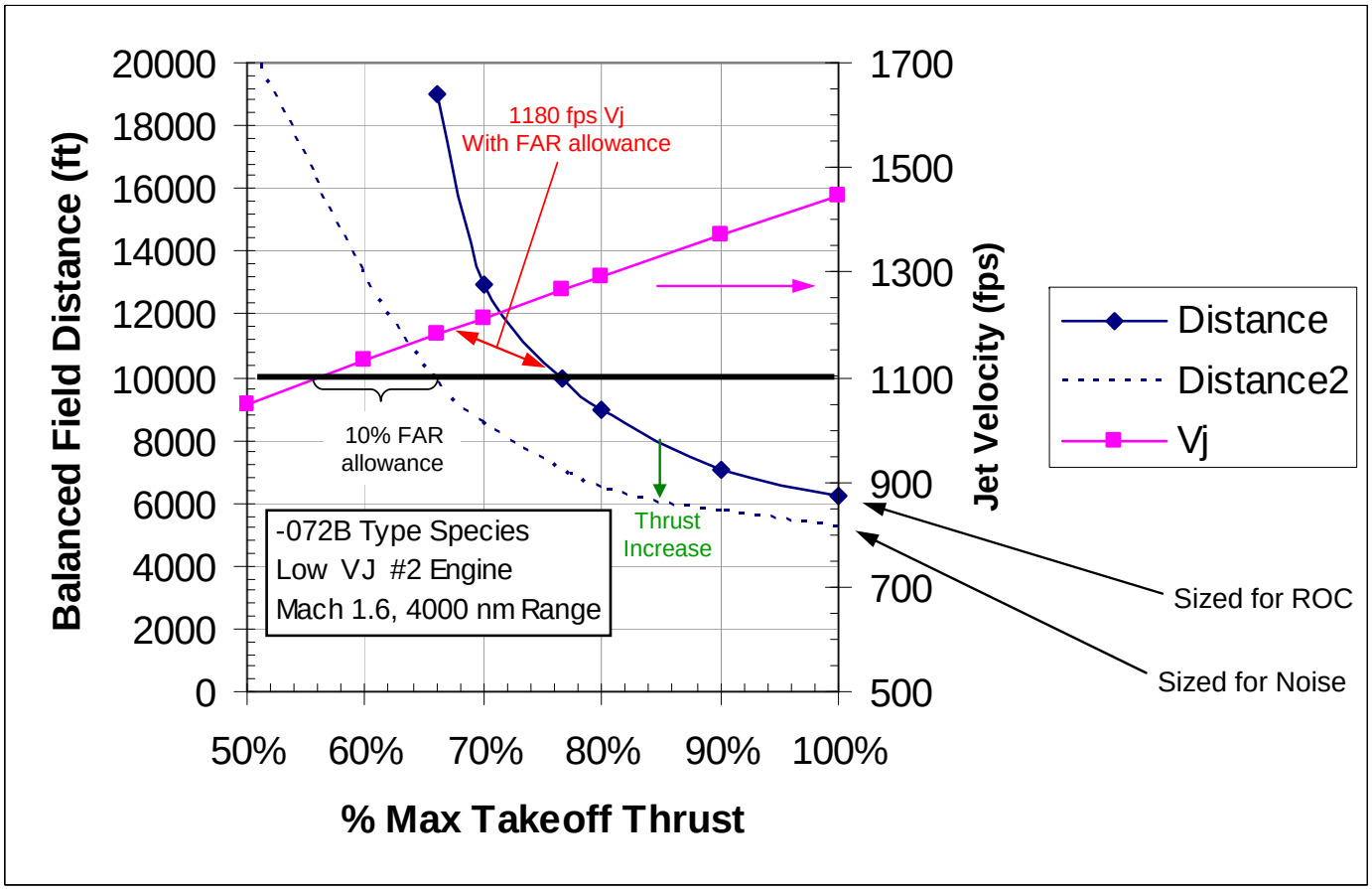

Figure 2.2.3.3 Sizing for 1100 fps Vj at Takeoff

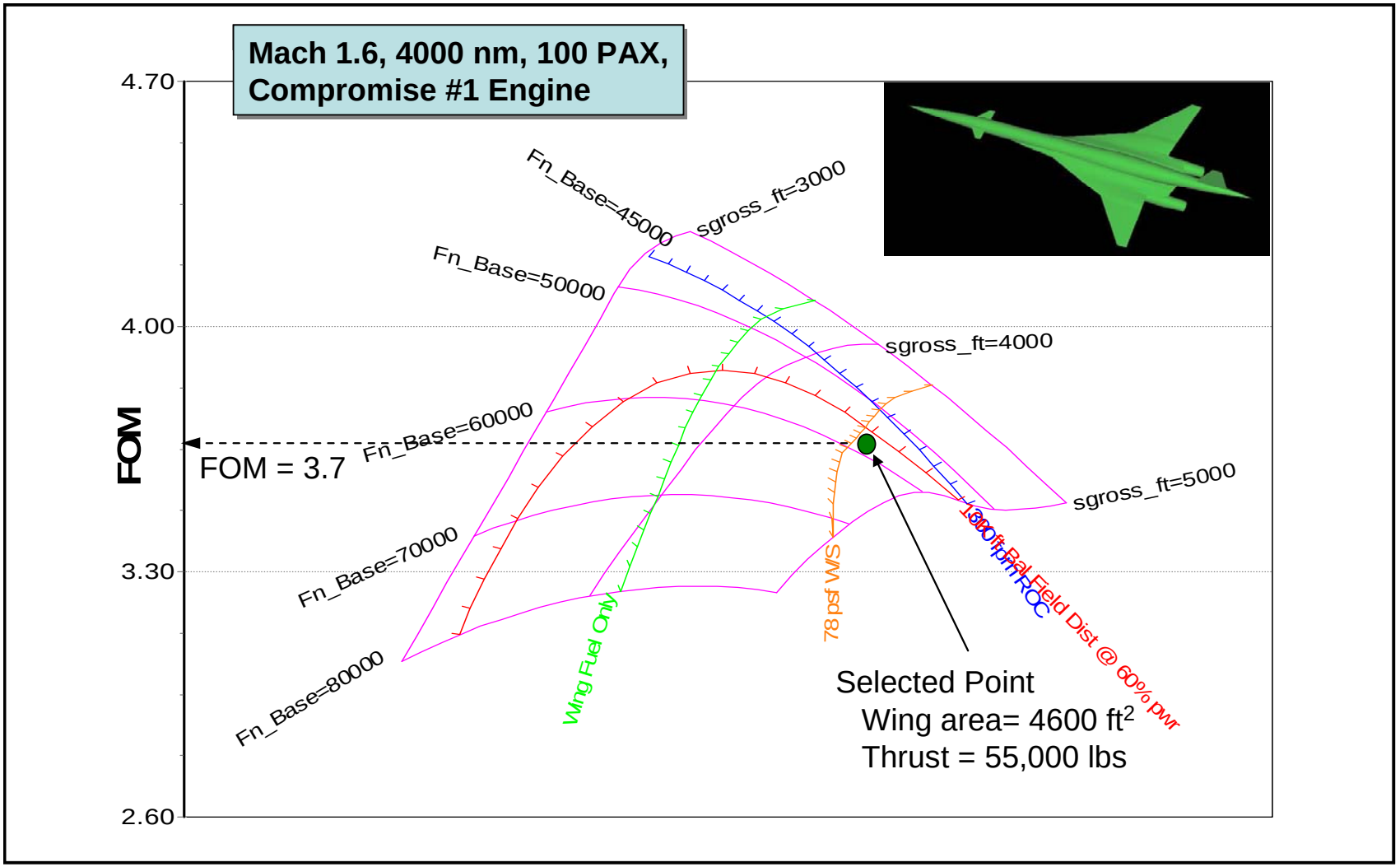

Figure 2.2.3.4 072B Type Species Carpet Plot

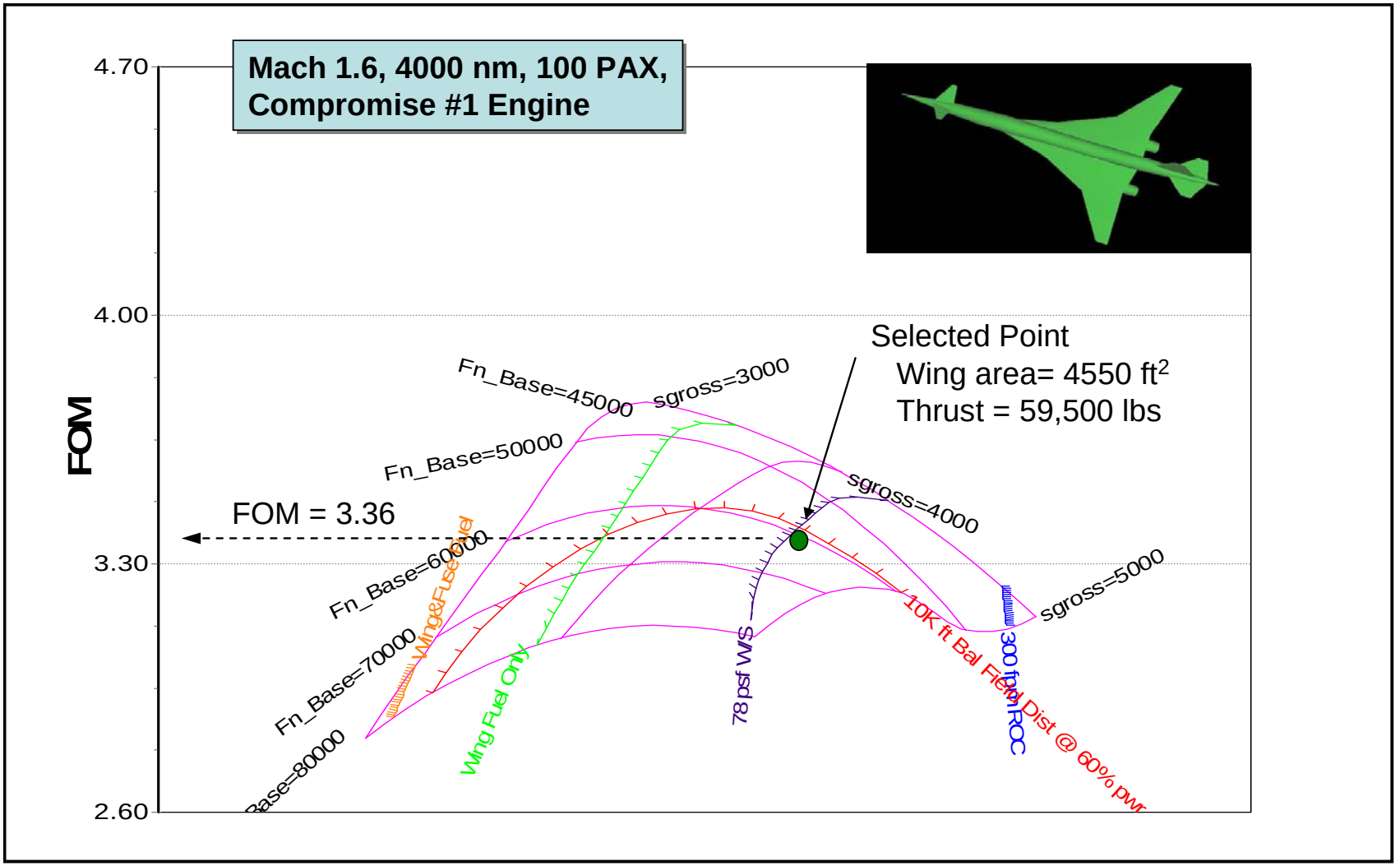

Figure 2.2.3.5 070 Type Species Carpet Plot

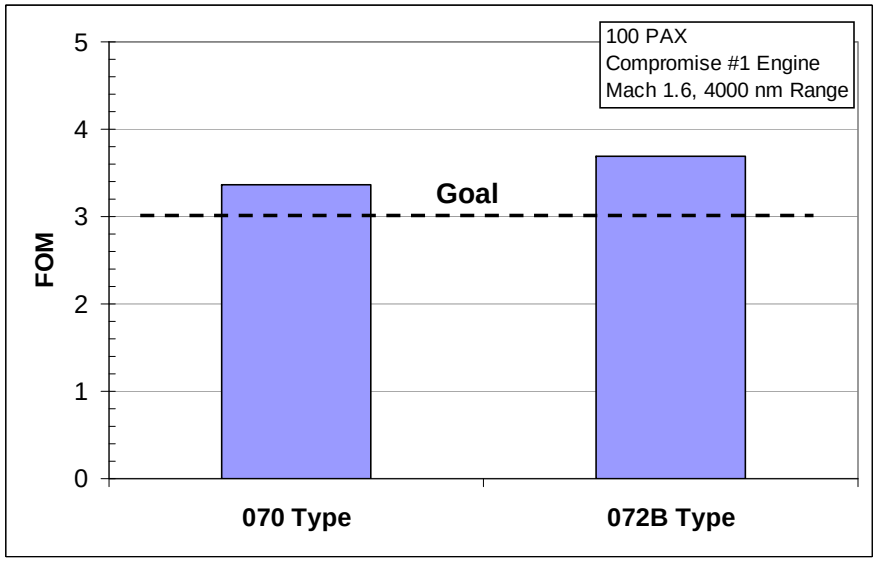

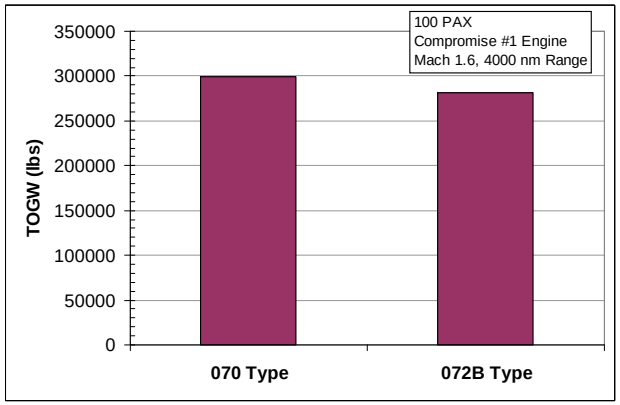

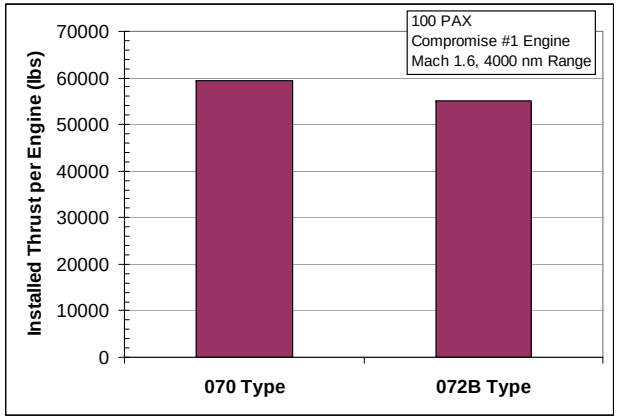

• Select 072B species for rest of trades

Figure 2.2.3.6 Species Trade Results

- Passengers laid out per IAC Short / Medium Dual Class rules, as BCA study
- Three “nominal” cross-sections developed

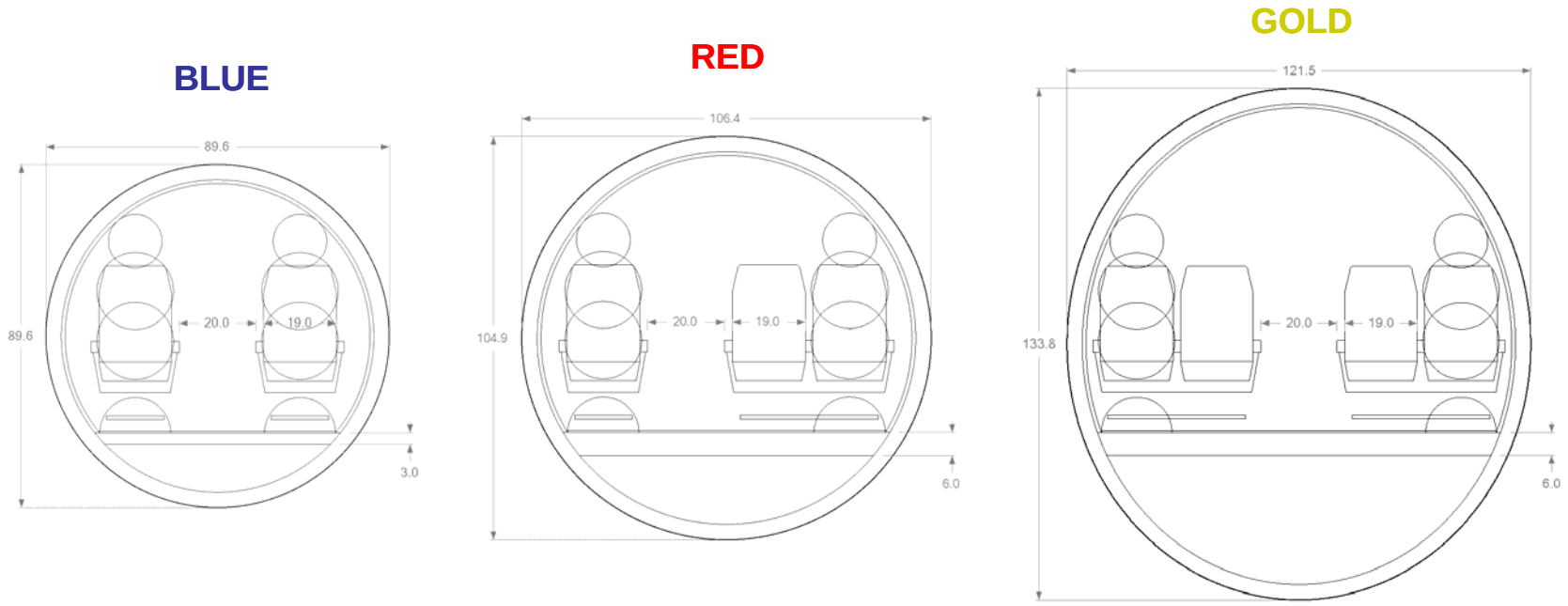

Figure 2.2.4.1. Passenger Layout for Number of Passengers Trade

- 100 Pax – 2+2 and 2+1, 2 x LD-4 baggage

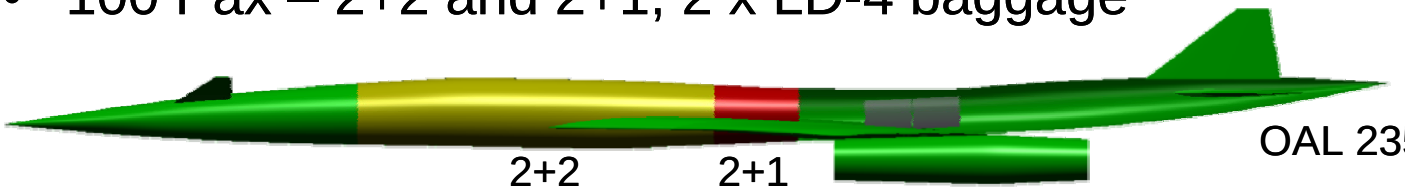

- 50 Pax – 2+1 and 1+1, 1 x LD-4 baggage

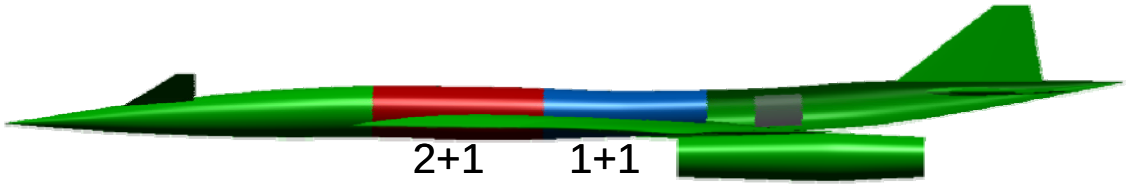

- 25 Pax – 2+1 and 1+1, Bulk baggage

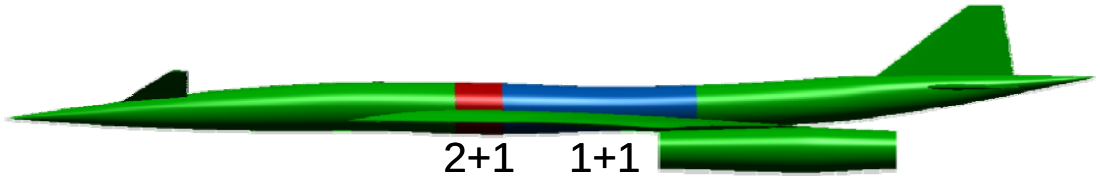

Fineness Ratio (l/d) ~ 21 for all

Figure 2.2.4.2 Payload and Fuselage Sizing

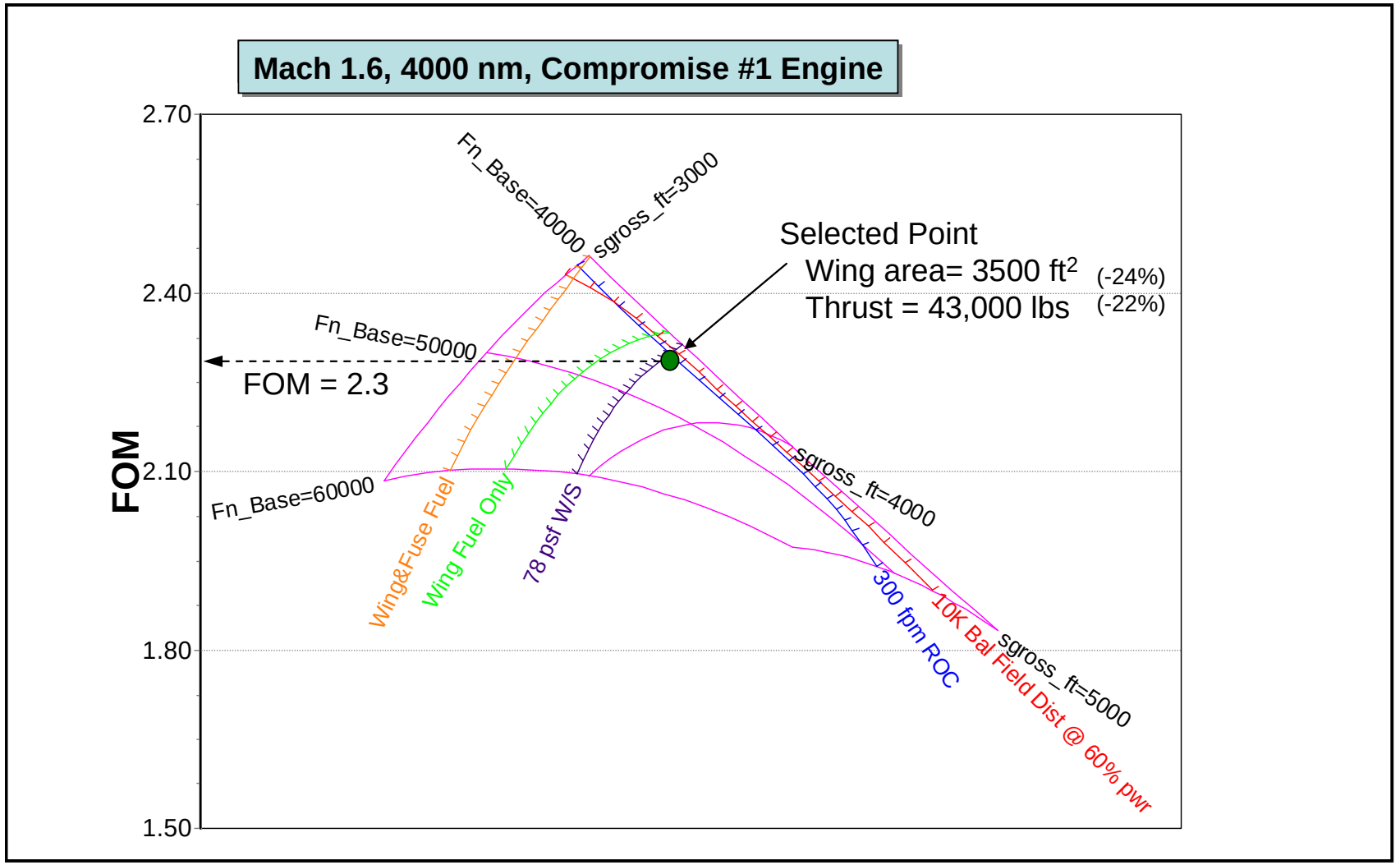

Figure 2.2.4.3 Carpet Plot for 50 Passenger Concept

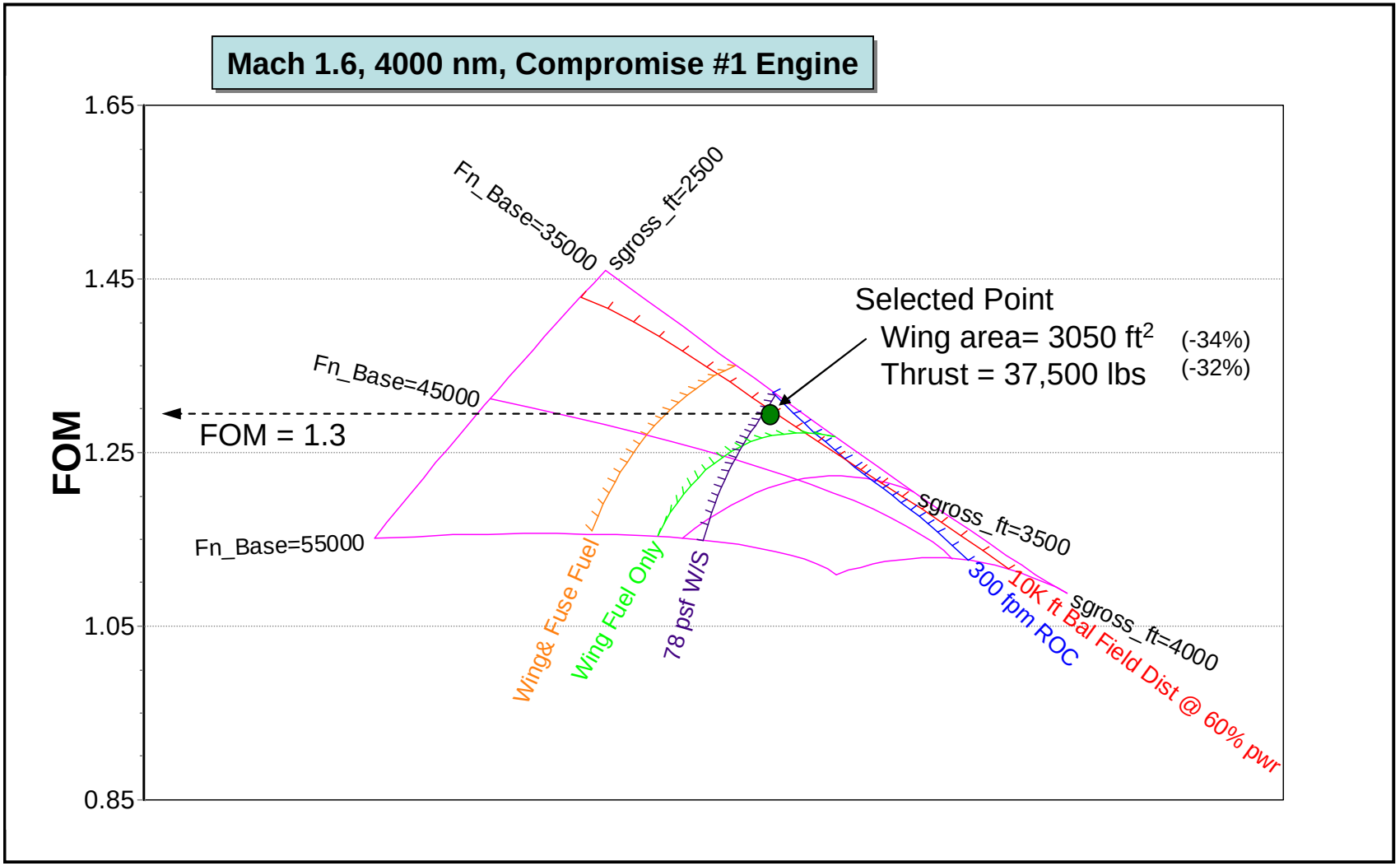

Figure 2.2.4.4 Carpet Plot for 100 Passenger Concept

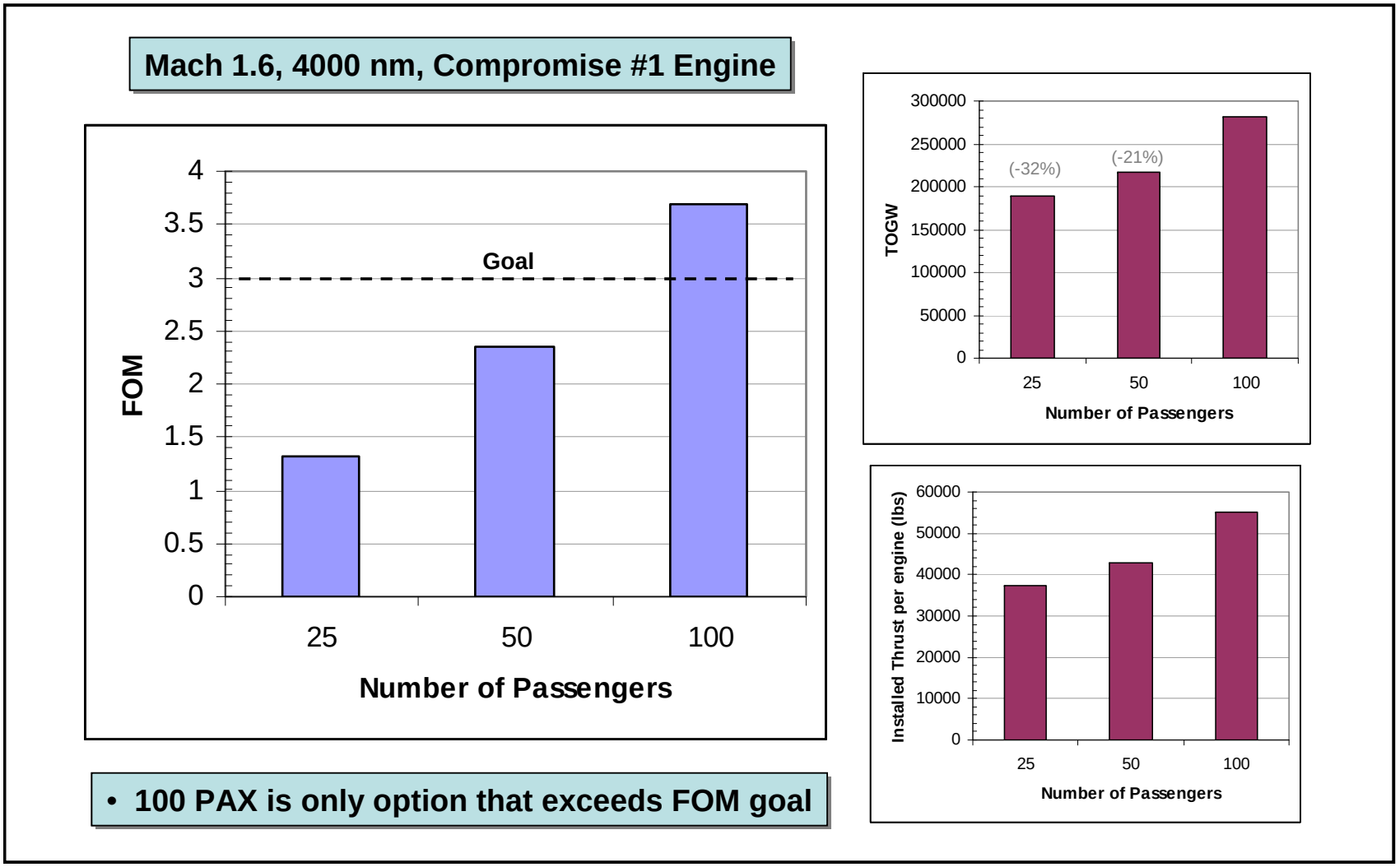

Figure 2.2.4.5 Passenger Trade Results Summary

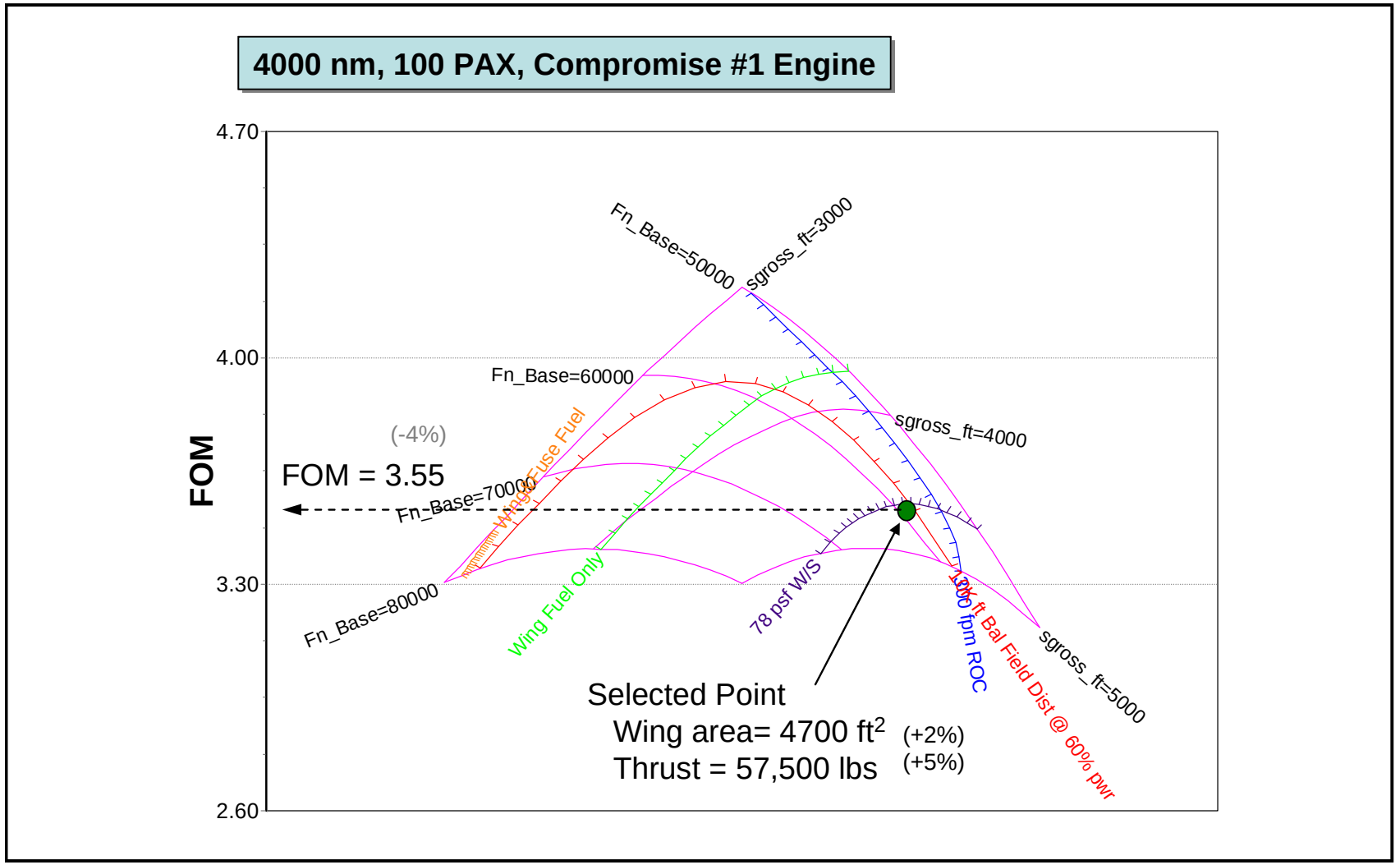

Figure 2.2.5.1 Carpet Plot for Mach 1.8 Concept

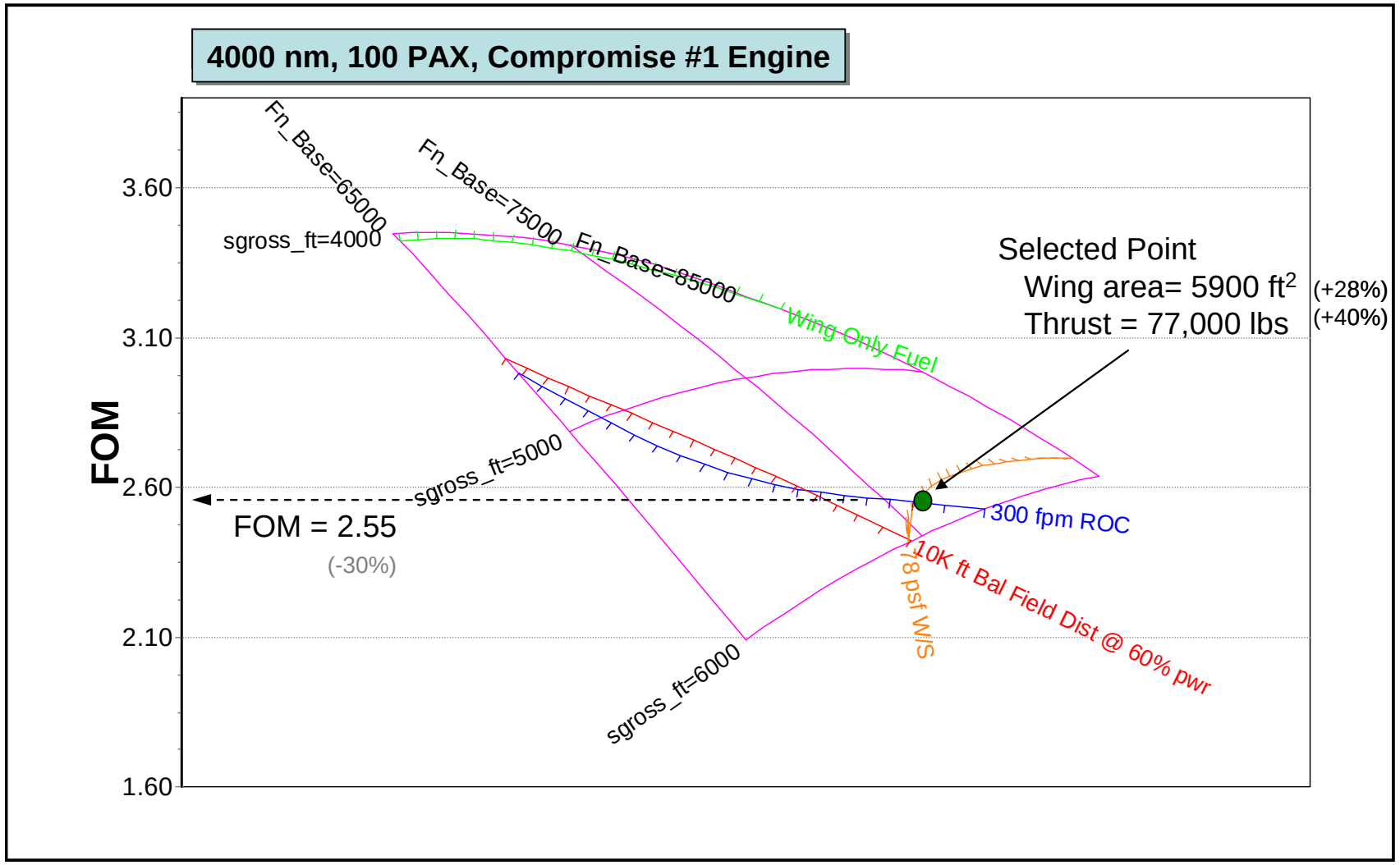

Figure 2.2.5.2 Carpet Plot for Mach 2.0 Concept

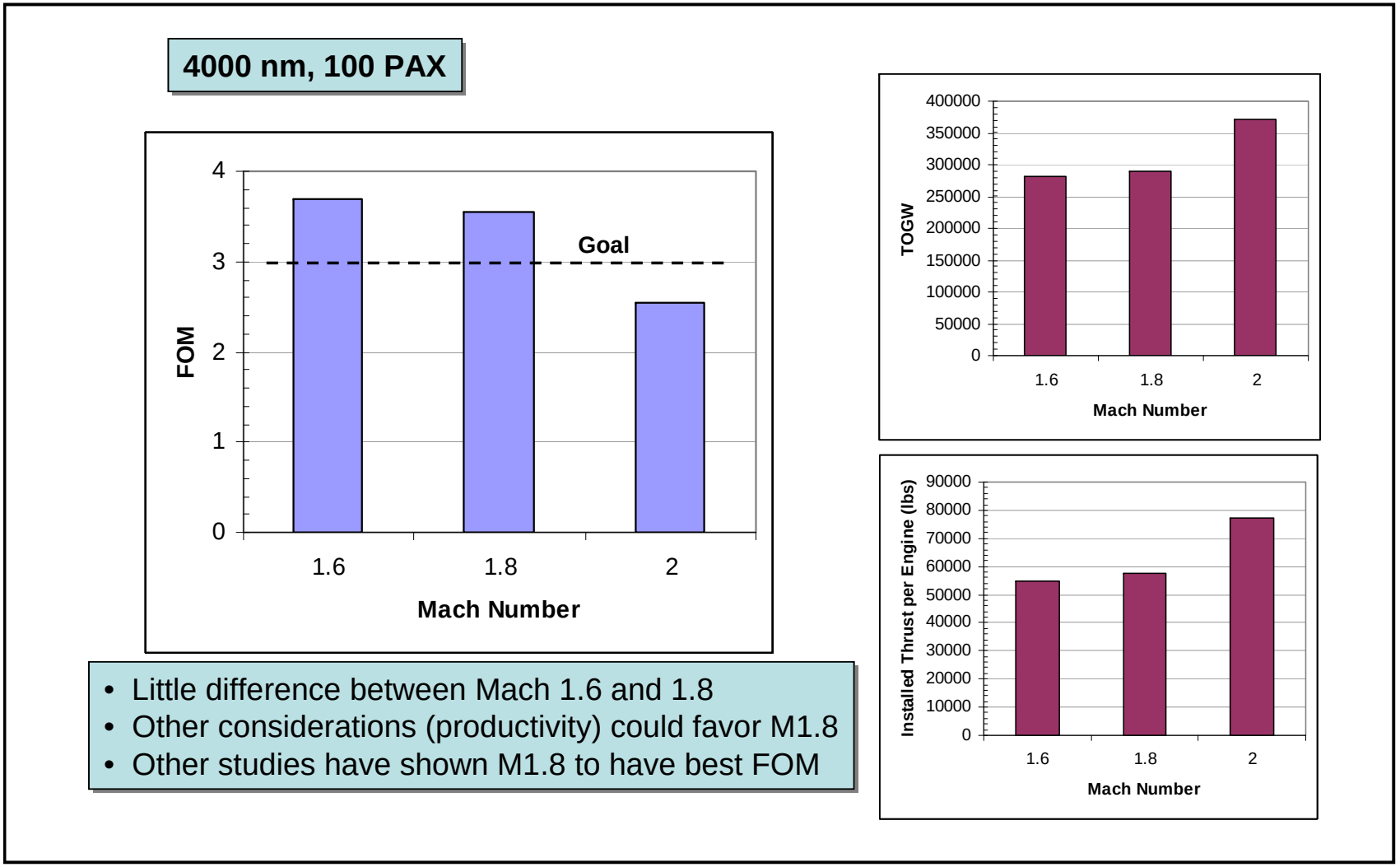

Figure 2.2.5.3 Cruise Mach Number Trade Results

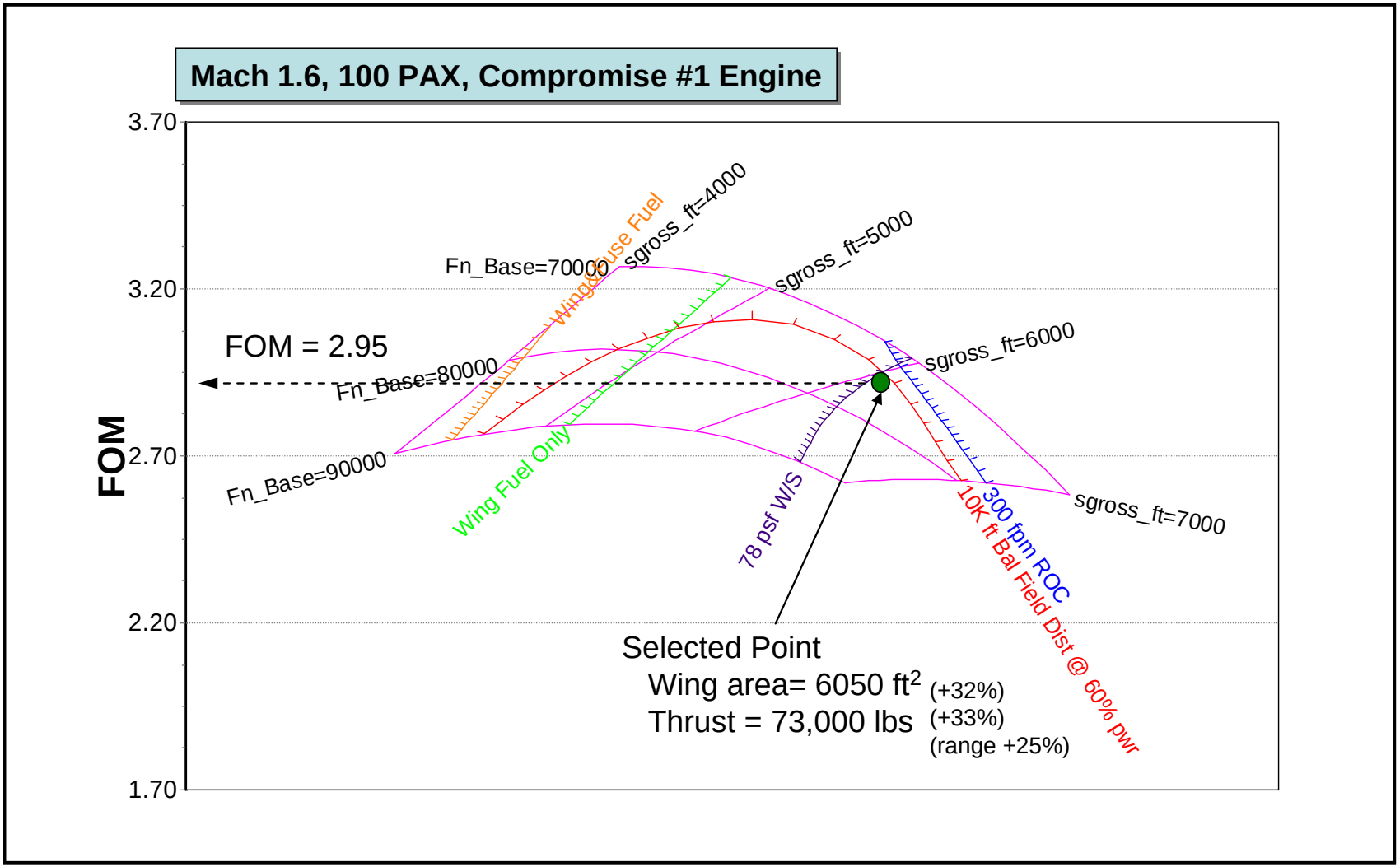

Figure 2.2.6.1 Carpet Plot for 5000 nm Range Concept

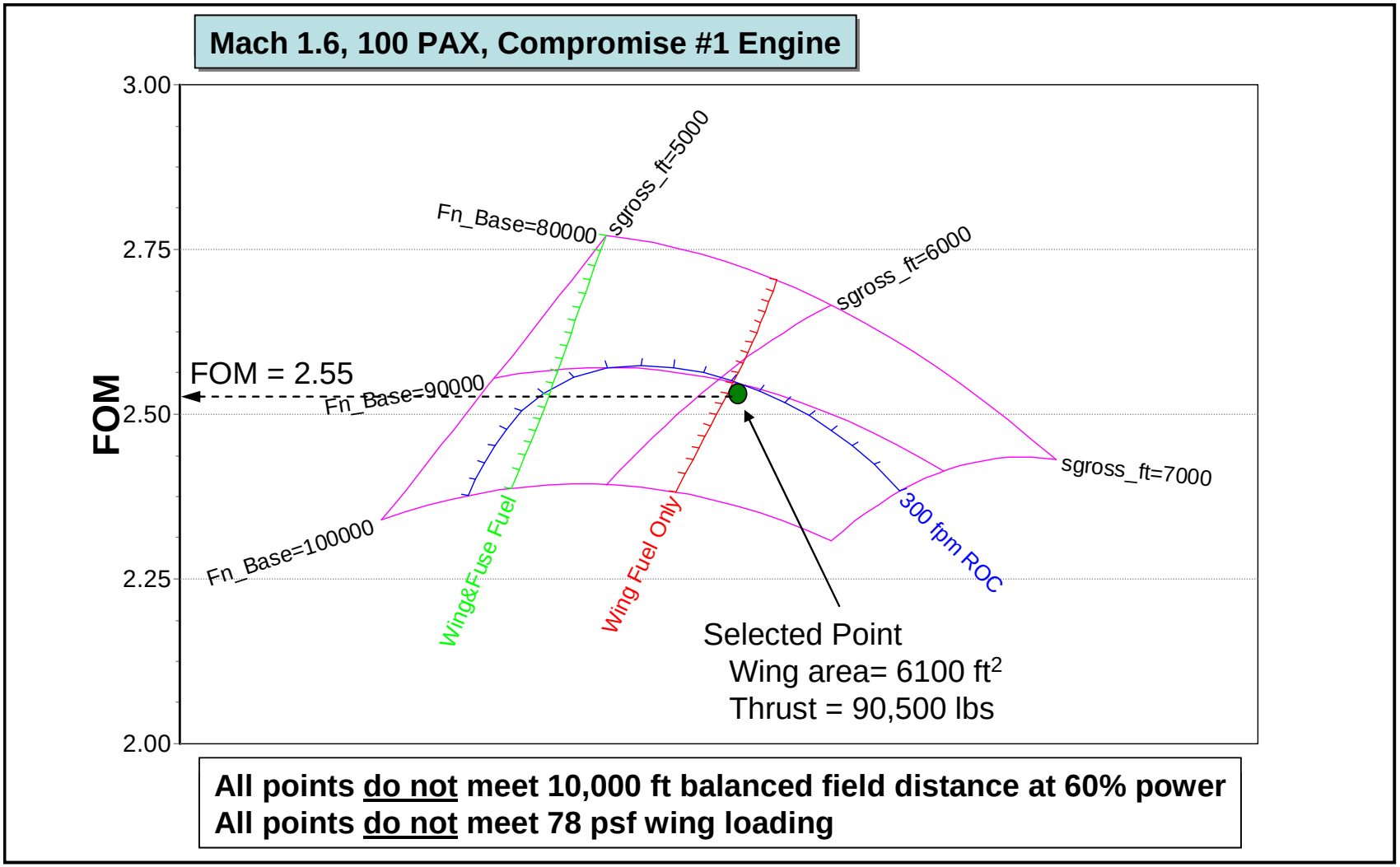

Figure 2.2.6.2 Carpet Plot for 6000 nm Range Concept

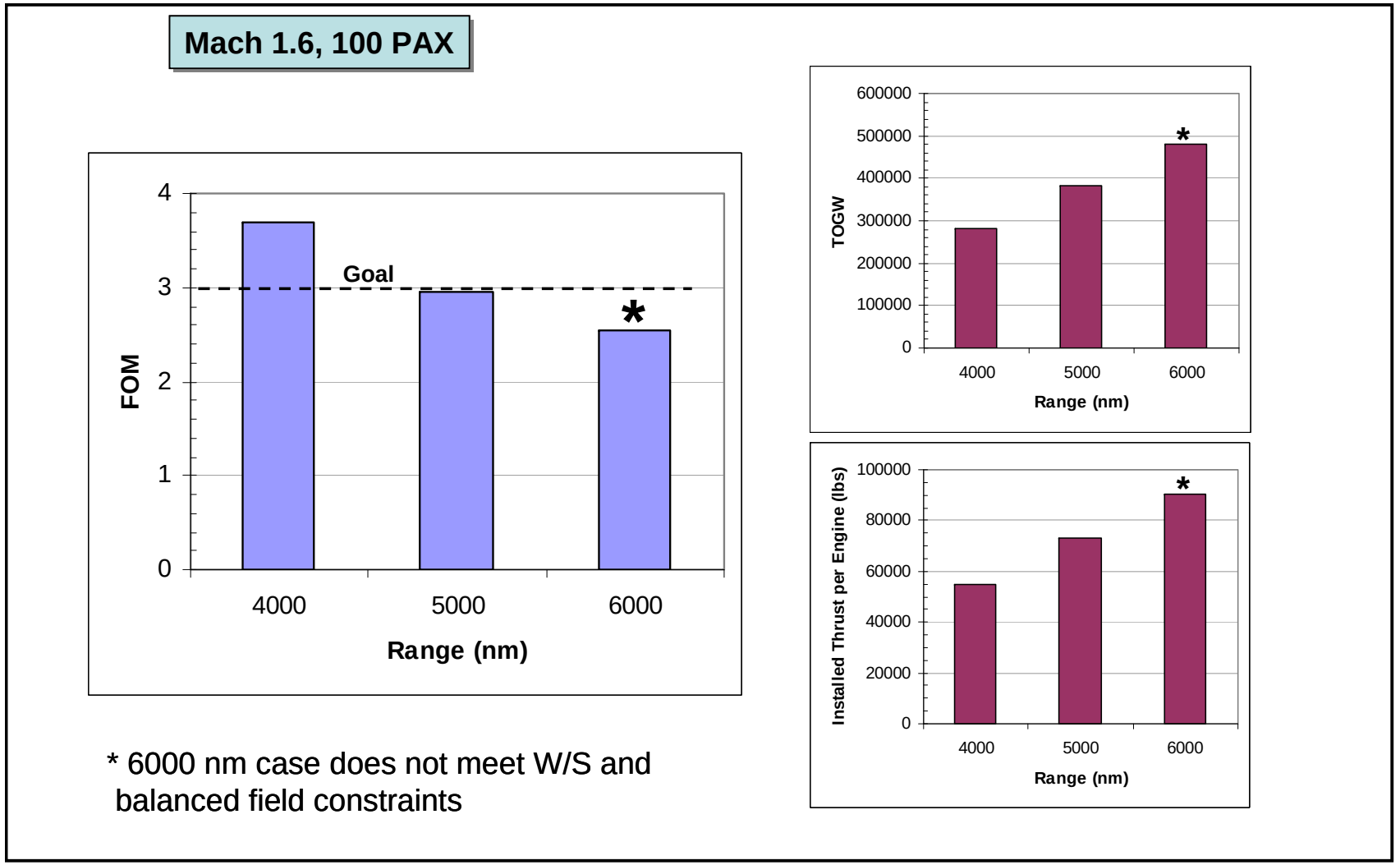

Figure 2.2.6.3 Range Trade Results

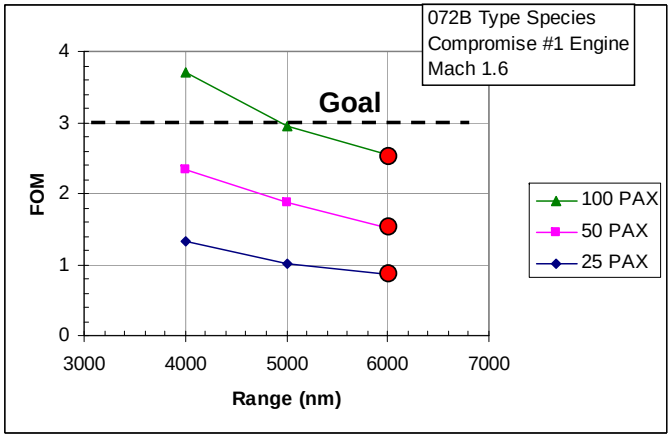

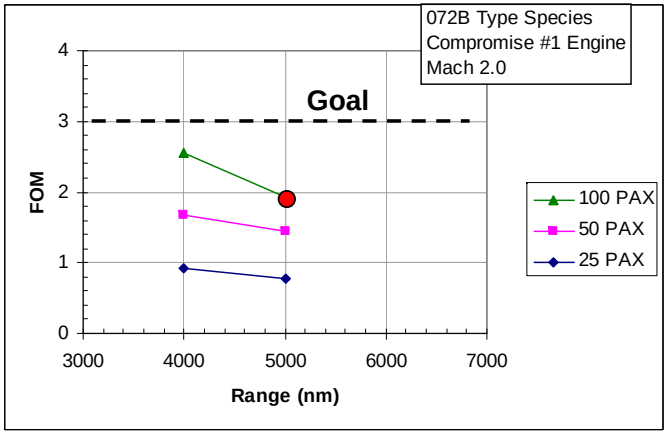

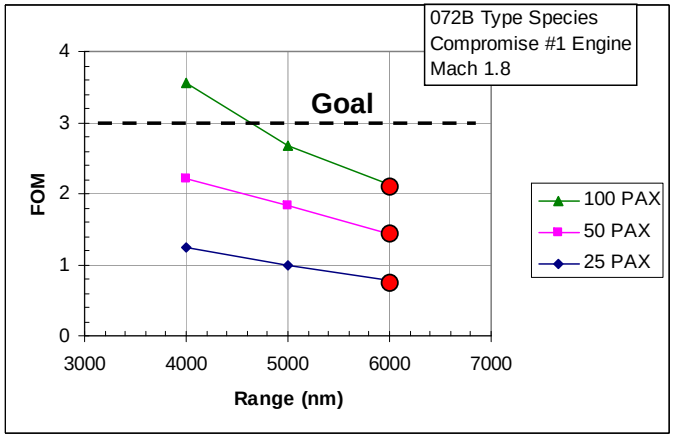

- Does not meet W/S constraint

- 4000 nm and 100 PAX exceeds FOM goal at Mach 1.6 and 1.8

Figure 2.2.7.1 Combined Range, Mach, Passenger Trade Results

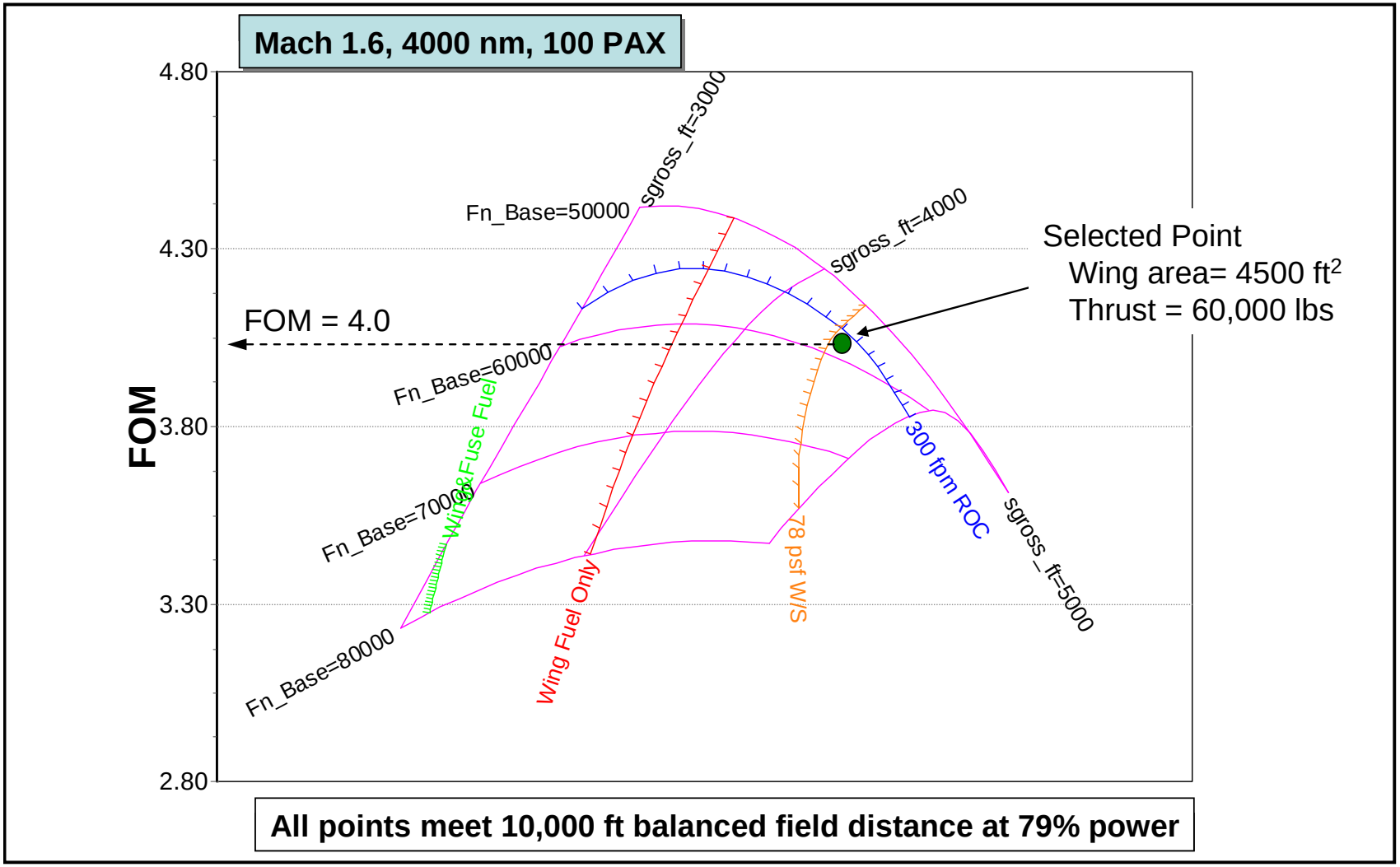

Figure 2.2.8.1 Carpet Plot for Low Jet Velocity #1 Engine

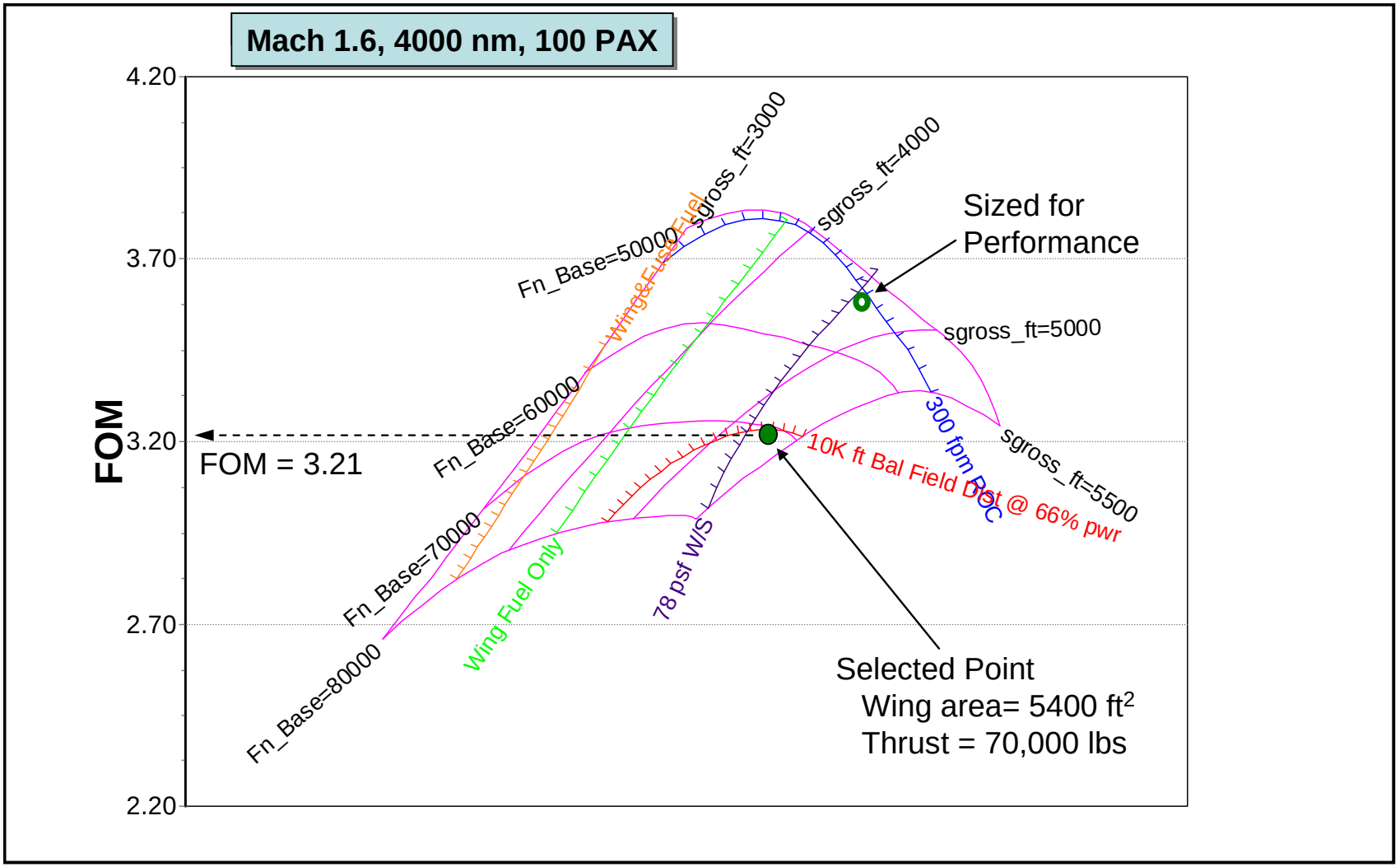

Figure 2.2.8.2 Carpet Plot for Low Jet Velocity #2 Engine

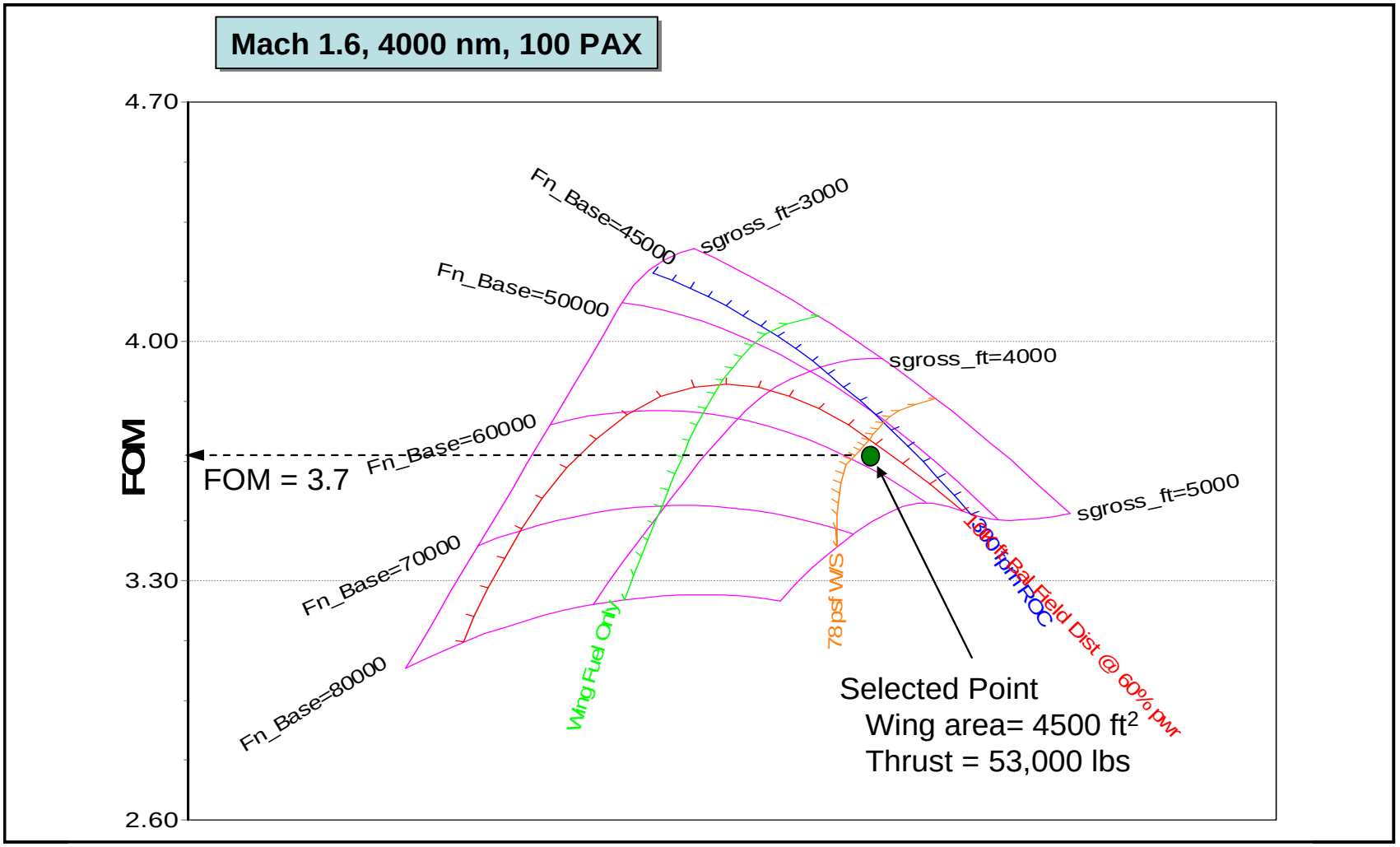

Figure 2.2.8.3 Carpet Plot for Compromise #1 Engine

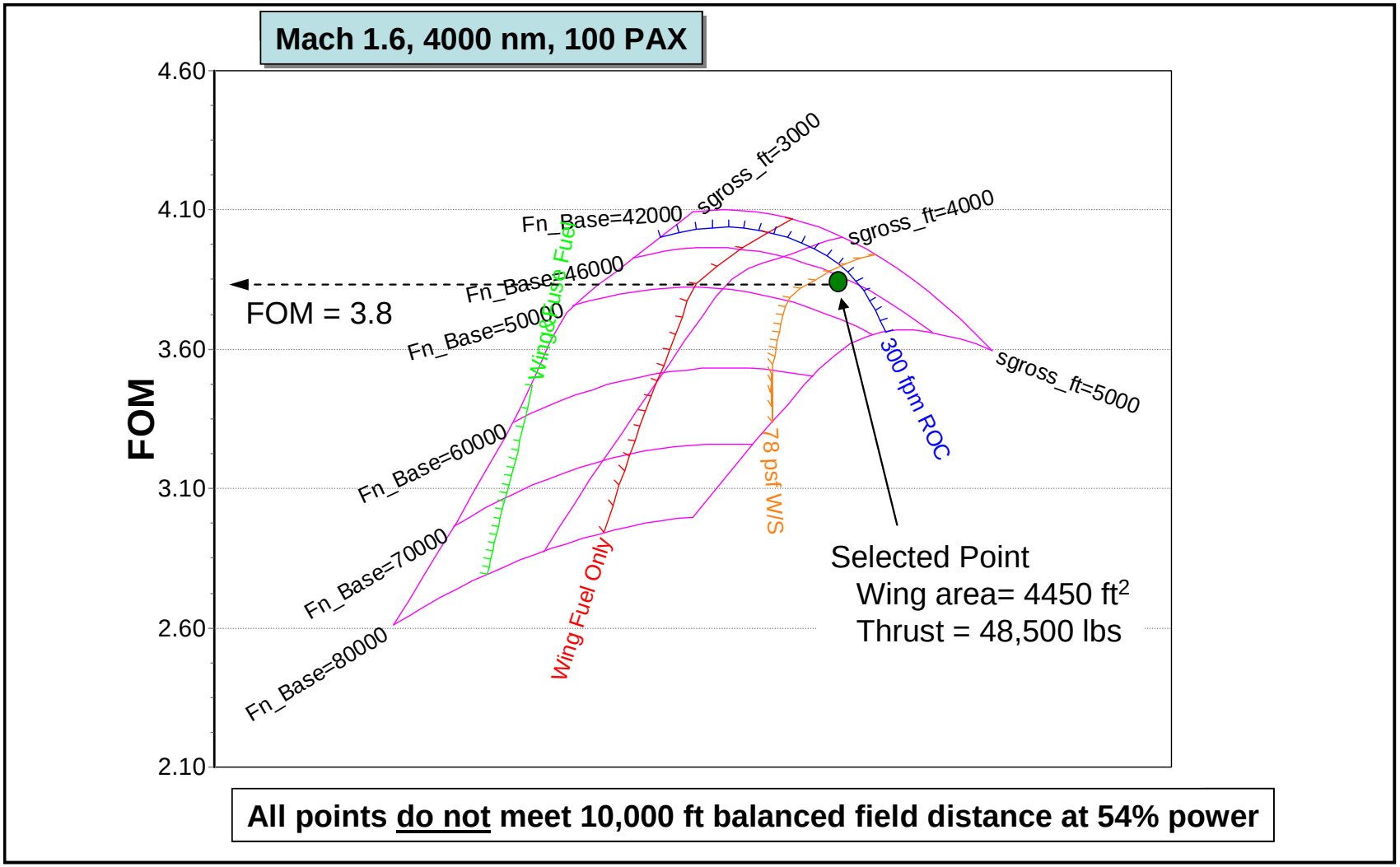

Figure 2.2.8.4 Carpet Plot for Compromise #2 Engine

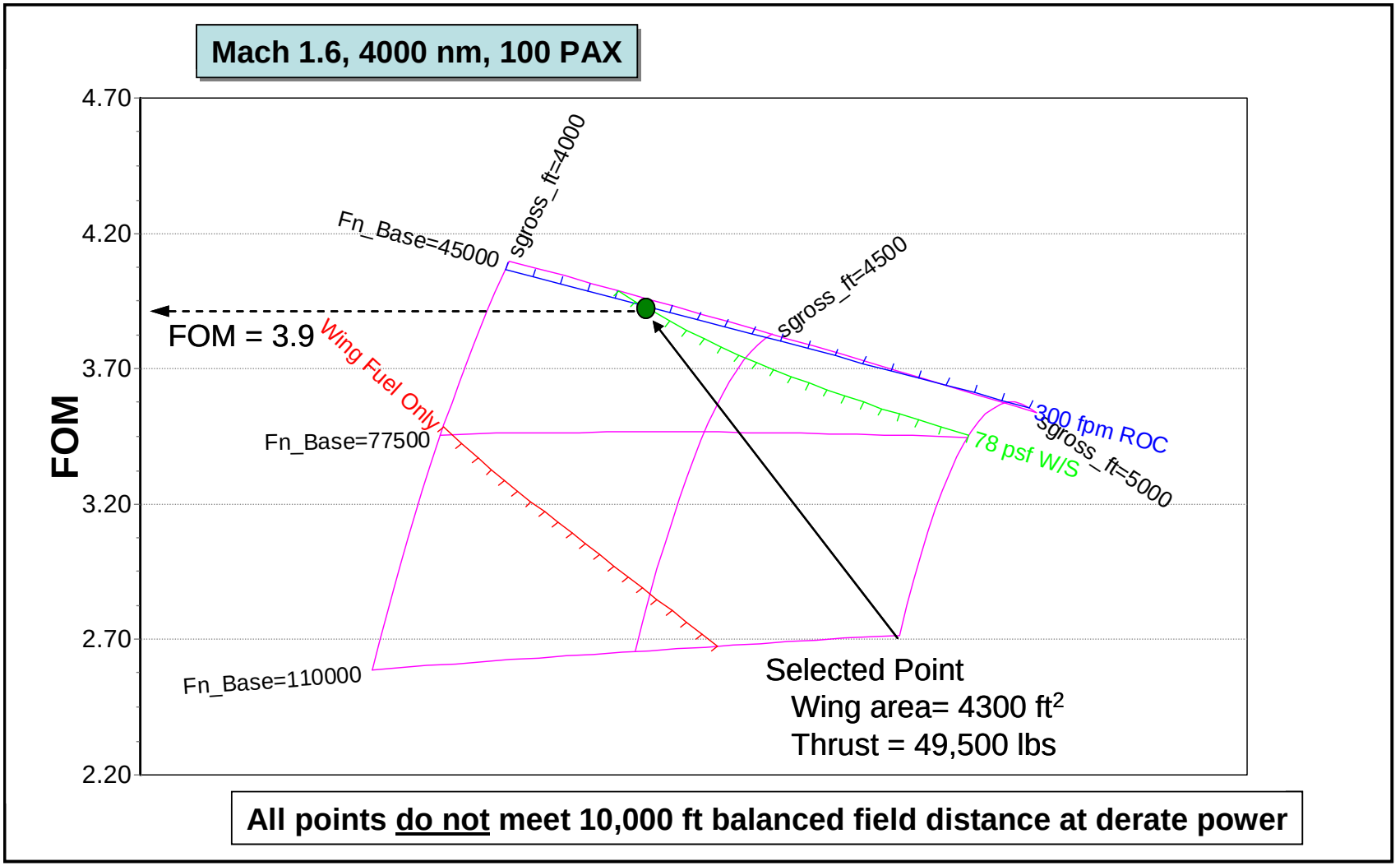

Figure 2.2.8.5. Carpet Plot for Low Diameter #1 Engine

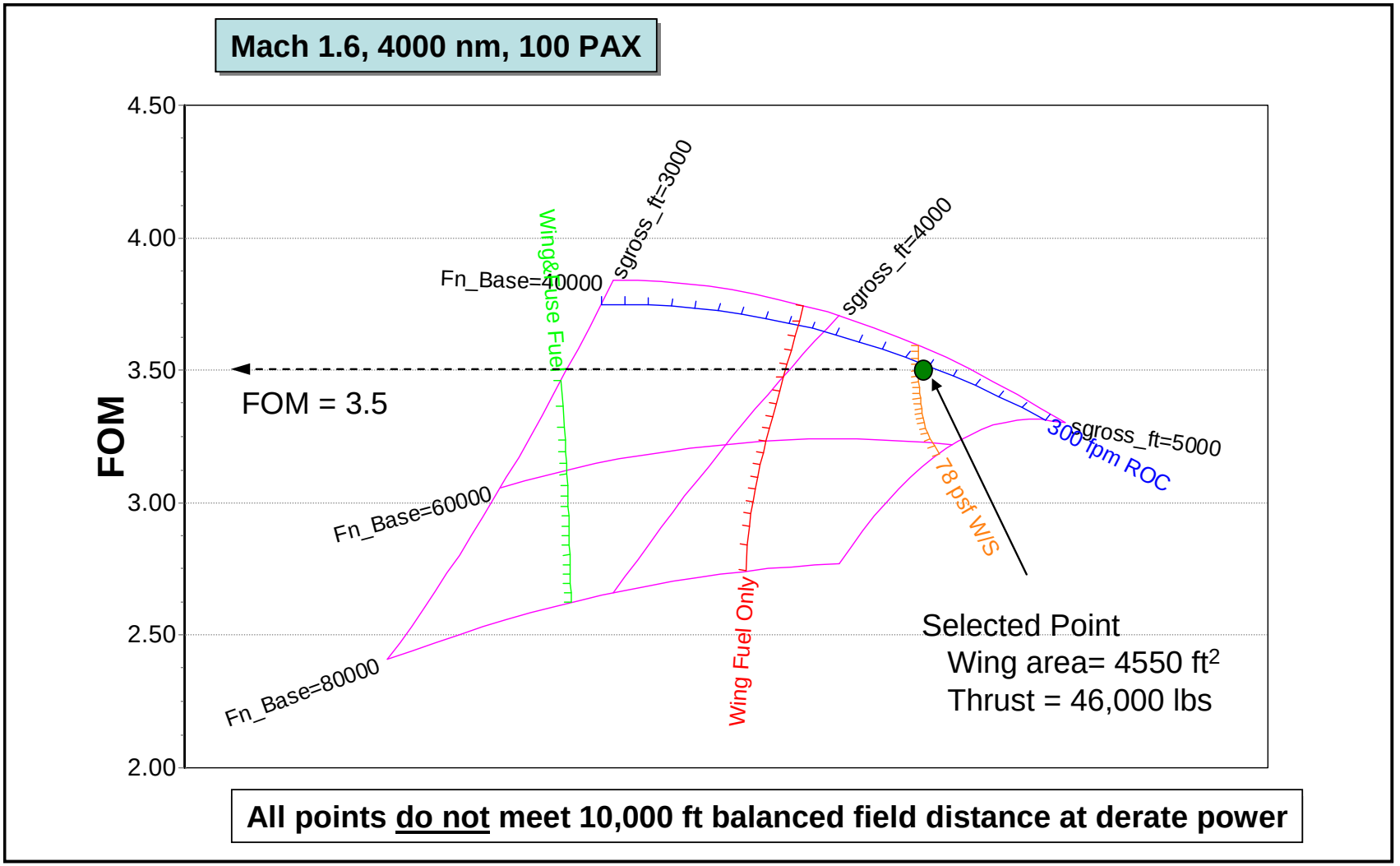

Figure 2.2.8.6. Carpet Plot for Low Diameter #2 Engine

Mach 1.6, 4000 nm, 100 PAX

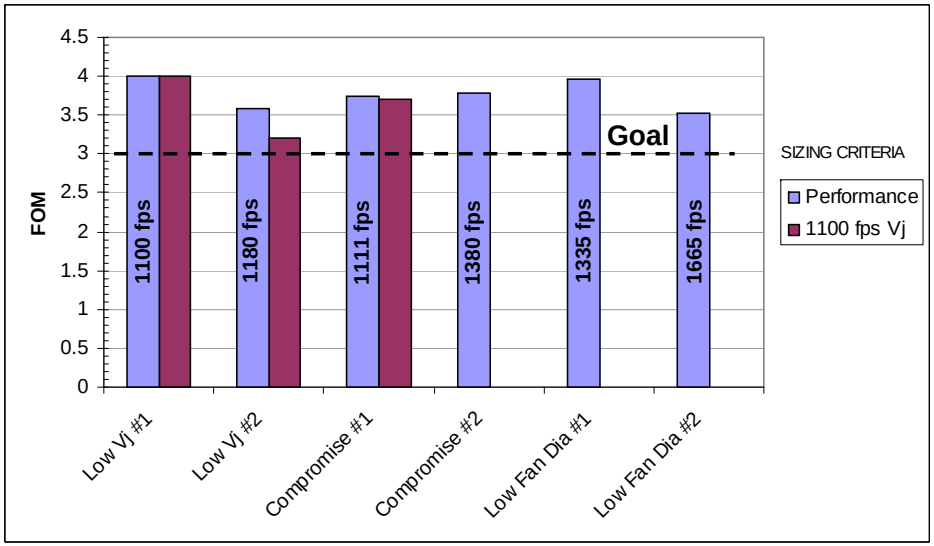

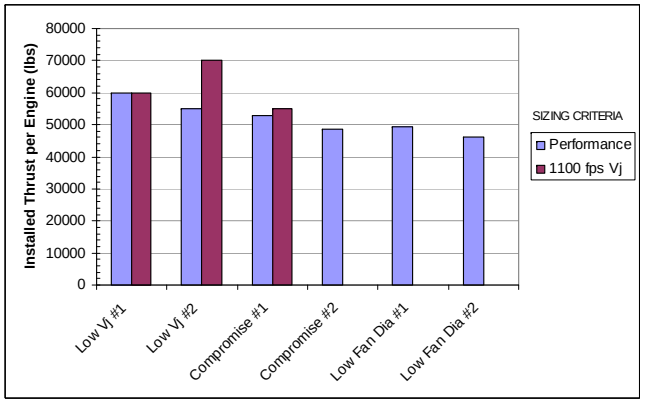

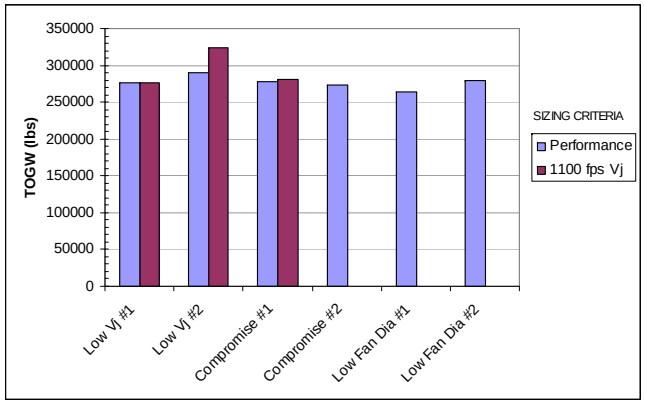

- Engine cycles are representative of different technology levels and jet velocities

We are selecting Compromise #1 engine cycle for Task 2.5

Figure 2.2.8.7 Engine Cycle Trade Results

Configuration	V2.1 Dec 17 Compromise 2	V2.5 (resized) Mar 12 Compromise 2
Wing Area (ESDU)	3527	3771
Wing Area (Gross)	**4450**	**4600**
Thrust per engine	**48,500**	**58,000**
Engine T/W	5	5
TOGW	273,834	291,098
OEW	129,940	135,320
Payload	21,000	21,000
Total Fuel	123,217	135,130
Block Fuel	105,725	116,346
Range	4000	4000
Supersonic Cruise		
Mach	1.6	1.6
Altitude	52,245	52,412
Weight	251,948	267,223
CL	0.1875	0.1833
L/D	9.698	9.486
SFC	1.0111	1.0107
Climb (pinch point)		
Mach	1.13	1.13
Altitude	40,550	40,550
Weight	261,221	277,651
CL	0.2224	0.2162
L/D	10.142	9.797
Thrust	27,125	29,641
SFC	0.8533	0.8533
ROC	360	322
Bal Field Dist. (100% pwr)	6441	7088
W/S (takeoff)	77.6	77.2
FOM	3.78	3.44

Note 1: V2.5 of the MDAO model has corrections to aero and engine scaling
Note 2: Engines were not de-rated to meet 1100 fps takeoff Vj
Note 3: V2.5 cases were constrained to 55,000 ft max cruise altitude

Figure 2.2.9.1 765-072B Performance Summary

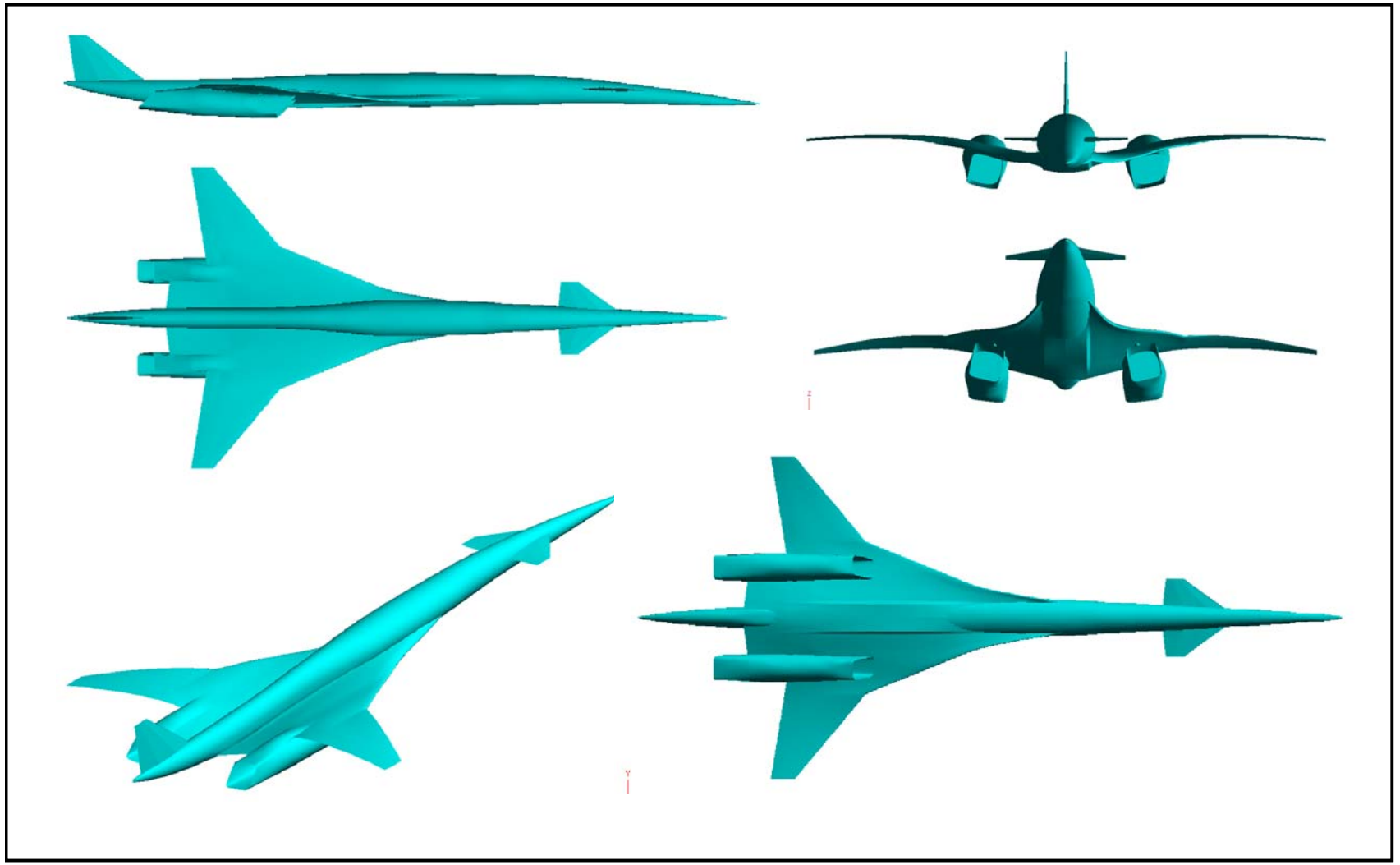

Figure 2.2.9.2 765-072B External Views

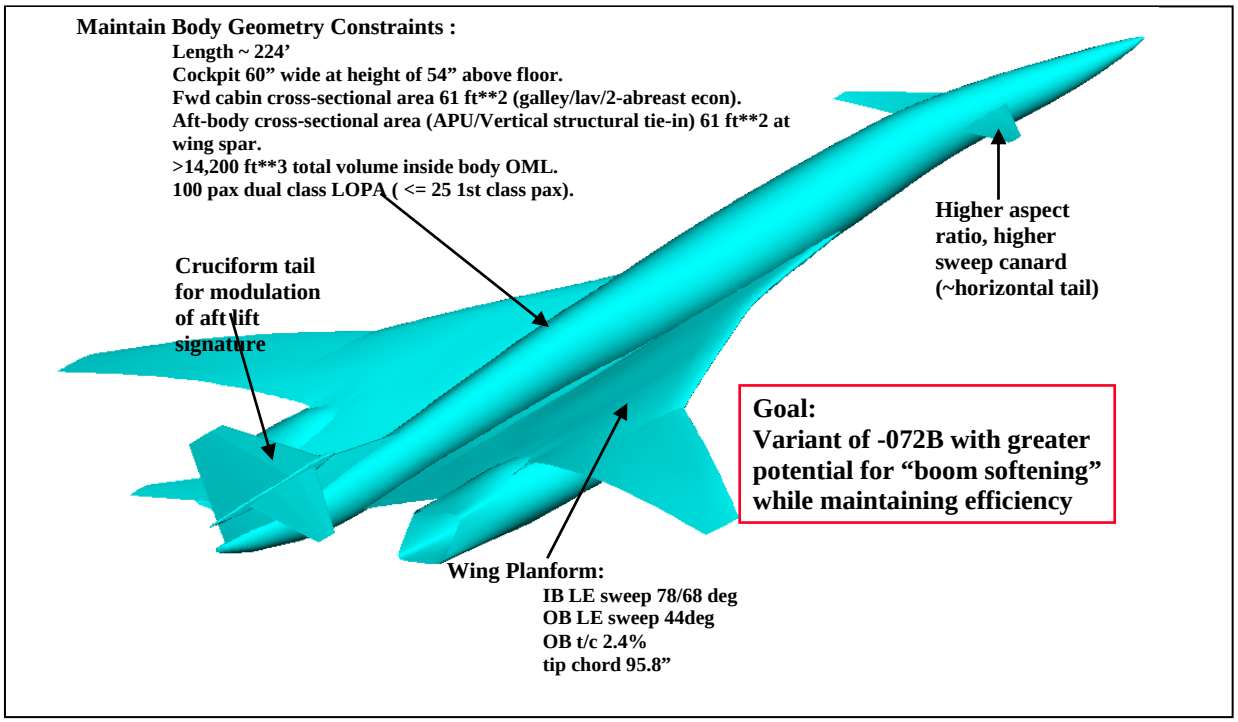

Figure 2.2.10.1 Features of the 765-078 boom softening airplanes.

model	DATA TABLE (as drawn airplane)				
Model 765-078A	Wing		Horizontal	Canard	Vertical
ITEM	ESDU	Total	Tail		Tail
Area to CL	4016.675	4366.2	161.99	300.84	409.14
Exposed			161.99	300.84	387.78
Reference	4016.675		161.99	300.84	387.78
Aspect Ratio	3.00	3.43	3.15	3.15	2.000
Taper Ratio	0.122449	-	0.25	3.150	0.241
LE Sweep angle		0.00	48	48	58
Dihedral, TE	12	55	10	0	0
T/C	0.024	0.024	0.000		0.030
Tail Volume		0.205	0.090	0.115	0.1355
Span , in	1317.84	903.808	271.07	369.41	236.31
Root Chord, In	782.0418	788.66	137.69	187.63	391.70
Tip Chord, in	95.76	56.000	34.42	46.91	94.52
M.A.C. IN	528.3255	728.109	96.38	131.34	273.38
X 1/4 mac	1713.465	1563.924	540.31	2525.89	2455.02
Y, Zmac	243.6007		96.213896	79.881	136.08
Tail Arm, IN.			1173.16	812.42	741.5502

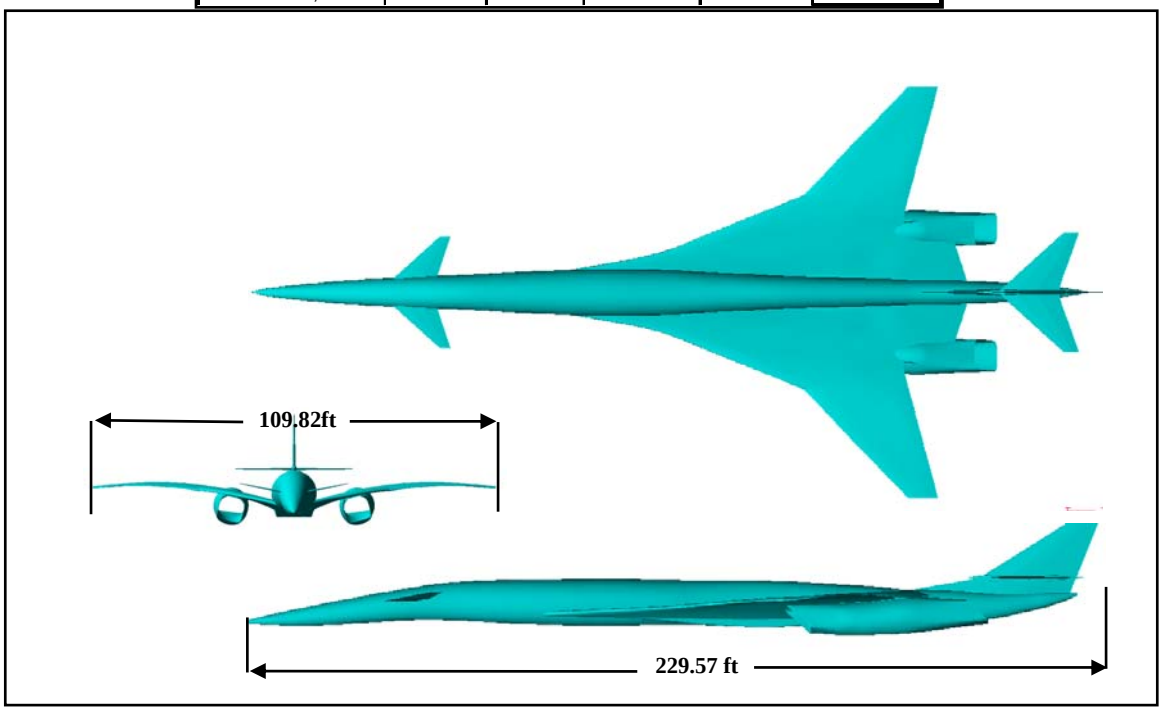

Figure 2.2.10.2 765-078A 3-view and characteristics.

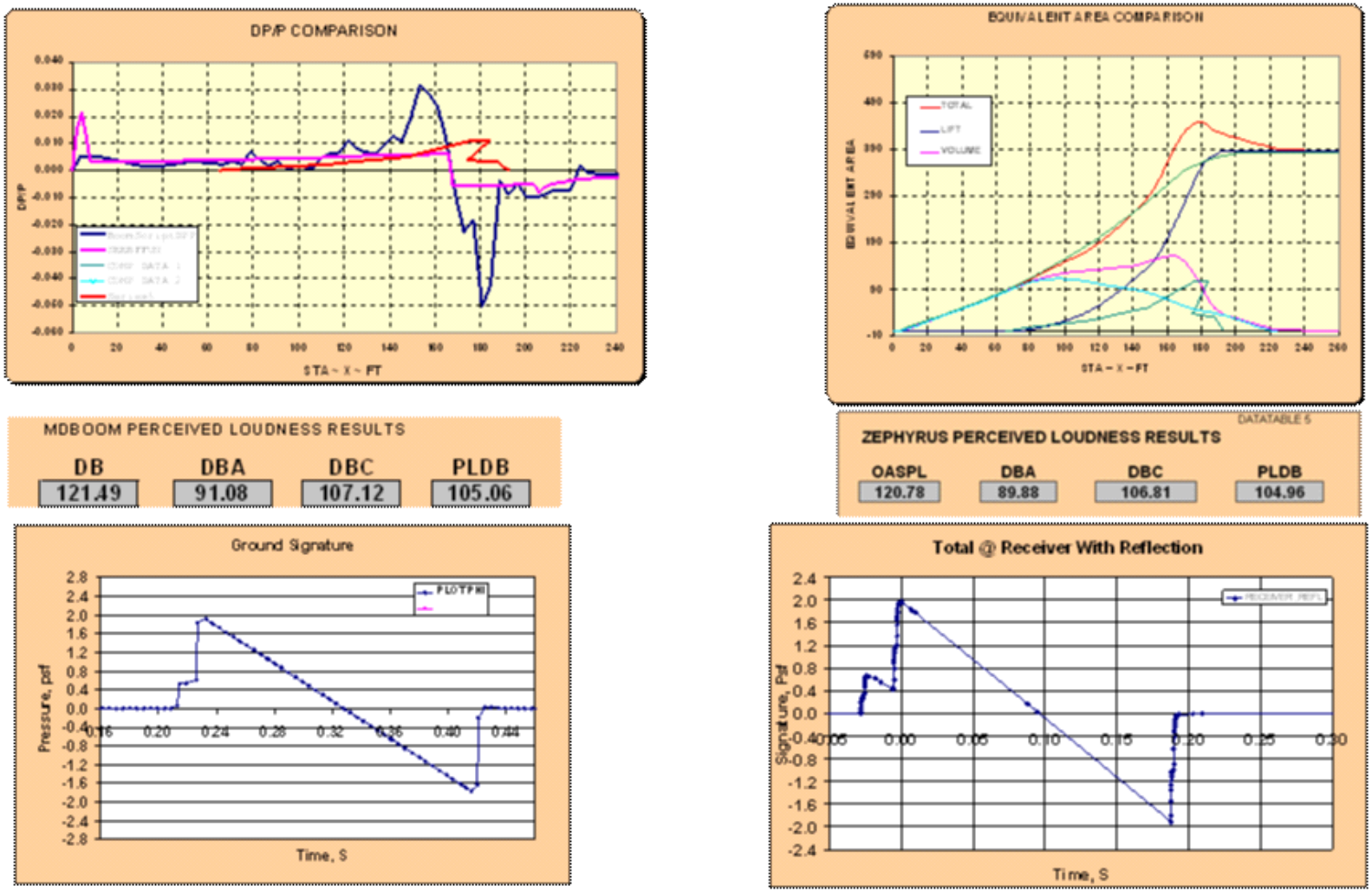

Figure 2.2.10.3 MDboom and Zephyrus predictions of boom for the 765-078A, M=1.8, 270,000lb, 51,000ft.

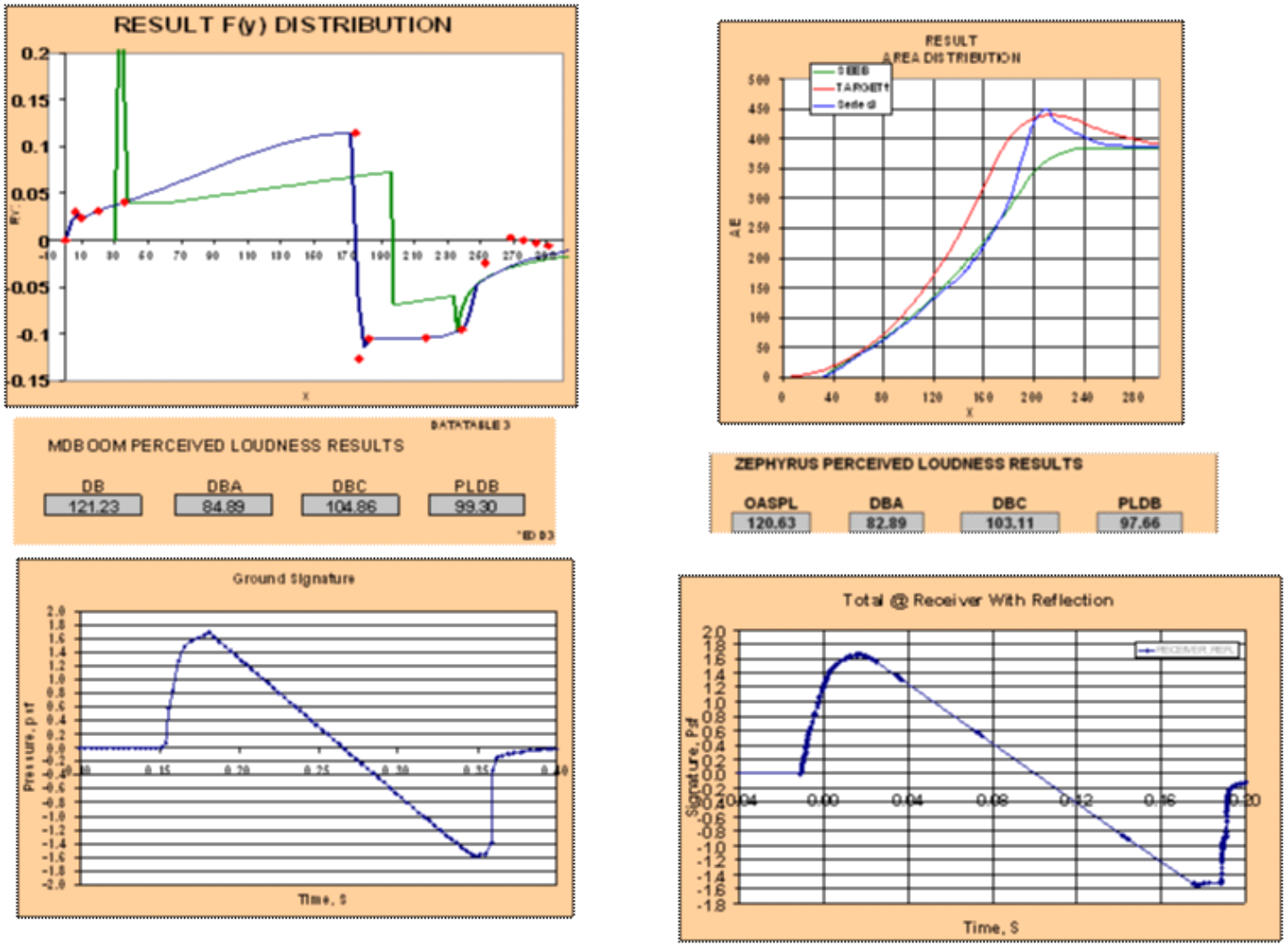

Figure 2.2.10.4 MDboom and Zephyrus predictions of boom for the 765-078B, M=1.8, 270,000lb, 51,000ft.

model	DATA TABLE (as drawn airplane)				
Model765-076E	Wing		V-tail	Aft Deck	Vertical
ITEM	ESDU	Total		flaperon	Tail
Area to CL	2516.509	2707.4	377.48		
Exposed			377.48		
Reference	2516.509		377.48	303.79	
Aspect Ratio	2.94	3.43	3.15	2.88	
Taper Ratio	0.171792	-	0.198	0.368	
LE Sweep angle		0.00	48	0	
Dihedral, TE	12	50	45	12	
T/C	0.024	0.024	0.030		
Tail Volume		0.283	0.146	0.1369	
Span , in	1033.032	903.808	413.79	354.77	
Root Chord, In	598.7239	788.66	219.35	180.29	
Tip Chord, in	102.856	56.000	43.38	66.32	
M.A.C. IN	409.2022	548.097	151.01	132.08	
X 1/4 mac	1243.924	1140.999	1641.14	1707.97	
Y, Zmac	197.4135		262.93	75.030	
Tail Arm, IN.			397.2	464.04	

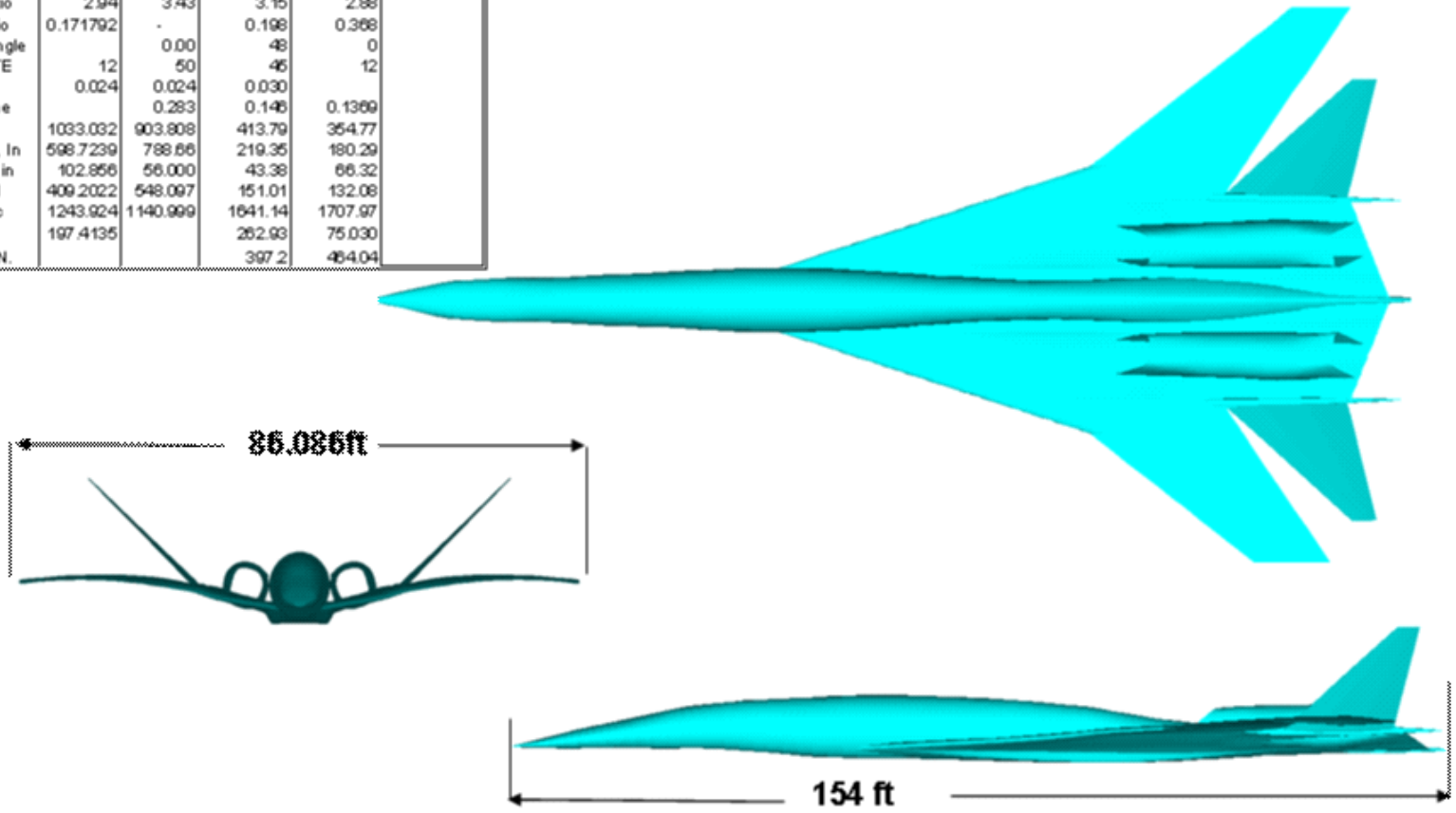

Figure 2.3.1 765-076E

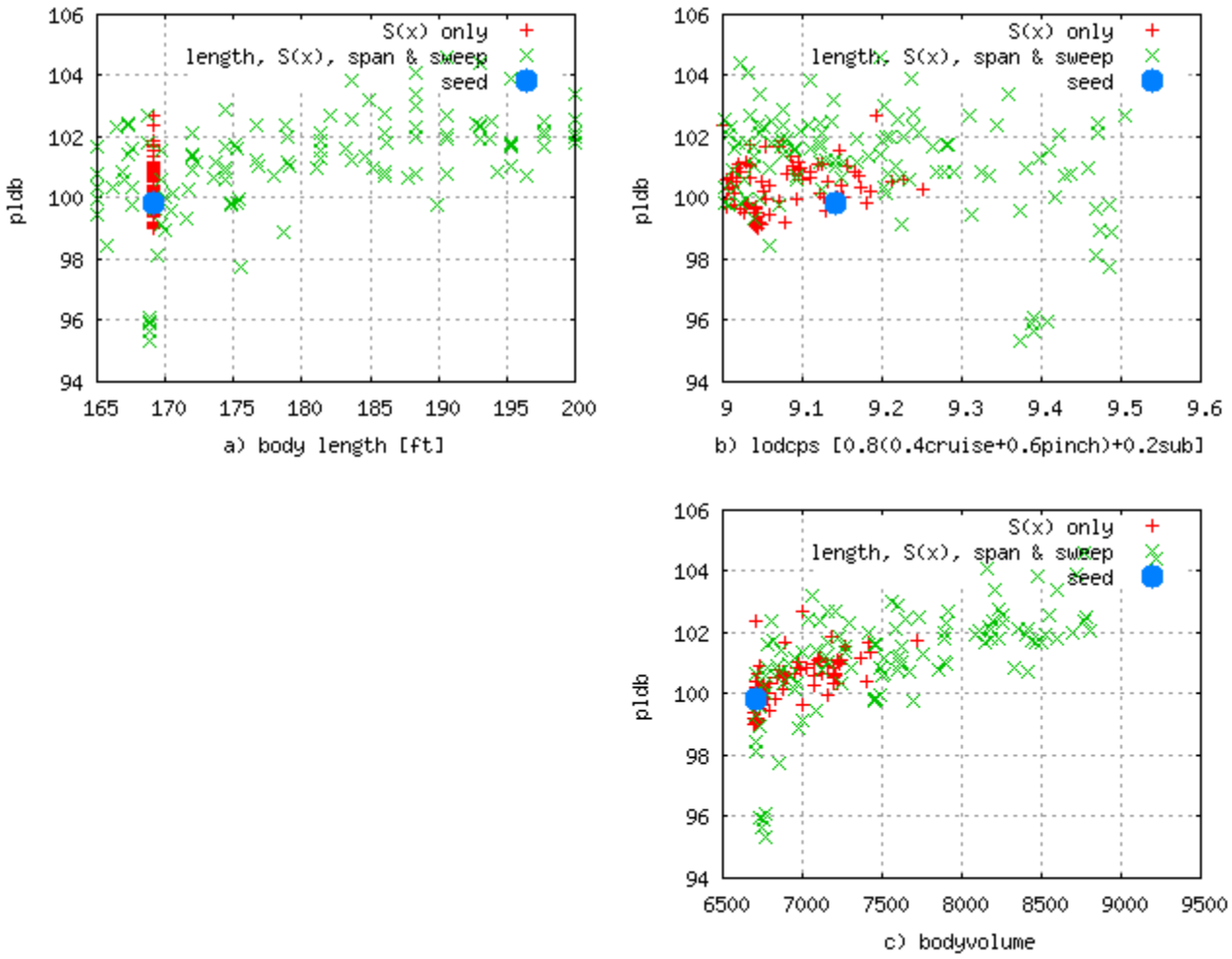

Figure 2.3.1.1 Early 765-076 study minimizing PLdB via body cross-section only (red +); and via body cross-section, body length, wing span and sweep (green x).

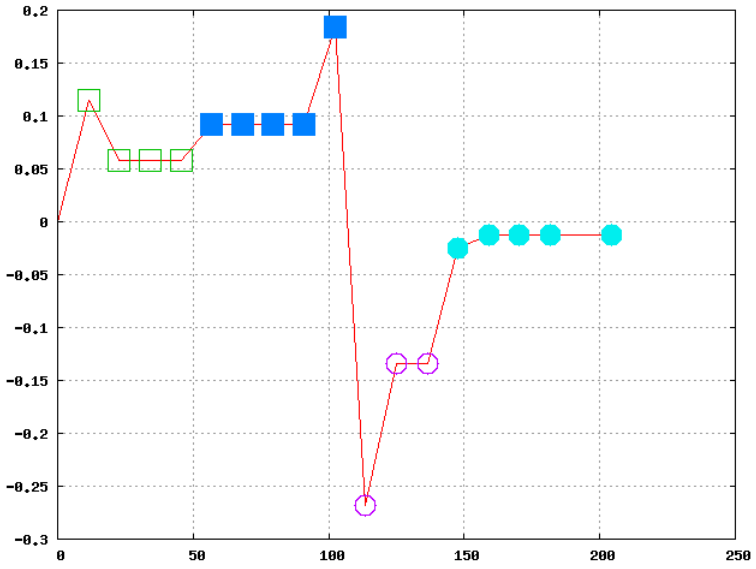

Figure 2.3.1.2 Typical parametrized F-function.

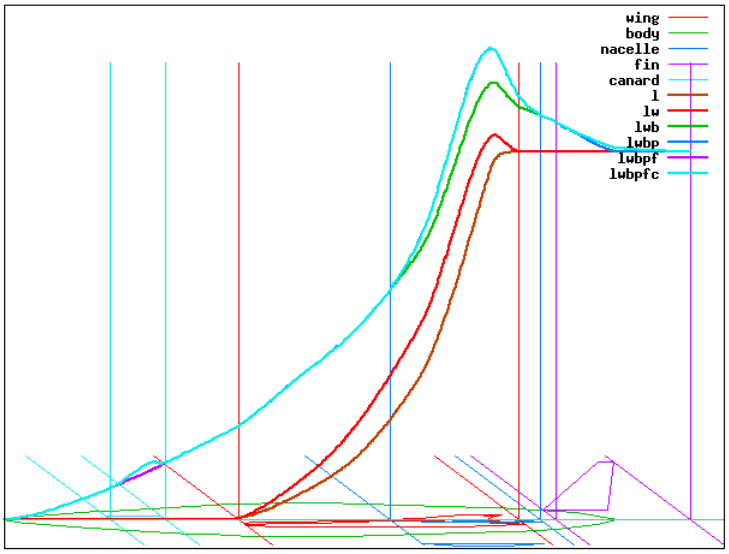

Figure 2.3.1.3 Mach-plane cuts through an actual geometry, and the corresponding features in the equivalent area distribution.

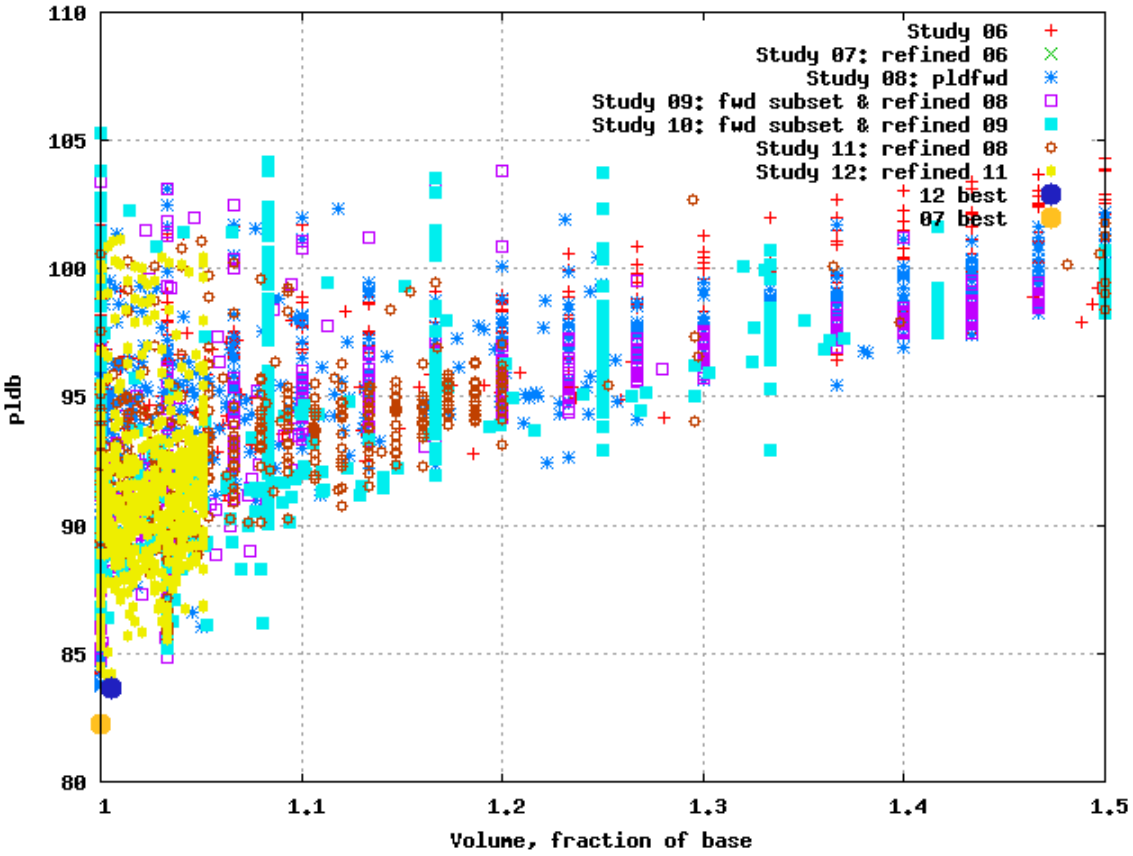

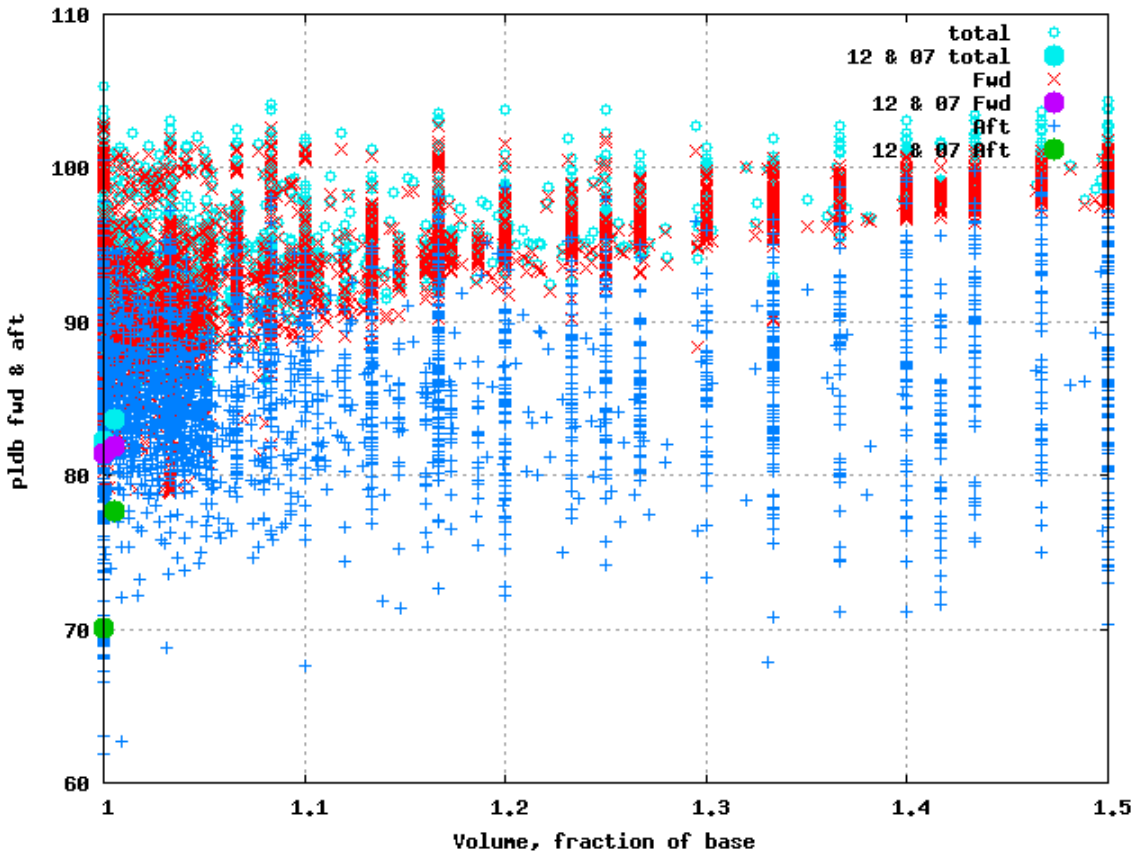

Figure 2.3.1.4 Data from studies of boom reduction potential for airplanes of the 765-076 size and configuration. Boom PLdB was minimized using parametrized F-function with constraints on equivalent area. a) PLdB versus overall volume of the equivalent body (volume + lift), as fraction of the baseline volume. b) Forward and aft components of PLdB versus volume.

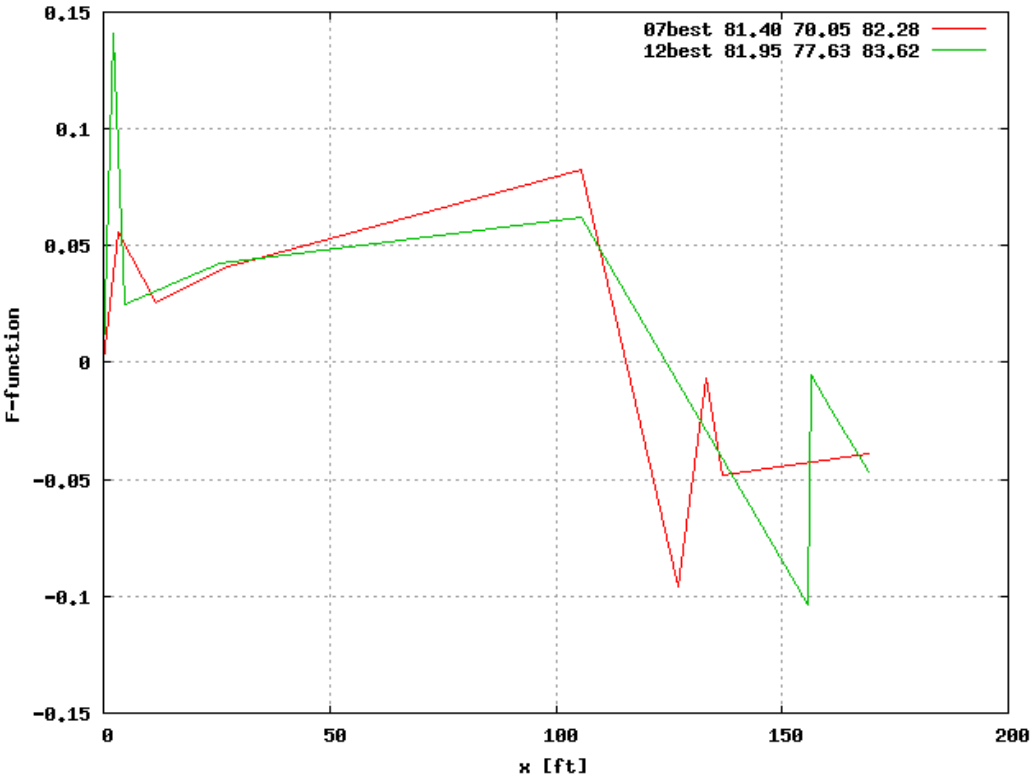

Figure 2.3.1.5 F-function of two best points from studies shown in Figure 2.3.1.4

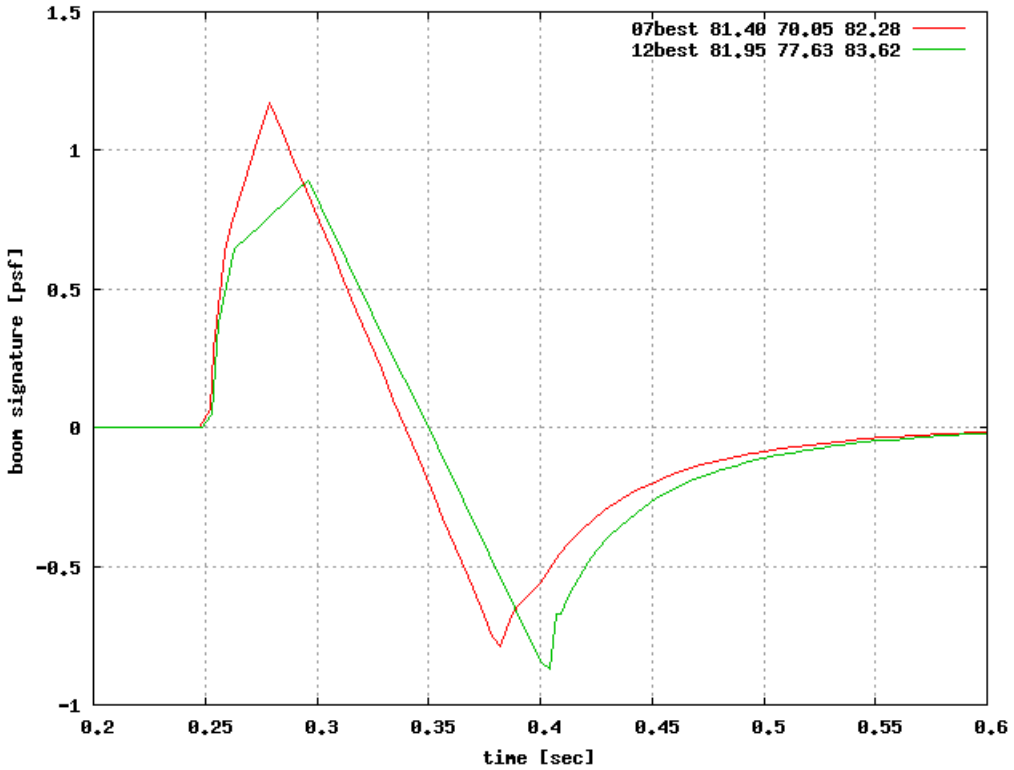

Figure 2.3.1.6 Ground signature from 50,000ft, according to MDboom, of the two best points from study shown in Figure 2.3.1.4.

Table 2.3.2.1. Pressure Drag variation with CG according to Tranair on Design 3.

Design	Cw	CC	Color	ΔCG to trim
076z3 (mod. no V-tail design)	-0.01485	0.000488	Green	3.5% aft
076z4 (43 wtV-tail mod./best design)	-0.01189	0.000125	Blue	2.8% aft
076v1 (1.6 deg more incidence than d4)	-0.01611	0.000489	Red	4.0% aft
076v2 (1 deg more incidence than d4	-0.02061	0.000284	Cyan	5.4% aft

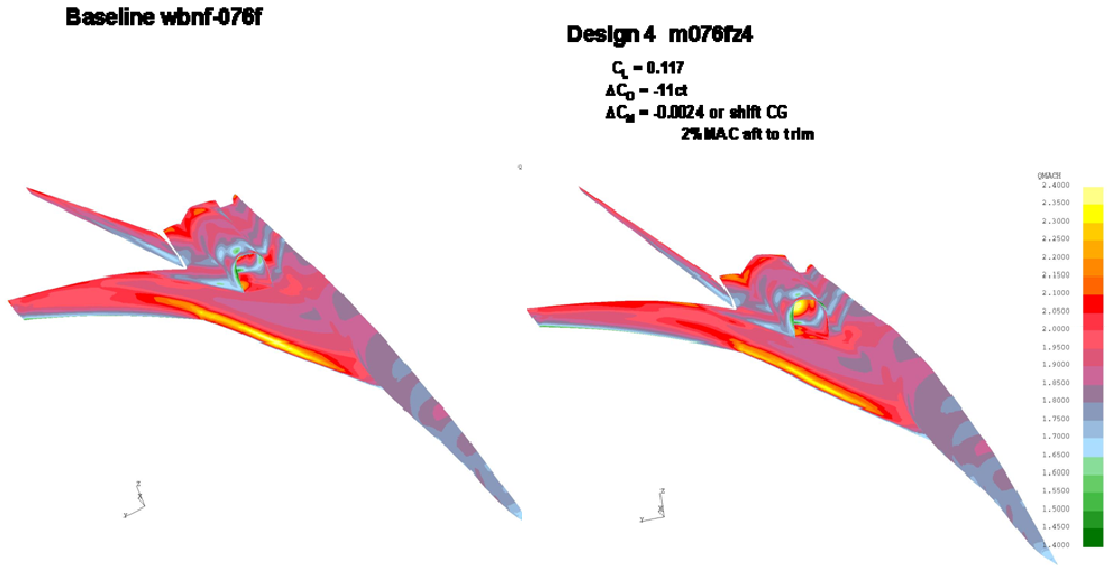

Figure 2.3.2.1 Contours of local Mach number from Tranair on baseline and Tranair designed configurations.

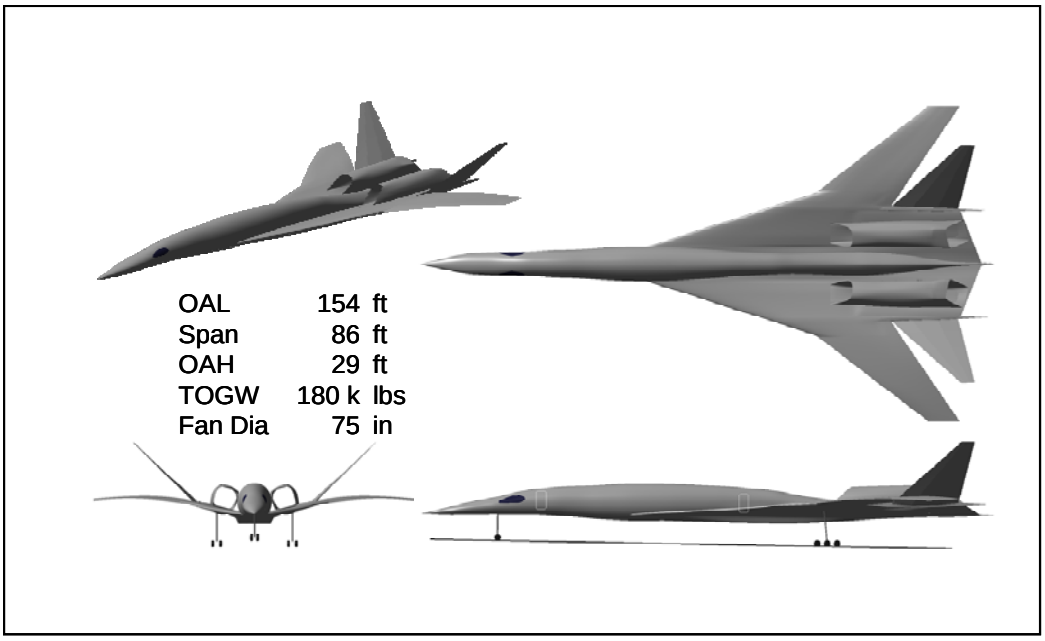

Figure 2.3.2.2 765-076E External Views

Configuration	V1.2 Mar 16 BSE 04B Engine
Wing Area (ESDU)	2517
Wing Area (Gross)	3344
Thrust per engine	**43,000**
Fan Diameter (in)	75.4
Engine Weight	9612
TOGW	171,793
OEW	92,950
Payload	6,300
Total Fuel	73,171
Block Fuel	62,029
Range	**3200***
Supersonic Cruise	
Mach	1.6
Altitude	49,895
Weight	159,939
CL	0.1457
L/D	8.513
SFC	0.9237
Climb (pinch point)	
Mach	1.13
Altitude	40,550
Weight	163,691
CL	0.1910
L/D	8.506
Thrust	19,966
SFC	0.9183
ROC	302
Bal Field Dist. (100% pwr)	5309 (58%)
W/S (takeoff)	68.3
FOM	1.55

Mach 1.6, 30 PAX, variable range

* Range and fuel load reduced until 300 fpm ROC constraint is met

Figure 2.3.2.3 765-076E Performance Summary

model	DATA TABLE (as drawn airplane)				
Model 765-076F	Wing		V-tail	Aft Deck	Vertical
ITEM	ESDU	Total		flaperon	Tail
Area to CL	2516.509	2707.4	377.48		
Exposed			377.48		
Reference	2516.509		377.48	303.79	
Aspect Ratio	2.94	3.43	3.15	2.88	
Taper Ratio	0.171792	-	0.198	0.368	
LE Sweep angle		0.00	48	0	
Dihedral, TE	12	50	45	12	
T/C	0.024	0.024	0.030		
Tail Volume		0.283	0.146	0.1369	
Span , in	1033.032	903.808	413.79	354.77	
Root Chord, In	598.7239	788.66	219.35	180.29	
Tip Chord, in	102.856	56.000	43.38	66.32	
M.A.C. IN	409.2022	548.097	151.01	132.08	
X 1/4 mac	1483.924	1380.999	1881.14	1947.97	
Y, Zmac	197.4135		262.85	75.030	
Tail Arm, IN.			397.2	464.04	

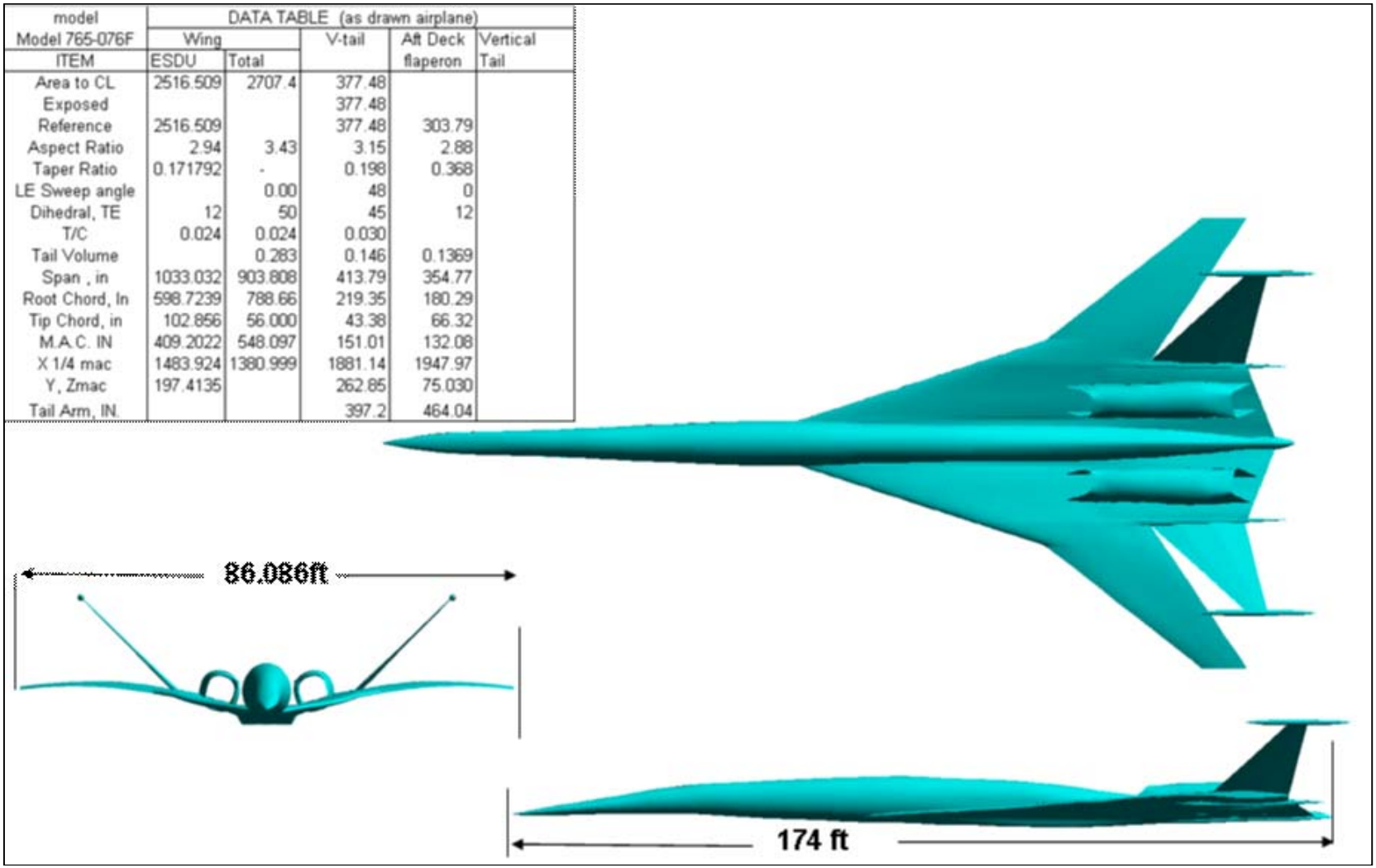

Figure 2.3.3.1 765-076F configuration.

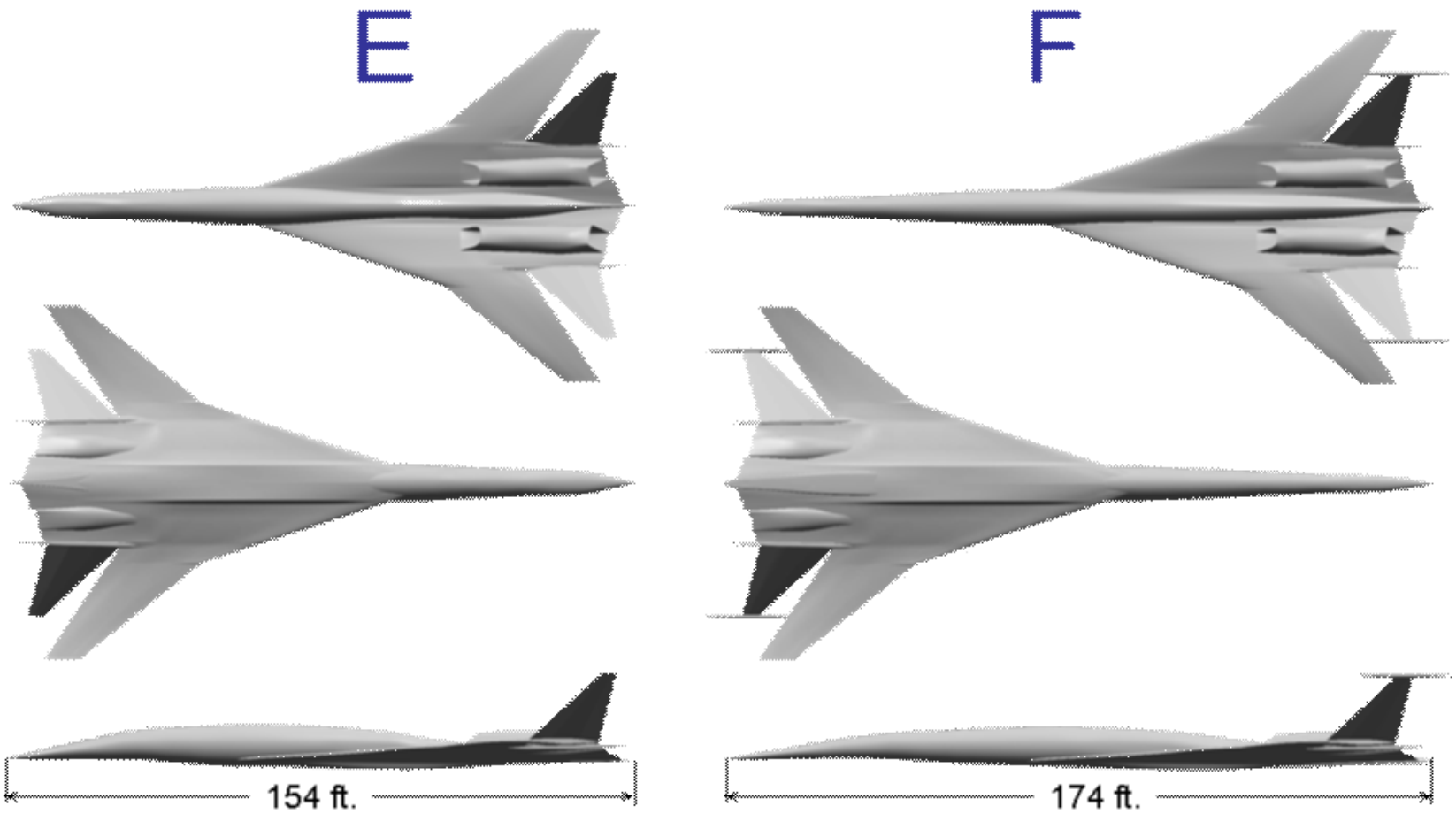

Figure 2.3-2. 765-076E and -076F Geometry Comparison

MDBOOM PERCEIVED LOUDNESS RESULTS

DB	DBA	DBC	PLDB
113.33	74.54	97.35	89.97

ZEPHYRUS PERCEIVED LOUDNESS RESULTS

OASPL	DBA	DBC	PLDB
113.13	70.91	94.68	85.15

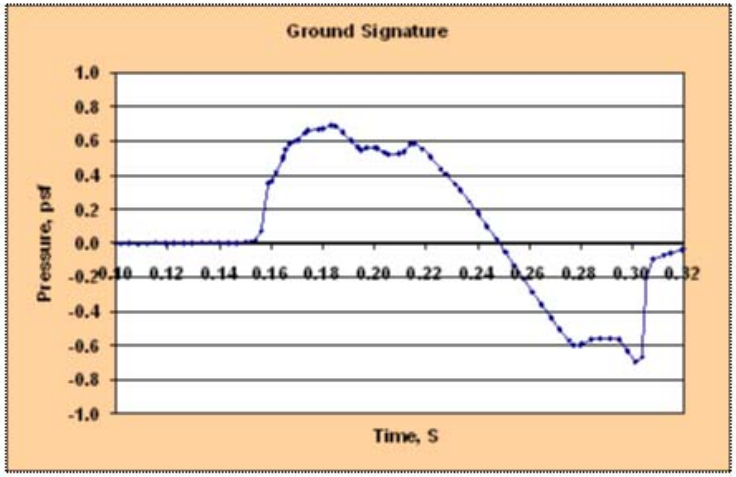

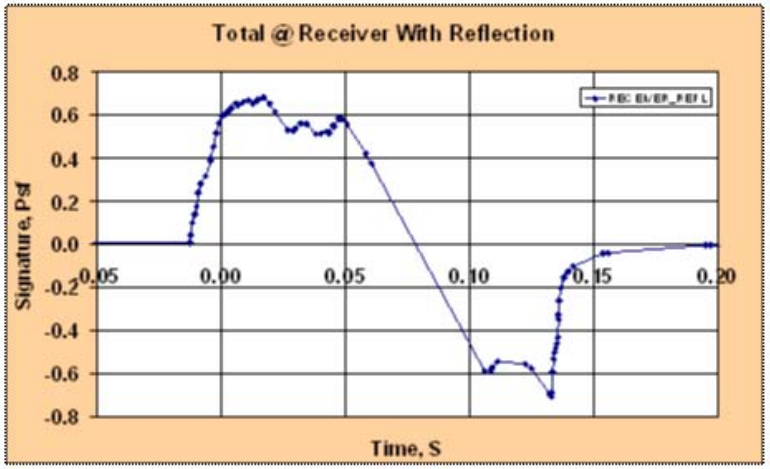

Figure 2.3.3.3 Boom PLdB and ground signature for the 765-076F.

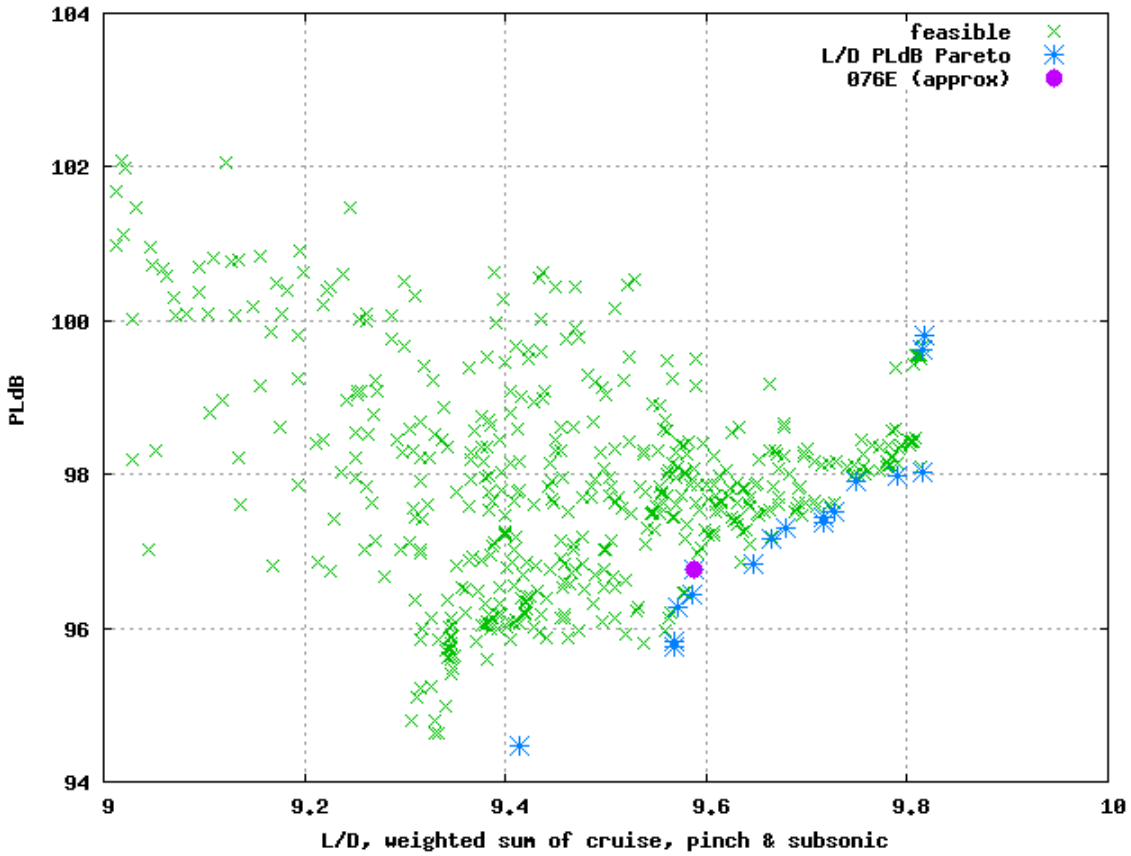

Figure 2.3.3.4 Pareto optimization starting from the 765-076E. Minimizes PLdB and maximizes L/D using body design variable while constraining cabin volume and overall body volume to be at least the baseline.

3.0 Propulsion Development

3.1 Trade Space Study Engines

The initial concept development work prior to final downselect employed proprietary Boeing Study Engines (BSE). They were selected by choosing a relevant airframe configuration, installing one of several available engines, then sizing both thrust and wing area to maximize range. Any other impact on the configuration was also assessed in case it might change the simple conclusion that range decides the best engine.

As an example, various engines were installed on the 1080-2015 ("2015TC") airframe and wing area and thrust were sized to maximize range at various Mach for 300,000lb MTOW. Figure 3.1.1 shows the resulting range. For this airframe, the BSE-2 engine provides superior range at Mach 1.8, and seems to be the natural choice. Figure 3.1.2 also supports the BSE-2 engine because wing area is minimized, suggesting minimum airframe weight. Also on the plot, in the gray patches at the ends of some bars, is evidence that wing area can vary, in concert with the engine, without greatly affecting range. But even the lower end of that range is not lower than the BSE-2 for all engines except the BSE-1601, and that engine provides significantly less range. Figure 3.1.3 shows the resulting thrust, and concludes the engine selection with the BSE-2 having the minimum sea level static thrust. Conventionally, that means the BSE-2 engine should be lighter and cost less than the others.

An identical exercise was performed with a different set of smaller engines installed on a smaller aft wing airplane at 180,000lb MTOW in an effort to choose a best engine for studying the 30 passenger low boom concept.

For the engine cycle trades in Section 2.0, a series of six candidate engines cycles were developed by Georgia Institude of Technology (GIT), three from P&W and three from RR, were evaluated. These were provided to the MDAO model in the form of installed thrust and fuel flow tables for a reference thrust. Results from those engines have been shown in Section 2.0.

3.2 RR NPSS Development and Cycle Trade Parameters

Georgia Tech, with guidance from Rolls Royce, the only participant in Option 2, modeled a dual spool, mixed-flow turbofan (MFTF) engine with a high pressure ratio fan. The MFTF architecture was selected because it is a proven architecture that has been used for years, and its modeling characteristics are well understood. A simple, block schematic of the MFTF is shown in Figure 3.2.1 – NPSS Model Schematic. The engine technologies, such as component efficiency, were modeled using public domain data which was then modified to reflect the technology level that will be ready for entry into service in the 2025 timeframe. Georgia Tech iterated with Rolls Royce until both groups thought that the technology levels modeled were appropriate. A list of all duct pressure drops and component design efficiencies can be found in Table 3.2.1 – MFTF Design Point Efficiencies for 072B Study (Including Tech Level Effects). The baseline efficiencies are not tied to a particular year, and may be adjusted by the *Technology Level Effects* described in Table 3.2.2. The *Technology Level Effect* used for the 072B and 076E configurations is 3.0.
The NPSS model was created using several modularized function files that allowed for easy updates to the model as new data or results were made available. A brief description of the NPSS file naming convention is shown in Table 3.2.3 – NPSS File Naming Convention.

3.2.1 - Engine Cycle Set-up and Control Methodology

MFTF Cycle Setup at SLS

The MFTF is a parametric model that allows the user to select values for the cycle parameters listed in Table 3.2.4. These parameters were chosen because they have the largest impact on engine characteristics of importance to this study including specific thrust, specific fuel consumption, lapse rate, fan diameter, and jet velocity. The NPSS solver is used to satisfy all of the following conditions at the SLS cycle setup point. These are high level discussions; however more detailed descriptions of the engine model are presented in subsequent sections.

- FPR is set directly from the user input.
- OPR is set directly from the user input by varying the on design HPC pressure ratio.
- Maximum T41 is a constraint and is used during maximum power calculations throughout flight envelope including takeoff conditions.
- Throttle ratio is used to set T41 at the SLS condition.
- Net Thrust at SLS is set by varying the SLS engine mass flow.
- Bypass ratio is varied by the solver until the user input extraction ratio is achieved.
- The cooling flows are sized using Equation in conjunction with Figure 3.2.2 through Figure 3.2.5. A fixed value of maximum T3 is used to size the cooling flows for all engine cycles. This was done to facilitate numerical convergence and decrease run time.
- During cycle setup the engine design point efficiencies from Table 3.2.1 are used. Size effects from Figure 3.2.6 through Figure 3.2.13 are applied to the base efficiencies.
- The engine is sized with the inlet installed.

Off-Design Operation

In off design mode the NPSS solver is reconfigured to calculate engine operating parameters, namely thrust and fuel flow, at any given ambient conditions.

- Maximum Power / Maximum Cruise / Maximum Climb
  - Vary fuel flow to run to 100% corrected fan speed unless constrained by max T4.1 limit or max T3 limit.
  - Exhaust nozzle throat area varied to maintain 22% Fan SMN.
- Part Power
  - Fuel flow is varied to run to desired percentage of max power net thrust.
  - Exhaust nozzle throat is area held fixed at current maximum power value.
- Throttle Hook
  - Function to run several points from max power to idle power to generate “hooks” at a specified altitude and Mach number
    - Runs Engine at maximum power.
    - Computes thrust target = max power thrust * percentage.
    - Executes model at desired part power setting.
  - The main use of this function is to generate thrust and fuel flow data for the Cases engine data pack.

Inlet Sizing and Operation

The inlet capture area is sized at a user specified top of climb altitude and Mach number. After the initial engine setup at SLS conditions the engine is ‘flown’ to the top of climb and run at maximum power. The inlet capture area is varied by the NPSS solver until the inlet size is matched to the cruise conditions using the recommended Mass Flow Ratio (MFR) from the inlet maps. This minimizes spillage drag and ensures better installed engine performance. Inlet performance is calculated during off-design using inlet recovery, spillage drag, bleed drag, and bypass drag maps provided by Boeing, shown in Figure 3.2.14, Figure 3.2.15, and Figure 3.2.16.

Nozzle Gross Thrust Coefficient

Nozzle losses were modeled using a gross thrust coefficient, or C_{fg}. Boeing provided a nozzle C_{fg} curve which provides the gross thrust coefficient as a function of nozzle pressure ratio. NPSS calculates nozzle pressure ratio at a given flight condition; the corresponding C_{fg} is then applied to the gross thrust in order to account for losses. Figure 3.2.17 shows the variation of C_{fg} with nozzle pressure ratio.

Takeoff De-rating

In the 072B initial studies, summarized in Table 3.2.5, the MFTF could not simultaneously satisfy the vehicle range, fan diameter, and takeoff jet velocity requirements. Further investigation revealed that the flight condition that constrained the engine size was usually the top of climb point; this resulted in excess thrust at the takeoff condition. Since the aircraft did not need maximum available power to meet the 10,000 ft takeoff field length requirement the engine could be de-rated for takeoff conditions. A user specified jet velocity input was created that limits the engine takeoff power to meet the user input. This allowed the MDO environment to conduct trade studies between takeoff field length and jet velocity. Jet velocity was chosen as a parameter because it is directly related to the jet noise requirement. The de-rating logic is as follows:

- Once engine is setup it is run in off design mode at the takeoff condition. (1,000 ft / 0.255 Mach)
- The engine is then throttled back until the specified exit jet velocity is attained.
- The corrected fan speed at this de-rated power is recorded as pcn2takeoff.
- For the takeoff power flight envelope the engine is operated by varying the fuel flow until the corrected fan speed is equal to pcn2takeoff.

Creating the CASES Engine Data Pack

The CASES data pack allows for different thrust and fuel flow values to be specified for takeoff, climb, and cruise. Maximum cruise and climb were both defined by the maximum power definition discussed previously. If the engine is de-rated to a particular takeoff jet velocity then the de-rating logic is used to determine takeoff power available, otherwise takeoff is defined as normal maximum power operation. Throttle hooks are generated for each flight condition defined in the flight envelope in Figure 3.2.18.

3.2.2 Parametric Model Effects

Several "public domain" curves were used in order to account parametric effects as the engine cycle was changed. For example, the leakage cooling flows are dependent on the combustor exit temperature. Iteration with Rolls Royce occurred until they were satisfied that the "public domain" curves represented the appropriate technology levels without divulging proprietary information. The following effects are included in the engine model:

- HPC Size Effect
- HPT and LPT Size Effects
- Technology Levels
- Fan, HPC, HPT, and LPT Reynolds Effects
- HPT and LPT Cooling Flows
- Fan and HPC Loading (Effect of design point efficiency vs. design pressure ratio)
- Weight Estimation

HPC Size Effects

The HPC size effect data came from a NASA report by Niedzwiecki, titled "Small Engine Technology Programs". The "current technology" curve shown in Figure 3.2.19 was selected from the report and the

only adjustment was to convert the polytropic efficiency to a delta on adiabatic efficiency. This was necessary because NPSS uses adiabatic efficiency in map and performance calculations.

Turbine Size Effects

The HPT and LPT size effect data came from a NASA report by Niedzwiecki, titled ""Small Engine Technology Programs". The '*current technology'* curve shown in Figure 3.2.20 the corrected flow axis to represent 40 lbm/s and 10 lbm/s, respectively.

Technology Levels

The technology levels are adders relative to a fixed baseline value. By changing the overall technology level of the engine all of the components are adjusted simultaneously.

Reynolds Effects

Reynolds effects were based on Bullock's "Analysis of Re and Scale Effects on Performance of Turbomachinery" (J. Engineering for Power, July 1964, pp.247-256). Equation describes the Reynolds effect calculation implemented in the MFTF. The NPSS model also has relationships to relate the flow and pressure ratio scalars to the efficiency adder. These are shown in the equations below. Graphs of the resulting Reynolds effects for each component were shown in Figure 3.2.6 through Figure 3.2.13. The NPSS compressor and turbine elements and Reynolds number sockets were modified to accept these curves.

$$\frac{1-\eta}{1-\eta_{RNI=1.0}} = RNI^{-0.2}$$

Equation 3.2.1 MFTF Reynolds Effects Equation

$$s\_w_P = s\_eff = 1+\frac{\Delta\eta}{\eta}$$

$$s\_\mathrm{Pr} = s\_w_P$$

Equation 3.2.2 MFTF Reynolds Effects on Pressure Ratio and Flow Rate

Turbine Cooling

A Coolit type algorithm is used with a cooling effectiveness factor of 1.0. This is equivalent to full coverage film cooling. The cooling logic in the MFTF takes the single blade row cooling calculations from Coolit and adapts them to a "Total Chargeable Cooling" curve. This assumes the chargeable cooling curves apply to the HPT first row blade and that the HPT first row blade accounts for 30% of the total turbine cooling. A metal temperature of 2000ºF is used to calculate the required cooling. This metal temperature was chosen because it represents the compromise between an aggressive temperature for a nickel based alloy, and a conservative temperature for a CMC material.

$$\phi = \frac{\left(T_{4.1,Max} + \Delta Deterioration\right) - T_{metal}}{T_{4.1,Max} - \left(T_{3,Max} - CCA\_\Delta T\right)}$$

Equation 3.2.3 Cooling Effectiveness

The curve for total chargeable cooling is shown in Figure 3.2.2. Cooling effectiveness is defined in Equation above.

Total Leakage is defined as a linear function of the Turbine Rotor Inlet Temperature and is shown in Figure 3.2.3.

Total cooling flow, shown in Figure 3.2.4, was distributed across the HPT and LPT to provide reasonable levels of cooling for the temperatures being investigated. The fractions in Figure 3.2.4 are multiplied by the total cooling air fraction obtained from Figure 3.2.2 to obtain the cooling flow for each component. The

fractions listed in Figure 3.2.5 represent the corresponding leakage flow distribution and are multiplied by the total leakage obtained from Figure 3.2.3 to set the leakage flow.

Fan and Compressor Loading

The fan and HPC polytropic efficiencies are parametric functions of the fan and compressor loading. A loading curve from Hill & Peterson, *Mechanics & Thermodynamics of Propulsion* (Addison-Wesley, 2nd edition, 1992) was supplemented with data from Creason & Baghdadi, *Design and Test of a Low Aspect Ratio Fan Stage*, AIAA paper 88-2816. This provided the fan and HPC loading curves shown in Figure 3.2.21. Since the Fan Pressure Ratio (FPR) varied from 1.8 to 3.0, the multistage fan loading curve was used.

Weight Estimation

Weight estimates are based on a simplified methodology provided by Rolls Royce and described by the equations below. The equations use basic flow scaling of components and Georgia Tech modified the reference values based on previous experiments with WATE++ studies. The reference values used in the various weight equations are found in Table 3.2.6. Specific works per stage values came from matching known cycles to stage counts for various engines. Since these values came from current engines they may be somewhat conservative for the N+2 timeframe.

$$\sum(\text{Turbomachinery Wts}) + \text{CDN Wt} + \text{AGB Wt} + \text{Misc Wt}$$

Equation 3.2.4 MFTF Weight Estimation Equation

$$\frac{\text{Weight}}{\text{Weight\_Ref}} = \left(\frac{\text{Wc}}{\text{Wc\_Ref}}\right)^{1.1} * \left(\frac{\text{Nstg}}{\text{Nstg\_Ref}}\right)^{n}$$

Equation 3.2.5 Turbomachinery Weight Equation

$$\text{Nstg} = \frac{\text{SpecifcWork}}{(\text{SpecificWork/Stage})}$$

Equation 3.2.6 Stage Count Equation

$$\frac{\text{CDN\_Weight}}{\text{Weight\_Ref}} = \left(\frac{\text{HPC\_Exit\_W c}}{\text{Wc\_Ref}}\right)^{1.1}$$

Equation 3.2.7 CDN Weight Equation

$$\frac{\text{AGB\_Weight}}{\text{Weight\_Ref}} = \left(\frac{\text{HPC\_Inlet\_ Wc}}{\text{Wc\_Ref}}\right)^{1.1}$$

Equation 3.2.8 AGB Weight Equation

$$\frac{\text{Misc\_Weigh t}}{\text{Weight\_Ref}} = \left(\frac{\text{HPC\_Inlet\_ Wc}}{\text{Wc\_Ref}}\right)^{1.1}$$

Equation 3.2.9 Misc Weight Equation

3.2.3 - MFTF Configuration and Cycle Selection for the 072B

Georgia Tech investigated the design space shown in Table 3.2.4 to find three candidate engine cycles for the 072B. From initial design space explorations it was found that the range of cycle parameters shown in Table 3.2.4 provides good performance for the 072B configuration. It was not possible to create an engine cycle with the assumed technology levels that simultaneously satisfied the jet velocity, fan diameter,

mission fuel burn requirements, and vehicle thrust requirements. For this reason Georgia Tech provided three engine cycles for mission analysis, one which met the jet velocity constraint, one which came closer to the fan diameter constraint, and one which was a compromise between the two objectives. This allowed Boeing to perform the trades required to determine which cycle was the best selection for the 072B. These cycles are not optimum solutions since they are a result of a discrete search of the design space; however, they are still useful in performing trade studies and may be good candidates as initial conditions in a gradient based search.

For the design space exploration 10,000 engine cycles were run using a Latin Hypercube which is a type of Design of Experiments, or DoE. By using a DoE the design space can be intelligently explored with far fewer engine cycles than would be required with a random grid search. A multivariate plot of the complete design space with all cycle inputs and relevant outputs such as fan diameter, SFC, and jet velocity is shown in Figure 3.2.22.

Cycles that did not meet the thrust requirements of the 072B at various flight conditions were filtered out of the design space, shown in Figure 3.2.23. The absolute minimum jet velocity of the cycles that survived the thrust requirement filtering was 1258 ft/s which did not meet the requirement of 1100 ft/s. The minimum fan diameter remaining was 86 inches which did satisfy the constraint imposed by Boeing for the 072B.

In order to select the three cycles to provide to Boeing, Georgia Tech examined the fan diameter and jet velocity Pareto front shown in Figure 3.2.24. Three cycles were selected, the ones with absolute minimum fan diameter, absolute minimum jet velocity, and a compromise solution. In Figure 3.2.24 these cycles are represented with the labels Case A, Case B, and Case C respectively. The compromise solution was selected using TOPSIS, or Technique for Order Preference by Similarity to Ideal Solution. By weighting the relevant importance of jet velocity and fan diameter a TOPSIS finds the cycle with the closest Euclidian distance to the ideal solutions of 1100 ft/s and 86". The three selected cycles and their performance is summarized in Table 3.2.5 and Table 3.2.7. As is to be expected the low fan diameter cycle has the highest FPR and a correspondingly high jet velocity. Also of interest is that the compromise cycle, Case C in Figure 3.2.3.3, has a lower maximum T4.1 than the other two selected cycles. This is because these cycles resulted from a discrete search of the design space. There are other cycles that are very close to Case C on the Pareto front that have different maximum T4.1's. This reiterates that need to use these cycles as initial points in a further MDO optimization.

3.2.4 - MFTF Updates for 076E Configuration

Minor updates to the MFTF NPSS model were made for the study of the low-boom 076E configuration. After discussing the results of the 072B study internally and with feedback from Rolls Royce, Georgia Tech reached the conclusion that the technology levels used in the 072B version of the MFTF were too conservative. The base efficiencies of the turbomachinery components and the burner were increased. The new efficiencies for the engines used in the 076E study are shown in Table 3.2.8. The efficiencies reflect the baseline efficiency added to the technology effect previously discussed in Section *3.2.2 Parametric Model Effects*.

3.3 The coupled NPSS/MDA Tool

The integration of NPSS into the MDAO process allowed the capability to optimize engine-airframe combination in a way previously unavailable. Without NPSS, the ModelCenter model used assumed nacelle scaling correlations to grow and shrink the nacelle based on the thrust required, while the thrust and fuel flow for the engine was merely scaled within CASES. NPSS allowed an engine deck to be created with each iteration, providing a more accurate sized engine for different thrust requirements. As the reference thrust for the engine deck is the required thrust, there is no longer any need to scale thrust and fuel flow in CASES, increasing the accuracy of the analysis. In addition, NPSS estimates the engine diameter, which allows more accurate inputs to geometry than the assumed correlations.

For the 765-072B configuration, the nacelle geometry was allowed to change with changes to the engine parameters, which provided a wide design space for the parametric engine. A weight was estimated based on an engine thrust-to-weight assumption of between 4.25 and 5.0.

When the 765-076E configuration was analyzed, an addition to NPSS was made available that estimated the engine weight internally, removing the necessity to roughly estimate engine weight based on thrust-to-weight. The 765-076E outer-mold-lines were fixed because of the low-boom requirements, and so the nacelle diameter was not allowed to grow, though it was allowed to shrink.

The first integration was between NPSS and the -072B species MDAO model. To check out this integration, we chose to do a comparison between the vehicle performance from the GTRR Compromise engine cycle dataset provided for the downselect trade studies (Section 2.0) and the NPSS output simulating the cycle inputs for this engine. On any design study, things are constantly changing, so it was impossible to do a completely "apples to apples" comparison. For example, the mission calculations had been revised to incorporate a maximum cruise altitude constraint of 55,000 ft (lower than optimum), which came out of the Market Study. The NPSS model had also been updated with lessons learned from the mid-term review, so the same inputs would not exactly produce the same outputs. Finally, the -072B MDAO aerodynamics analysis had been updated slightly as a result of completing the model validation exercise.

Figure 3.3.1 shows a comparison of the (updated) vehicle characteristics with the GTRR compromise engine (Column 1) to the NPSS generated engine with the same cycle inputs (Column 2). In both examples the thrust and wing area had been resized to meet the ROC and W/S constraints. No attempt was made here to derate the engine for takeoff. So the balanced field distances shown are for an engine at 100% power. The conclusion is that with the revised NPSS deck integrated into the MDAO model requires about 5% more thrust for the same cycle parameters. This additional thrust results in a slightly larger engine, higher TOGW, more fuel and larger wing to meet the same aircraft performance requirements. The resulting FOM drops from 3.44 to 3.06.

3.4 072B Optimization

For the cycle optimization with the -072B species MDAO model, the primary objective was to maximize FOM. This optimization would be subject to several constraints, as follows.

- ROC greater than 300 fpm anywhere in the mission
- Sufficient fuel volume in the wing (desired) or no more than 47,200 lbs of fuel in the fuselage, below the passenger compartment (required)
- Takeoff W/S less than 78 psf (approximates a 155 kt approach speed)
- Balanced field distance less than 10,000 ft
- Takeoff Vj less than 1100 fps (derated)

Initial attempts at the optimization showed that the design space did not have any feasible solutions for a 10,000 ft balanced field distance with 1100 fps Vj. Therefore, Vj was changed from a constraint to an optimization goal. Thus we now had a multiple objective optimization problem.

The selected optimizer for this study was Design Explorer. This is a Boeing developed optimizer, which has been licensed to Phoenix Integration for use in Model Center. The optimizer uses an algorithm (SEQOPT) that is more effective on "noisy" data or design spaces with multiple peaks and valleys than a traditional gradient search algorithm. Design Explorer has a limitation of a single objective function. Since we had a multi-objective optimization, we elected to conduct the following three optimizations and compare the results.

- Maximize FOM
- Minimize Vj
- Maximize FOM/Vj

We anticipated that each of these would result in a significantly different "optimum" engine cycle.

The design variables for the optimization and their allowable ranges are as follows.

	Lower	Upper
• Fan Pressure Ratio (Fan_PR)	1.8	2.9
• Overall Pressure Ratio (Overall_PR)	25	35
• Extraction Ratio	0.9	1.1
• Max Turbine Temperature (Max_T41) (deg R)	2700	3700
• Throttle Ratio	1	1.2
• Inlet Design Altitude (ft)	40,000	55,000
• Jet Velocity (Vj) (fps)	1100	2000
• Net Thrust (lbs)	50,000	70,000
• Wing Area (sgross_ft)	4000	6000

The limits for the cycle design variables were established by Georgia Tech and Rolls Royce as representative of N+2 technology level. The limits for thrust and wing area were chosen based on experience from the earlier trade studies. The upper limit for the inlet design altitude was the same as the max cruise altitude constraint. We observed that the inlet design altitude always optimized at the upper limit of 55,000 ft. It was eventually eliminated as a design variable and simply set at 55,000 ft. This reduced the dimensionality of the optimization problem. The lower limit for the jet velocity was the project goal for takeoff. The upper limit was made as low as possible, but still result is feasible design solutions for the 10,000 ft balanced field distance. The reader will note that Vj is both a design variable and an optimization objective. There are actually two Vj design variables in the NPSS model (zVjet, Vj). One is an input and the other is an output. When the NPSS derate switch is turned on, these two variables are made equal. For the maximize FOM the derate switch was turned off. For the other two optimizations, the derate switch was turned on.

The optimization needs a set of starting values for the design variables. It seems to work better if the set results in a feasible design. The values for the GTRR Compromise engine from the trade study analysis were used as the starting point. This concept does not exactly match the concept shown in Figure 3.3.1 because the inlet design point was changed from Mach 1.8, 43000 ft to Mach 1.6, 55,000 ft for this comparison. This concept was designated the Benchmark. Each of the optimizations was compared to it to determine if it improved FOM, Vj, or both. For design space with many peaks and valley, it is possible that a different starting point for the design point for the design variables will result in a different optimum solution. This is known as a local optimum, as opposed for the global optimum that we hoped to find. In a large, multi-dimensional design space is very difficult to determine for sure if an optimization has found a true global optimum. For this study, once an optimum was found, we tried a couple of different starting points to see if they would arrive at the same optimum solution. This is clearly not a rigorous way to make the determination, but it provided some level of confidence that a global optimum was obtained.

The results of the first optimization to maximize the FOM are shown in Figure 3.4.1, along with the Benchmark GTRR compromise engine cycle. The optimization changed all the design variables with a significant increase in fan pressure ratio and Max T41. This allowed the thrust and wing area to be reduced, while still meeting the constraints. The FOM for the optimum concept increased from 3.14 to 3.43. However, the Vj also increased from 1375 to 1640 fps for a 10,000 ft balanced field distance with a derated engine.

The results of the second optimization to minimize Vj are shown in Figure 3.4.2 along with the Benchmark. The optimization again changed all of the design variables. The max T41 was again significantly increased. This time, however, the fan and overall pressure ratios were reduced. The required thrust increased, but the wing area decreased. The optimized FOM increased slightly from 3.14 to 3.17 and the optimized Vj significantly dropped from 1375 to 1194 fps for a 10,000 ft balanced field distance with a derated engine. The Vj did not achieve the goal of 1100 fps.

The results of the third optimization to maximize FOM/Vj are shown in Figure 3.4.3 along with the Benchmark. The optimization again changed all of the design variables. The max T41 went to the limit of 3700 deg R. The overall pressure ratio increased, but the fan pressure ratio decreased. The required thrust

increased, but the wing area decreased. The optimized FOM increased from 3.14 to 3.22 and the Vj dropped from 1375 to 1204 fps.

The three optimizations are shown compared to each other in Figure 3.4.4. In deciding how to choose from the three optimizations for the competing objectives, we observed that all resulted in an FOM greater than the project goal of 3. None resulted in a Vj below the project goal of 1100 fps. Therefore, we selected the optimization that provided the lowest Vj (optimization 2 – minimize Vj).

Appendix 1 contains some visual details of the 072B.

3.5 076E Optimization

As discussed in section 2.3.4, the -076E species MDAO model had fixed external mold lines and a maximum allowable takeoff gross weight, due to the boom signature constraints. This meant that the optimization objectives, constraints, and design variables would be different for the -076E. The -072B optimization used a fixed 4000 nm range and variable TOGW, while the -076E has a fixed 180,000 lb maximum TOGW and a variable range. We elected to conduct the following three optimization for the -076E and compare the results.

- Maximize Range
- Minimize Vj
- Maximize Range/Vj

. This optimization would be subject to several constraints, as follows.

- ROC greater than 300 fpm anywhere in the mission
- Sufficient fuel volume in the wing
- Takeoff W/S less than 78 psf (approximates a 155 kt approach speed)
- Balanced field distance less than 10,000 ft
- Fan diameter less than 75.4 inches
- TOGW less than 180,000 lbs

Many of these are the same constraints as for the -072B. The fan diameter constraint was added to reflect the fixed external mold lines of the -076E. The design variables for the optimization and their allowable ranges are as follows.

	Lower	Upper
Fan Pressure Ratio (Fan_PR)	1.9	3.4
Overall Pressure Ratio (Overall_PR)	20	50
Extraction Ratio	0.9	1.1
Max Turbine Temperature (Max_T41) (deg R)	2800	4000
Throttle Ratio	1	1.2
Jet Velocity (Vj) (fps)	1100	1300
Net Thrust (lbs)	30,000	50,000
Range (nm)	3500	4000

The limits for the cycle design variables were extended beyond what was used for the -072B by Georgia Tech and Rolls Royce after preliminary optimizations showed it would be difficult to find feasible solutions for the -076E. These limits are representative of something between N+2 and N+3 technology levels. The 4000 nm upper limit for the range was the recommended value from the earlier trade studies, while the 3500 nm lower limit was the least we could tolerate with a transcontinental mission. The thrust limits were what preliminary analyses showed would result in feasible designs. The 1100 fps lower limit for Vj was the project goal, while the 1300 fps upper limit was what preliminary analyses showed would result in feasible designs. The philosophy was that even while maximizing FOM, we didn't want the Vj to get too high. The wing area was eliminated as a design variable, due to the fixed external mold lines. The range is both a design variable and an optimization objective. In the MDAO model there is an input range and an

output range. The first is the design variable and the second is the objective. When the MDAO model iterates to close the mission solution, these two variables are made equal.

The starting point cycle for the -076E optimization was selected to be the optimum cycle from the -072B optimization the resulting concept is designated the Benchmark. The point of departure engine cycle for the -076E (Section 2.5) was the proprietary BSE 04B engine. It was not possible to simulate this cycle in NPSS for this non-proprietary study, so it was not used as the benchmark.

The results of the first optimization to maximize the FOM are shown in Figure 3.5.1, along with the Benchmark GTRR compromise engine cycle. For this optimal solution, the Max T41 went to its upper limit of 4000 deg R. The overall pressure ratio also increased, but the fan pressure ratio decreased. To meet the ROC constraint the thrust increased. The range increased from 3700 nm to 3910 nm. This is reasonably close to the goal of 4000 nm. The Vj decreased from 1510 to 1250 fps for a 10,000 ft balanced field distance with a derated engine.

The results of the second optimization to minimize Vj are shown in Figure 3.5.2 and yielded a significantly different cycle. Both the fan and overall pressure ratios decreased from the bench mark. The max T41 increased, but did not reach its limit. The range went to its lower limit of 3500 nm in an attempt to minimize the TOGW and thrust. The resulting Vj decreased from 1510 to 1164 fps, which is close to the project goal of 1100 fps.

The results of the third optimization to maximize range/Vj are shown in Figure 3.5.3 and again yielded a significantly different cycle. The max T41 again went to the upper limit of 4000 deg R. The overall pressure ratio increased, but the fan pressure ratio decreased. The thrust also increased. In this optimization, the range increased slightly from 3700 to 3799 nm and the Vj decreased significantly from 1510 to 1197 fps.

The three optimization results are compared in figure 3.5.4. There were two competing project objectives: 4000 nm range and 1100 fps Vj. None of the three optimizations achieved either of these objectives. The max range optimization achieved the best range, the min Vj optimization achieved the lowest Vj, and the max range/Vj optimization was a compromise. Without any clear knowledge of the relative importance of range versus Vj, we chose the compromise optimization 3 (max range/Vj) for the preferred engine cycle.

3.6 Selected Cycle Parameters

The selected optimum engine cycle parameters for the -072B and -076E concepts are as follows.

- 765-072B
  - Fan Pressure Ratio (Fan_PR) 2.10723
  - Overall Pressure Ratio (Overall_PR) 34.4961
  - Extraction Ratio 1.05938
  - Max Turbine Temperature (Max_T41) (deg R) 3666.8
  - Throttle Ratio 1.12539
  - Inlet Design Altitude (ft) 55,000
  - Derate Jet Velocity (Vj) (fps) 1194
  - Net Thrust (lbs) 64,688
- 765-076E
  - Fan Pressure Ratio (Fan_PR) 2.20176
  - Overall Pressure Ratio (Overall_PR) 39.2188
  - Extraction Ratio 0.9
  - Max Turbine Temperature (Max_T41) (deg R) 4000
  - Throttle Ratio 1.10039
  - Inlet Design Altitude (ft) 55,000
  - Derate Jet Velocity (Vj) (fps) 1197
  - Net Thrust (lbs) 41,133

Both the -072B and -076E are twin engine concepts. The -072B is a larger 100 passenger aircraft, while the -076E is a smaller 30 passenger aircraft. As expected, the -072B engine produces more thrust than the -076E engine. The -076E is a more constrained aircraft which required higher levels of Max T41, overall and fan pressure ratios in order to achieve reasonable flight performance.

The cycle selected by Boeing for the 076E configuration has a very high turbine inlet temperature of 4000ºR. For the 076E study Georgia Tech thought that by examining higher TIT's the resulting increased engine efficiency might help to bridge the gap between the vehicle performance and requirements. This high temperature takes advantage of future material technologies that will be present at the time of entry into service. The cooling flow model in NPSS assumes a metal temperature of 2460ºR. As discussed in *3.2.2 Parametric Model Effects*, this temperature, along with the appropriate cooling flows, is compatible with the material available in the N+2 timeframe. Due to the increased allowable metal temperature the total cooling and leakage flow for the selected cycle are at a reasonable value of 32.2% of the HPC inlet flow. Additionally the difference between the cooling gas temperature and gas path temperature is similar to current engines.

The MDO optimization chose a low FPR because it lowers the jet velocity by increasing the engine bypass ratio. The secondary effect of low FPR is a worse thrust lapse rate which means that the engine has to be even more oversized at takeoff to meet top of climb thrust requirements. Therefore the engine must be further de-rated to lower the jet velocity.

The throttle ratio corresponds to a theta break of approximately Mach 1.55 at the cruise altitudes. This is to be expected since the engine should be operating near the maximum T3 and T4.1 in order to achieve the best cycle efficiency.

The amount of cooling air required for the high TIT of 4000R may be reduced by the addition of cooled cooling air (CCA) technology. In the NPSS model provided to Boeing for the 076E study the CCA feature was not enabled; however the CCA feature is enabled in the final model delivered to Boeing. The CCA implementation, as shown in Figure 3.5.5, cools compressor discharge air using fan bypass duct air before it is used to cool the turbine blade. The reduction in cooling air required is accounted for by the CCA_ ΔT term in Equation 3.2.3.

To draw the 2-D flowpath of the down-selected cycle Georgia Tech elected to use NASA's WATE++ tool due to its integration with NPSS. Georgia Tech designed a flowpath using WATE++ and iterated with Rolls Royce until they were satisfied with the final WATE++ drawing. Rolls Royce used the final WATE++ output to draw the final CAD model.

Tables and Figures for Section 3.0

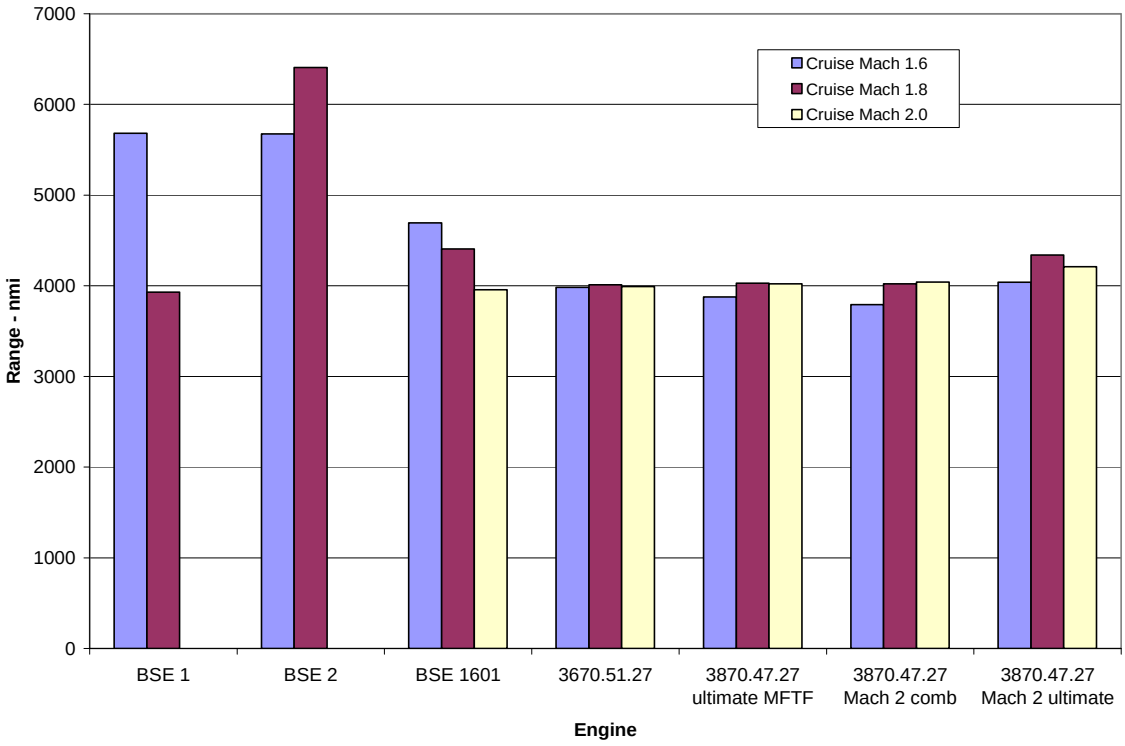

Figure 3.1.1 Thrust and area sizing results for various engines on a scaled 2015TC airframe.

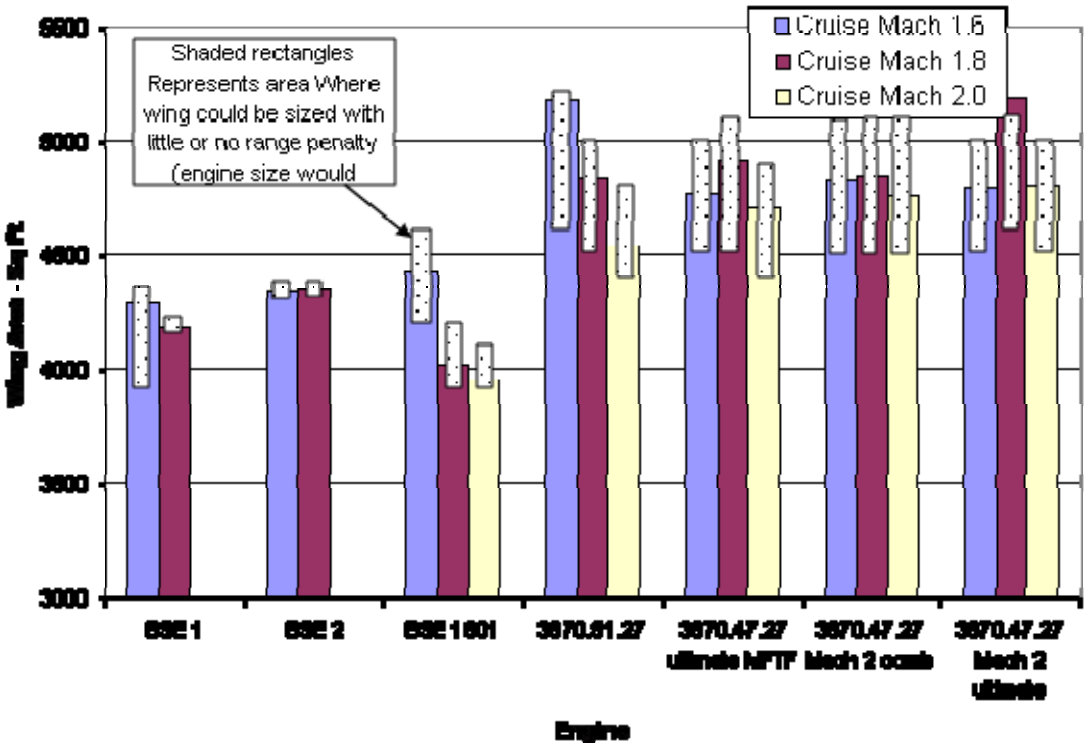

Figure 3.1.2. Wing area resulting from engine/airframe sizing on a scaled 2015TC airframe.

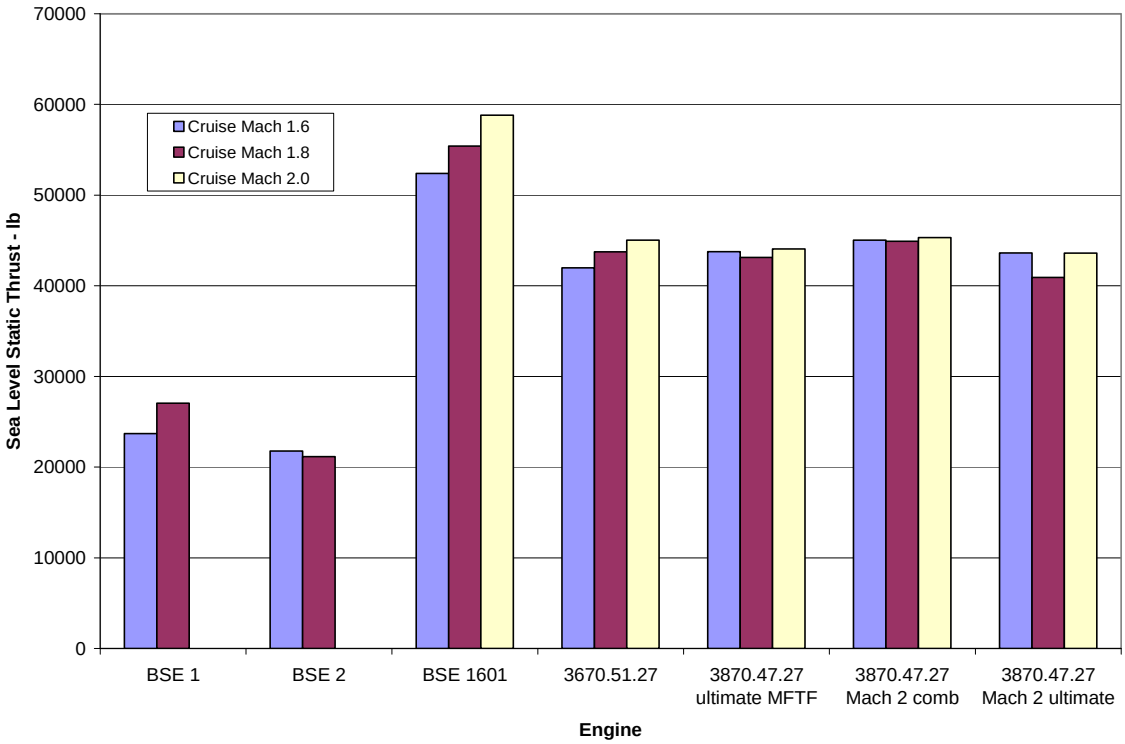

Figure 3.1.3. Thrust resulting from engine/airframe sizing on a scaled 2015TC airframe.

Table 3.2.1 MFTF Design Point Efficiencies for 072B Study (Including Tech Level Effects)

NPSS Component Name (Description)	Value
Duct1 (Swan Neck Duct)	Pressure loss = 1.0%
Fan design point efficiency	0.90 (polytropic)
Duct2 (HPC to Burner)	pressure loss = 2.0%
HPC design point efficiency	0.886 (polytropic)
Fuel LHV	18400
Burner efficiency	0.997
Burner design point	pressure loss = 2.7%
HPT design point efficiency	0.917 (adiabatic)
LPT design point efficiency	0.93 (adiabatic)
Duct3 (TEGV duct)	pressure loss = 1.0%
Duct5 (Bypass duct)	pressure loss = 5.0%
Duct4 (Tailpipe)	pressure loss = 0.5%
Nozzle	Discharge flow coefficient and velocity coefficient are functions of NPR. Curves were provided by Boeing.

Table 3.2.2 Technology Level Effects

Tech. Level	**Fan** η_{poly}	**HPC** η_{poly}	**Burner** η	**HPT** η_{ad}	**LPT** η_{ad}
0	0	0	0	0	0
1	0.008	0.012	0.002	0.01	0.01
2	0.016	0.025	0.005	0.03	0.02
3 (Study Value)	0.025	0.030	0.007	0.05	0.03
4	0.035	0.035	0.009	0.06	0.04

Table 3.2.3 NPSS File Naming Convention

GT MFTF NPSS Naming Convention	
.mdl file	Defines the engine model general configuration
.fnc files	Declares variables and defines functions used in the .run file
.run file	Executes the design and off-design points
.map files	Defines operating characteristics of the engine components
.view files	Defines the output files dynamically
.case_xxxx	Defines a set of flight conditions to execute the engine model.

Table 3.2.4 Rolls Royce MFTF Design Space for 072B

Rolls Royce MFTF Design Space	
Overall Pressure Ratio	26 – 36
Fan Pressure Ratio	1.8 – 3.0
Takeoff Thrust	68,000 –90,000 lbf
Extraction Ratio	0.9 – 1.1
T41 max	3000 – 3800 °R
Throttle Ratio	1.0 – 1.16

Table 3.2.5 Summary of Cycles Selected for MFTF/072B

	Low Fan Diameter	Low VJ	Compromise
Design FPR	2.94	2.25	2.48
Design OPR	29.46	31.26	32.95
Design TTR	1.05	1.07	1.05
Design EX TR	0.930	1.058	1.032
T4.1 Max (°R)	3668	3618	3523
Rated SLS FN	81648	89421	89475
Rated SLS SFC	0.5917	0.4849	0.512
Cruise SFC (start)	1.101	1.076	1.06
Design BPR	1.93	3.56	2.84
Design W2R	1425	2148	1932
Fan Diameter (in)	85.32	104.70	99.33
VJ @ 0K/0.25/52900	1715	1258	1375

Table 3.2.6 Weight Estimation Reference Values

Component	Weight_Ref	Wc_Ref	Nstg_Ref	SpecWork/Stg	n (Equation)
Fan	0.82	1.0	1	19.56	0.9
HPC	4.38	1.0	9	20.79	1.0
HPT	32.69	1.0	2	208.34	0.5
LPT	10.68	1.0	3	53.09	0.9
CDN	20.67	1.0	-	-	-
AGB	0.69	-	-	-	-
Misc	4.81	-	-	-	-

Table 3.2.7 Continued Summary of MFTF/072B Cycles

Altitude (ft)	Mach	Target FN (lbs)	Thrust Margin (%)		
			Case A	Case B	Case C
1,500	0.388	52,900	32.47	33.15	37.48
11,215	0.700	39,600	30.11	26.08	30.61
28,000	0.850	21,300	33.84	31.42	34.19
39,000	0.950	15,100	20.90	19.67	22.36
40,550	1.129	19,540	1.69	3.69	2.55
40,550	1.229	21,670	0.68	0.56	0.58
40,550	1.429	22,230	20.79	21.04	19.52
40,550	1.629	23,590	28.32	27.09	24.66
40,550	1.800	24,700	28.17	27.77	24.02
46,800	1.800	22,330	6.20	5.90	2.69
46,800	1.800	21,900	8.28	7.98	4.70
50,250	1.800	18,400	8.20	7.87	4.60
54,700	1.800	14,900	7.95	7.59	4.31

Table 3.2.8 Efficiency Updates to MFTF for 076E (Including Tech Level Effects)

Fan	0.905 (polytropic)
HPC	0.915 (polytropic)
HPT	0.92 (adiabatic)
LPT	0.93 (adiabatic)
Burner	0.997

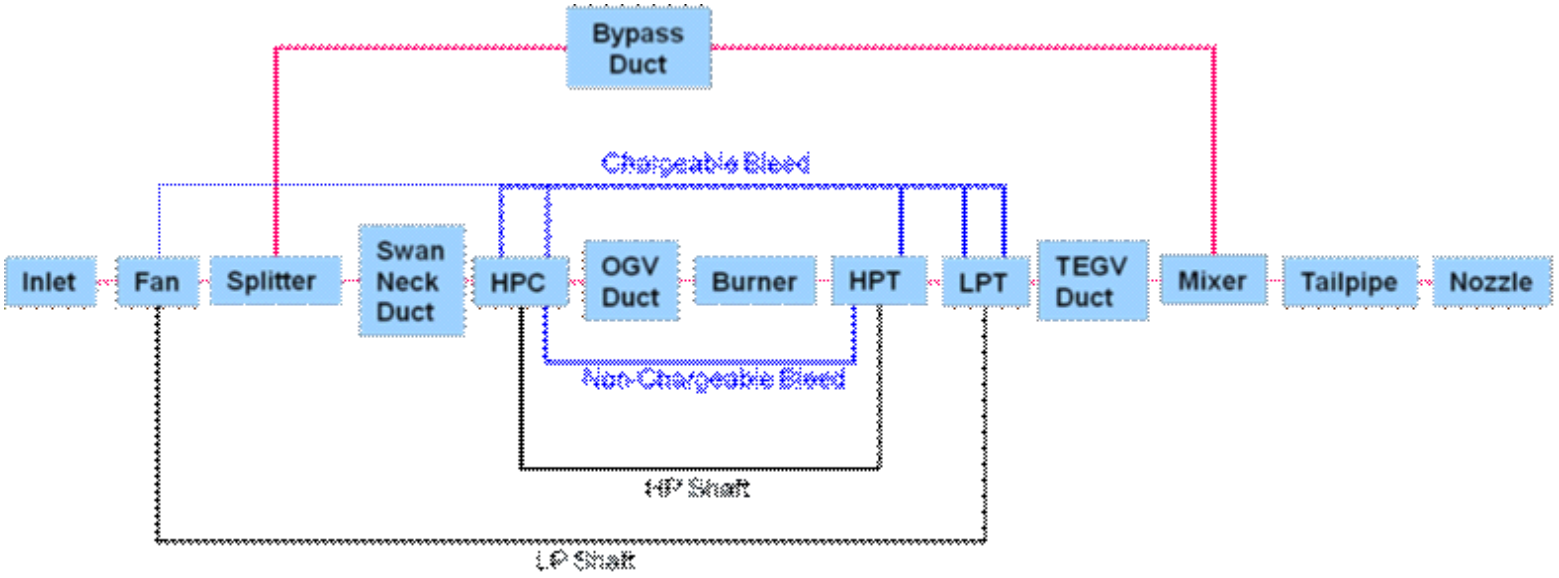

Figure 3.2.1 NPSS Model Schematic

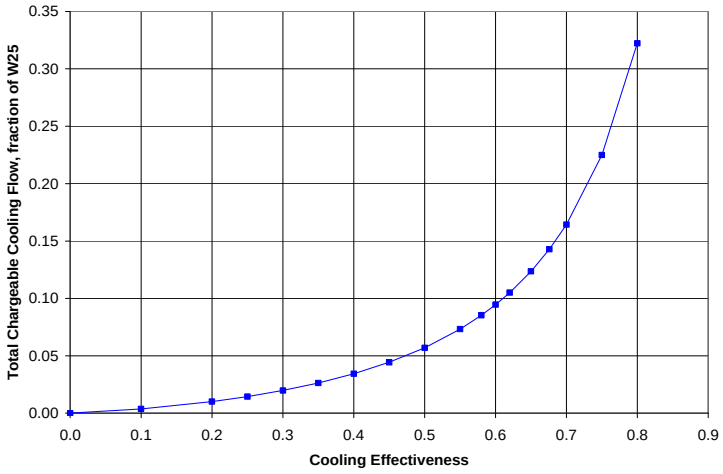

Figure 3.2.2 Total Chargeable Cooling

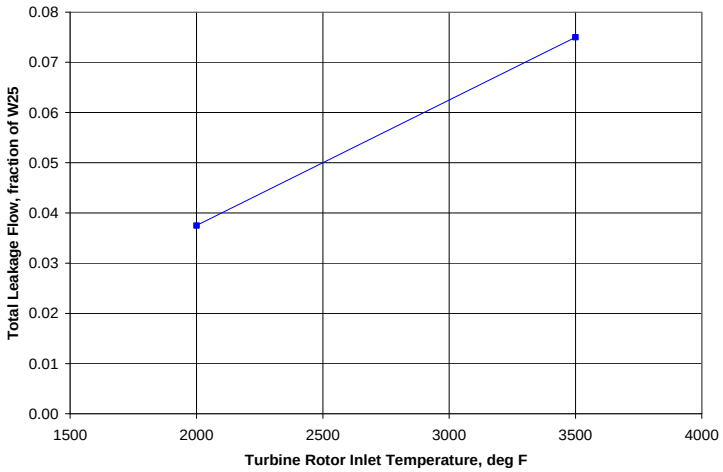

Figure 3.2.3 Turbine Total Leakage Flow

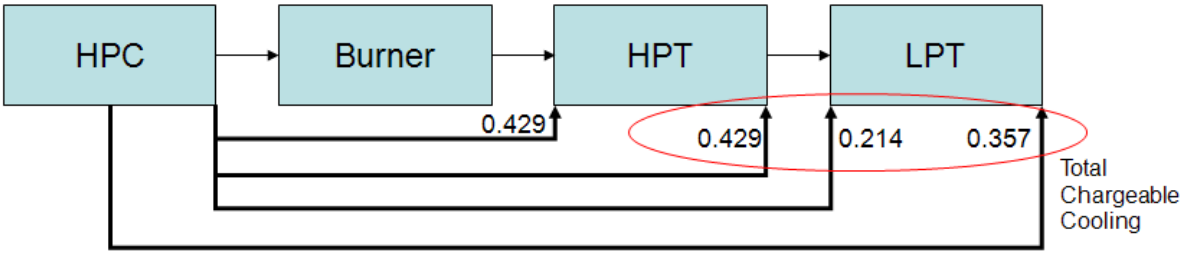

Figure 3.2.4 Turbine Cooling Flow Distribution

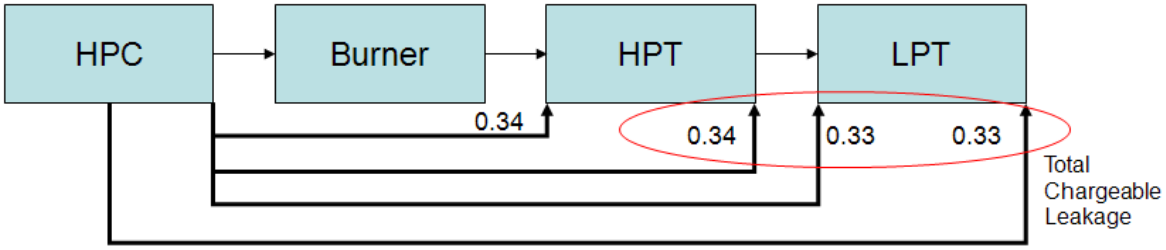

Figure 3.2.5 Turbine Chargeable Leakage Flow Distribution

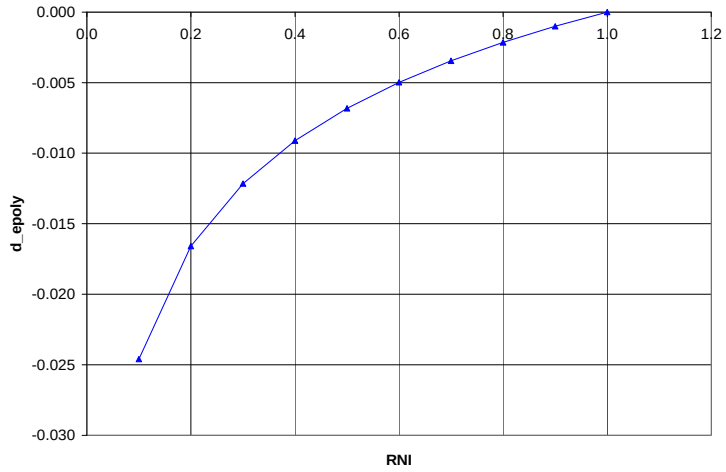

Figure 3.2.6 Fan Reynolds Effects (Efficiency)

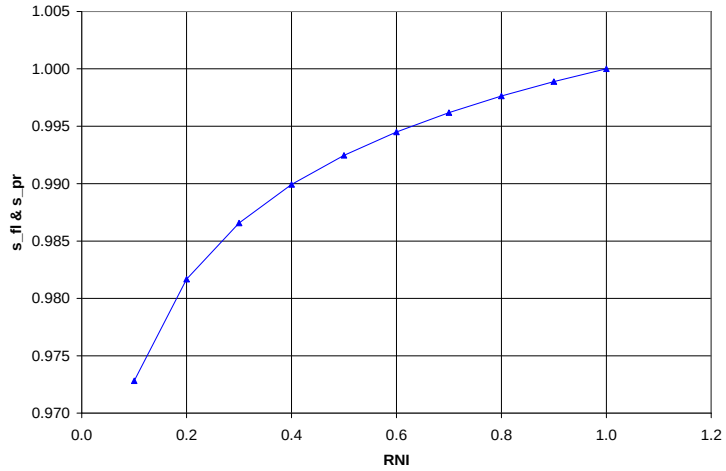

Figure 3.2.7 Fan Reynolds Effects (Flow & Pressure Ratio)

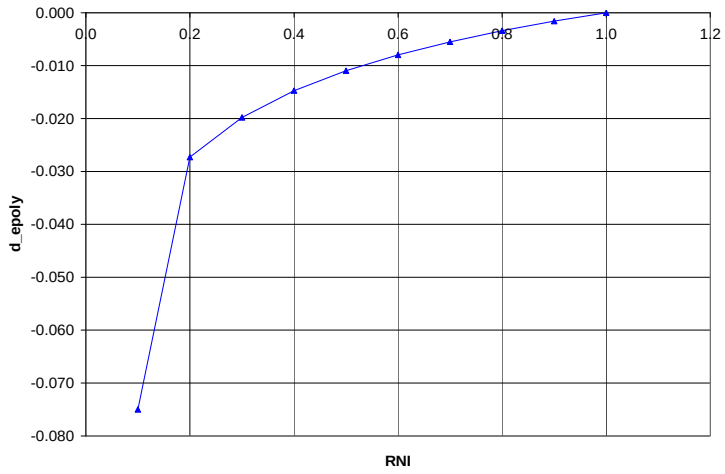

Figure 3.2.8 HPC Reynolds Effect (Efficiency)

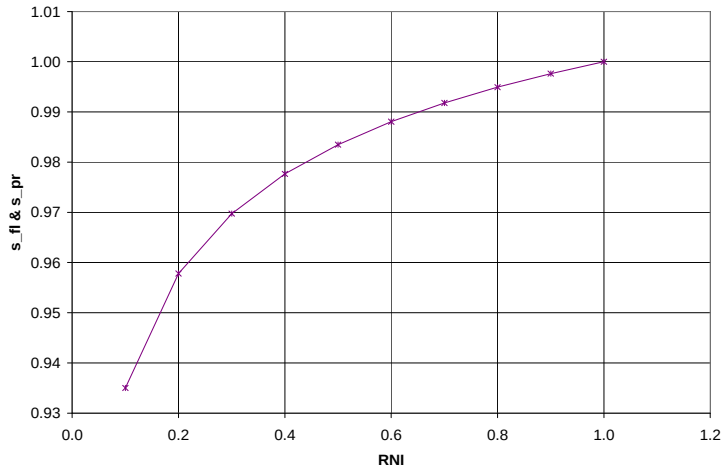

Figure 3.2.9 HPC Reynolds Effect (Flow & Pressure Ratio)

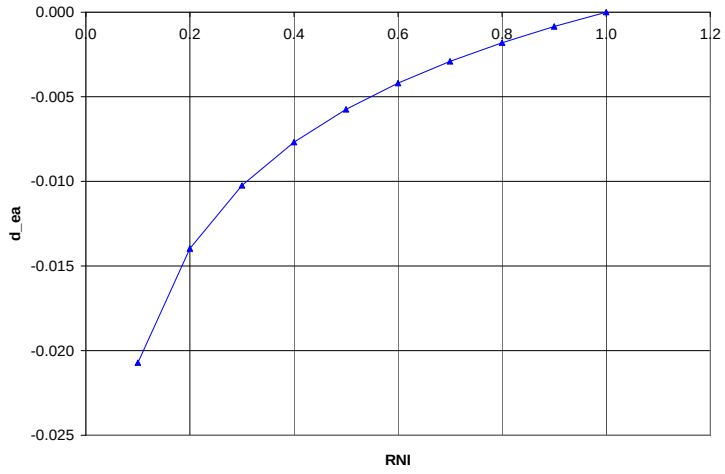

Figure 3.2.10 HPT Reynolds Effect (Efficiency)

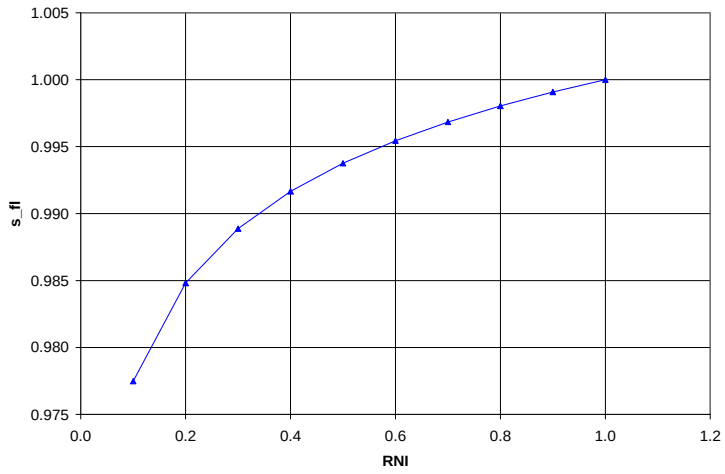

Figure 3.2.11 HPT Reynolds Effects (Flow & Pressure Ratio)

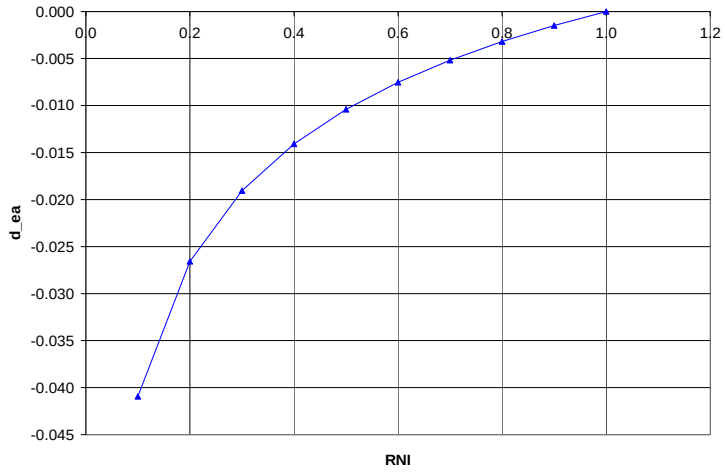

Figure 3.2.12 LPT Reynolds Effects (Efficiency)

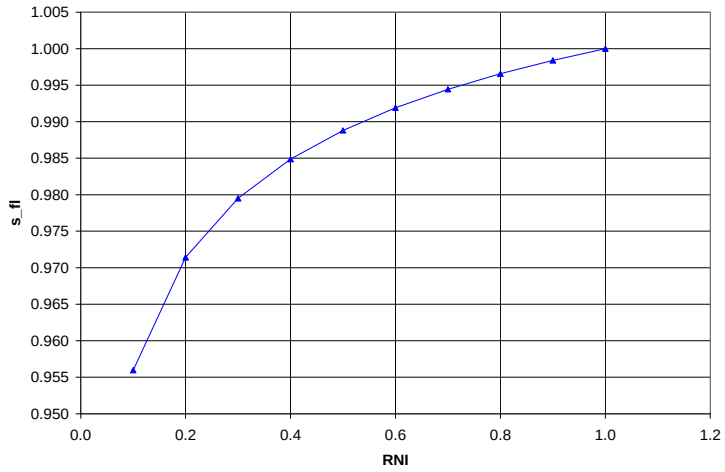

Figure 3.2.13 LPT Reynolds Effects (Flow & Pressure Ratio)

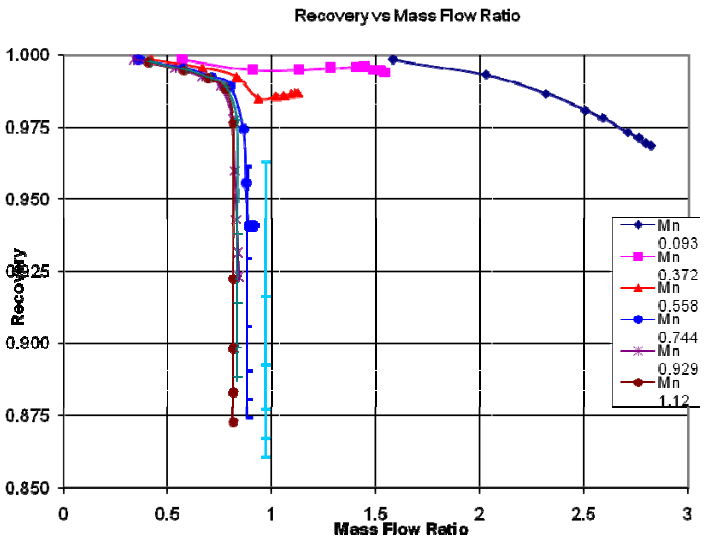

Figure 3.2.14 Inlet Recovery

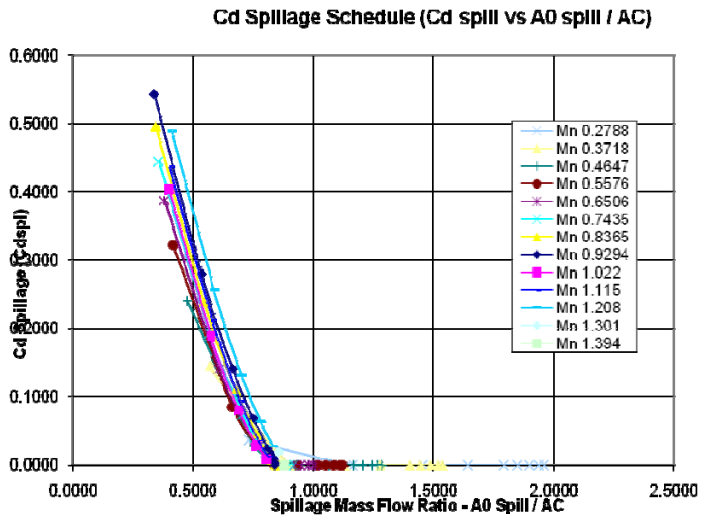

Figure 3.2.15 Inlet Spillage Drag Coefficient

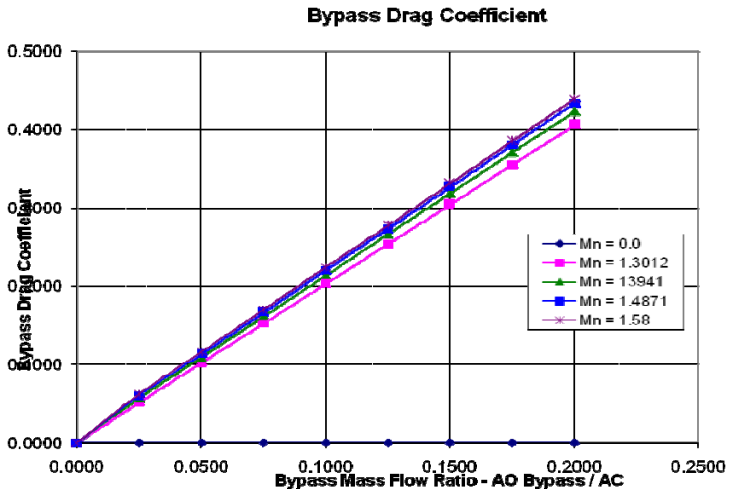

Figure 3.2.16 Inlet Bypass Drag

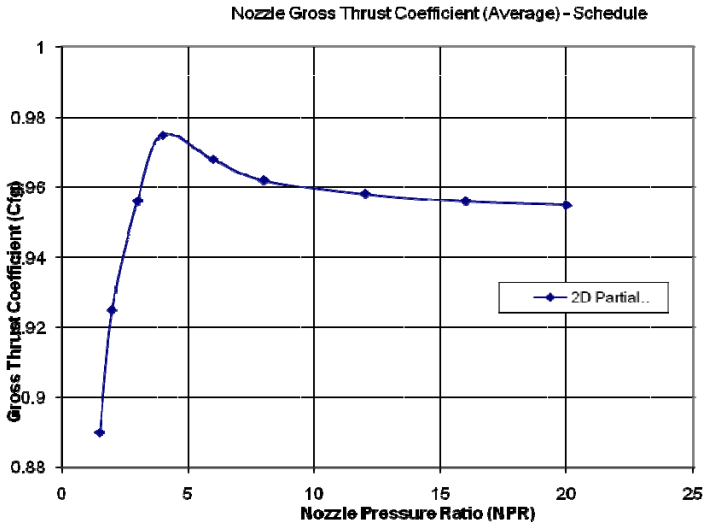

Figure 3.2.17 Nozzle Gross Thrust Coefficient

Max Continuous / Max Climb / Cruise Powerlines / Idle

Altitude (ft)	Mach Number																				
0	0	0.2	0.3	0.4	0.5																
1500	0	0.2	0.3	0.4	0.5	0.6															
5000	0	0.2	0.3	0.4	0.5	0.6	0.7														
10000			0.3	0.4	0.5	0.6	0.7	0.8													
15000				0.4	0.5	0.6	0.7	0.8	0.9												
20000					0.5	0.6	0.7	0.8	0.9	0.95	0.98	1									
25000						0.6	0.7	0.8	0.9	0.95	0.98	1									
30000							0.7	0.8	0.9	0.95	0.98	1	1.05	1.1	1.2	1.3					
33000							0.7	0.8	0.9	0.95	0.98	1	1.05	1.1	1.2	1.3	1.4				
36089							0.7	0.8	0.9	0.95	0.98	1	1.05	1.1	1.2	1.3	1.4	1.5	1.6	1.8	2.0
39000								0.8	0.9	0.95	0.98	1	1.05	1.1	1.2	1.3	1.4	1.5	1.6	1.8	2.0
43000								0.8	0.9	0.95	0.98	1	1.05	1.1	1.2	1.3	1.4	1.5	1.6	1.8	2.0
47000										0.95	0.98	1	1.05	1.1	1.2	1.3	1.4	1.5	1.6	1.8	2.0
50000										0.95	0.98	1	1.05	1.1	1.2	1.3	1.4	1.5	1.6	1.8	2.0
53000										0.95	0.98	1	1.05	1.1	1.2	1.3	1.4	1.5	1.6	1.8	2.0
55000												1	1.05	1.1	1.2	1.3	1.4	1.5	1.6	1.8	2.0
60000													1.05	1.1	1.2	1.3	1.4	1.5	1.6	1.8	2.0
Thrust	MCT	MCL	90%	85%	80%	70%	60%	40%	20%	Idle											

Figure 3.2.18 MFTF Flight Envelope

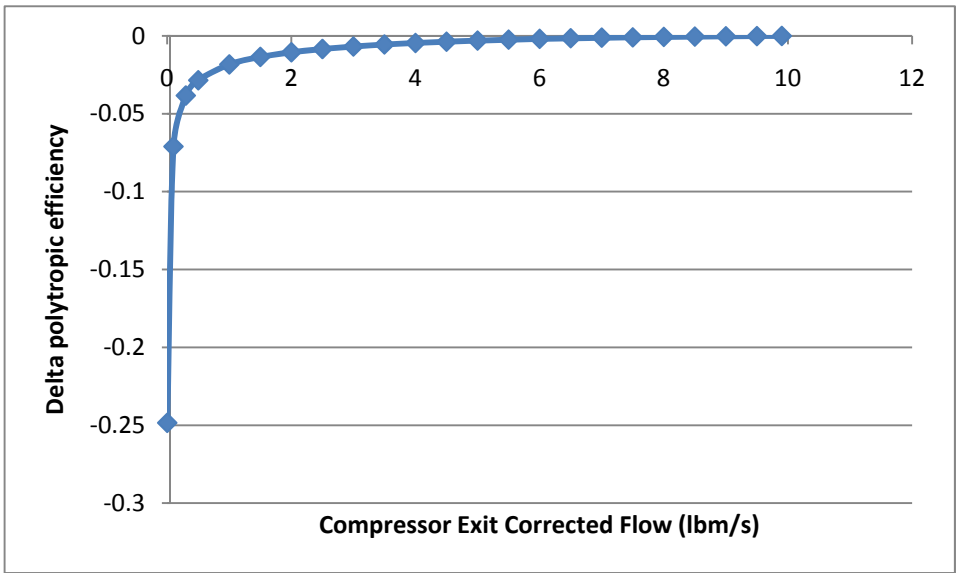

Figure 3.2.19 Public Domain HPC Size Effect

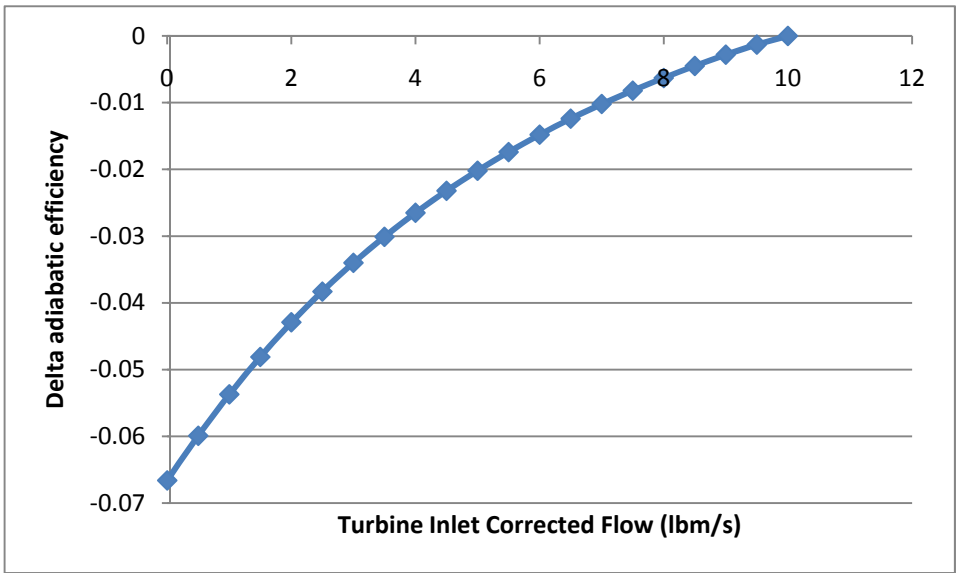

Figure 3.2.20 Public Domain HPT/LPT Size Effect

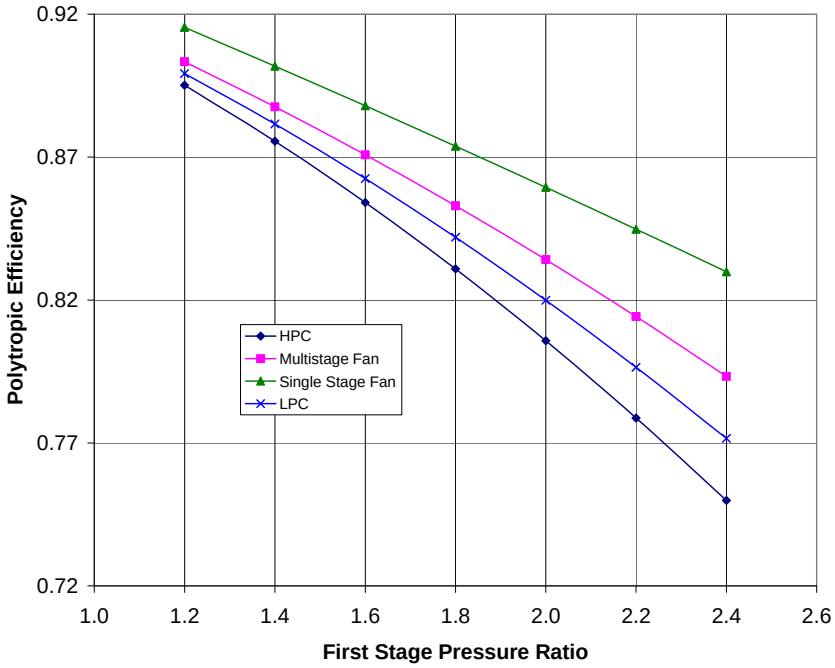

Figure 3.2.21 MFTF Fan and HPC Loading vs. Efficiency

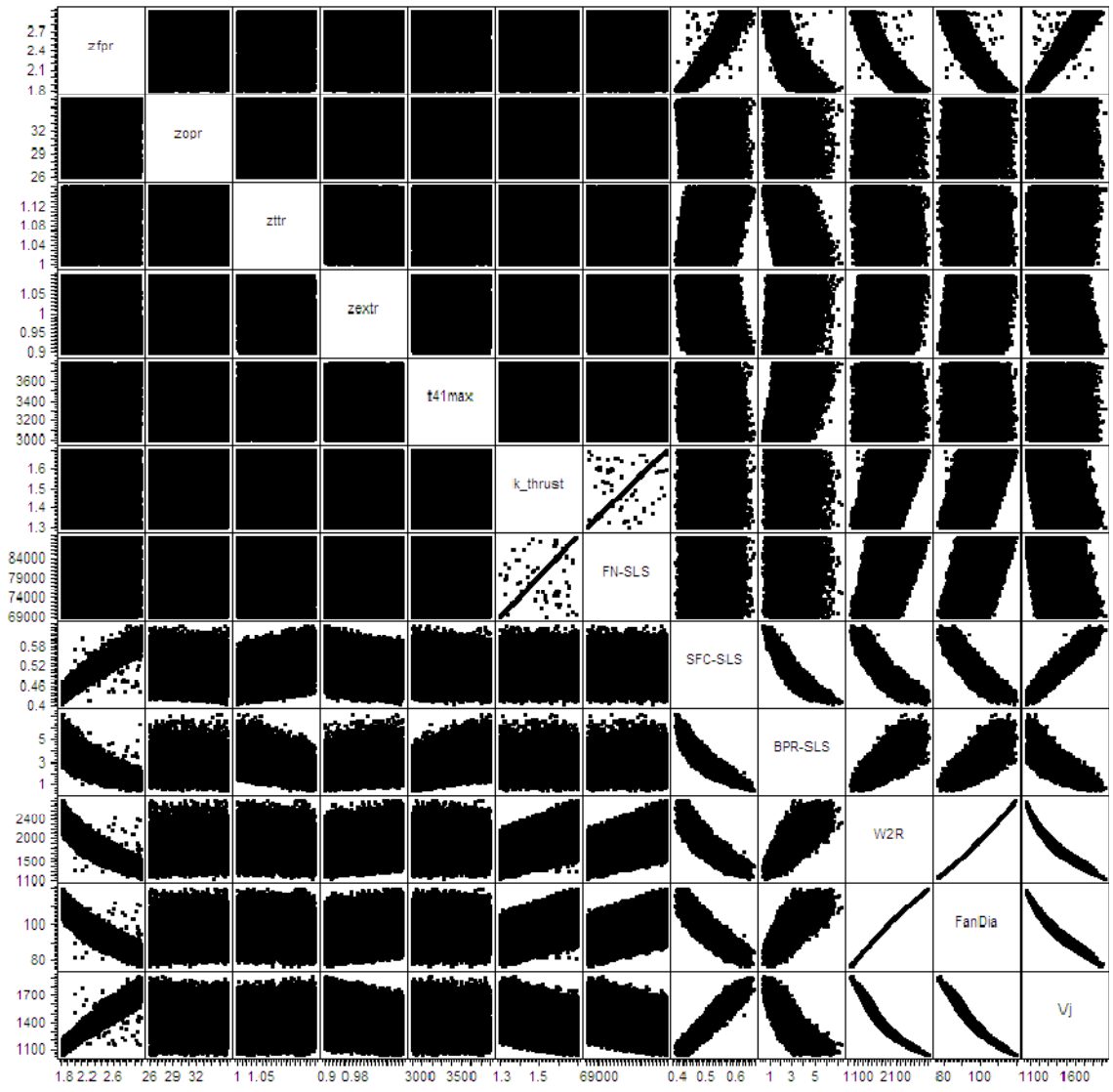

Figure 3.2.22 Unfiltered Rolls Royce MFTF 072B Design Space

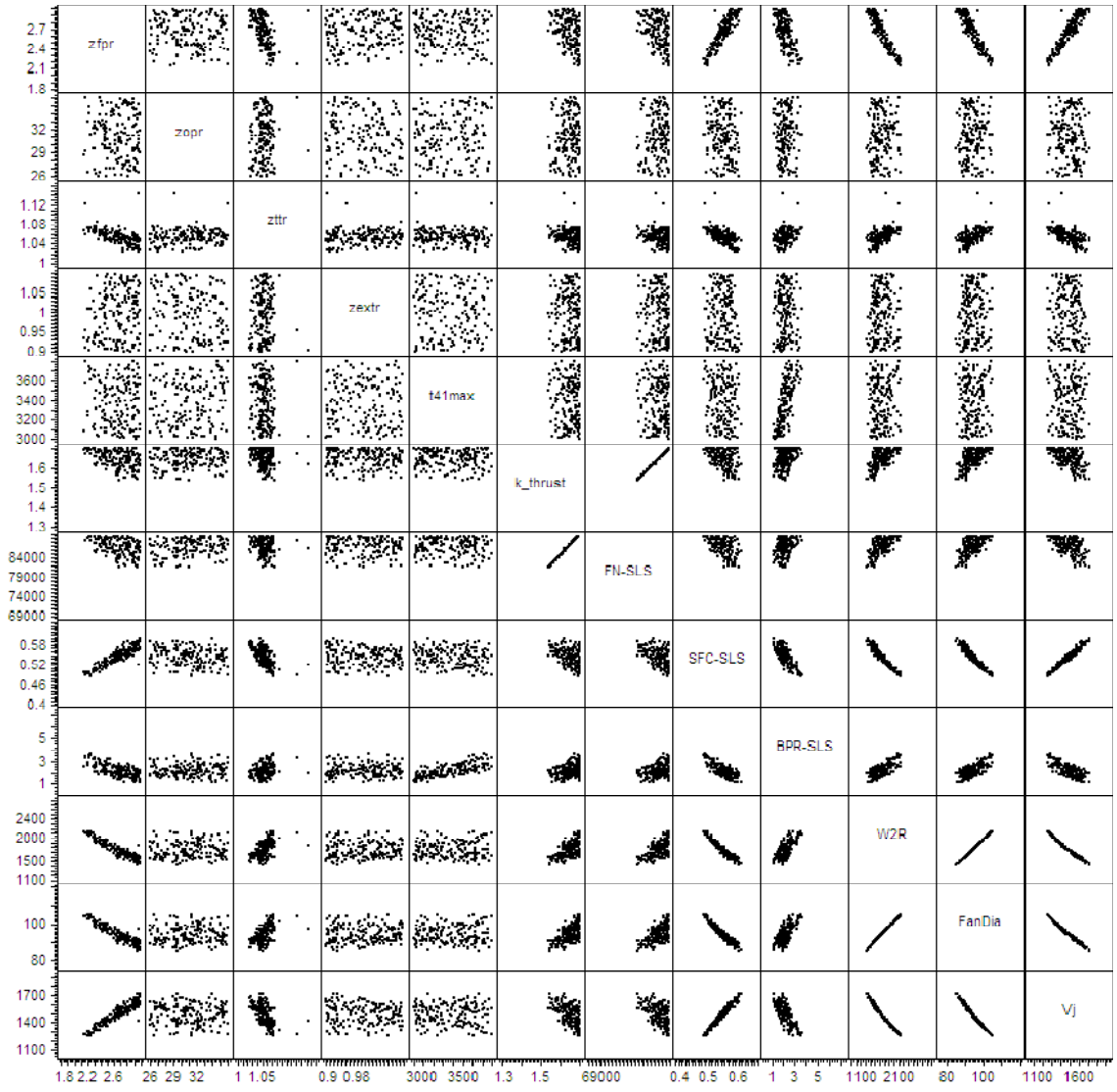

Figure 3.2.23 Rolls Royce Filtered Design Space for 072B

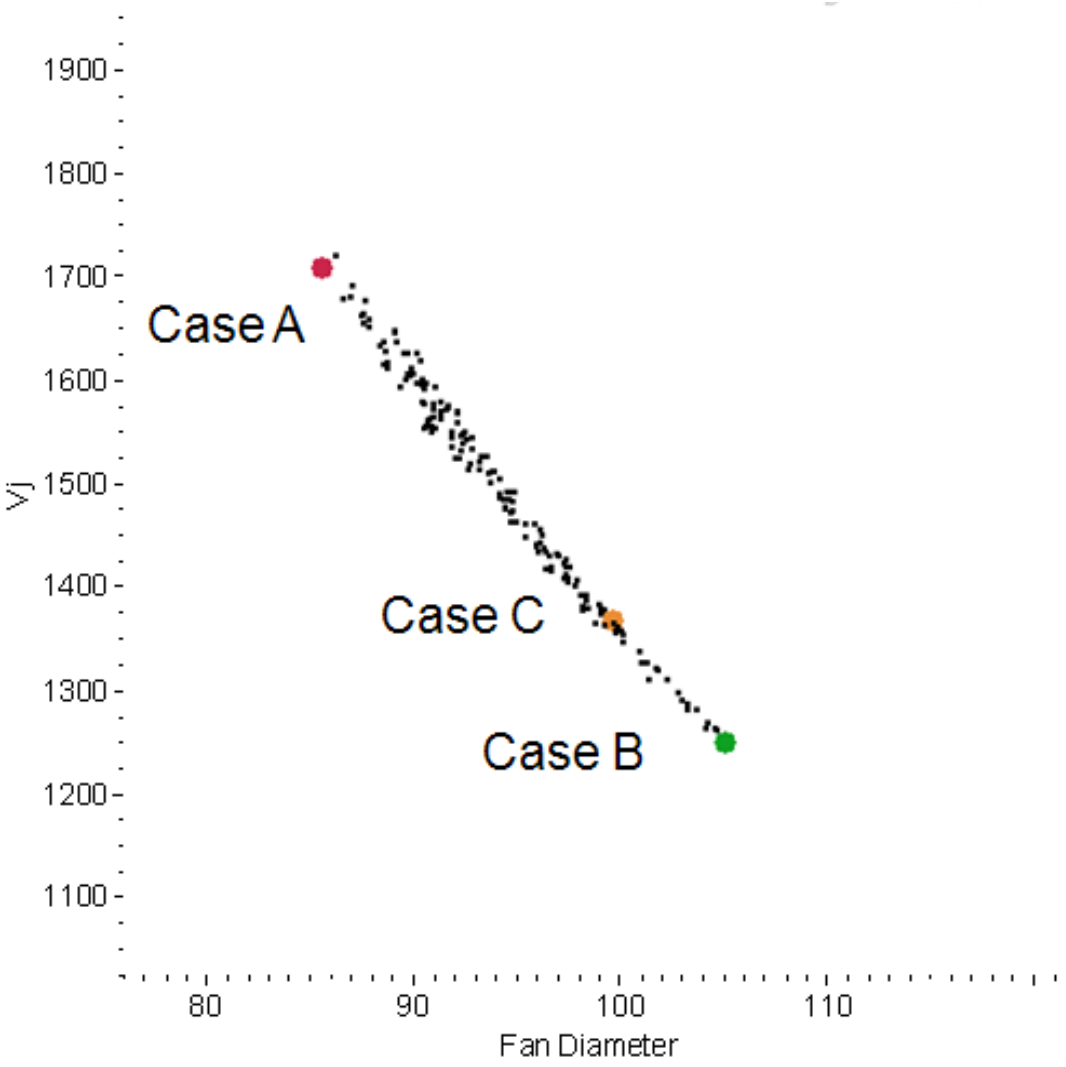

Figure 3.2.24 Rolls Royce Fan Diameter/Vj Pareto Front

Configuration	V2.5 (resized) Mar 12 Compromise 2	V2.5+NPSS (resized) Mar 12 Sim RR Comp
Wing Area (ESDU)	3771	4099
Wing Area (Gross)	**4600**	**5000**
Thrust per engine	**58,000**	**61,000**
Engine T/W	5	5
TOGW	291,098	317,499
OEW	135,320	146,420
Payload	21,000	21,000
Total Fuel	135,130	150,561
Block Fuel	116,346	130,557
Range	4000	4000
Supersonic Cruise		
Mach	1.6	1.6
Altitude	52,412	51,731
Weight	267,223	293,649
CL	0.1833	0.1794
L/D	9.486	9.214
SFC	1.0107	1.012
Climb (pinch point)		
Mach	1.13	1.13
Altitude	40,550	40,550
Weight	277,651	303,826
CL	0.2162	0.2177
L/D	9.797	9.418
Thrust	29,641	33,666
SFC	0.8533	0.8318
ROC	322	318
Bal Field Dist. (100% pwr)	7088	6192 (??%)
W/S (takeoff)	77.2	77.5
FOM	3.44	3.06

Mach 1.6, 4000 nm, 100 PAX

Note 1: V2.5 of the MDAO model has corrections to aero and engine scaling
Note 2: NPSS produces different thrust & fuel flow for the same cycle inputs
Note 3: None of the engines were de-rated to meet 1100 fps takeoff Vj
Note 4: V2.5 cases were constrained to 55,000 ft max cruise altitude

Figure 3.3.1 765-072B Performance Comparison for NPSS Engine Cycle

- Both Optimization 1 and GTRR Compromise were resized to meet constraints
- Both meet 55,000 ft "threshold" max cruise altitude limit
  - Changed GTRR Compromise engine design cruise point to Mach 1.6, 55,000 ft (originally M1.8, 43,000 ft)

Max FOM	Benchmark
Optimized Design (307)	GTRR Compromise Engine
Fan_PR=2.891406	Fan_PR=2.24754
Overall_PR=36	Overall_PR=35.0555
Extraction_Ratio=0.9984375	Extraction_Ratio=0.91115
Max_T41=3453.906	Max_T41=3127.96
Throttle_Ratio=1.1	Throttle_Ratio=1.14895
Net_Thrust=53,008	Net_Thrust=61,000
Sgross_ft=4535	Sgross_ft=5000
---	---
FOM=3.43	FOM=3.14
ROC=311 fpm	ROC=360 fpm
Fuselage Tank Vol=18,923 lb	Fuselage Tank Vol=11,480 lb
Bal Field Distance=9905 ft	Bal Field Distance=9868 ft
W/S_takeoff=77.4 psf	W/S_takeoff=76.6 psf
100% Vj=1891 fps	100% Vj=1600 fps
De-rate Vj=1640 fps	De-rate Vj=1375 fps

Optimization improved on GTRR Compromise cycle at the expense of Vj

Figure 3.4.1 765-072B Optimization #1 Summary (Maximize FOM)

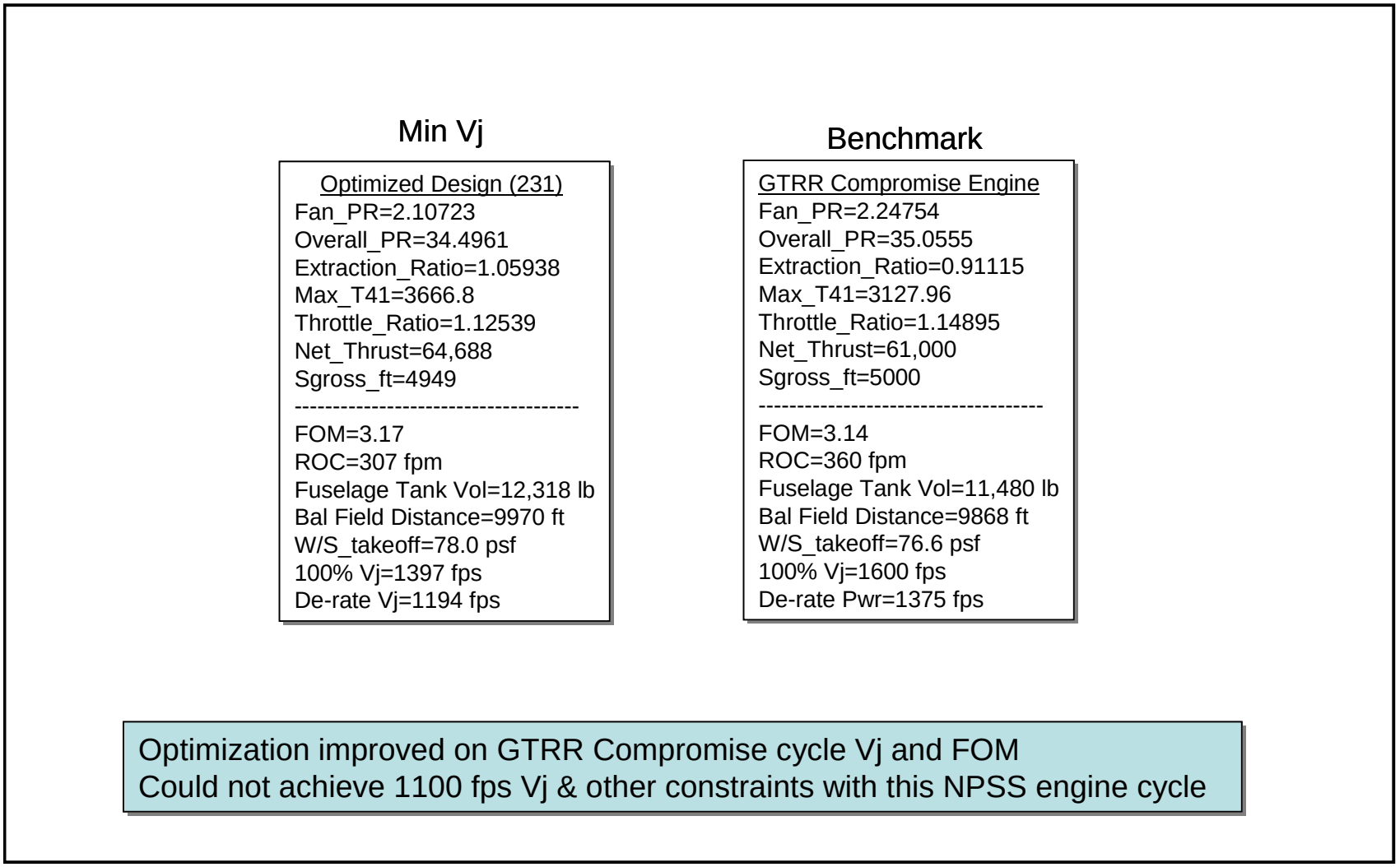

Figure 3.4.2 765-072B Optimization #2 Summary (Minimize Vj)

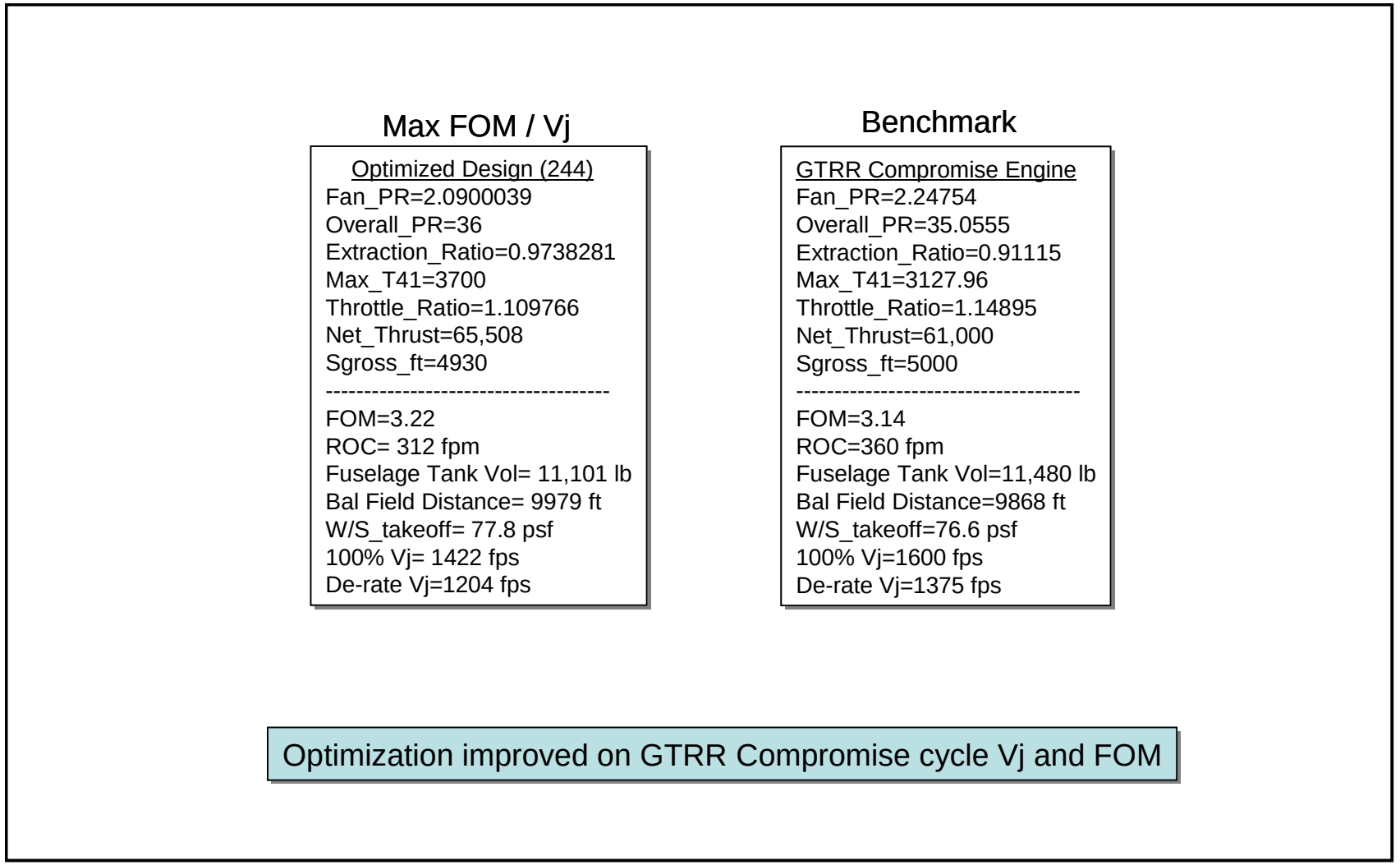

Figure 3.4.3 765-072B Optimization #3 Summary (Maximize FOM/Vj)

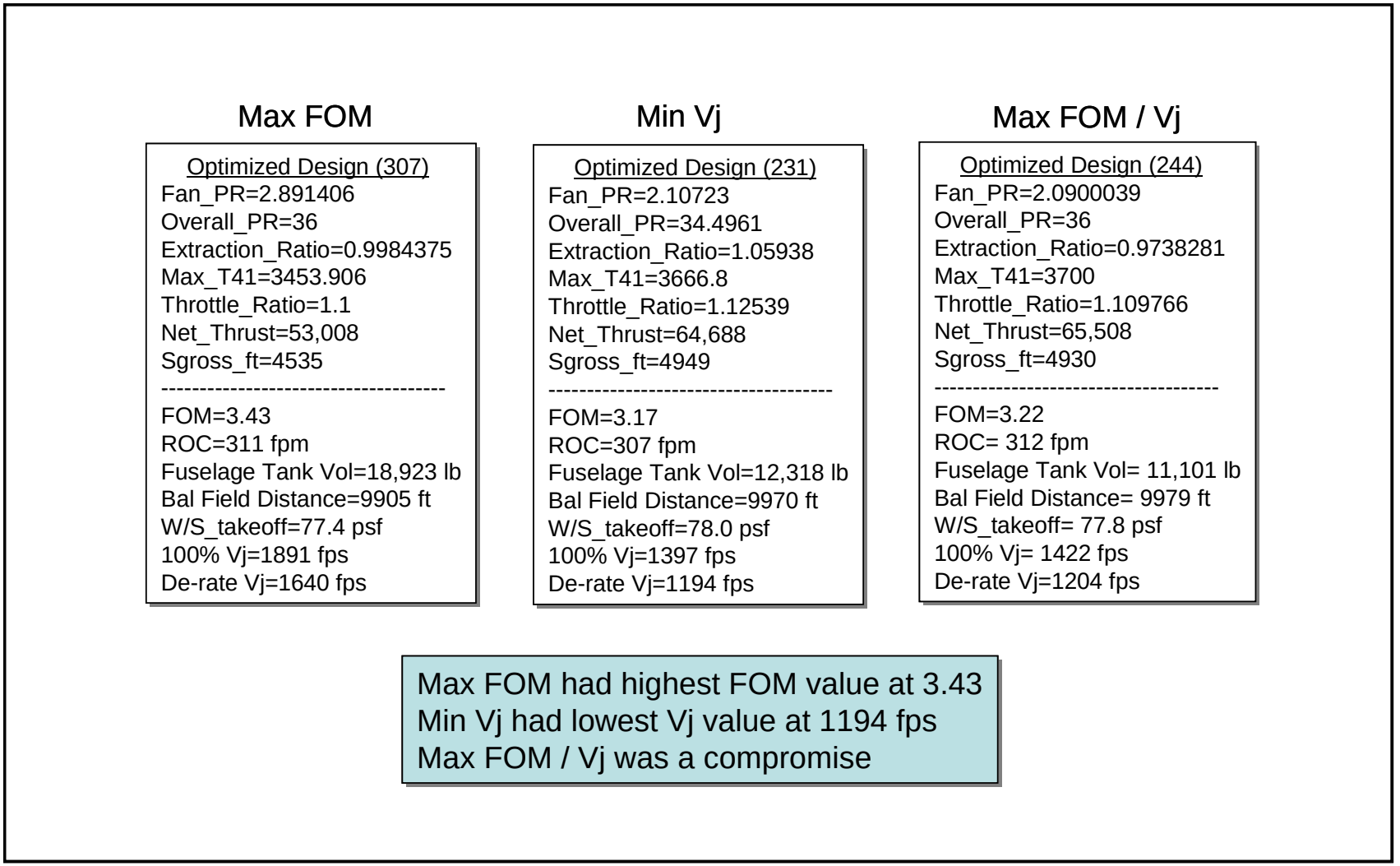

Figure 3.4.4 765-072B Optimization Comparison

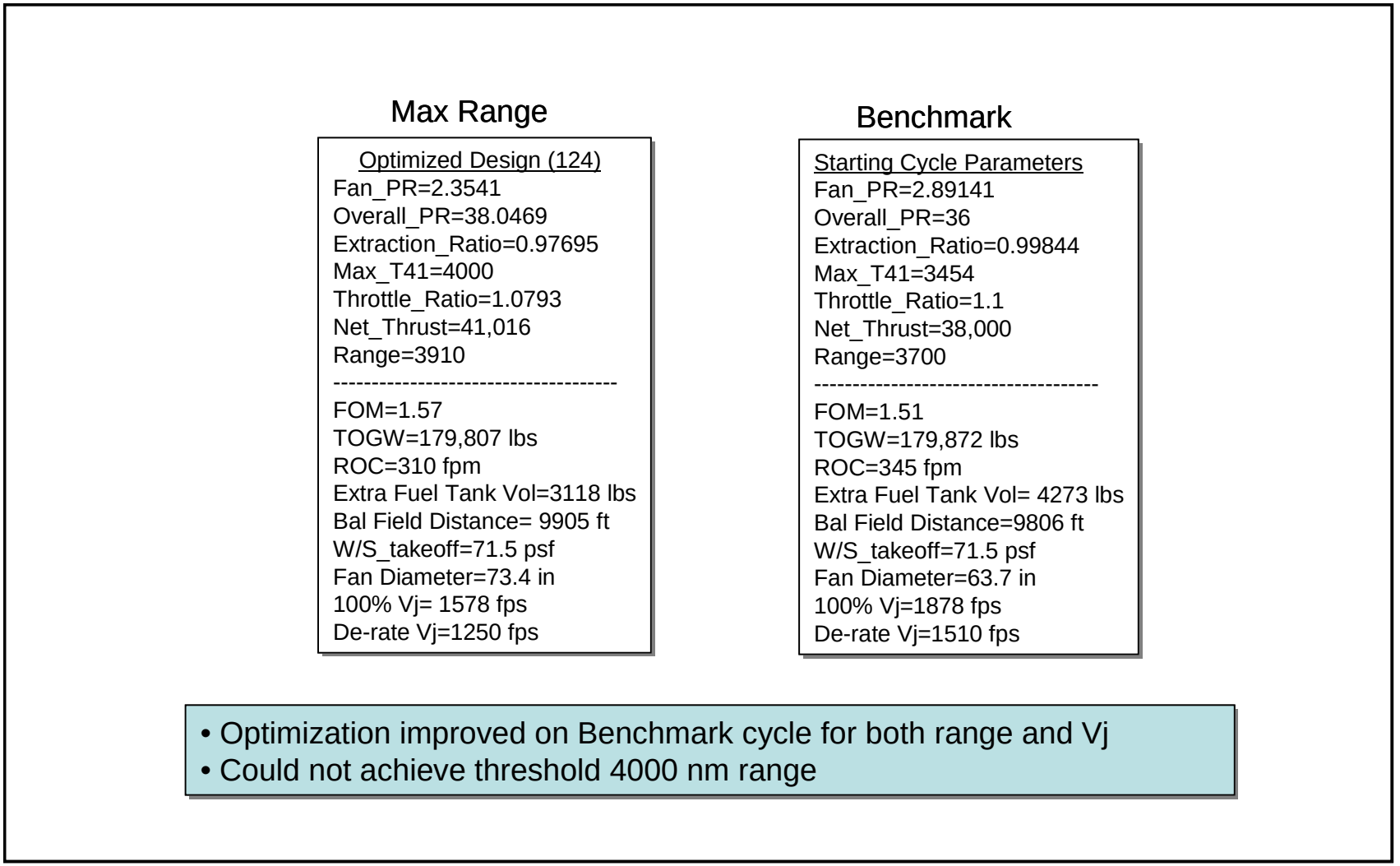

Figure 3.5.1 765-076E Optimization #1 Summary (Maximize Range)

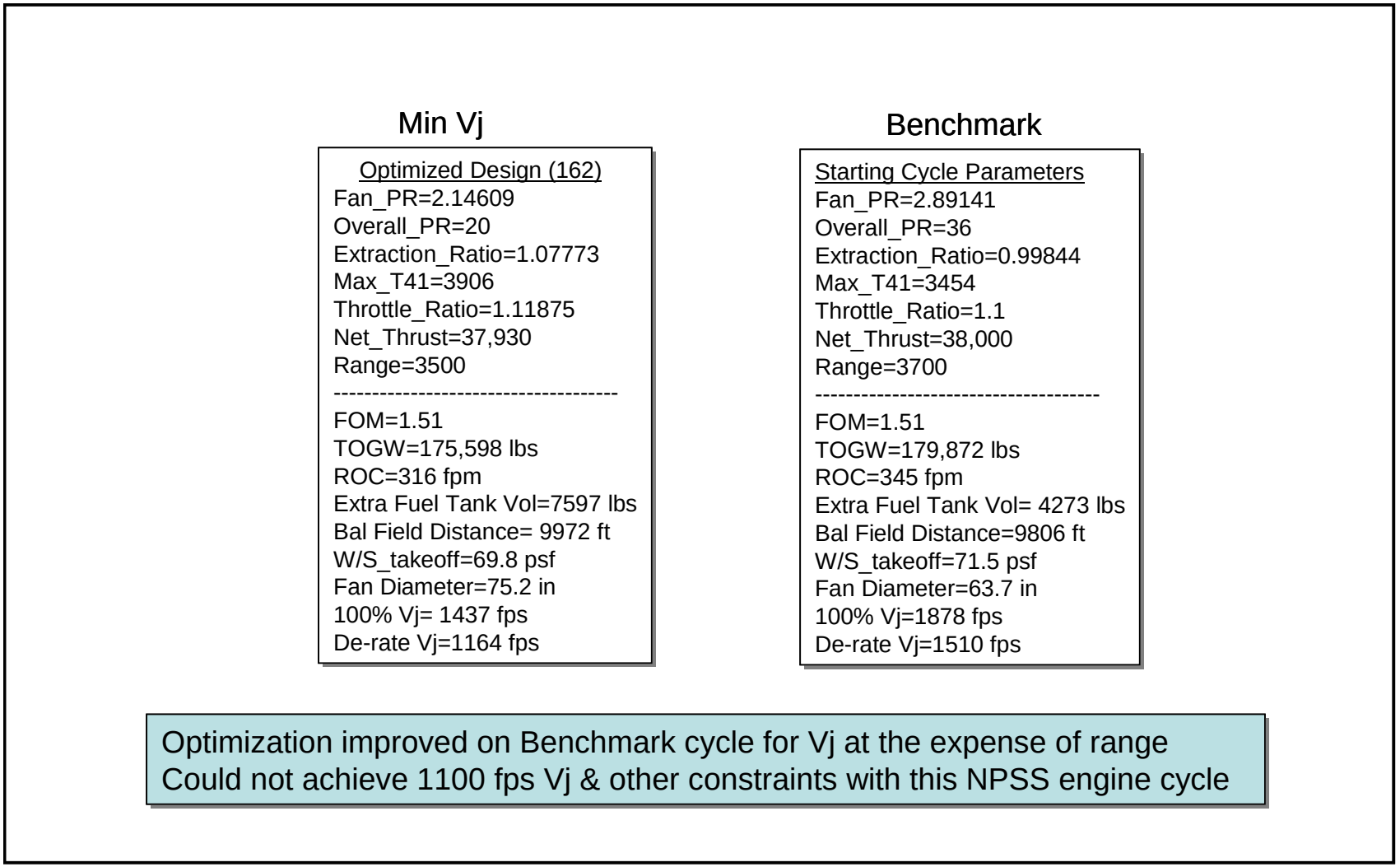

Figure 3.5.2 765-076E Optimization #2 Summary (Minimize Vj)

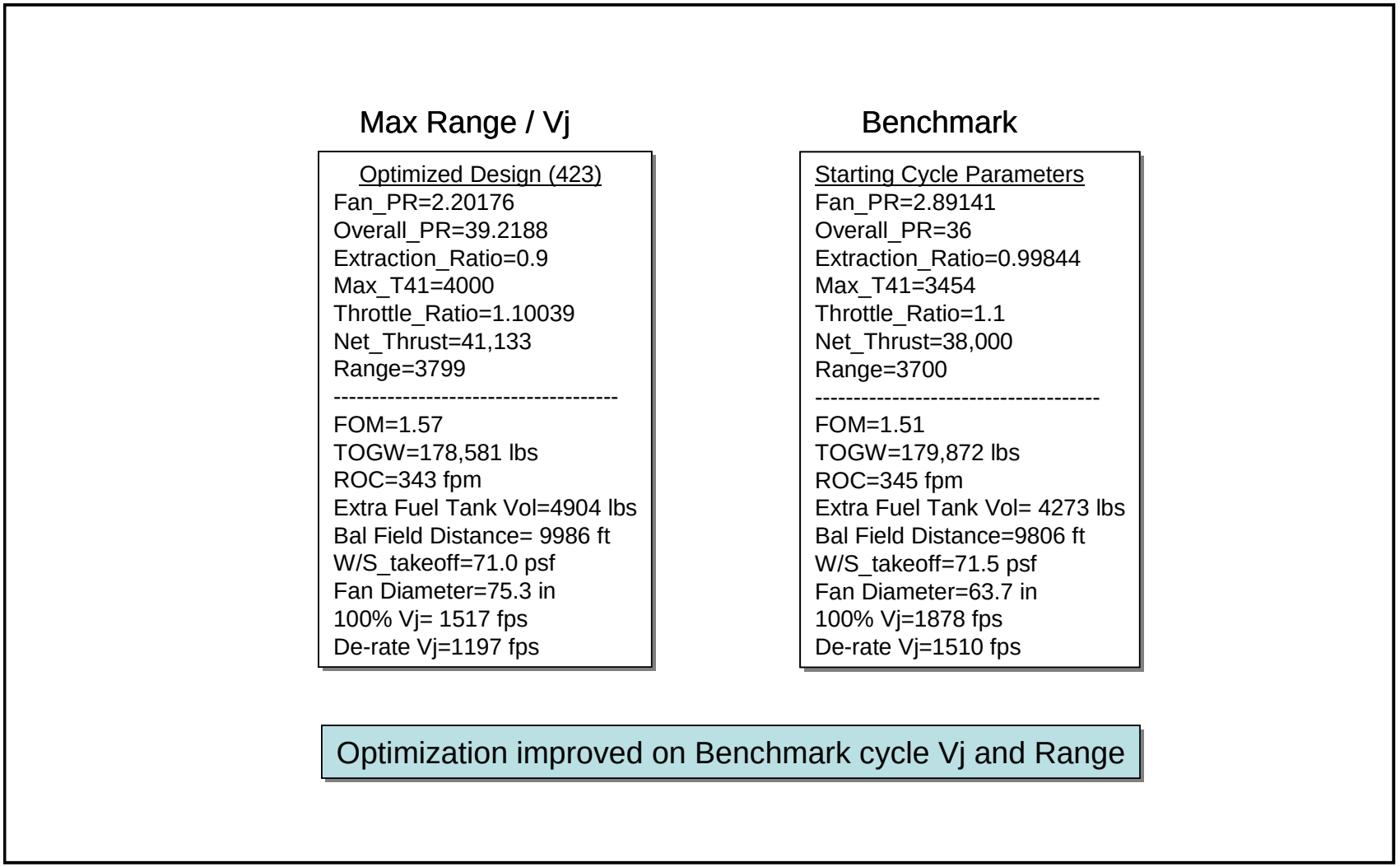

Figure 3.5.3 765-076E Optimization #3 Summary (Maximize Range/Vj)

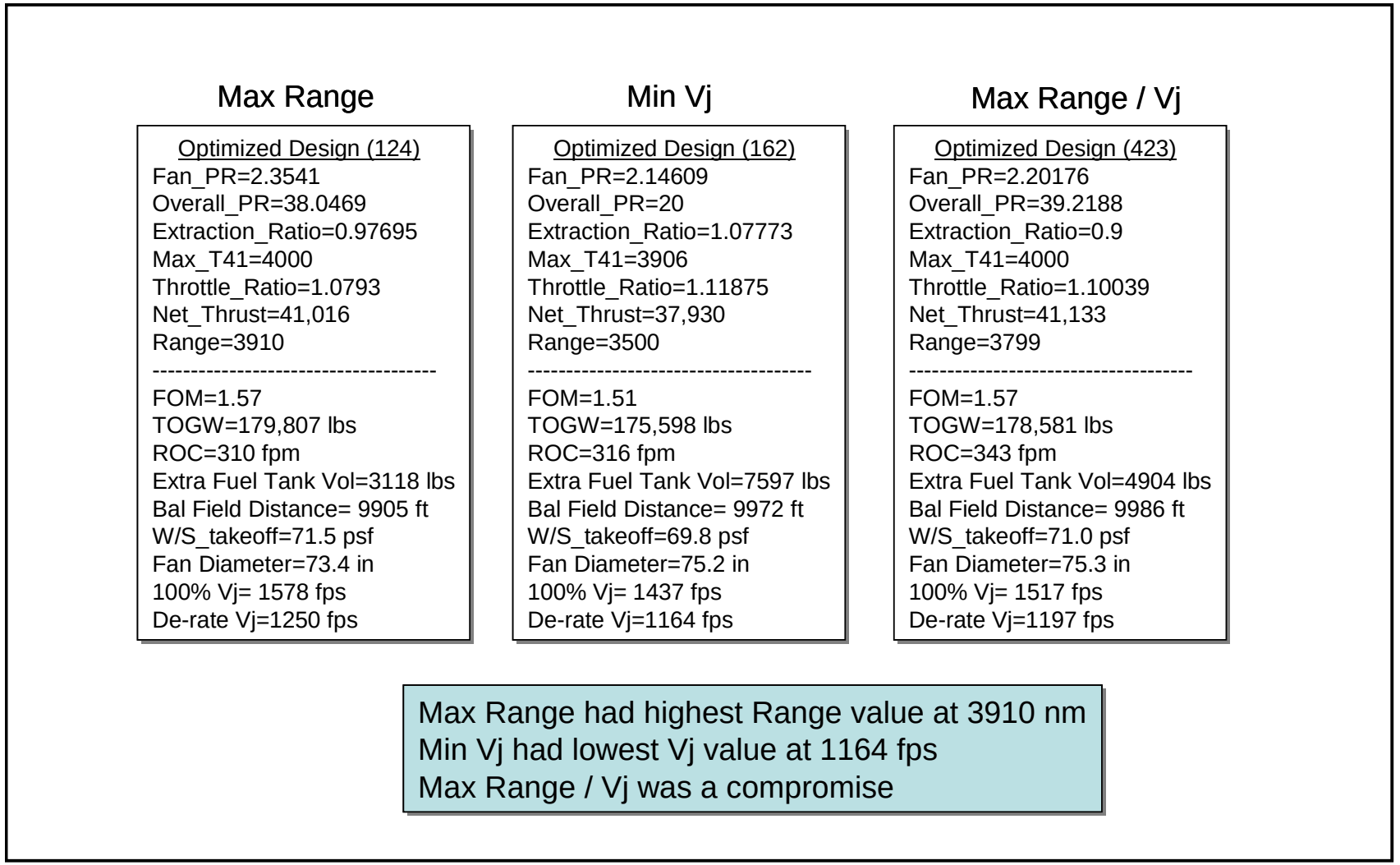

Figure 3.5.4 765-076E Optimization Comparison

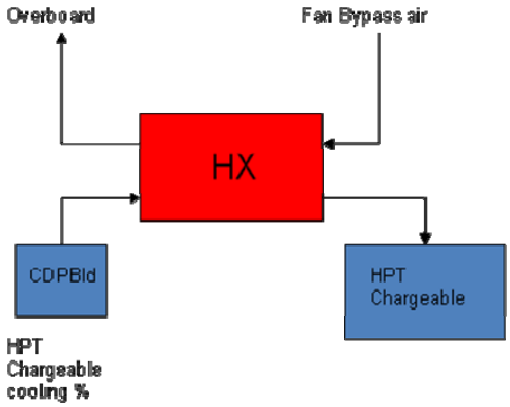

Figure 3.5.5 CCA Diagram

4.0 Non-Proprietary Small Supersonic Aircraft

4.1 Concept Selection

The 076E was selected as the deliverable small supersonic aircraft because of its low boom characteristics. The mission performance rules are contained in Figure 4.1.1. The performance of the concept is shown in Figure 4.1.2

4.2 Description of the 076E

The model 765-076E was conceived as compromise configuration between sonic boom mitigation and airplane productivity. Some of the high level features of the configuration are shown in Figure 4.2.1. Since one of the primary drivers of sonic boom noise level is weight, the passenger capacity of the airplane was limited to 15-45. The performance of the airplane was analyzed with 30 passengers.

Configuration Description

The general arrangement of the aircraft is shown in Figure 4.2.2. An IGES file for this outer mold line is delivered with this report in a separate file titled "765-076E_ContractDeliverable.igs. A CFD quality OML IGES file is also included and it is titled "t65-076E_CFD_Ready.igs.

The model 765-076E has a highly integrated arrangement with heavily shaped surfaces for improved supersonic drag and noise characteristics. The surface definition was created from a required area distribution to achieve a desired sonic boom, with sufficient constraints to ensure the ability to package internal components after the fact. The linear analysis that created the lofted geometry produced surfaces sufficient for the level of analysis done under this contract, but with design refinement the predicted sonic boom and cruise performance goals should be achievable with higher order analysis tools and experimental validation.

Wing

The wing has a highly swept planform with a large glove and aft deck to accommodate the integration of the upper mounted engine nacelles. The wing planform is shown in Figure 4.2.3.
The outboard wing is of solid titanium construction. The inboard wing is of built-up titanium construction. An overview of the wing structure can be seen in the general arrangement drawing. The wing uses a drooped leading edge, midboard flaps, and an aileron, as well as two aft elevator surfaces.

Tail

The tail uses similar construction as the wing, with the outboard portion constructed of solid titanium, and the inboard portion constructed of built-up titanium. An overview of the tail structure can be seen in the general arrangement drawing. The tail is all-flying and is controlled by an actuator attached to the rear spar, turning about a spindle attached to the front spar.

Body

The body does not have a constant section and contains the passengers and crew, as well as baggage, landing gear, and subsystems. The body is constructed of built up titanium. The forward pressure bulkhead is slanted to allow the nose landing gear to be mounted further aft. Frames are distributed through the body on nominal 20 inch spacing on center. There are 28, 10 inch diameter passenger windows. A conceptual structural arrangement can be seen on the general arrangement drawing.

Landing Gear

The landing gear is a conventional tricycle type. The main landing gear has 2 struts, with 6 wheels per strut. The truck is levered (similar to 777) such that the airplane rotates about the aft tire. The tires are high pressure (320 psi) and are 21.5 x 9. The MLG folds inboard and forward into the wing / body fairing. Two diagonal braces replace the traditional drag and sway braces to accommodate the shorter trunion. The nose landing gear has 2 tires which are 20 x 9. The nose landing gear folds forward in front of the forward pressure bulkhead, so there is no NLG pressure deck.

Systems

The flight deck is a conventional side-by-side arrangement with Pilot and Copilot. No provisions are made for a drooping nose or forward windscreen, so synthetic vision will be required. Windows to the side are provided, so synthetic vision will only be required to the front. The cockpit vision provided is shown in Figure 4.2.4.

The electronics and avionics are located in the E/E bay behind the aft pressure bulkhead. Behind that are the ECS packs, and behind that the APU. A layout of the systems bays can be seen in Figure 4.2.5.

The fuel is distributed among 10 tanks throughout the inboard wing and aft fuselage. A layout of the fuel tanks can be seen in Figure 4.2.6. Fuel can pumped from tank-to-tank to actively manage the airplane center of gravity for improved performance and reduced sonic boom. The fuel tanks can accommodate a total of 85,300 lb of fuel.

Propulsion

The propulsion system was developed as a part of contract Option 2, and will be discussed in that portion of the report.

Payloads

As many as 45 passengers can be accommodated on the 765-076E. Two notional Layouts of Passenger Accommodations (LOPAs) can be seen in Figure 4.2.7. Four type 1 emergency exits are provided, 2 in the front cabin, and 2 over the wing. The aft door cannot be serviced without walking on the wing, so the cabin will be serviced from the forward door only.

Weights

The 765-076E aircraft was sized to 180,000 lbs Maximum Takeoff Gross Weight (MTOGW) in order to meet low-boom and performance targets. The Operational Empty Weight (OEW) was calculated using the QWIKO weight estimation tool; a parametric supersonic aircraft weight estimation tool that was developed jointly with Boeing and McDonnell Douglas during the HSR program. QWIKO has been used successfully on several supersonic aircraft studies in the past, including the High Speed Civil Transport and Quiet Supersonic Platform studies. QWIKO includes allowances for N+2 technology and weight savings.

The initial QWIKO weight statement is shown in Figure 4.2.8. This weight statement utilizes a BSE engine. The fuel weight was based on the calculated OEW and the design TOGW. QWIKO assumes that the structure is laid out efficiently and that there is sufficient structural depth to carry loads. The 765-076E configuration is very thin structurally in order to meet the low-boom requirements and preliminary FEM results indicate that the 180,000lb TOGW target may be unrealistic and very difficult to reach. This is discussed further in the Option 2 FEM section.

A preliminary center of gravity diagram was constructed for the 765-076E configuration as shown in Figure 4.2.9. Due to the integrated nature of a low-boom configuration, the 765-076E was analyzed “as-is” and there was no additional tail sizing or wing shifting performed.

The Operational Empty Weight center of gravity was determined using QWIKO and by geographically locating large components such as the APU and EE Bay. The nose landing gear was located forward of the forward slant bulkhead and the main landing gear was placed as far aft as possible without interfering with the wings rear spar. This gear layout resulted in approximately 2% of the OEW on the nose wheel, and 5% of MTOGW on the nose wheel.

During supersonic flight the center of pressure moves aft, so separate C.G. envelopes were needed for supersonic and subsonic flight. The aft limit was notionally set at 2% Mean Aerodynamic Chord (MAC) ahead of the main landing gear. The subsonic forward limit was set by the Maximum Zero Fuel Weight (MZFW) of the forward-most payload case, 30 passengers. A notional supersonic forward limit was set 5% in front of the aft limit, which is comparable to the High Speed Civil Transport's envelope.

The preliminary 765-076E weights were revised to include the findings from the NPSS engine study and initial performance runs. The TOGW was reduced to 178,737 lbs and the OEW was recalculated using QWIKO. The 765-076E performance weight statement can be found in Figure
4.2.10.

4.3 Sonic Boom Discussion

The 765-076E Signature was designed using the Boeing MTA tool. It was based on a linear design and the signature was analyzed with MDBOOM and Zephyrus wave propagation codes. Zephyrus results are believed to be more accurate, because it applies molecular relaxation throughout the wave propagation. The MDBOOM code is utilized in off-body signature analysis, because it is easier to use. The wave propagation results are shown in Figure 4.3.1. The Zephyrus code yields a ground signature of 91.5 PLdB, while the MDBOOM code yields a ground signature of 93.8 PLdB. The 765-076E configuration should be able to provide ~91 PLdB after Non-linear CFD-based boom optimization.

The off-body Euler CFD was conducted to see how effective the linear design was in shaping the front and aft signature. Figure 4.3.2 shows the near-field pressure distribution produced by the Cart3d CFD code. A comparison of the off-body F-Function, Cart3d vs. the linear theory, is shown in Figure 4.3.3. Note that the Cart3d & linear theory agree on some prominent features. Cart3d captures the wave advance neglected by Linear Theory. It spreads the length and steepens the shocks. The ground signature is shown in Figure 4.3.4 for the original design condition, Mach=1.8, weight=162,000 lbs, and altitude=49,000 ft. Other conditions analyzed, included Mach=1.6 & 1.8 at altitudes=49,000 and 55,000 ft. The ground signature results for these alternate conditions can be found in Figures 4.3.5, 4.3.6, and 4.3.7. Examining the figures shows that there is some signature shaping on the front side of the sonic boom signature, but essentially an N-wave feature for the aft side of the sonic boom signature. The progression of one of the signatures with altitude is shown in Figure 4.3.8 to further illustrate the off-body CFD results. These signature differences (CFD vs. linear) prevents using only the linear tools for design. So the process is to develop concepts and seeds in linear theory and then optimize with Cart3d to realize the linear theory level.

In summary the 765-076E was designed using linear-based methods (Boeing MTA) to provide ~91 PLdB shaped sonic-boom signature. Off-body CFD-based signature analysis (Cart3d Euler) shows a partially shaped front signature and an N-wave aft signature with ~ 97 – 100 PLdB. These results are typical and expected for an initial design without non-linear CFD-based boom optimization. Non-linear CFD-based boom optimization will be conducted in a separate N+2 System Level Experimental Validation contract.

4.4 Goal Compliance

The N+2 study identified some guidelines or goals for a variety of metrics. These are summarized in Table 4.4.1. The capabilities of the two study concepts (-072B and -076E) are also shown in the table. This table shows that the -072B will meet the performance goals, but will not meet the environmental goals. While

the -076E has a lower boom signature, it still does not meet the study's environmental goals. It also does not meet the minimum range or FOM goals of the study.

4.5 Propulsion

The propulsion system used for the mission analysis was a NPSS optimized cycle as described in section 5.

Tables and Figures for Section 4.0

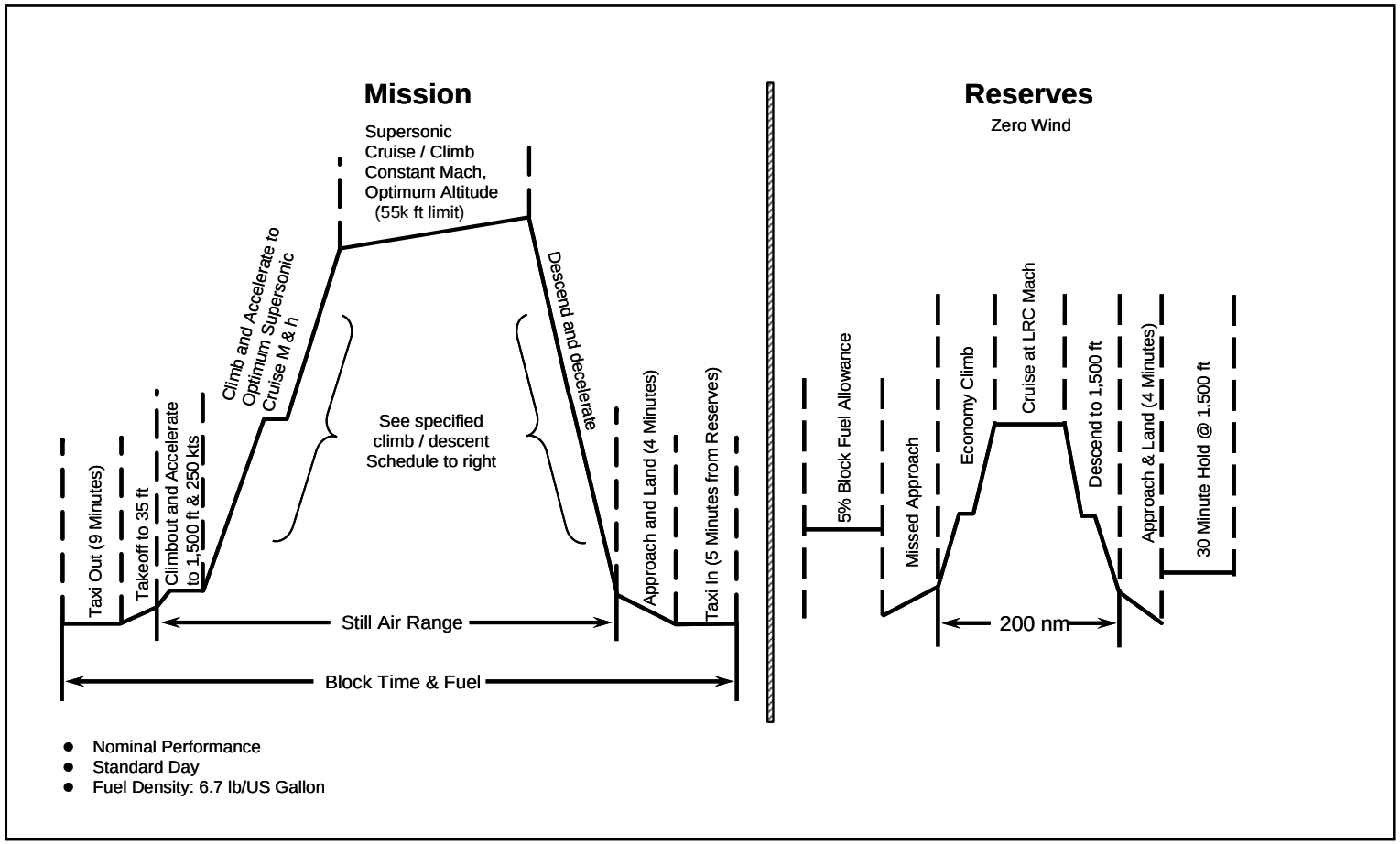

Standard N+2 Mission

Figure 4.1.1 765-076E Mission Profile

Configuration	Preferred Optimization 3 Maximum Range / Vj NPSS GTRR Cycle
Wing Area (ESDU)	2517
Wing Area (Gross)	3344
Thrust per engine	41,133
Fan Diameter (in)	75.3
Engine Weight	7271
TOGW	178,581
OEW	88,390
Payload	6,300
Total Fuel	84,373
Block Fuel	72,740
Range	3799
Supersonic Cruise	
Mach	1.6
Altitude	51,784
Weight	161,165
CL	0.1726
L/D	8.72
SFC	0.985
Climb (pinch point)	
Mach	1.13
Altitude	40,550
Weight	170.066
CL	0.1985
L/D	8.551
Thrust	20,739
SFC	0.8096
ROC	343
De-rate Vj (10k ft takeoff)	1197
W/S (takeoff)	71.0
FOM	1.57

Mach 1.6
30 PAX
variable range

Figure 4.1.2 765-076E Non-Proprietary Small Supersonic Aircraft Deliverable Performance Summary

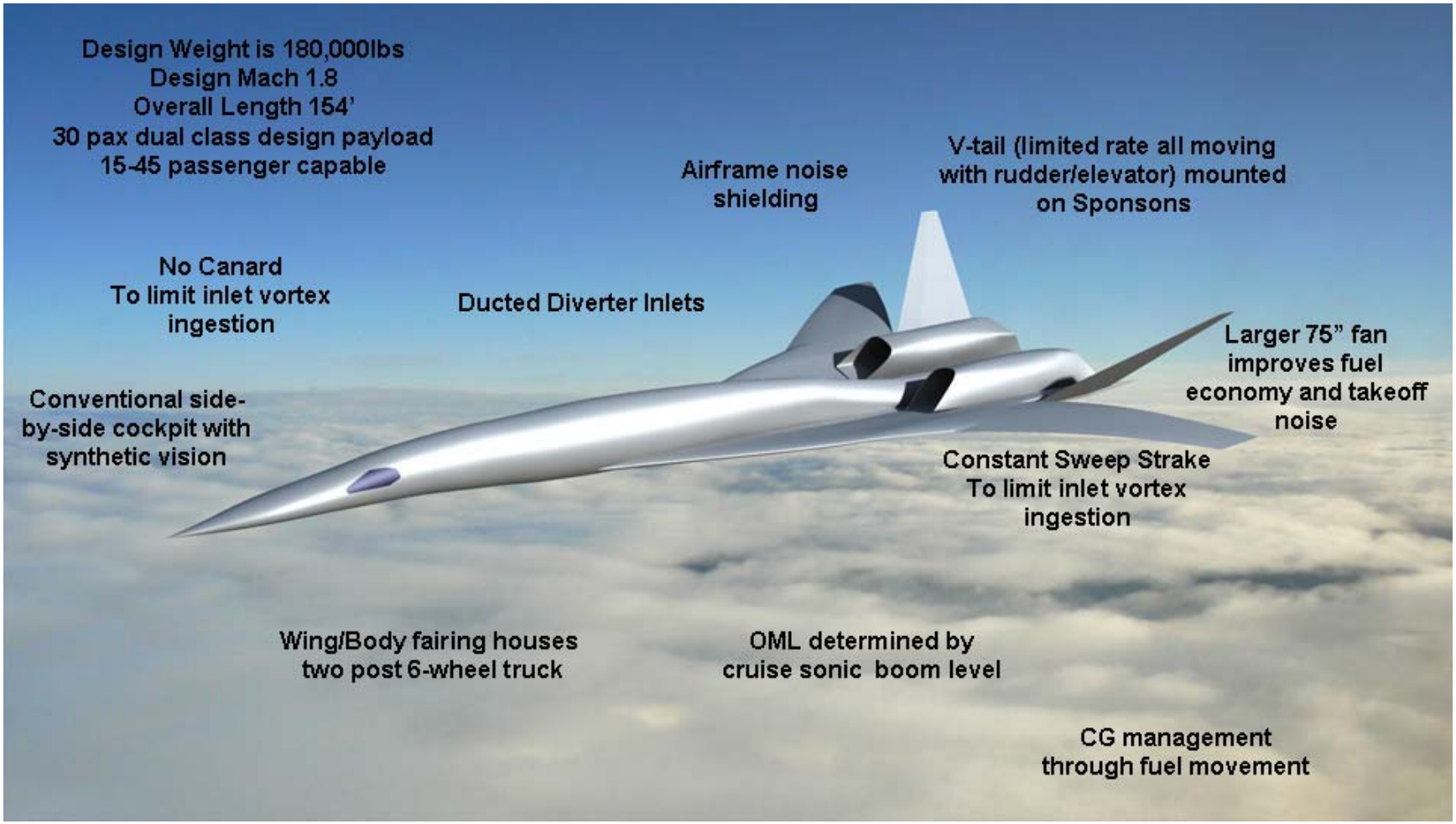

Figure 4.2.1 Model 765-076E Features

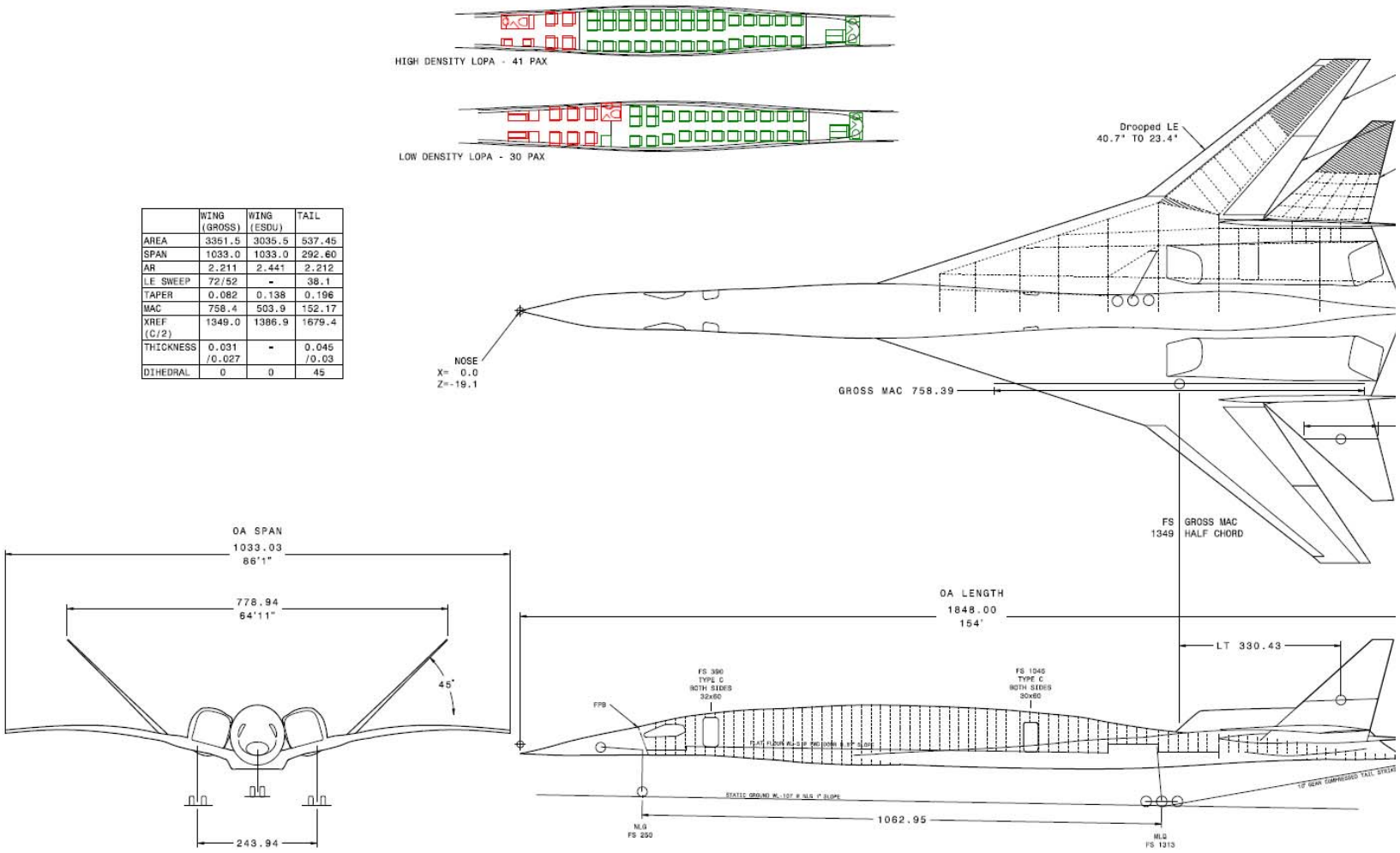

	WING (GROSS)	WING (ESDU)	TAIL
AREA	3351.5	3035.5	537.45
SPAN	1033.0	1033.0	292.60
AR	2.211	2.441	2.212
LE SWEEP	72/52	-	38.1
TAPER	0.082	0.138	0.196
MAC	758.4	503.9	152.17
XREF (C/2)	1349.0	1386.9	1679.4
THICKNESS	0.031 /0.027	-	0.045 /0.03
DIHEDRAL	0	0	45

Figure 4.2.2 765-076E General Arrangement, 1/200 scale.

Projected	Units	Wimpress
Area	sqft.	3180.0
Aspect Ratio		2.330
Taper Ratio		0.082
Span	In.	1033.0
Root Chord	In.	1254.3
Tip Chord	In.	102.9
M.A.C.	In.	485.6
Sweep C/4	Deg.	64.41
Ave. Exposed Chord	In.	426.1
Chord S.O.B.	In.	1159.8
Dihedral	Deg.	0.00

Reference Plane	Units	
Sweep C/4	Deg.	64.41
Sweep Leading Edge	Deg.	72.00 / 52.00 / 48.00
Sweep Trailing Edge	Deg.	-21.62 / -84.99 / 34.00
Slat Area	Sqft.	126.71
Plain Flap Area	Sqft.	156.12
Aileron Area	Sqft.	82.44
Control Surface Area	Sqft.	117.89

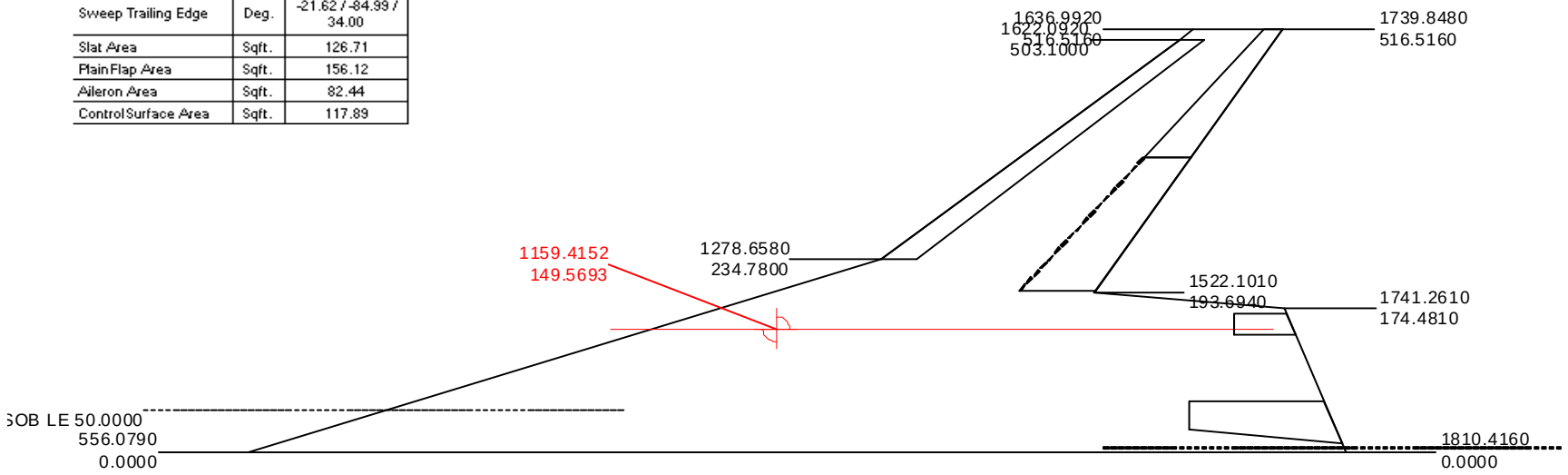

Figure 4.2.3 076E Wing Planform

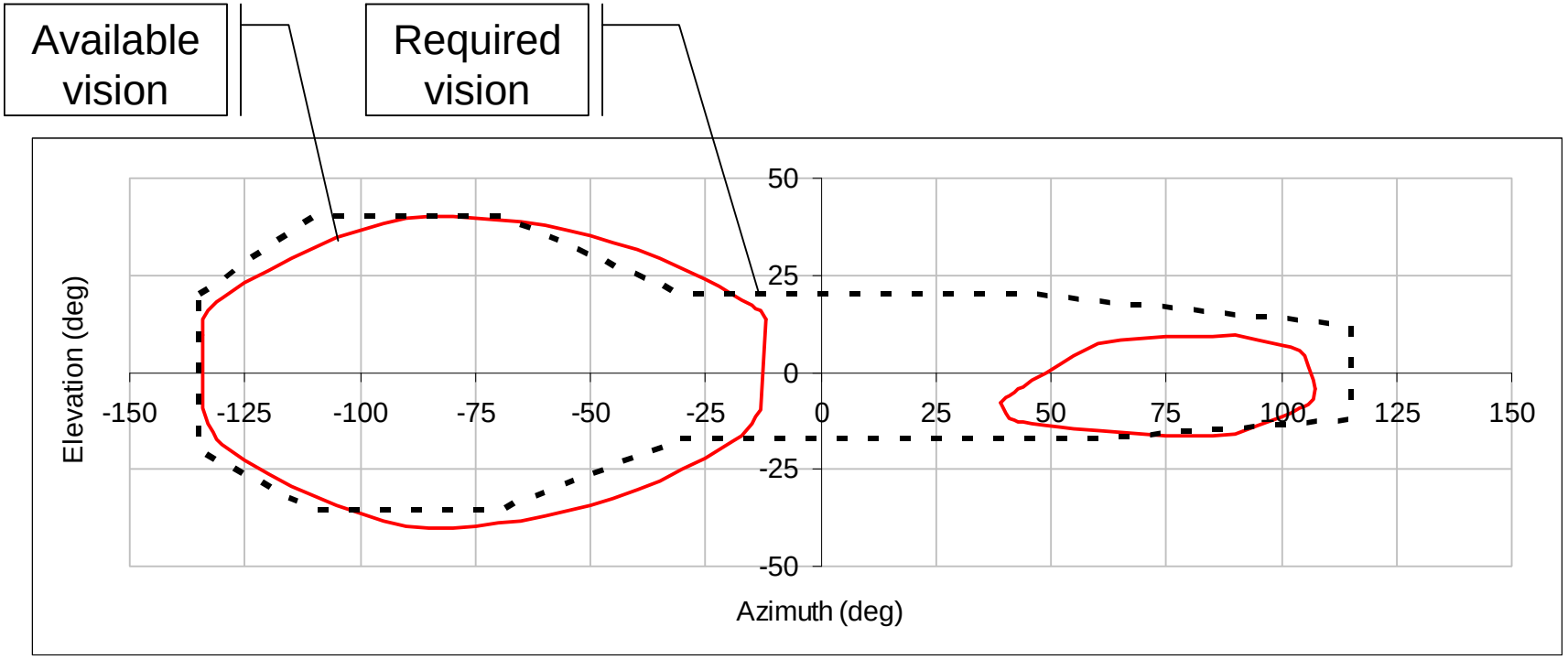

Figure 4.2.4 076E Cockpit Vision

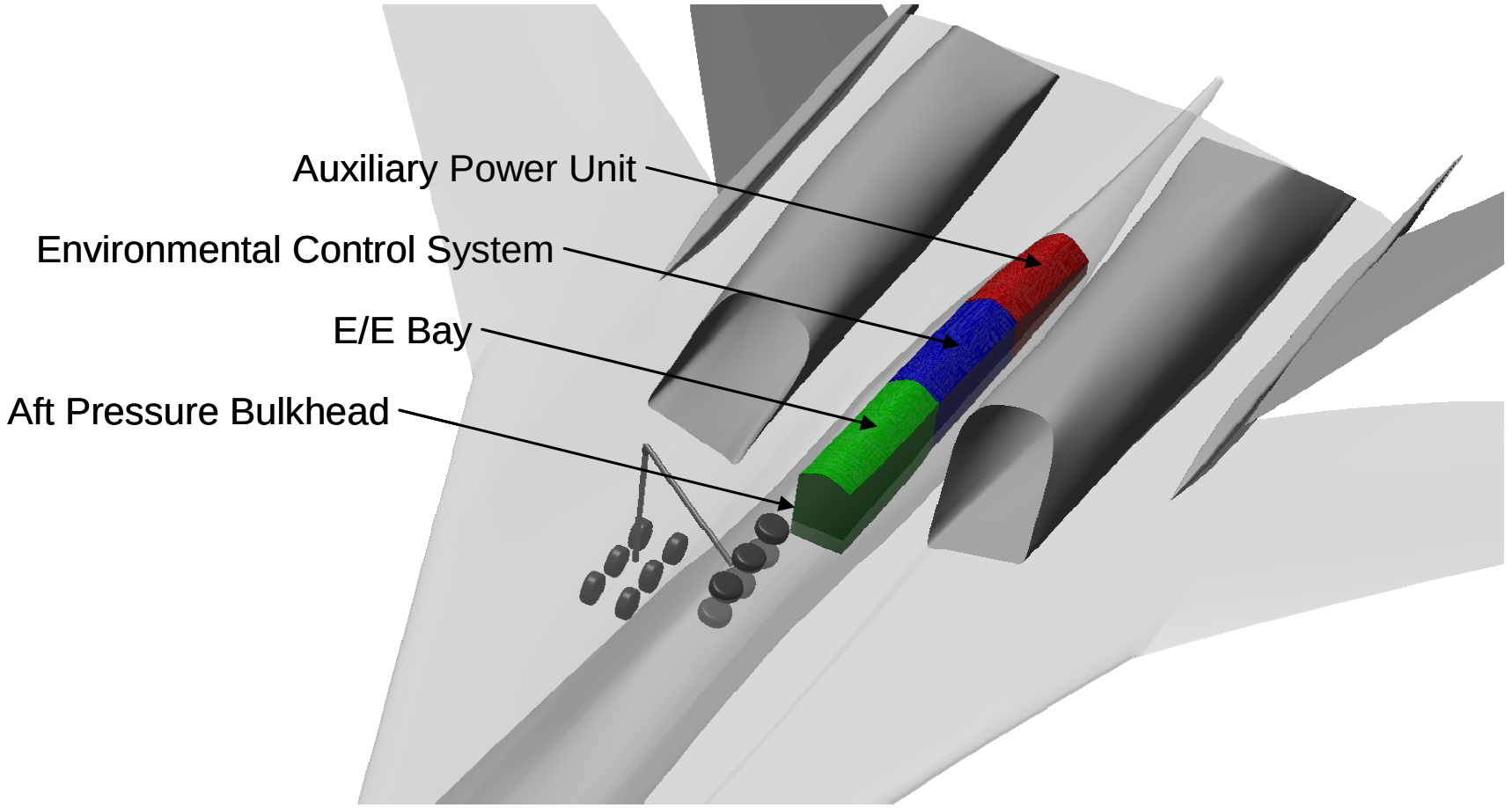

Figure 4.2.5 076E Subsystem Layout

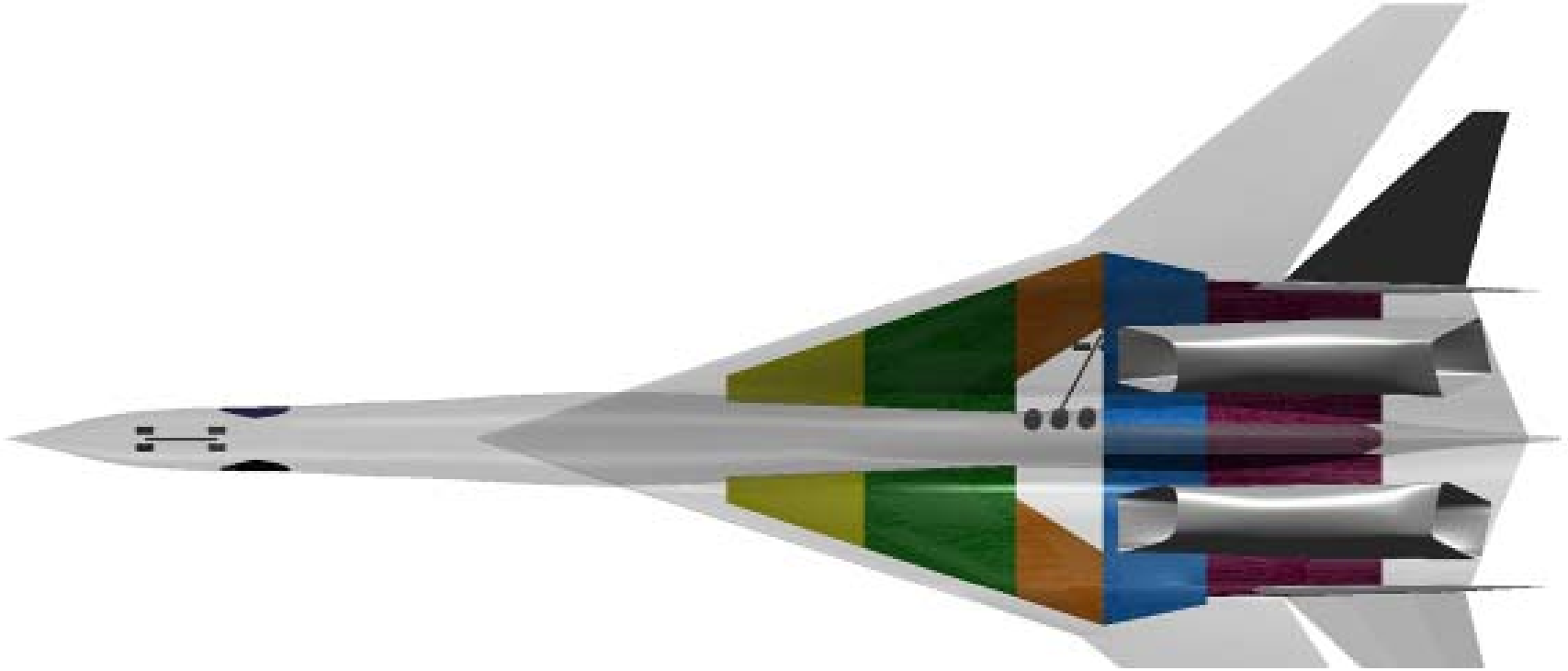

Figure 4.2.6 076E Fuel Tank Layout

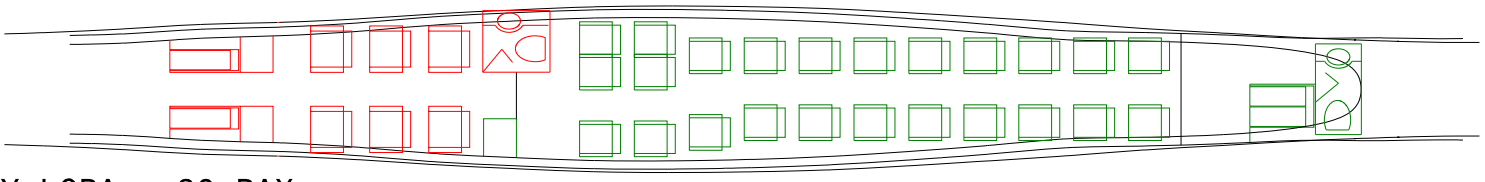

LOW DENSITY LOPA - 30 PAX

	Class %	Carts	Cart Ratio	Lav Ratio	Closet Ratio	Attendant Ratio
First	20	2	0.333	6	7	6
Economy	80	2	0.083	24	1	24
Total	-	4	0.133	-	-	15

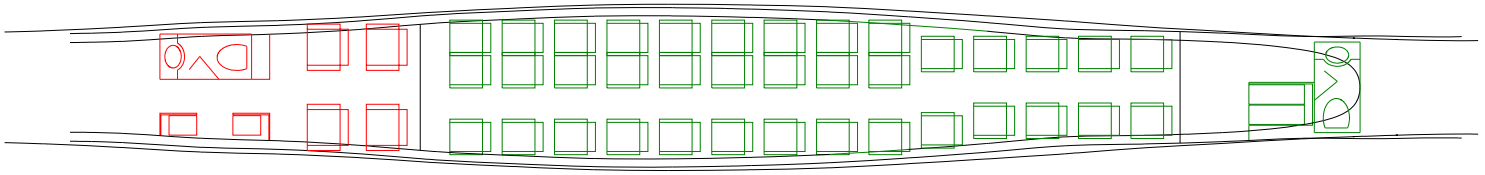

HIGH DENSITY LOPA - 41 PAX

	Class %	Carts	Cart Ratio	Lav Ratio	Closet Ratio	Attendant Ratio
First	9.8	1	0.250	4	2	4
Economy	90.2	2	0.051	39	0	39
Total	-	3	0.073	-	-	21

Figure 4.2.7 076E Layout of Passenger Accommodations

		Growth 180,000 lb	
FC	**Description**	**Weight**	**CG**
01	Wing Structure	26670	1409
02	Horizontal Tail Struture	3110	1667
03	Vertical Tail Structure	10	1667
04	Fuselage Structure	9600	911
05	Main Landing Gear	4330	1285
07	Nose Landing Gear	620	241
08	Forebody Controls	0	0
	Structure Total	**44,340**	**1,291**
09	Inlet Structure and Systems	2840	1458
10	Cowling	1560	1590
11	Pylon/Strut	1040	1583
12	Engine	19220	1567
13	Nozzle	1020	1715
14	Installation (incl. fairings)	1360	1583
15	Engine Accessories, Controls, & Start System	200	1605
	Propulsion Pod Total	**27,240**	**1,564**
23	Fuel System	2500	1306
24	APU/EPU	450	1577
24	Instruments	830	459
24	Surface Controls	2010	1240
24	Hydraulic Power System	1300	1187
24	Pneumatic System	0	0
24	Electrical System	1920	1474
24	Electronics	510	1294
24	Flight Provisions	760	320
24	Passenger Accomodations	6010	841
24	Cargo Compartment	550	1368
24	Emergency Equipment	180	818
24	Environmental Control Systems	980	1262
24	Ice Protection	200	1424
24	Exterior Markings	380	1168
24	Load and Handling	0	0
24	Customer Options	800	500
	Systems & Fixed Equipment Total	**19,380**	**1,055**
	Manufacturer's Empty Weight (MEW)	**90,960**	**1,323**
97	Standard and Operational Items	3140	891
	Operational Empty Weight (OEW)	**94,100**	**1,308**
	Payload	6300	879
	Max Zero Fuel Weight (MZFW)	**100,400**	**1281**
	Fuel	79,600	1328
	MTOGW	**180,000**	**1,302**

Figure 4.2.8 Preliminary 765-076E Performance Weights

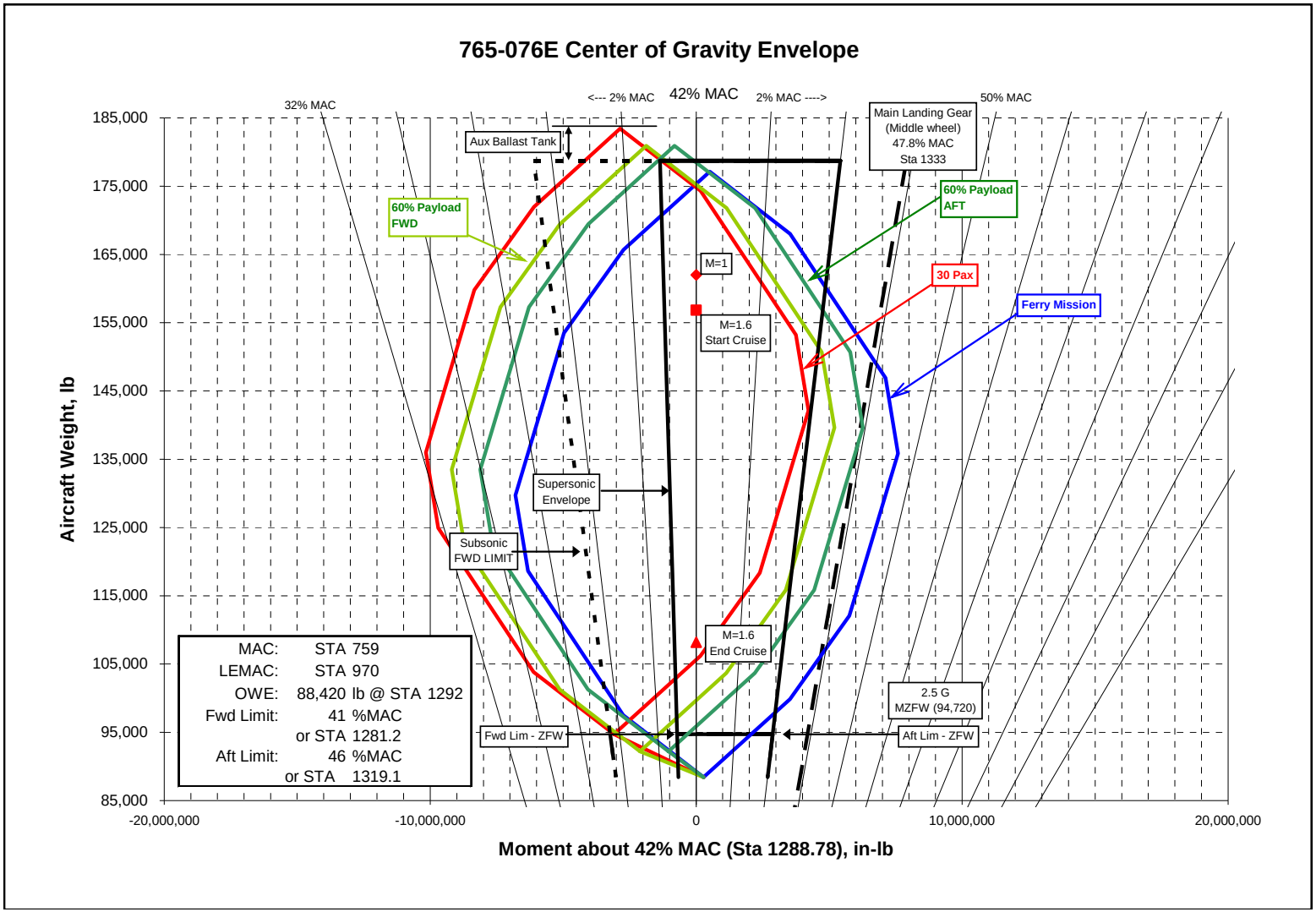

Figure 4.2.9 Preliminary 765-076E Center of Gravity Envelope

FC	Description	Weight	CG
01	Wing Structure	26590	1409
02	Horizontal Tail Struture	3110	1668
03	Vertical Tail Structure	10	0
04	Fuselage Structure	9590	911
05	Main Landing Gear	4290	1285
07	Nose Landing Gear	620	241
08	Forebody Controls	0	0
	Structure Total	**44,210**	**1,291**
09	Inlet Structure and Systems	2840	1458
10	Cowling	1560	1590
11	Pylon/Strut	760	1582
12	Engine	14540	1567
13	Nozzle	960	1715
14	Installation (incl. fairings)	1040	1582
15	Engine Accessories, Controls, & Start System	200	1605
	Propulsion Pod Total	**21,900**	**1,563**
23	Fuel System	2420	1306
24	APU/EPU	450	1577
24	Instruments	830	459
24	Surface Controls	2000	1240
24	Hydraulic Power System	1290	1187
24	Pneumatic System	0	0
24	Electrical System	1810	1476
24	Electronics	510	1294
24	Flight Provisions	760	320
24	Passenger Accomodations	6010	841
24	Cargo Compartment	550	1368
24	Emergency Equipment	180	818
24	Environmental Control Systems	980	1262
24	Ice Protection	200	1424
24	Exterior Markings	380	1168
24	Load and Handling	0	0
24	Customer Options	800	500
	Systems & Fixed Equipment Total	**19,170**	**1,052**
	Manufacturer's Empty Weight (MEW)	**85,280**	**1,307**
97	Standard and Operational Items	3140	891
	Operational Empty Weight (OEW)	**88,420**	**1,292**
	Payload	6300	879
	Max Zero Fuel Weight (MZFW)	**94,720**	**1265**
	Fuel	84,017	1311
	MTOGW	**178,737**	**1,286**

Figure 4.2.10 765-076E Performance Weights

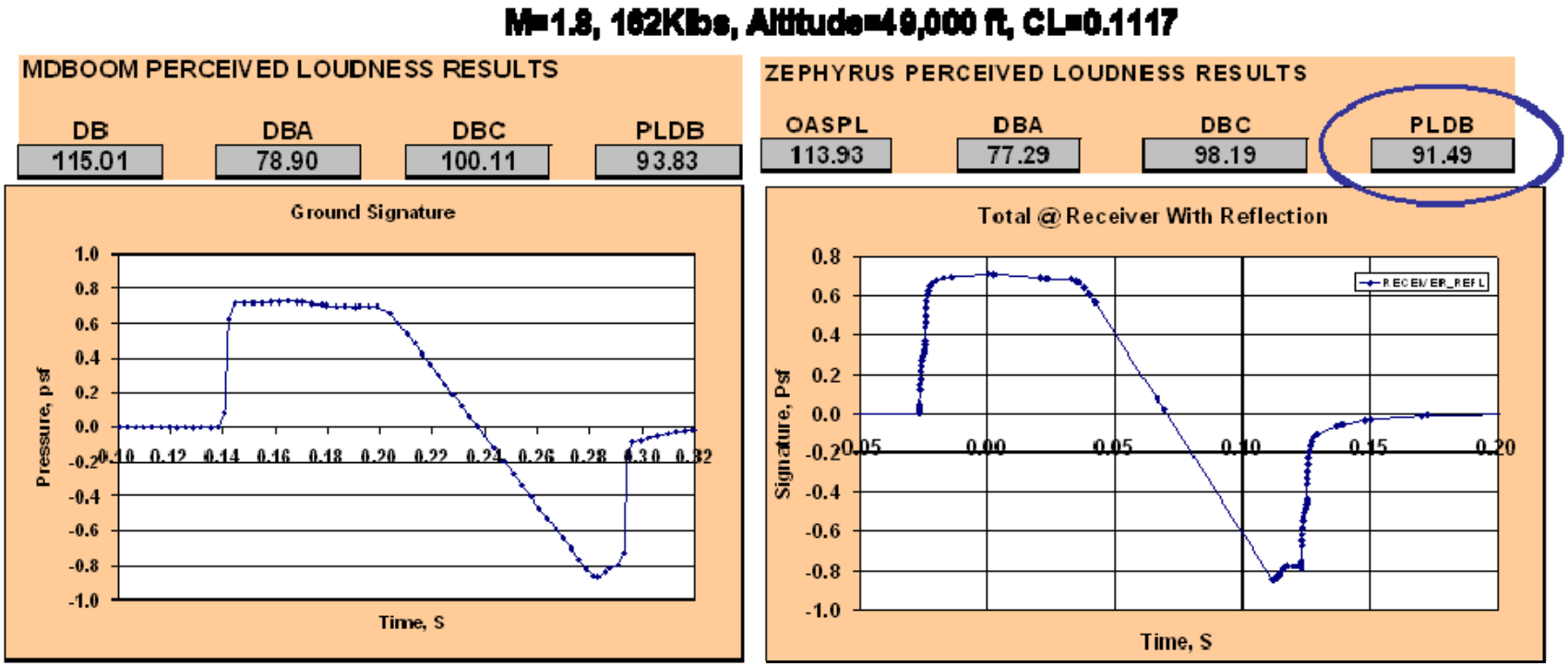

Figure 4.3.1 765-076E As-Designed Shaped Ground Signatures

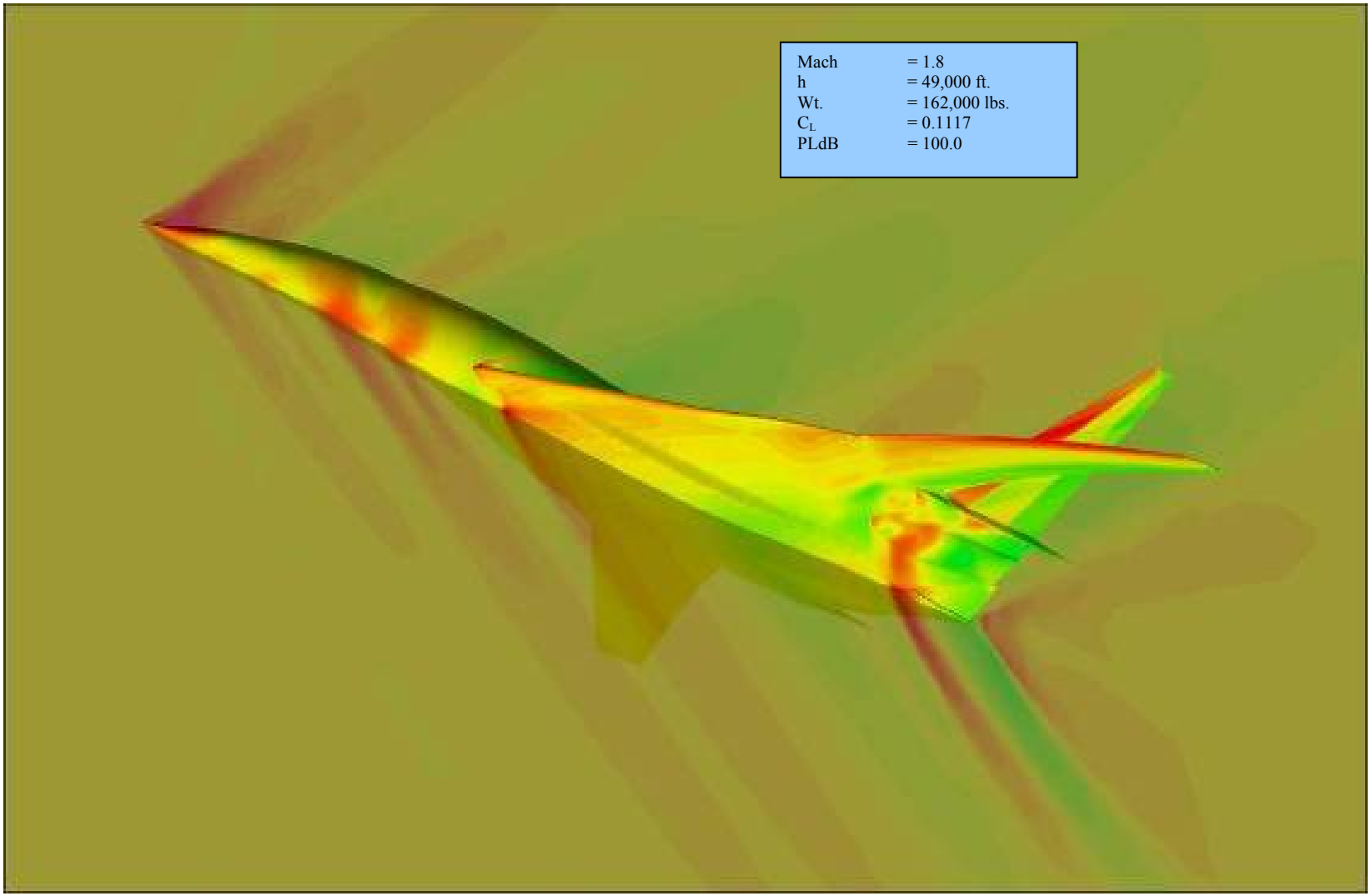

Figure 4.3.2 765-076E CART3D CFD Euler Solution

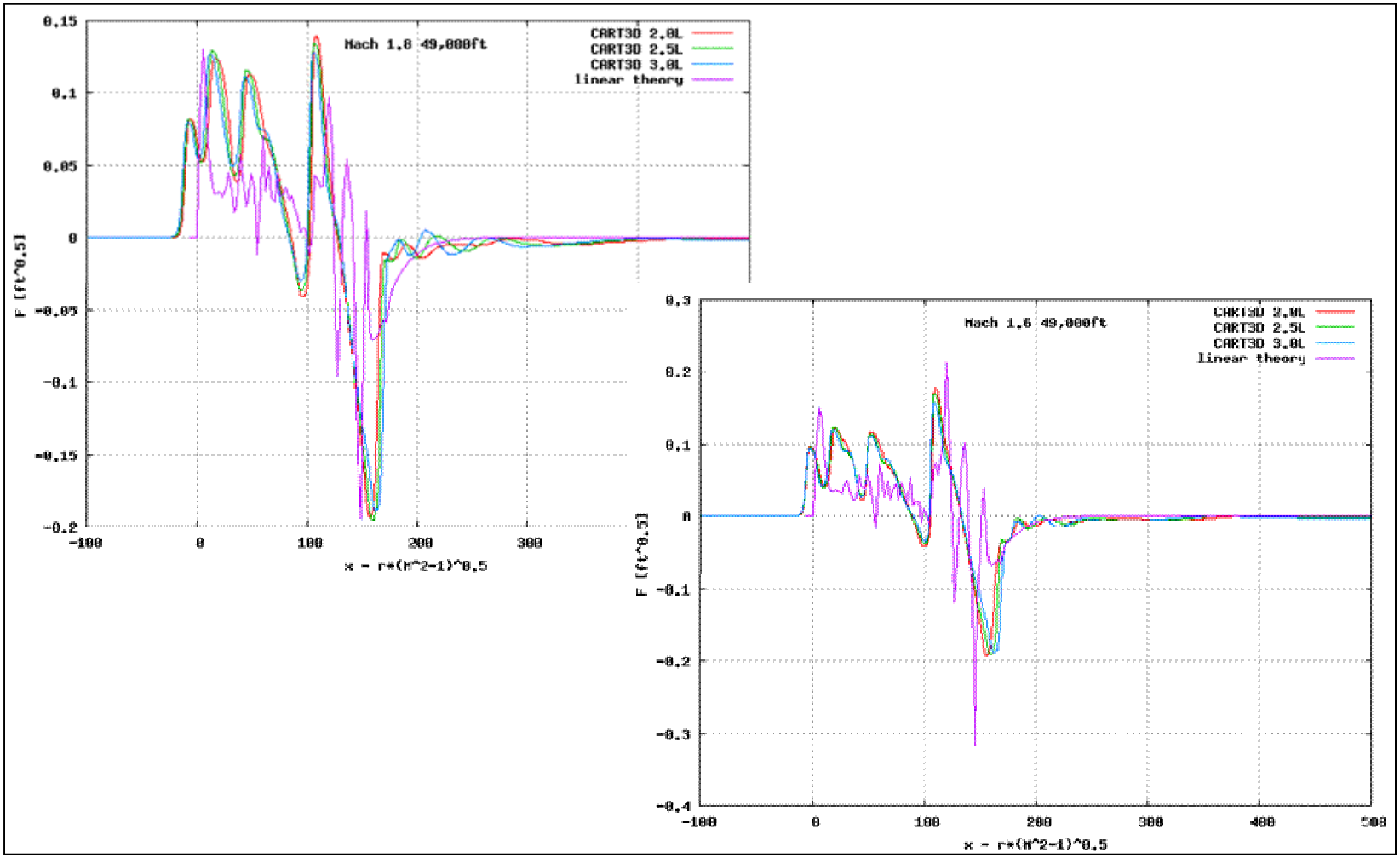

Figure 4.3.3 765-076E Off-Body F-Function CART3D vs. Linear

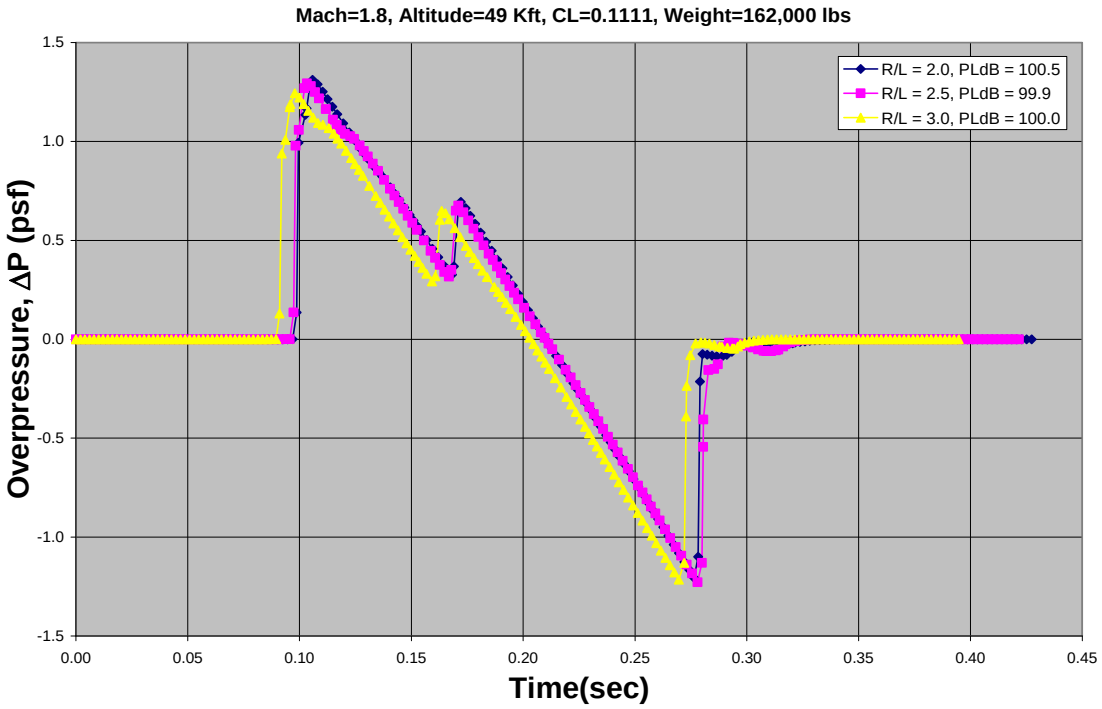

Figure 4.3.4 765-076E Ground Signatures

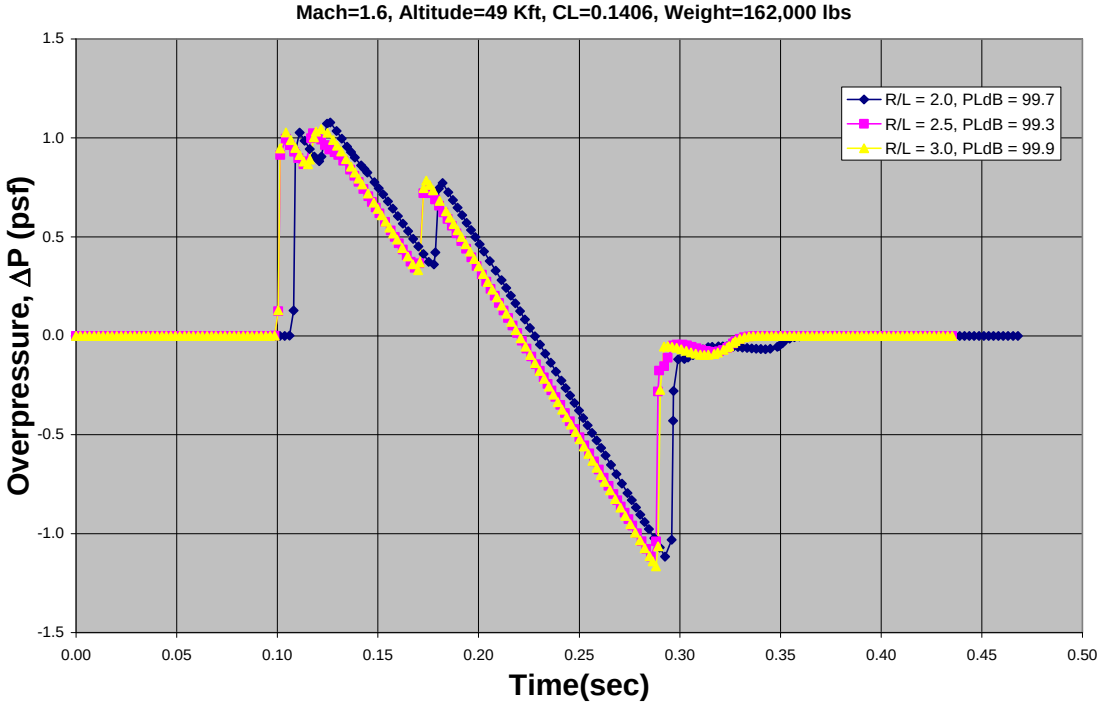

Figure 4.3.5 765-076E Alternate Ground Signature Results

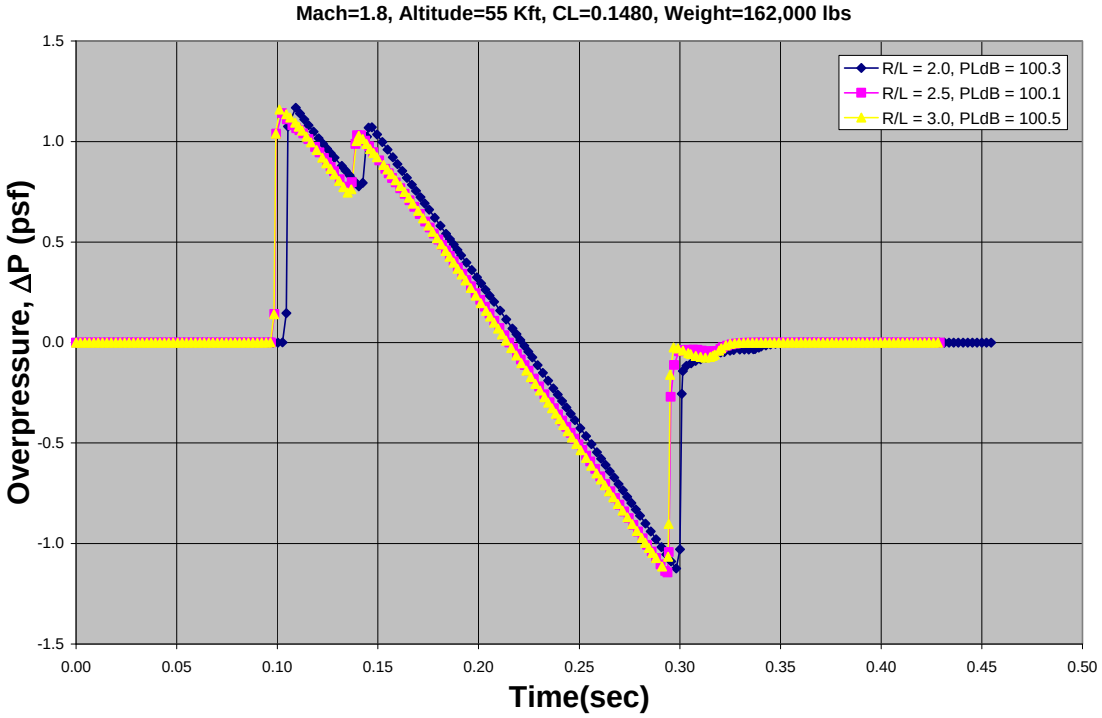

Figure 4.3.6 765-076E Alternate Ground Signature Results

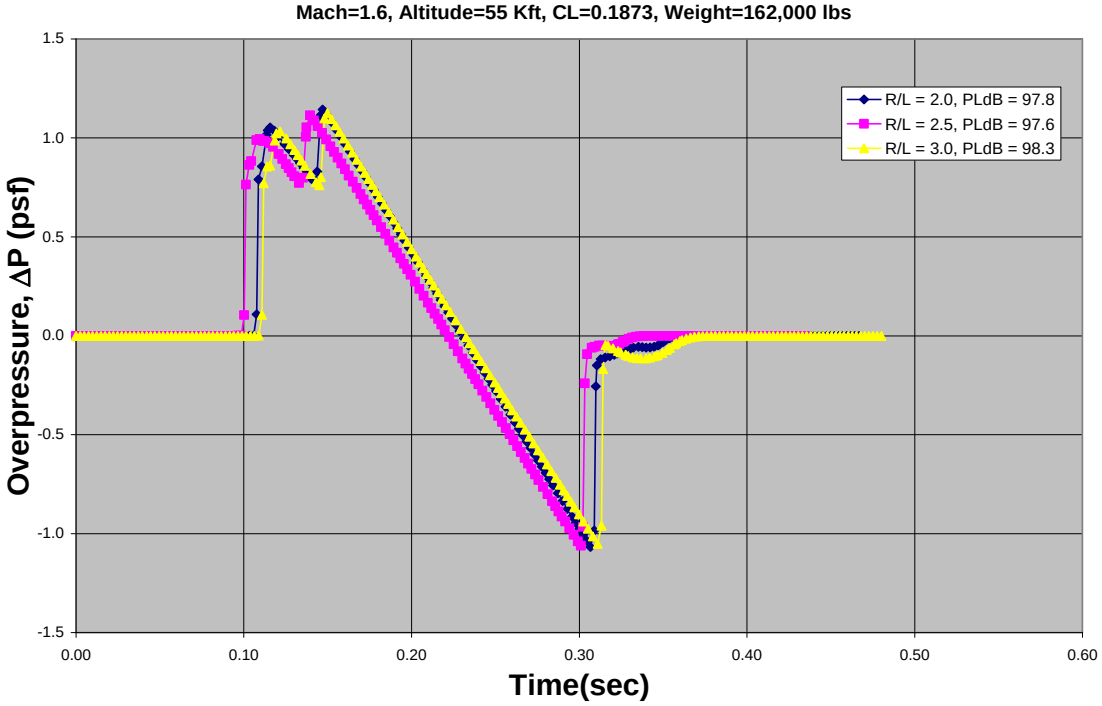

Figure 4.3.7 765-076E Alternate Ground Signature Results

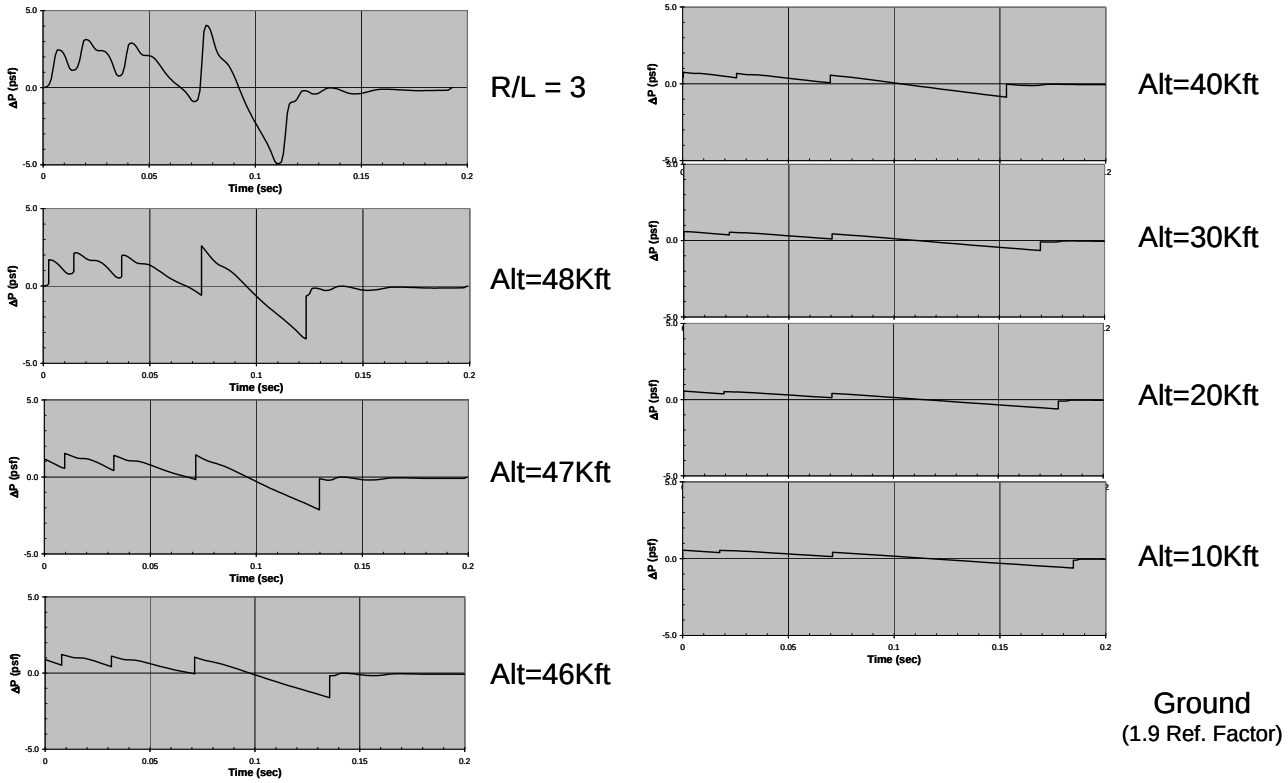

Figure 4.3.8 Progression of Signature with Altitude(Mach=1.6, Alt=49 kft, Weight=162 klbs)

Table 4.4.1 N+2 Study Compliance Matrix

	Guidelines for Study	765-072B	765-076E
Environmental Goals			
Sonic Boom (Linear Theory Goal)	65-70 PLdB	~ 100	~ 90
Airport Noise (cum below Stage 3)	Stage 3 –10 to 20 dB (1100 fps Vj)	1194 Vj	minus 15
Cruise Emissions (NOx g/kg of fuel)	Limited Consideration	Not evaluated	Not evaluated
Performance Goals			
Cruise Mach	1.6 to 2.0	1.6	1.6
Range (nm)	4000 to 6000	4000	3799
Payload (passengers)	25 to 100	100	30
Fuel Efficiency (passenger-miles per pound of fuel)	>3.0	3.17	1.57

5.0 Second Iteration Analysis of Baseline Concept

5.1 Structural Analysis (Option 1)

The structural analysis and sizing of the selected configuration begins with the OML geometry and basic structural layout provided by the configuration design engineer. A finite element model (FEM) was developed based on this data utilizing Boeing 'rapid FEM' development tools. Initial sizing was estimated and material properties obtained for the baseline materials of carbon composites and aluminum selected for this analysis. A 2nd cycle of analysis was executed to improve the loads paths, evaluate alternate material usage and revised criteria.

The flight envelope is shown in Figures 5.1.1. The dive speed envelope was defined as 1.15% of the cruise speed envelope. A limited set of conceptual design level structural design criteria was developed for initial sizing of the airframe primary components. These consisted of symmetrical pull-up conditions, steady roll, 3–point landing (@ 1.6 g), 0.5 g ground turn, and cabin pressurization. The cabin is assumed to be pressurized to a design pressure altitude of 6000 Ft mean sea level. It is assumed that the pressure relief valve is set to 0.5 psi. Figure 5.1.2 lists the flight load conditions. Loads were developed for the target MTOW condition of 180,000 lbs.

A weights statement together with parametric weight was prepared by the weight and balance group and shown in section 4.0. The weights group provided the distribution of the nonstructural weight items to the FEM for use in the loads and structural analyses

A set of design loads conditions were generated from the initial FEM and used in the sizing analysis using MSCNASTRAN Solution 200. The final sizing analysis has produced structural weights that exceed the parametric weight estimates. The Maximum Take-Off Weight (MTOW) has been defined as 180,000 lbs and therefore the maximum fuel load has been reduced commensurate with the difference in the parametric structural weight estimates and the sized structure. The reduction in fuel load results in a reduction in mission range that falls below minimum requirements and decreases the value of the final sized FEM for use in further analyses.

The following subsections provide additional detail and results for the structural analysis activities.

5.1.1 FEM and Sizing

Challenges

Due to the unique configuration of the 765-076E airplane, there are a number of structural challenges for the team to address. Two of these challenges are the thin aft deck and the outboard and inboard wing joint.

- Thin Aft deck, Figure 5.1.3: The aft deck configuration presents a significant challenge for the structure team, as it averages only 7 inches thick and require to carry the engine and the tail load.

- Outboard and Inboard Wing Joint, Figure 5.1.4: The joint between the outboard and inboard wing also presented a significant structural challenge, as the depth is about 7 inches in that area.

Assumptions

The structural analysis task under this NRA is a low-fidelity analysis on a conceptual design model, therefore a number of assumptions had to be made for the analysis. The following is a list of assumptions used in this analysis:

- The tails will act as all moving control surfaces. This assumption is made because the control surfaces and the control laws have not been fully developed, and the fact that a huge tail load is required to perform the pitch maneuver

- 10% improvement for material stress and strain allowable. This assumption is made to reduce vehicle weight and is deemed valid because the vehicle is designed to be a 2025 airplane
- Assuming the control surface actuators will fit into the limited space in the airplane
- The sizing analysis is a strength only analysis, so no buckling or dynamic constraints were considered
- Control surfaces will not be sized. They are model to transfer the aero loads to the structure, and has weight assigned by the parametric tool

Materials Used in the Finite Element Model

- Sandwich Panel:

	E11 (ksi)	**E22 (ksi)**	**Poisson Ratio**	**Shear Modulus (ksi)**	**Density (lb/in^3)**
Carbon Fiber Face Sheet	23000	1600	0.34	800	0.056
Aluminum Honeycomb	187	0.187	0.4	0.013	0.00329

- Isotropic Materials:

	E (ksi)	**Poisson Ratio**	**Density (lb/in^3)**
Titanium	10000	0.33	0.101
Aluminum	16000	0.31	0.162
Carbon-Carbon	18460	0.34	0.065

- The application of materials can be seen in the Figures 5.1.5 & 5.1.6:

Finite Element Model

Structural Layout

The structural layout of the 076E airplane is shown in Figures 5.1.7. This layout is the result of previous sizing analysis cycle, where the high running loads indicated issues with the aft deck stiffness and outboard and inboard wing joint. This can be seen in plots of the running loads, as shown in Figures 5.1.8 & 5.1.9. To enhance the structure, a number of improvements were added to the vehicle:

- Tail torque box: Because of thin aft deck, a torque box was used to carry the tail load forward to the trailing edge of the wing. This is to relieve the load in the carry through structure in the aft deck, as the depth there are insufficient to carry the tail load and the engine weight effectively.
- Keel structure, Figure 5.1.10: A set of keels were added to the inboard wing in the streamwise direction to add bending stiffness to the wing. This addition was deem necessary after initial sizing analysis indicating the need to increase the rigidity of the inboard wing and aft deck
- Aft deck elevator surfaces: A set of elevator surfaces were added to the aft deck to relieve the tail load
- Solid wing and tail tips: Solid core were used at the tip of the outboard wing and tail. This is due to the limited internal volumes at these locations.

Structural Analysis Process

The structural analysis process, shown schematically in Figure 5.1.11, utilized a variety of COTS tools as well as Boeing developed processes. The analysis began with an OML geometry of the airplane, which was then taken into Catia V5 to prepare for finite element modeling. The preparation includes the creation of internal structural layout, and the payload structure in the fuselage. All the surfaces are also split to make the meshing process easier. Once that is completed, it was taken into Patran to create finite element and aeroelastic model. A number of Boeing process was used to rapidly prepare the FEM for the loads and structural sizing analysis

Setup for Sizing Analysis

The sizing of the 076E FEM utilized SOL200 solver from MSC Nastran 2005R3. The objective of the sizing analysis is to find global minimum for weight based on strength sizing. There are a total of 1096 design variables in the model, which is high for a conceptual design model. This is needed to try to achieve the aggressive weight target, which was calculated by Boeing's parametric weight tool to be 31,430 pounds. These design variables include the following:

- Ply thickness of composite panels
- Shell thickness of titanium structures
- Cross sectional area of caps

The sizing analysis was based on the strength of the vehicle, so strain allowables were used as the constraints for the panels and stress allowables were used as constraints for the caps. The sizing analysis performed here was based strictly on the linear static analyses of the vehicle, so other considerations such as flutter, buckling, and dynamic gust will need to be studied to yield the final weight and structure design.

The load for each load cases (see table below) were first generated in Nastran SOL144 static aeroelastic analysis, and then mapped to Nastran FORCE cards. These FORCE cards are then combined with other load conditions if necessary, such as inertial load for the landing and the pressure loads for the fuselage. The usages of FORCE cards allow the analysis to run faster, as the loads are not updated with each design cycle update.

Case	Description	Mach	Q	NX	NY	NZ	Roll Rate	Pressure	Inertial Load (G)
1	2.5G Pull-Up @ M 0.836 x 1.15	0.961	4.373	0.0	0.0	2.5	0.0	5.52	N/A
2	1.2G Pull-Up @ M1.600 x 1.15	1.84	6.47	0.0	0.0	1.2	0.0	9.55	N/A
3	-0.5G Push Over @ M 0.836 x 1.15	0.961	4.343	0.0	0.0	-0.5	0.0	5.52	N/A
4	0.0G Push Over @ M 1.600 x 1.15	1.84	6.47	0.0	0.0	0.0	0.0	9.55	N/A
5	25 deg/sec @ M 0.836	0.836	3.306	0.0	0.0	0.0	0.436	5.52	N/A
6	3-point landing	0.235	0.568	0.0	0.0	1.0	0.0	0.00	-1.6
7	0.5G Lateral Ground Maneuver	0.0	0.0	0.0	0.5	0.0	0.0	0.00	1.0
8	1.5G Pitch Up @ M 1.600 x 1.15	1.84	6.47	0.0	0.0	1.5	0.0	9.55	N/A
9	Overpressure	0.0	0.0	0.0	0.0	0.0	0.0	18.29	-1.0
10	25 deg/sec @ M 0.836	0.836	3.306	0.0	0.0	1.6	0.436	5.52	N/A

Sizing Results

	Parametric Weight	FEM Weight	Difference
Fuselage	6,050	**11,936**	**5,886**
Total Wing	22,260	**35,390**	**13,130**
Tail & HPOD	3,120	**5,307**	**2,187**
Total	31,430	**52,633**	**21,203**

The final sized FEM yield a weight of 52,633 pounds, as shown in table above. This is 21,203 pounds heavier than the value predicted by the parametric weight tool. There are a number of reasons why the FEM weight is heavier than the parametric weight:

1. The parametric tool is based on empirical data of previous supersonic vehicles. These vehicles did not have configuration similar to this 076E airplane, which has thin aft deck supporting large tail loads and heavy engines.
2. The airplane has a 10% static margin, and a short moment arm for pitch maneuver. This means the tail will need to generate large forces in order to achieve the 2.5 G maneuvers, which means significant amount of structure is needed in the aft deck to support this large load.
3. The limited volume in the wing and the aft deck does not provide efficient load path. In order to carry the loads, more structures are required which yield heavier weight.

The structure team believed that the airplane structure has yet to achieve its minimal weight, and is optimistic that more weight can be removed. However, this will require more iteration in structural layout and interactions with the aerodynamic team to improve the configuration of the airplane. Here are the recommendations to improve the airplane's structure and to reduce the structure weight:

1. Increase the depth of the aft deck to allow more load bearing structures for the engine and tail
2. Increase the depth of the inboard and outboard wing joint to allow higher bending moment of inertia
3. Improve the structural layout so more spars are used to carry the load from outboard wing to the inboard wing box
4. Incorporate keel beam in the fuselage to carry load from fuselage bending
5. Conduct trade study to determine if usage of aluminum yields lighter weight

Conclusion from Sizing Analysis

A comparison of the running loads analysis between this latest sized FEM and the previous iteration shows a significant reduction in the loads. This is the results of the updated structural layout as well as the updated loads criteria. Two of the critical running load cases are shown in Figures 5.1.12 and 5.1.13.

The weight statement for the vehicle has also been updated, in Table 5.1.1, with the data from the sizing analysis. The MTOGW of the vehicle is still constrained at 180,000 pound, due to the requirement for sonic boom performance. Because of this, it was necessary to lower the fuel volume in order to counter the increase in structural weight, and achieve the target weight.

Although it is possible to reduce the structural weight further to regain some of the fuel volume, using the recommendations in the previous section, it is possible that this airplane cannot achieve the range and payload requirement as an 180,000 pound airplane. It is likely that MTOGW will need to be increased to accommodate the structure that will be necessary to meet performance and certification requirements. Therefore, to be able to close the design and to have a valid finite element model for further structural analyses, this airplane will need to be iterated among the disciplines within the team to ensure the final vehicle configuration can and will address all performance requirements. Until then, this finite element model will serve as a good lead-in to the next design iteration, but is likely not valid for further structural analyses.

Other Analyses

The original plan called for completion of a flutter analysis, gust loads assessment and development of state space models. These analyses have not been completed based upon the maturity of the FEM relative to the overall design and performance requirements.

5.2 Propulsion System Analysis (Option 2)

5.2.1 WATE ++

5.2.1.1 - Limitations of WATE++

While designing the flowpath Georgia Tech ran into some difficulty using WATE++ to draw a reasonable flowpath because the tool is designed to provide a weight estimate, not to create a realistic flowpath. Inherent limitations such as restricted compressor and turbine geometries, the inability to specify individual stage loadings, the restriction of constant hub, tip, or meanline designs, and other factors meant that GT had to create several design rules which allowed GT to create a feasible flowpath from WATE++ on the first pass which could then be tuned with input from Rolls Royce in order to arrive at the final design.

5.2.1.2 - WATE++ Flowpath Design Rules

All of the design rules were implemented into NPSS/WATE++ using the built in solver functionality. The aeromechanical design point for the WATE++ model was set as the top of climb point; however, WATE++ records maximum pressures and temperatures over the entire flight envelope to calculate duct thickness and other parameters that depend on upper limits.

Fan and HPC Tip Speeds

The Fan and HPC tip speeds are set as a function of the first stage pressure ratio. Since the shaft speed helps to determine the turbine radial location it was important to give the designer control over this parameter. By relating the blade tip speed to pressure ratio it allows the designer to make intelligent choices that scale with engine size. The curve, shown in Figure 5.2.1, used to determine the fan tip speed was taken

without modification from "Preliminary Estimation of Engine Gas-Flow-Path Size and Weight" by Sanghi. The HPC tip speed was created by supplementing the fan tip speed curve with data in Hill & Peterson.

Fan Inlet Mach Number

The thermal cycle analysis executed by NPSS calculates a fan diameter based on the SLS mass flow, an assumed fan specific flow of 40 lbm/ft^2, and a hub to tip ratio listed in Table 5.2.1. The engine-vehicle optimization performed for the 076E made use of the fan diameter calculated in the thermal cycle analysis. Therefore it is important to keep the fan hub to tip ratio and specific flow in the WATE++ model equal to the ones specified in the NPSS thermodynamic cycle. The fan inlet Mach number is varied to maintain the specified fan specific flow.

HPC / HPT / LPT Inlet Mach Numbers

Average stage flow coefficients, listed in Table 5.2.1 for the HPC and turbines, were set by varying the inlet Mach number until Equation 5.2.1 is satisfied. The rotational speed falls out from the tip speed set for the fan or HPC. The turbine radius is calculated by WATE++ using the turbine loading parameter and the enthalpy rise per stage.

$$\phi = \frac{C_{ax}}{(\omega r_{mid})}$$

Equation 5.2.1 Flow Coefficient

Turbine Loading

WATE++ allows the user to specify a turbine loading parameter. In order to simplify the calculations a constant mean line turbine with symmetrical velocity diagrams is assumed. While this would be a highly unlikely result for the actual design, it serves to provide a simple and quick method of relating the turbine loading to other input parameters. According to *Analysis of Fan-Turbine Efficiency Characteristics in Terms of Size and Stage Number* by Warner L. Stewart, the flow coefficient can be related to the turbine loading parameter and stator inlet angle, α_1, by Equation 5.2.2. By using this relationship the designer only has to choose a flow coefficient and stator inlet angle. Table 5.2.1 shows the final stator inlet angles.

$$\frac{C_{ax}}{U} = \left(\frac{\lambda + 1}{2\lambda}\right)\cot(\alpha_1)$$

Equation 5.2.2 Turbine Loading Parameter / Flow Coefficient Relationship

In order to keep the turbine loading within reasonable values a Smith chart is used to constrain the maximum possible turbine loading for the initial design pass. A Smith chart, shown in Figure 5.2.2, relates zero clearance turbine efficiency to the loading parameter and flow coefficient. The Smith chart is not corrected for tip clearance because it is assumed there will be active clearance control that greatly reduces tip losses. Furthermore, the actual efficiency values on the Smith chart come from test data, so they do not represent possible advances in technology.

Specific Speed

Specific speed is not used as an input into the MFTF WATE++ model; instead it serves as a sanity check on the combination of flow coefficients, first stage pressure ratios (i.e., rpm), and other inputs. Specific speed, as defined in Equation allows the designer to determine whether or not the component is designed in a way that will allow it to operate in an efficient manner. Curves corresponding to axial flow machines in Figure 5.2.3 and Figure 5.2.4 from "Introduction to Turbomachinery" by Japikse were used to determine whether the specific speeds that resulted from other WATE++ inputs were within reason.

$$n_s = \frac{\omega_{shaft}\sqrt{\dot{m}/\rho}}{(\Delta h)^{0.75}}$$

Equation 5.2.3 Definition of Specific Speed

Stage Count Calculation

It was found that WATE++ had very poor numerical convergence properties if the stage count was not specified for each component. To overcome this, WATE++ is provided with the stage count resulting from for each component using the simplified weight estimation routine.

WATE++ Material Selection

The built in WATE++ material database does not include the newest high temperature alloys or the advanced materials that are anticipated in 2025. Georgia Tech used appropriate materials for the various components, but the volume factors for each component were adjusted until the overall weight of each component generally agreed with the Rolls Royce simplified weight estimation method based on flow scaling. Rolls Royce believes the weights provided using their method are more representative of future material technologies. The materials used in the WATE++ model are listed in Table 5.2.2. Aspect ratio distributions were held constant and are listed in Table 5.2.3.

5.2.1.3 - Georgia Tech MFTF Flowpath for 076E

Using the design rules established for WATE++ Georgia Tech proceeded to design a flowpath for the cycle selected for the 076E configuration. Inputs were varied until a flowpath that did not violate any intrinsic mechanical constraints resulted. The final flowpath is shown in Figure 5.2.5. Pertinent input and outputs from the WATE++ model are summarized in Table 5.2.1. It should be noted that some of these parameters, such as the LPT flow coefficient, are outside of the ranges of normal design. This is due to the limitations of WATE++ and the inability to custom-tailor stage loading and radii distributions. The definition of the loading parameter used in Table 5.2.1 is shown in Equation 5.2.4. Table 5.2.4 lists the total engine dimensions and weight.

$$\psi = \frac{\Delta h}{U^2}$$

Equation 5.2.4 Definition of Turbine Loading Parameter

5.2.2 – Flowpath

Starting with the WATE++ flowpath defined by Georgia Tech and discussed above, Rolls-Royce used design architectures drawn from several Rolls-Royce engines to develop the engine cross section shown in Figure 5.2.6.

The conventional combustor section and two stage turbine architecture shown in the WATE++ flowpath are similar in concept to the AE3007 engine. The AE3007 is a civil aircraft engine currently powering the Embraer 145 among other aircraft.

The fan drive turbine of the WATE++ flowpath appeared to be most similar to fan drive turbines used to drive the large high bypass ratio fans in the Rolls-Royce family of engines. This design architecture was modeled to develop the fan drive turbine for the drawing.

The process used in developing the general arrangement drawing was to scope out the space allocated by WATE++ flowpath (axial and radial) for each component. Then each component was scaled to match the

WATE++ flowpath retaining mechanical details where possible. Finally, the similarity to the "host" engines was modified to merge the final engine cross section into one design concept. Different challenges were encountered in each area of adaptation and will be dealt with in turn.

Fan Scaling

Even though similar Rolls-Royce engines feature a two stage fan of similar stage pressure ratios as the target engine, in attempting to scale the components to the WATE++ Flowpath, the Rolls-Royce design team found that the WATE++ airfoil aspect ratios were necessarily higher than other engines. This compressed the geometry somewhat in the axial direction. For the fan flowpath, this compression and the resulting aspect ratios were within Rolls-Royce design practice. However high aspect ratio blading at these stage pressure ratios is sometimes difficult to achieve meeting all aero elastic criteria normally associated with fan blade design. Further iterations towards lower aspect ratio blading would help the construction.

Fan to HPC Swan Neck Scaling

The "swan neck" space claim from the WATE++ flowpath was found to be acceptable, but the shape as presented was more severe than can be accomplished with current (known) aerodynamics. The issue is flow separation from the duct inner wall as it descends to the HPC. In order to develop the general arrangement drawing, a duct from a similar sized engine was scaled to the WATE ++ flowpath resulting in the duct shape shown. The Rolls-Royce team was able to find a swan neck duct that fit the space and appears to be workable. However, by 2025, flow control on the surfaces may result in shorter duct lengths and/or more severe duct wall angles which would favor the WATE++ shape duct.

High Pressure Compressor Scaling

The 11 stage compressor as defined by the WATE++ space claim (axial length) requires blade and vane aspect ratios higher than those associated with today's proprietary highly loaded compressors. However, the blade and vane aspect ratios from the WATE++ flowpath are quite similar to previous generation compressor flowpaths. As the technology has improved to permit higher loading per stage, the blade and vane airfoils have progressively become lower in aspect ratio. The relationship is not quite as linear with loading as this discussion implies, but the trend is certainly true.

Combustor and High Pressure Turbine Scaling

Rolls-Royce aerodynamic components were found to be quite compatible with the space claim of the WATE++ flowpath when scaled to the engine size by flow. There was little compromise required to fit the geometry into the flowpath in this area. Looking forward, future turbines will almost certainly produce more work at reasonable efficiency. The HP spool may be driven by a single stage. It probably makes sense to limit the HP compressor work to that compatible with the best available single stage turbine technology.

Inter-turbine Transition and Low Pressure Turbine Scaling

The maximum flow angle found to be acceptable at the exit of the HPT (shrouded blade geometry) is 12º. This angle was adopted together with a shrouded second stage blade to establish the HPT to LPT turbine transition duct which was compatible with the space claim shown in the WATE++ flowpath. This provided sufficient room to include a structure through the interturbine duct so that an aft bearing could be included for the aft end of the HP shaft as well as a forward bearing for the LPT rotor modeling other Rolls-Royce engine architecture in this area.
The Rolls-Royce team elected to "straddle" mount the LPT with both a forward and aft bearing. This permits a smaller fan drive shaft diameter than might otherwise be considered. An aft structure was added to support the LPT aft bearing, again modeling similar Rolls-Royce architectures.

Engine Flowpath

The resulting engine meets the WATE++ overall dimensions in terms of length and diameter as shown in Figure 5.2.7.

5.2.3 Inlet & Nozzle Flowpath

The nacelle outer mold lines for the 076E configuration were fixed prior to selecting the engine cycle, as described in Sections 3. Because of this, some inlet and nozzle design features and flexibility were constrained. A single pass through the design process for the inlet and nozzle flow path was performed. As a result, some concerns and potential short coming with the nacelle configuration selected exists and will be identified in this section.

Figure 5.2.8 shows the inlet and nozzle flowpath for the selected 75 inch diameter engine for the 076E aircraft. The inlet is described as 3-D external compression configuration. It incorporates isentropic ramp to provide "nearly ideal" free-stream compression prior to throat shock. It is assumed that the baseline configuration will incorporates flow control technologies for optimal shock placement and stability at both cruise and off-design points. The take-off and low speed airflow demand will be accommodated via auxiliary inlet apertures located downstream of throat as shown in Figure 5.2.9. Inlet performance will be high at on-design flight conditions, high power, low speed with aux inlet open and cruise condition. The mechanical integration of aux inlet should be straightforward. The short diffuser length will require some form of flow control devices (e.g., micro vanes) to reduce potential for shock induced separation and energize diffuser flows, but may not satisfy performance and operability targets. In addition, the fixed ramp, bleedless inlet may not provide adequate shock control to satisfy traditional engine operability demands across flight envelope and power settings.

The nozzle is incorporated into the top mounted nacelle arrangement with variable nozzle area ratio (a8/a9). The nozzle is an internal 2D-CD configuration with an integrated thrust reverser concept. There are volume reserves in the nacelle for secondary flow geometry that could be used for reducing jet noise as shown in Figure 5.2.10. The design assumes the baseline configuration will incorporates flow control technologies for matching engine exit stream with secondary airflow. At target type trust reverser concept is shown in Figure 5.2.11. The nacelle design and configuration constraints create some integration concerns. The fixed external aft nacelle compromises off design nozzle performance. The scarfed nozzle exit plane results in suboptimal nozzle vector, impacting both performance and aircraft control. The ultra short nozzle duct, particularly on top, provides little length to mix exhaust and turn flow axially; performance and discharge characteristics may be compromised. The upper nozzle flap is not long enough to completely block flow for reverse operation. In addition, secondary flow / bypass and thrust reverser share deployment mechanisms, complicating failure mode management. The scarf nozzle design will require high temperature sidewall / throat seals to minimize leakage and temperature damage to nearby aircraft structure.

5.2.4 Jet Noise Certification Assessment

Introduction

At the outset of this contract it was realized that the scope of the noise certification assessment should be limited to the conceptual detail provided by the aircraft and engine performance databases. Therefore we selected limiting the noise prediction to screening the jet noise component at the three noise certification reference conditions (i.e. flyover, lateral and approach). We reached a general consensus between the airframe and engine team members that the most difficult noise goal condition to meet would be the lateral condition during the takeoff condition to meet takeoff field length and aircraft range requirements.

The lateral condition would be dominated by the jet noise component from the engine exhaust and therefore we selected a jet noise exhaust velocity in the range of 1100 feet per second for the engine design cycle based on knowledge of past subsonic and supersonic aircraft noise certification data. Therefore the noise assessment would provide a comparison of the jet noise estimate to the absolute total noise goal set to meet the NASA N+2 contract noise certification goal range.

Supersonic N+2 Noise Goal Assumptions

The NASA N+2 noise goal was to meet FAR Part Stage 3 minus 10 to 20 EPNdB.

The two engine 076E configuration was sized to meet a 10,000 feet field length for an aircraft range of about 4000 nmi. The sizing resulted in producing a maximum takeoff weight (MTOW) = 180,000 lbs and maximum landing weight (MLW) = 144,000 lbs

It was decided to initially shoot to meet Stage 3 minus 15 EPNdB (a midway position).Therefore we determined the absolute noise values needed to meet this requirement as follows:

- The absolute noise levels to achieve Stage 3 minus 15 EPNdB limits would need to be typically:
  Flyover = 92.0 – x EPNdB
  Lateral = 97.1 – y EPNdB
  Approach = 100.7 – z EPNdB
- The proposed initial delta goal increments relative to Stage 3 were selected as follows:
  x = 7, y = 3 and z = 5 for a total of – 15 EPNdB
  Hence the absolute goals were set at:
  Flyover = 85.0 EPNdB
  Lateral = 94.1 EPNdB
  Approach = 95.7 EPNdB

Another benchmark in setting these absolute goals was the fact that from an operational point of view it is well documented that the noisiest stage 3 aircraft existing in today's fleet (e.g. retrofitted older Stage 2 aircraft and MD-80 types) during departure have been perceived to be as objectionable neighbors in the communities surrounding the airports. For example, the MD80 noise certification Lateral level for an engine sea level static takeoff thrust of 20,850lbs = 96.0 EPNdB. Therefore the initial goal of 94.1 EPNdB for the 96E configuration is in the favorable lower noise direction.

Noise Certification Measurement Reference Locations

The FAR Part 36 reference noise certification measurement locations are illustrated in Figure 5.2.12 for the Flyover, Lateral and Approach conditions.

Noise Screening Assumptions

Unsuppressed jet noise was estimated at FAR Part 36 measuring locations for the following reference day conditions:

ISA+10º C day
70% Relative Humidity
Zero Wind
Sea Level

The plan was to assess the need for jet noise suppression devices to meet total noise goals including margins available for the contribution of fan (forward & aft) , turbine, core and airframe noise sources form the unsuppressed jet noise screening results

Jet Noise Prediction Assumptions

We used the ANNOP jet noise prediction code for a mixed flow turbofan cycle with internal mixer that uses the mass weighted jet velocity of the fan and core flows at the nozzle exhaust exit station. Additionally we assumed the following:

Assumed fully mixed flow at nozzle exit (i.e. No hot spots)
Assumed axi-symmetric nozzle exit

No account taken for potential self noise contribution of mixer
No account taken for any possible shielding of distributed jet noise sources by twin verticals (lateral) and aft deck platform (flyover)

Jet Noise Prediction Results

The following jet noise prediction results were obtained for the 076E configuration

FAR Part 36 Reference Conditions - Ground Rules

The ground rules for the three reference conditions were as follows:

a) Flyover Conditions
- Monitor point at 21325 ft (6500m)from brakes release
- MTOW
- Maximum takeoff power (de-rated) from brakes release to meet TOFL requirements
- V2+10 TAS climb-out speed
- First screening without cutback procedure
- If needed thrust cutback at approx 4000 feet before monitor to engine power to maintain level flight with one engine inoperative or 4% gradient power whichever is higher
- Assume an instantaneous cutback flight profile

b) Lateral Conditions
- MTOW-
- Maximum Takeoff power (de-rated) to meet TOFL requirements
- V2+10 TAS climb-out speed
- Noise monitor at 1476 feet (450m) to the side of the runway extended centerline
- Assume peak lateral noise occurs at 1000 feet AGL. This represents an angle of elevation from monitor to aircraft of 34.1º (Slant range = 1782 feet)
- Assume lateral attenuation from ANOPP
- No impact of cutback procedure on peak Lateral noise
-

c) Approach Conditions
- MLW
- Approach monitor at 6560 ft (2000m) from runway threshold (394 feet)
- Aircraft to maintain -3 degree glide-slope
- Define noisiest configuration - dirtiest aerodynamic - highest drag condition (30 deg flap)
- Front and main gear down
- Low speed high lift devices out
- Vref+ 10 TAS approach speed

And the results are:

Flyover (No cutback)
Altitude = ~ 2800 feet
V2+10 True Airspeed = 201 knots
Total Net Thrust = 39,588lbs
Vj = 1235 fps
Predicted Jet Noise Level = 87.3 EPNdB
Total Noise Level Goal = 85.0 EPNdB
Difference relative to goal = +2.3 EPNdB

Lateral (1476 ft from runway centerline)
Altitude = 1000 feet
V2+10 True Airspeed = 201 knots
Total Net Thrust = 42,522 lbs
Vj = 1238 fps

Predicted Jet Noise Level = 91.7 EPNdB
Total Noise Level Goal = 94.1 EPNdB
Difference relative to goal = -2.4 EPNdB

Approach

Altitude = 394 feet
Vref+10 True Airspeed = 165 knots
Total Net Thrust = 26,538 lbs
Vj = 979 fps
Predicted Jet Noise Level = 93.6 EPNdB
Total Noise Level Goal = 95.7 EPNdB
Difference relative to goal = -2.1 EPNdB

Jet Noise Screening Conclusions

Based on the jet noise screening results we can draw the following conclusions:

1. Engine cycle (Vj = 1238 fps) at de-rated power adequate to achieve lateral total noise goal (jet noise -2.4 EPNdB below goal). Below benchmark MD-80 noise certification level
2. Flyover Jet noise (without cutback) needs to be further reduced to achieve a reasonable margin relative to total noise goal (current jet noise at 2.3 EPNdB above goal)
3. A larger approach jet noise margin relative to total noise goal needed to account for other noise sources (fan, turbine, core & airframe) contributing to total noise (current jet noise – 1.9 EPNdB below goal)
4. Stage 3 – 15 EPNdB should be doable
5. Stage 3 – 20 EPNdB (i.e. to meet probable Stage 5 limits in 2016 will be a stretch)

5.2.5 Derated Takeoff and Jet Velocity Relationship

The NPSS parametric engine model and Model Center optimization focused on maximizing fuel efficiency while meeting the community noise goal. To do this, mixed jet velocity is used as surrogate for community noise. A target jet velocity of 1100 ft/sec was set. Derated takeoff thrust capability and Automatic Takeoff Thrust Control System (ATTCS) FAR Part 25 regulations were used to minimize takeoff jet velocity. The transonic pinch point and the top of climb flight conditions are engine sizing conditions. To take advantage of this relationship, Logic was added to the NPSS model to allow input of jet velocity which set the derated takeoff thrust rating. Figure 5.2.13 shows that a 21% lower jet velocity, at lateral and flyover conditions, are obtainable relative to the full thrust capability of the engine. Also, shown on the figure is the 39% derate available while still meeting the 10,000 ft balanced field distance.

Tables and Figures for Section 5.0

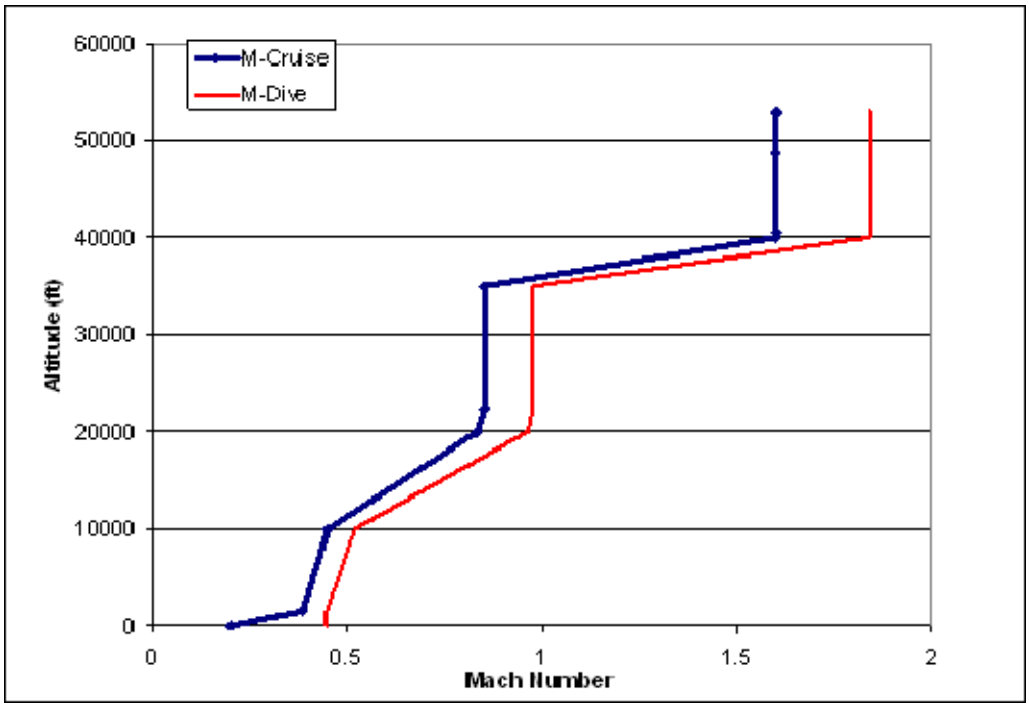

Figure 5.1.1 Flight Envelope for Design Loads Development.

Flight Load Conditions

- **Subsonic**
  - **2.5g (431 knots, M=0.95)**
  - **-1.0g (375 knots, M=0.838)**
  - **25 deg/sec roll(431, M=0.95) @ 1.7g**
- **Supersonic**
  - **1.2g (524 knots, M=1.84)**
  - **1.5g (524 knots, M=1.84)***
  - **0.0g (524 knots, M=1.84)**

Cabin pressure:
6.62 psig @ 20K alt
9.65 psig @ 40K Alt

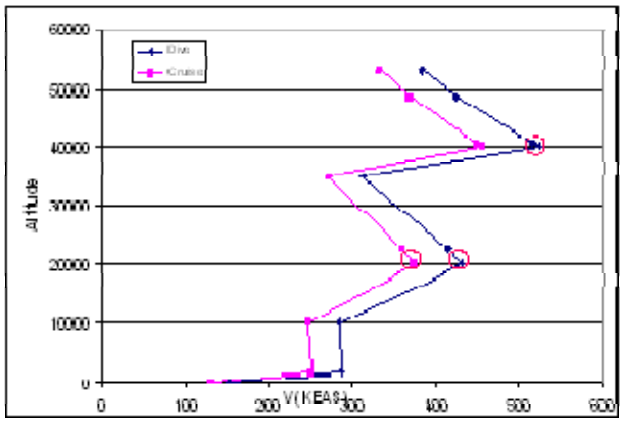

*** This condition represents a transient loading case and is balanced with pitch acceleration**

Figure 5.1.2 Design Load Conditions

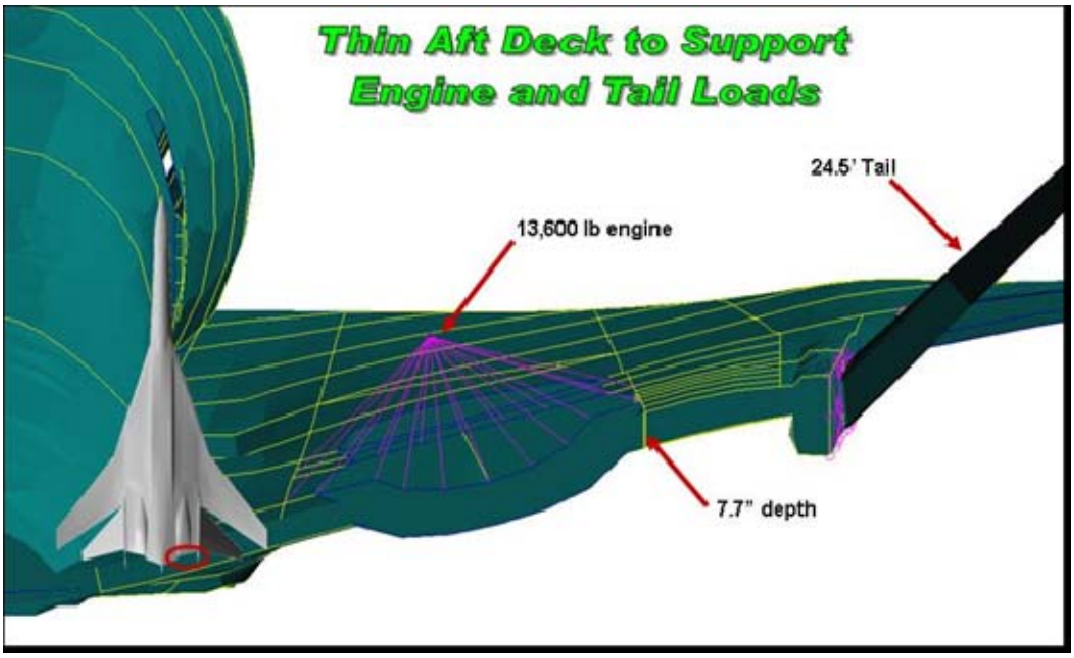

Figure 5.1.3. Aft Deck and Tail Joint

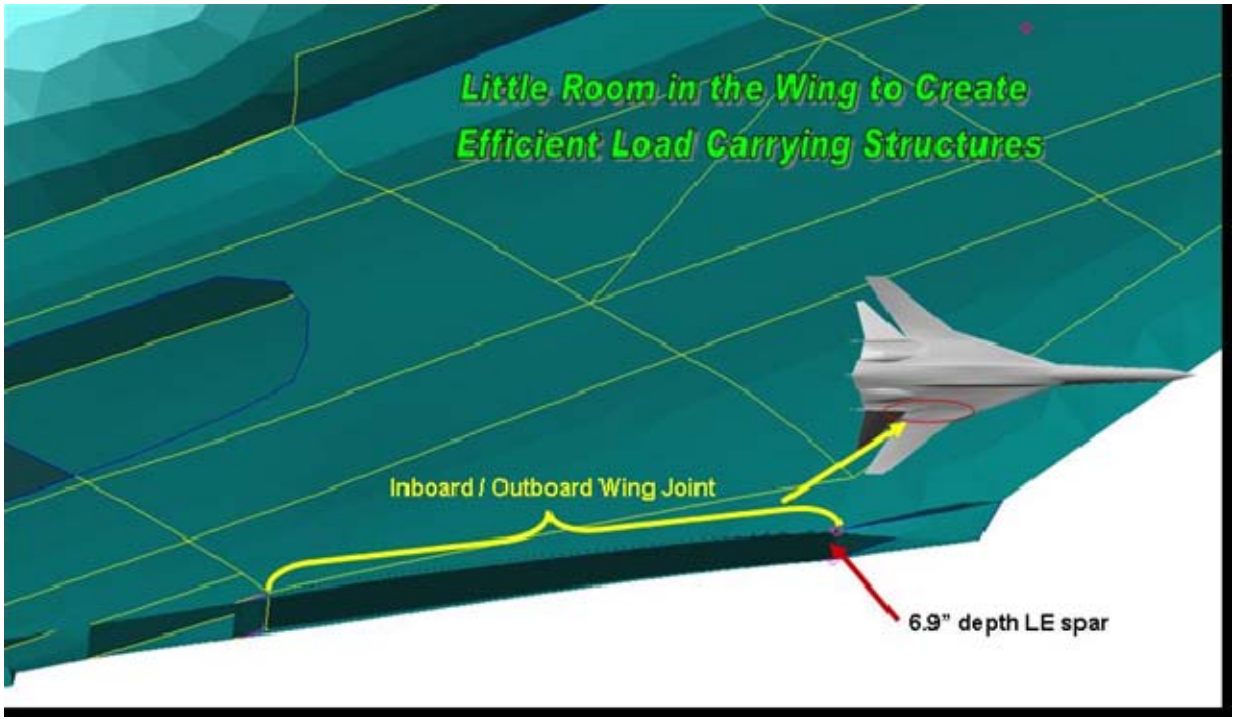

Figure 5.1.4. Inboard and Outboard Wing Joint.

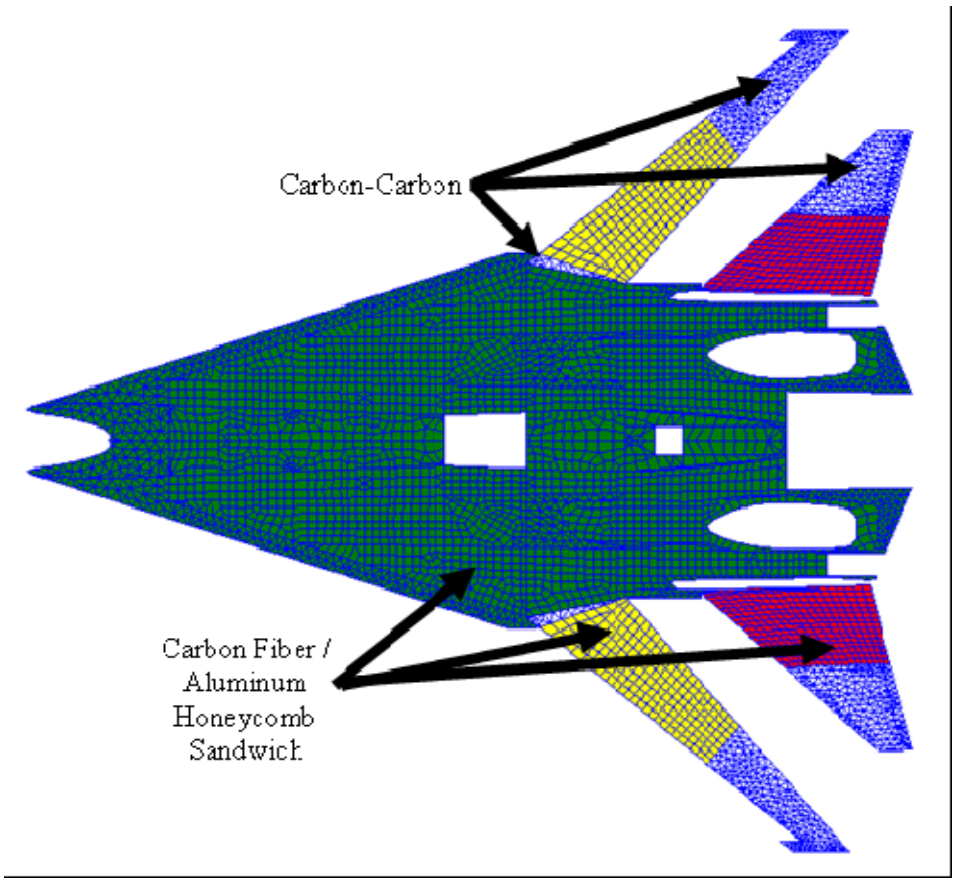

Figure 5.1.5. Wing & tail skin materials.

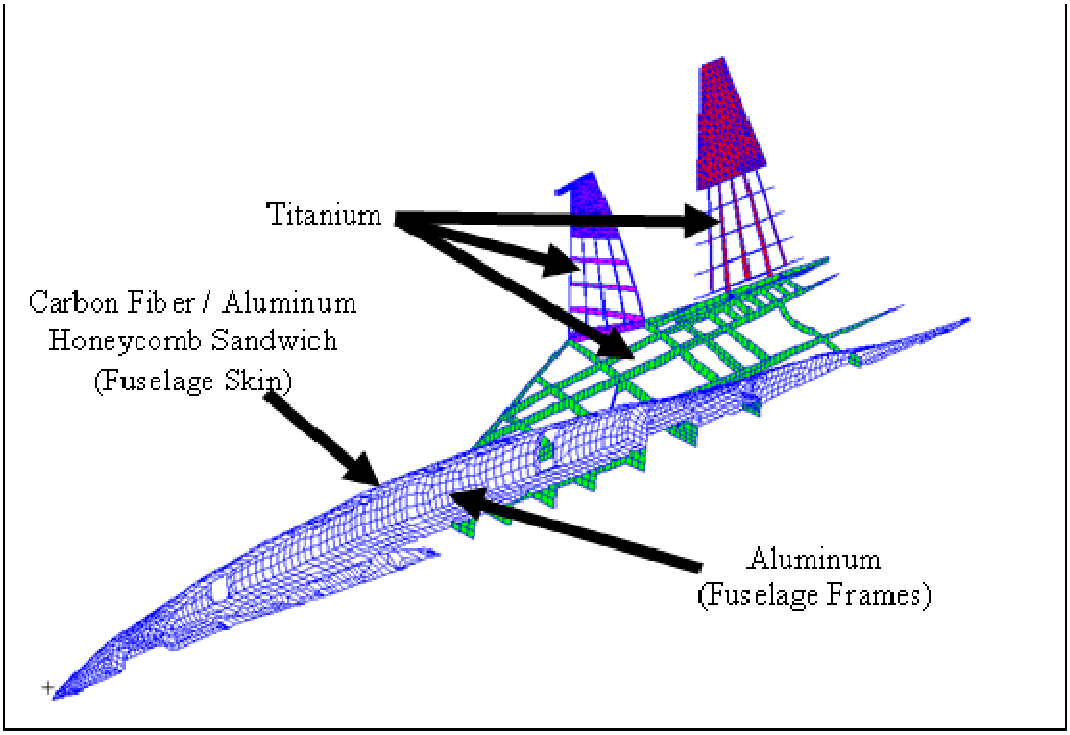

Figure 5.1.6. Internal structure materials.

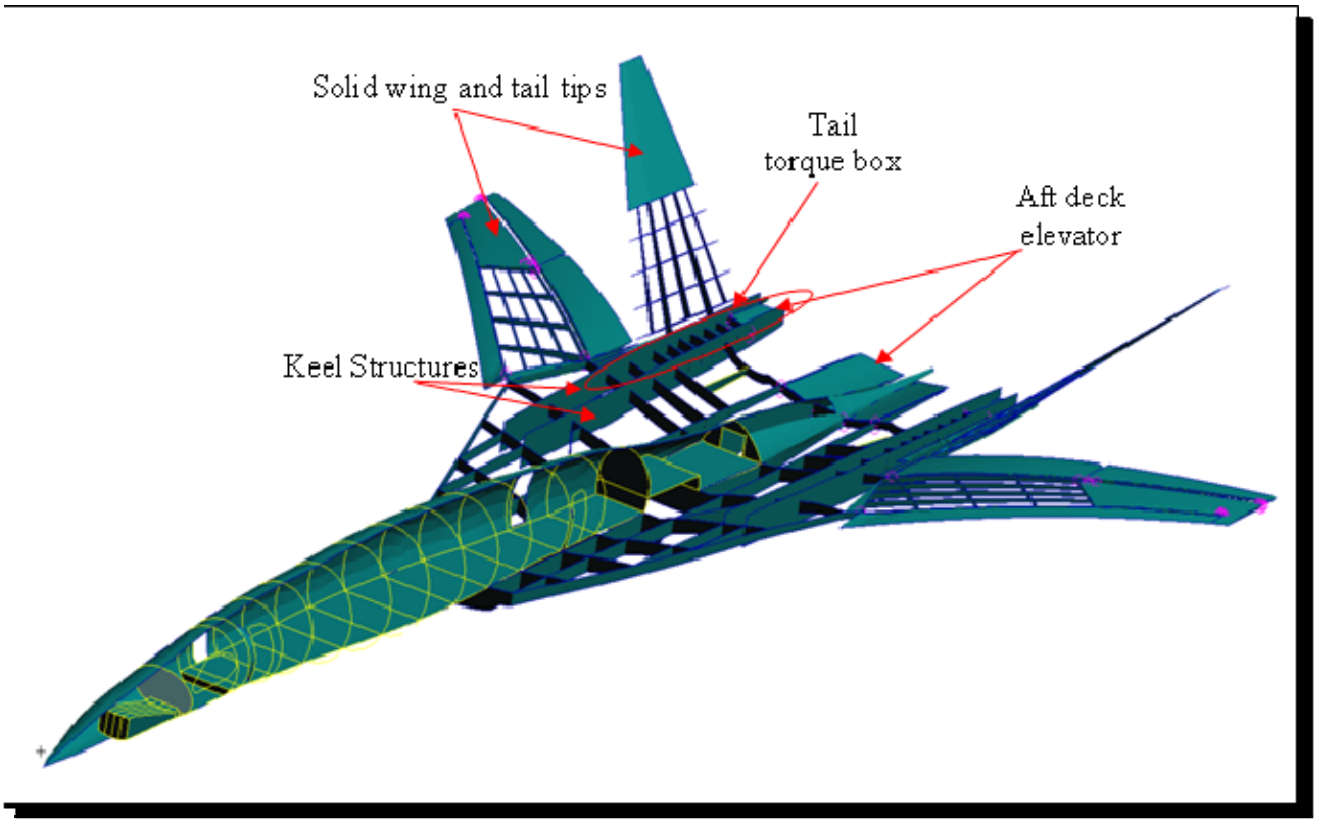

Figure 5.1.7 076E Structural Layout.

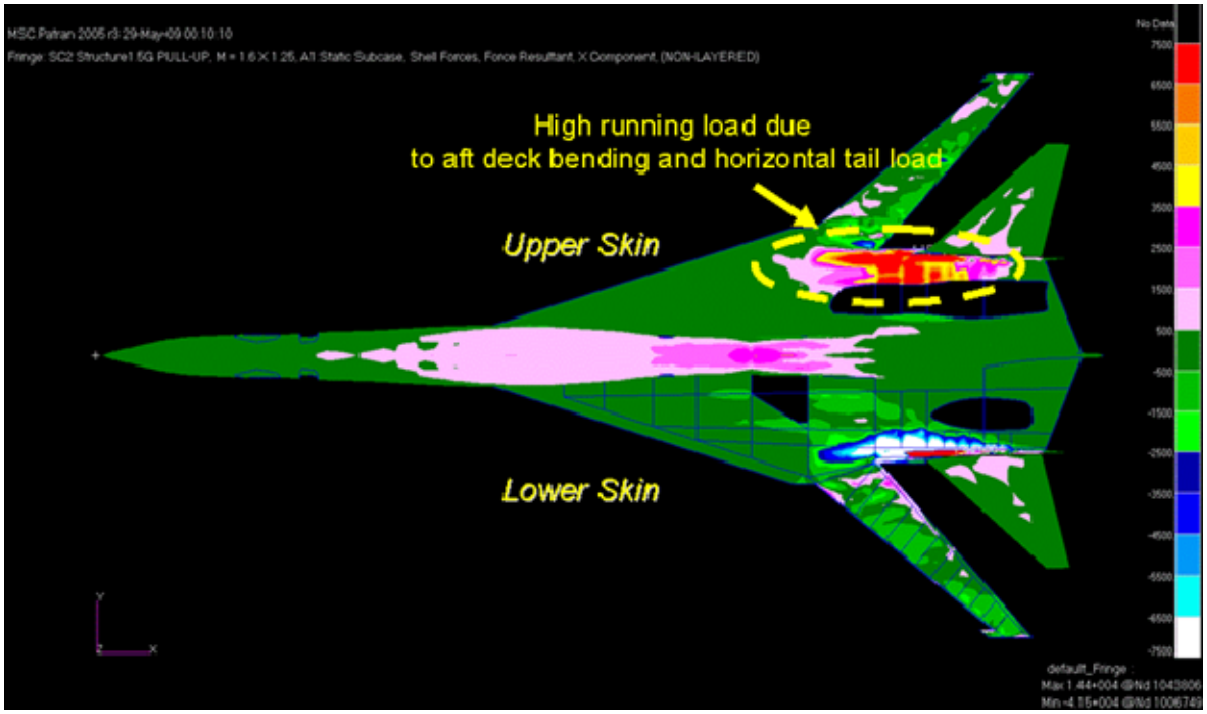

Figure 5.1.8. Streamwise Running Load Plot, 1.5G Pull-Up at Supersonic Dive Speed.

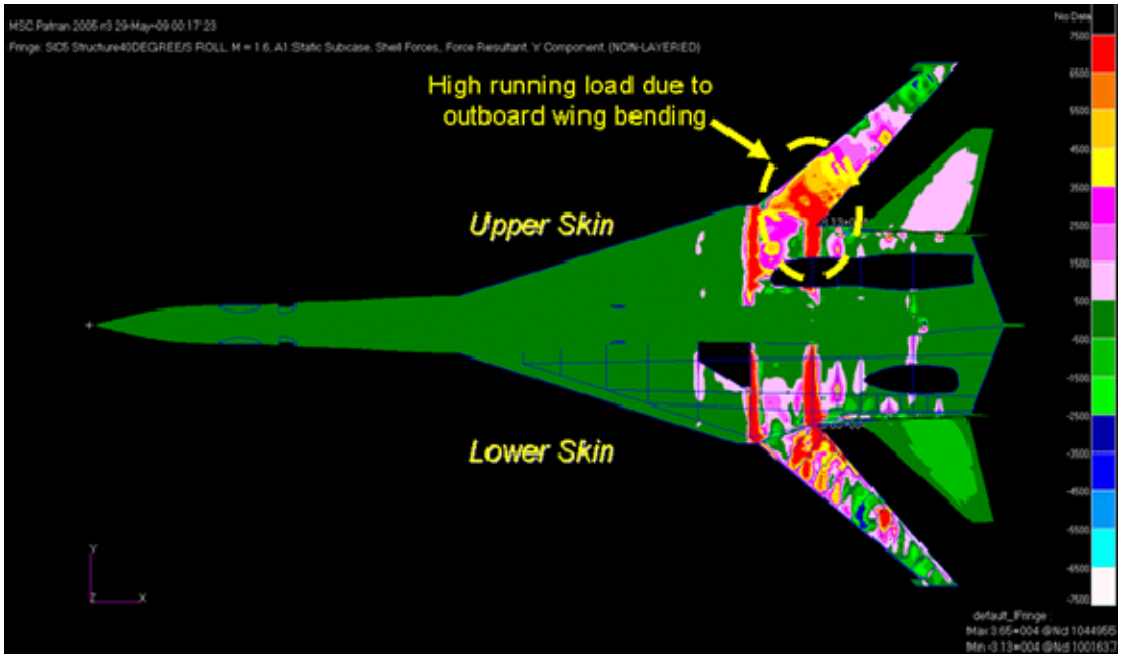

Figure 5.1.9. Spanwise Running Load Plot, 40 degree/sec Roll at Subsonic Speed.

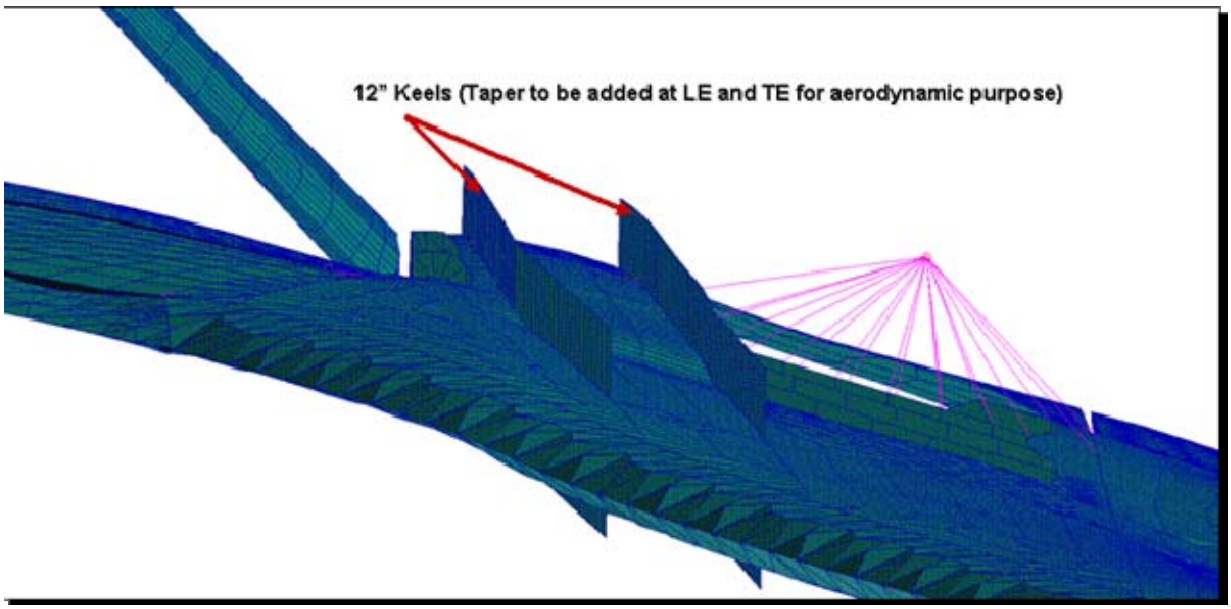

Figure 5.1.10 076E Keel Structure.

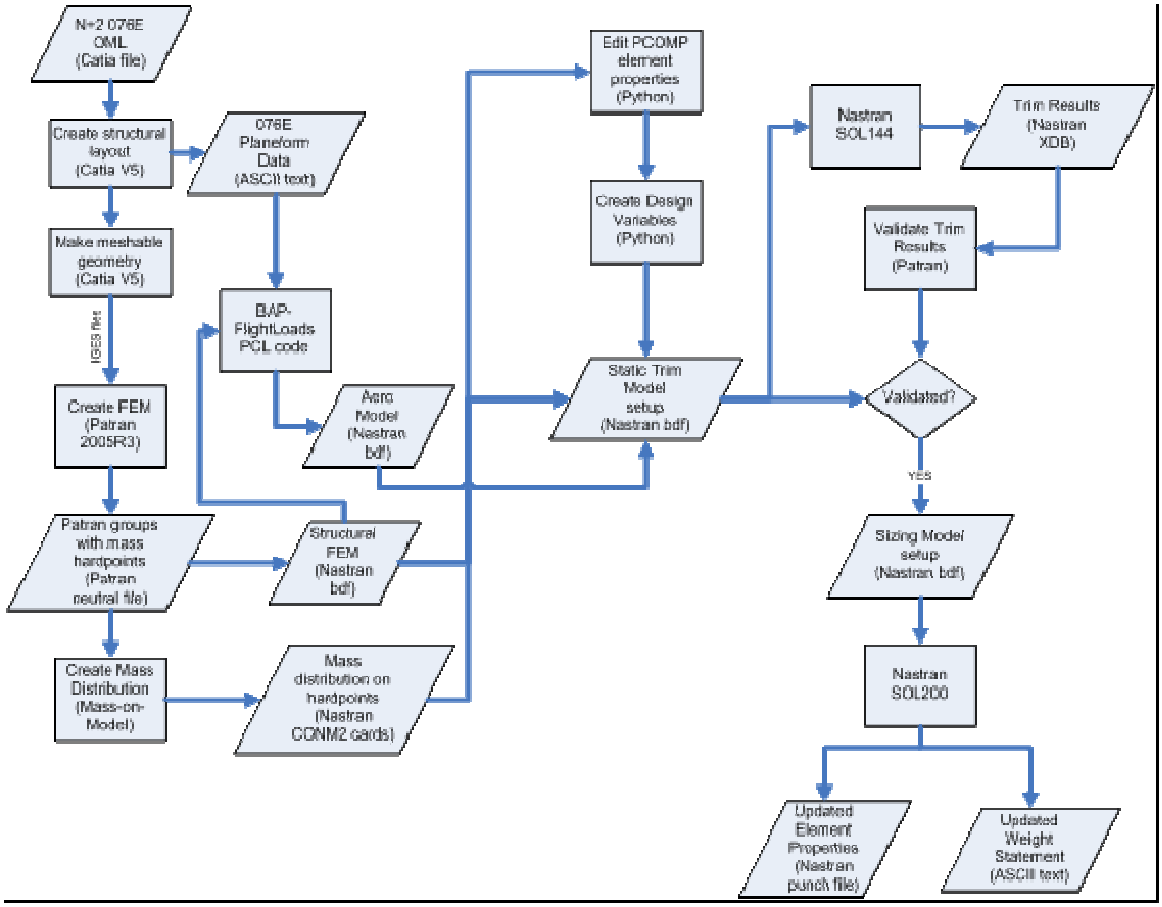

Figure 5.1.11. 076E Structural Analysis Process.

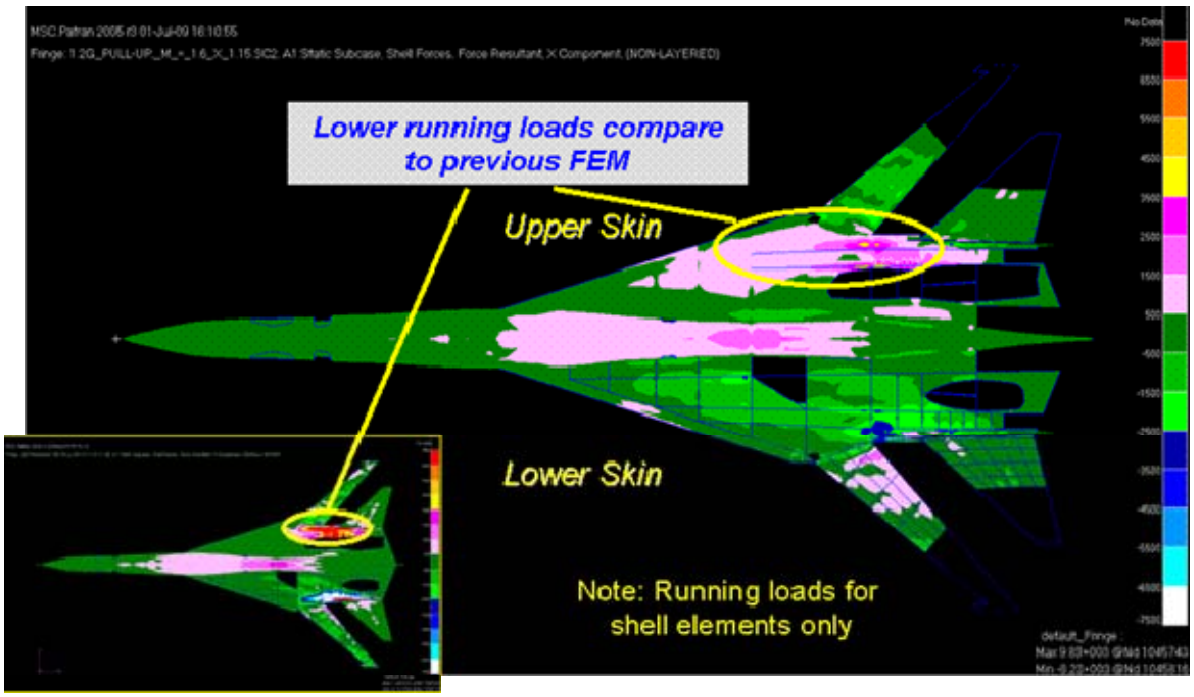

Figure 5.1.12 Comparison of Streamwise Running Loads during supersonic pull-up maneuver.

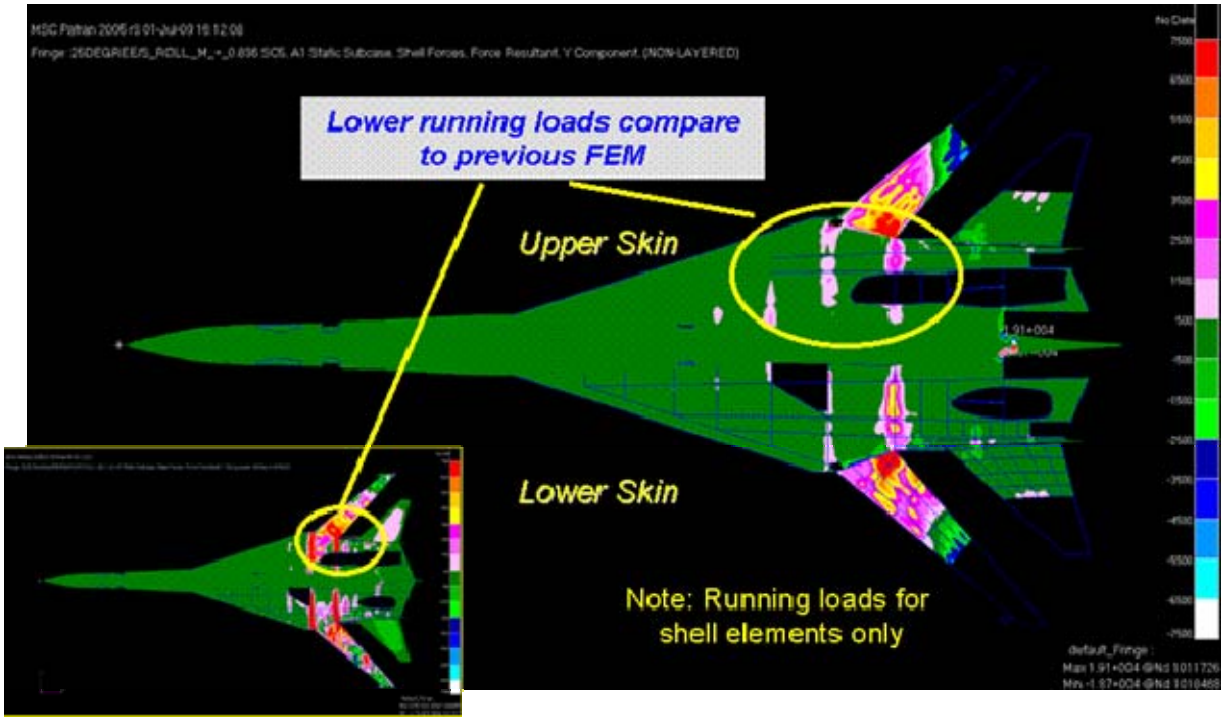

Figure 5.1.13 Comparison of Spanwise Running Loads during subsonic roll maneuver.

Table 5.1.1 Weight Statement Update using Sized Structural Weight.

Description	QWIKO Wts Weight	FEM Wts Weight
Wing Structure	26670	39800
Horizontal Tail Struture	3110	5297
Vertical Tail Structure	10	10
Fuselage Structure	9600	15486
Main Landing Gear	4330	4330
Nose Landing Gear	620	620
Forebody Controls	0	0
Structure Total	**44,340**	**65,543**
Propulsion Pod Total	**27,240**	**27,240**
Systems & Fixed Equipment Total	**19,380**	**19,380**
Manufacturer's Empty Weight (MEW)	**90,960**	**112,163**
Standard and Operational Items	3140	3140
Operational Empty Weight (OEW)	**94,100**	**115,303**
Payload	6300	6300
Max Zero Fuel Weight (MZFW)	**100,400**	**121,603**
Fuel	79,600	58,397
MTOGW	**180,000**	**180,000**

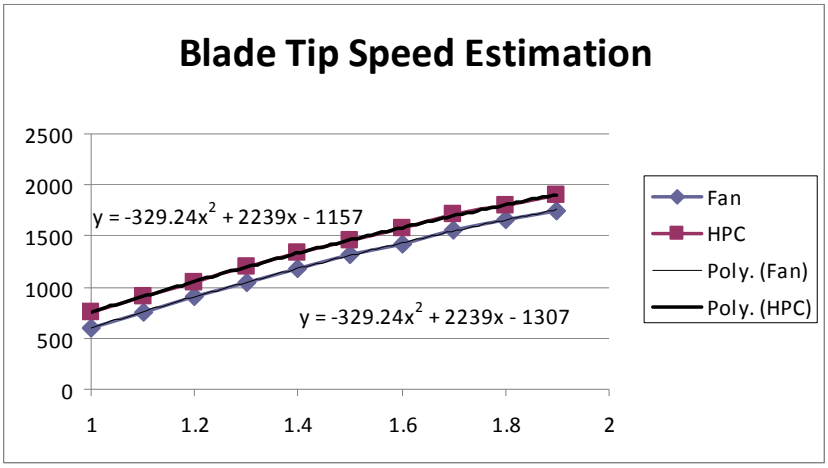

Figure 5.2.1 Fan and HPC Tip Speeds vs. First Stage PR

Table 5.2.1 WATE++ Component Information

	Fan	HPC	HPT	LPT
Pressure/Expansion Ratio	2.146	16.821	4.24	3.56
Hub to Tip Ratio	0.35	0.68	0.905	0.87
Stage Count	2	11	2	4
Rotor Speed (RPM)	4476	9730	9730	4476
Design Flow Coefficient	0.638	0.81	0.35	1.2
Stage Loading Parameter (per stage)	-	-	2.25	2.93
First Stage Stator Inlet Angle			67º	74º
Corrected Tip Speed (ft/s)	1394	1168	-	-
Component Weight (lbm)	3154	1040	684	1211
Hub to Tip Ratio	0.35	0.681	0.91	0.87
Length (in)	44.66	25.32	6.76	15.73

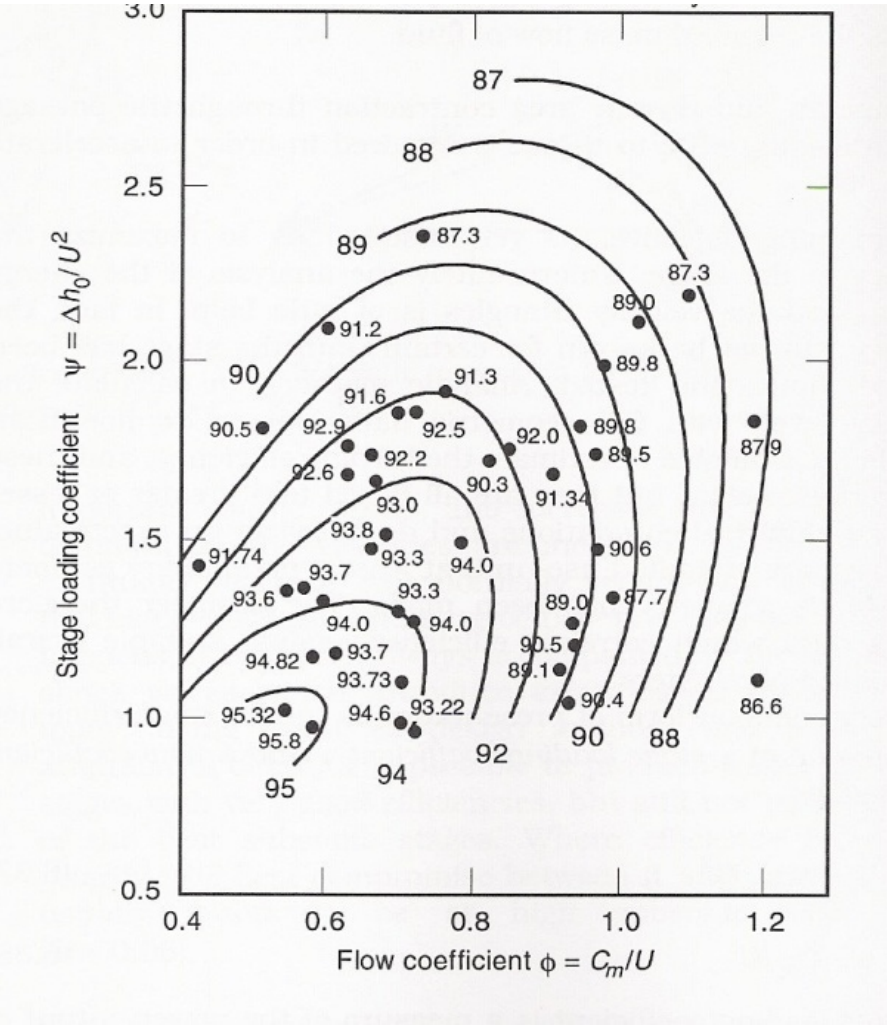

Figure 5.2.2 Smith Chart

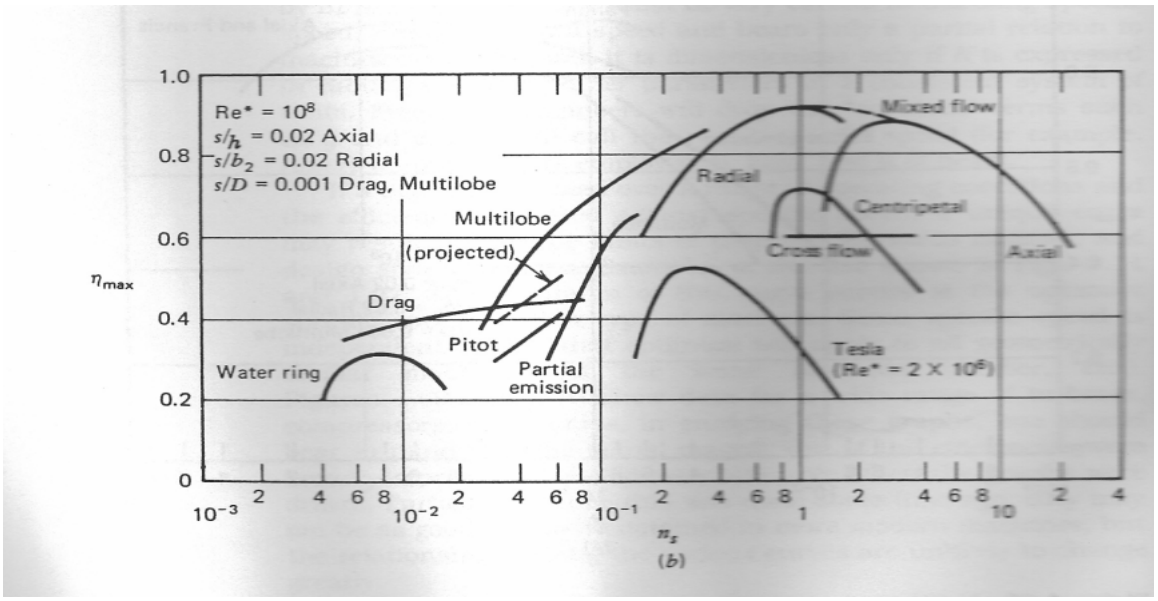

Figure 5.2.3 Compressor Efficiency vs. Specific Speed

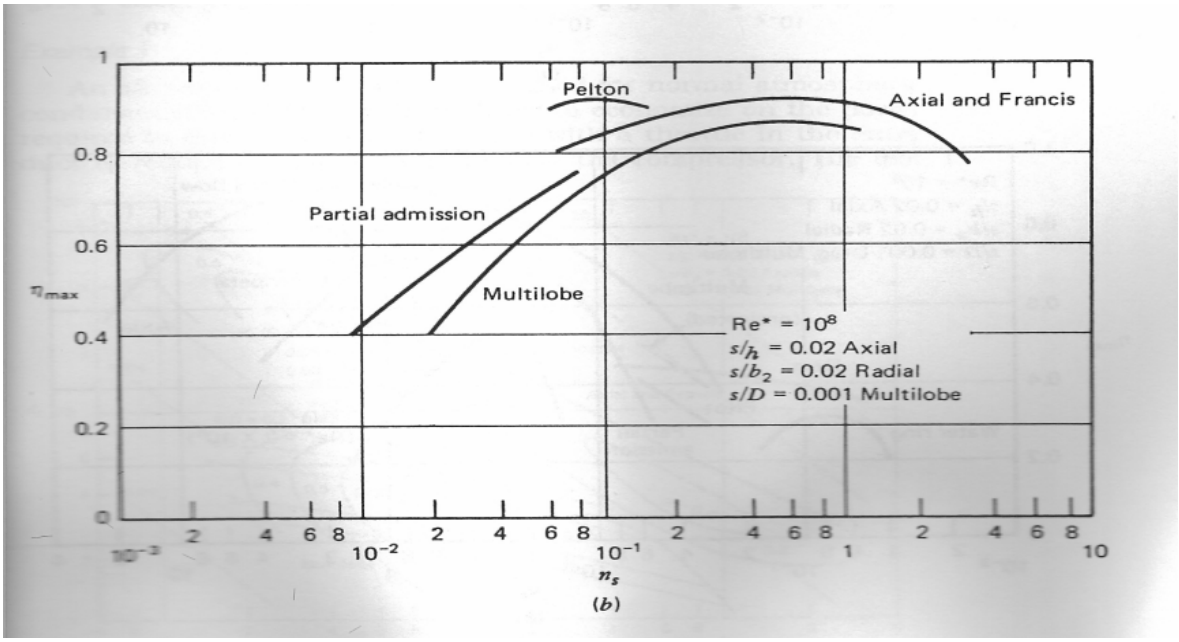

Figure 5.2.4 Turbine Efficiency vs. Specific Speed

Table 5.2.2 WATE++ Material Selection

Component	*Blade Material*	*Disk Material*
Fan	Ti-6Al-2Sn-4Zr-2Mo	Inconel 718
HPC	If(max Temp < 1250ºR) Ti-6Al-2Sn-4Zr-2Mo If(max Temp > 1250ºR) Inconel 718	Inconel 718
HPT	MAR-M247	Udimet 700
LPT	Udimet 700	Rene 95

Table 5.2.3 WATE++ Aspect Ratio Distributions

Component	*First stage Aspect Ratio*	*Last Stage Aspect ratio*
Fan	3.2	2.7
HPC	2.5	1.5
HPT	1.25	2.0
LPT	3.3	5.3

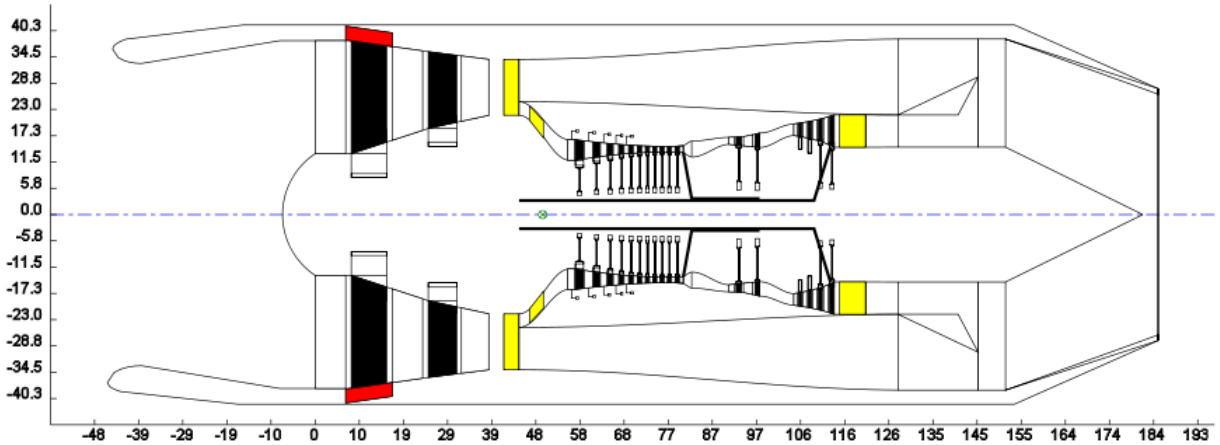

Figure 5.2.5 GT WATE++ Flowpath for MFTF

Table 5.2.4 External Engine Dimensions

Total Weight (lbm)	7523
Total Length (in)	225
Total Diameter (in)	83

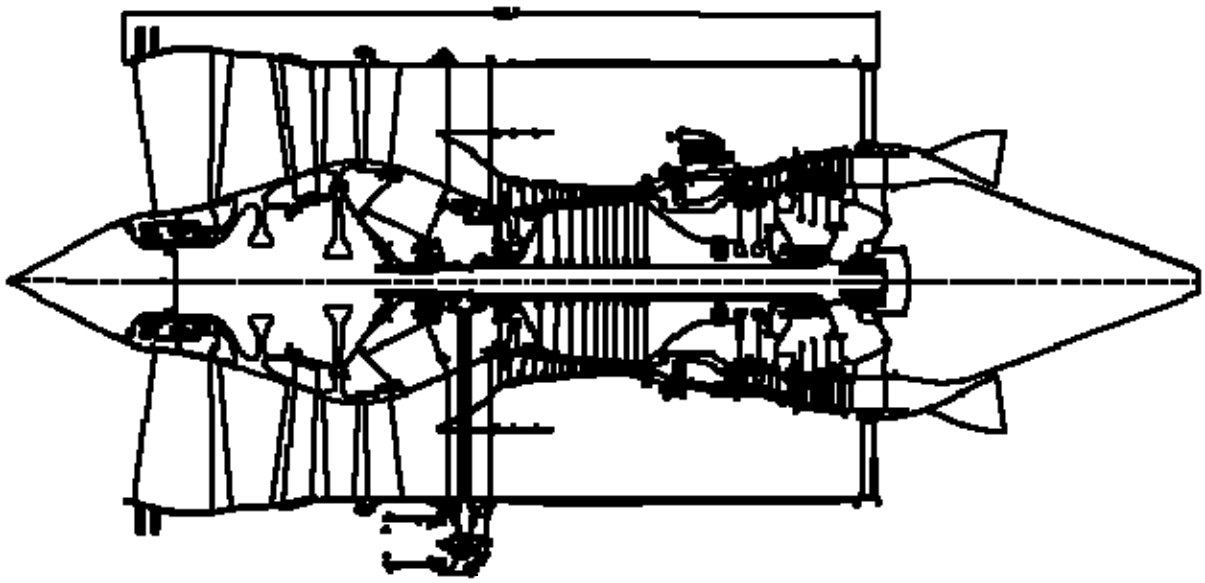

Figure 5.2.6 Engine General Arrangement developed by Rolls-Royce from WATE++ flowpath and cycle information provided

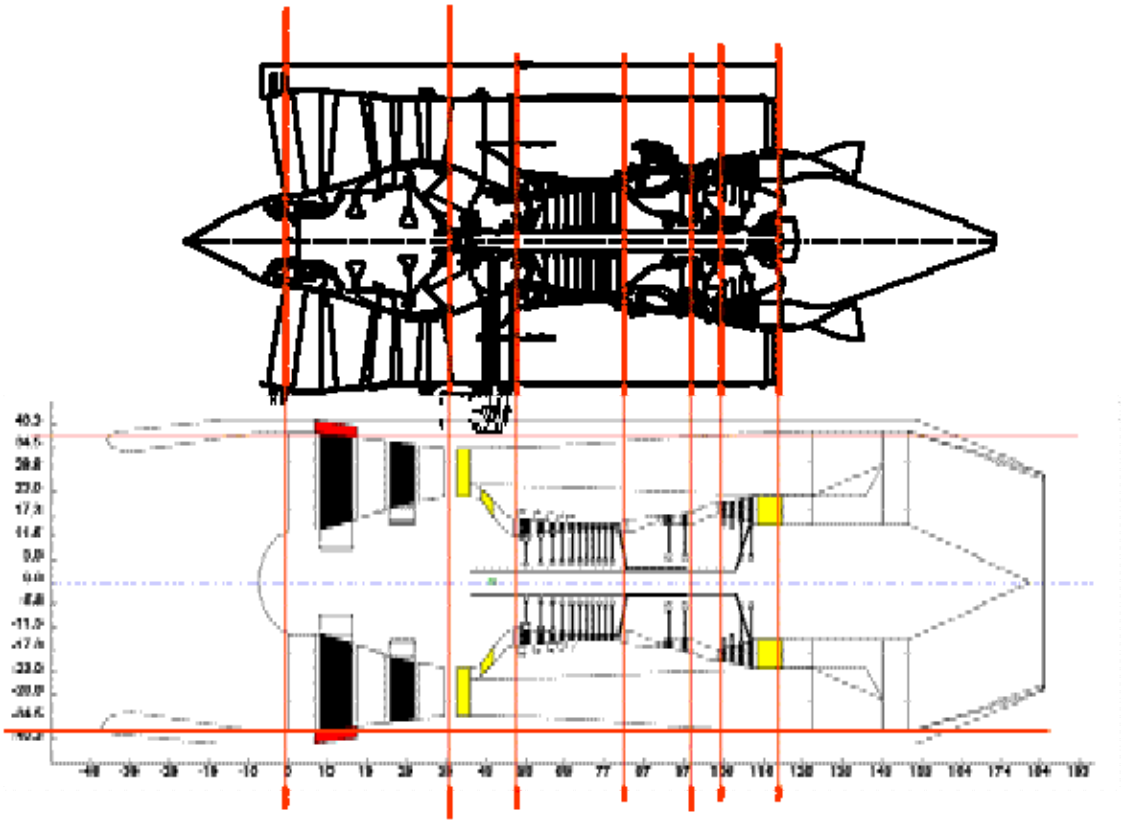

Figure 5.2.7 The R-R General Arrangement Matches the WATE++ Flowpath

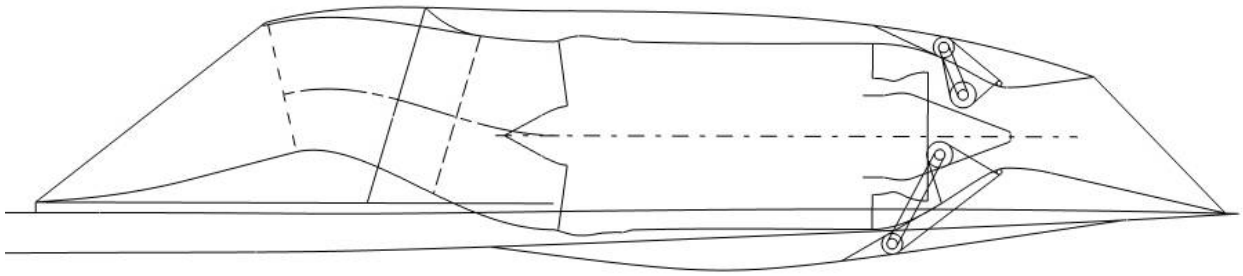

Figure 5.2.8 Inlet and Nozzle Flowpath with Engine Fan Diameter of 75 inches

Translating Cowl Aux Inlet Concept

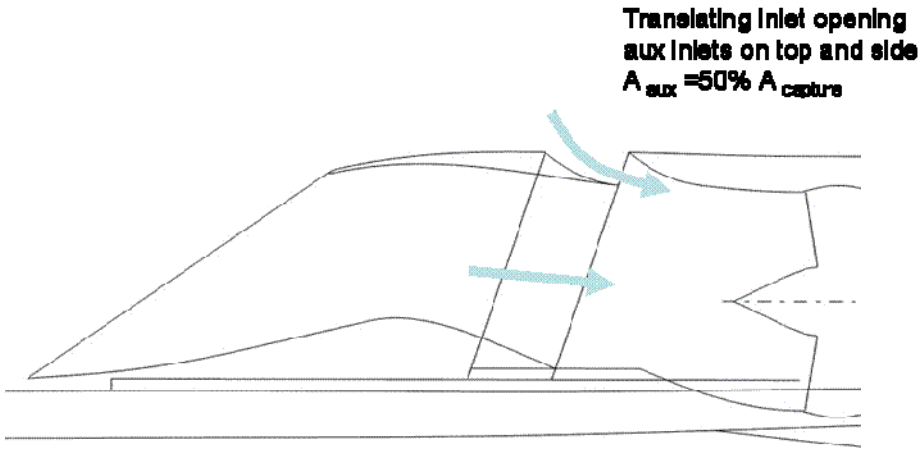

Figure 5.2.9 076E Inlet with Auxiliary Inlet

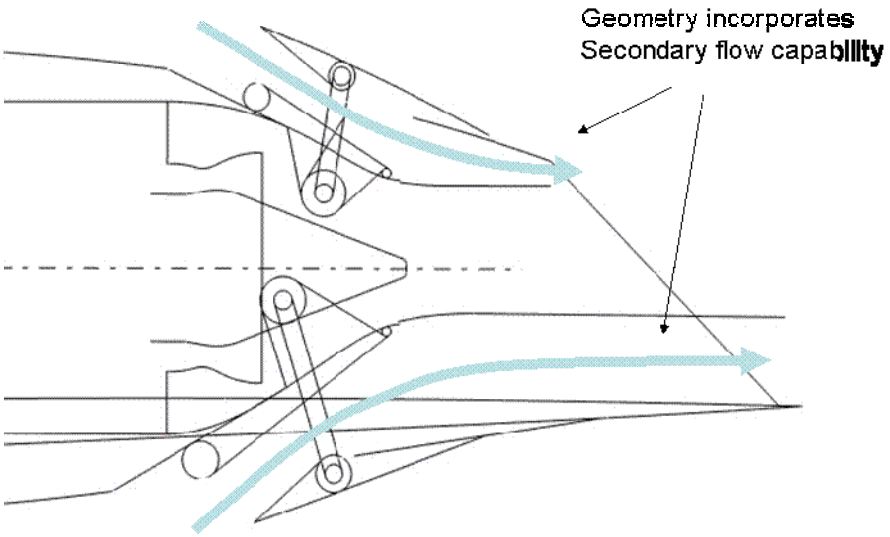

Figure 5.2.10 076E Nozzle w/ Secondary Flow Geometry

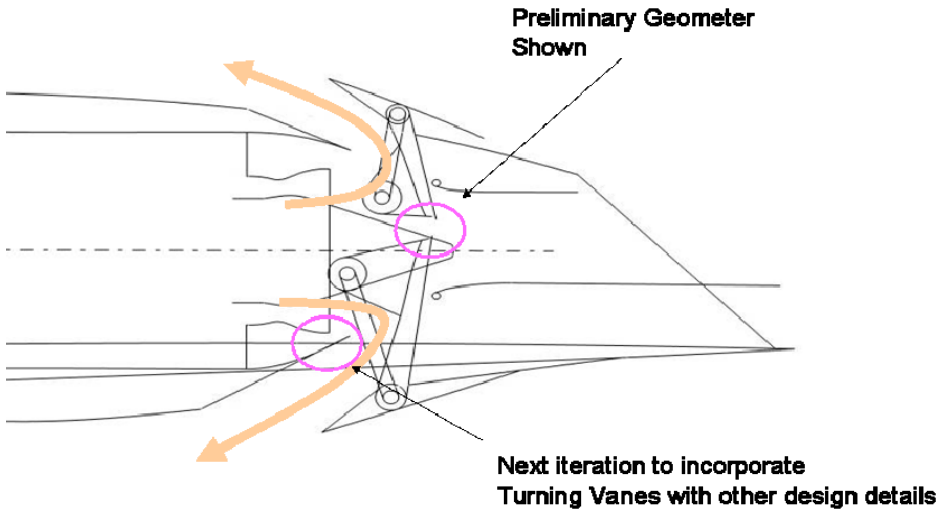

Figure 5.2.11 076E Nozzle w/Thrust Reverser Deployed

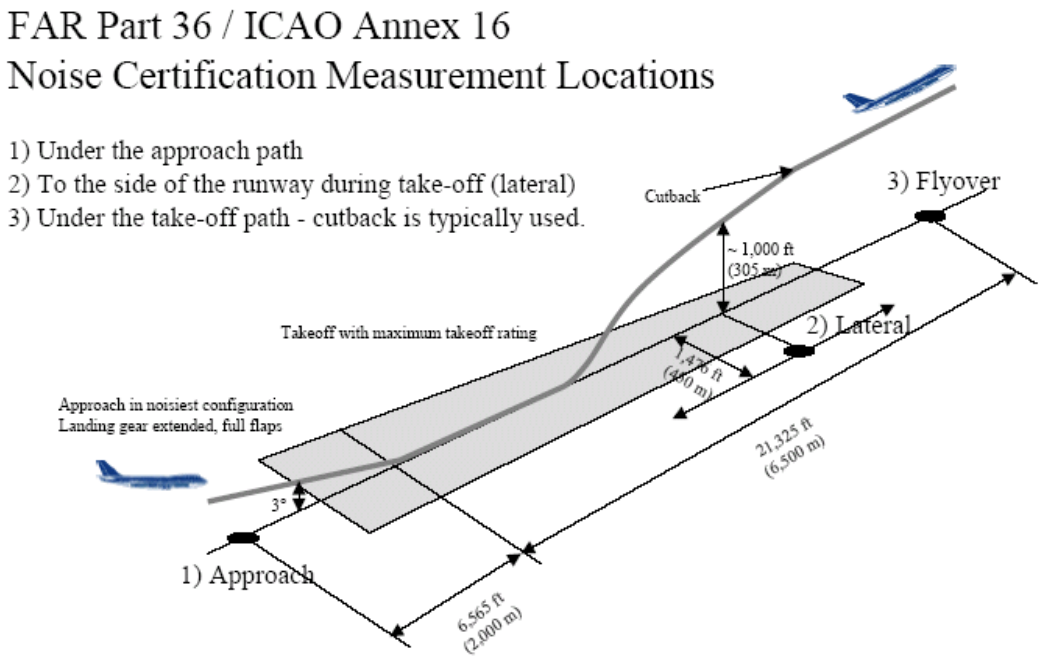

Figure 5.2.12 - Noise Measurement Reference Locations

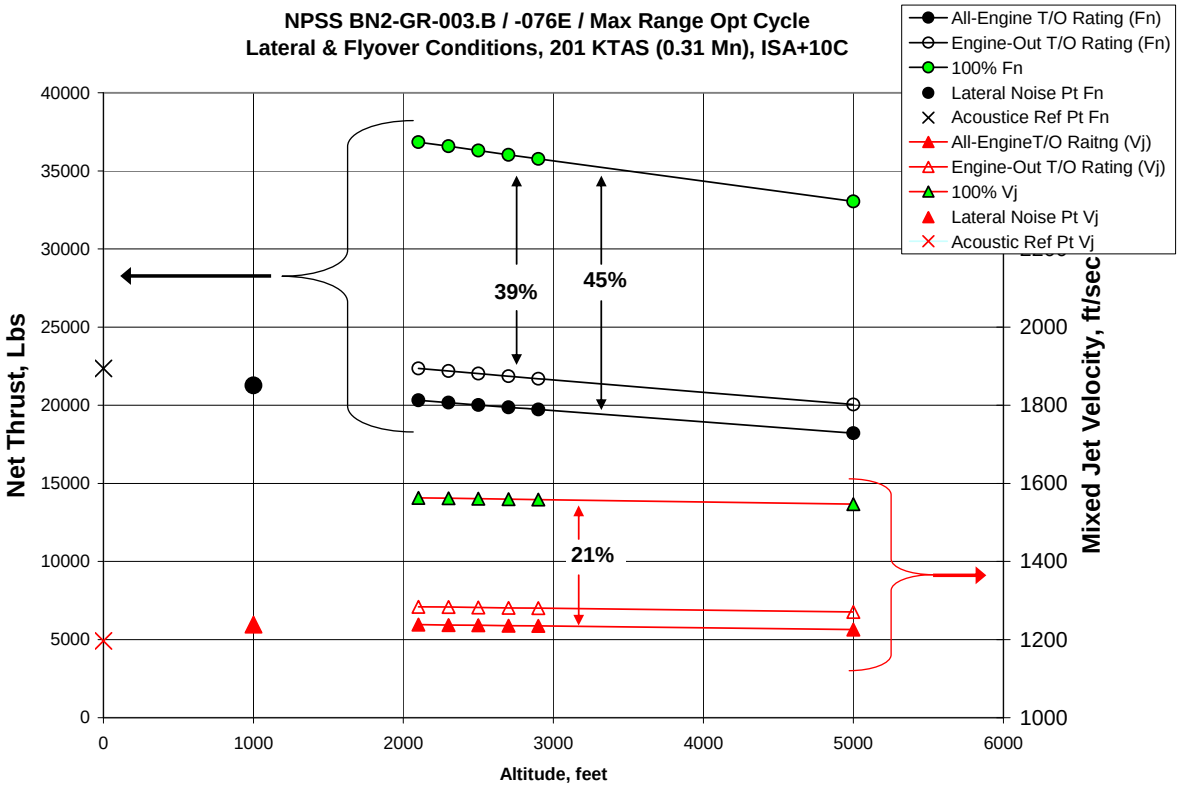

Figure 5.2.13 Benefit of Derated Takeoff On Jet Velocity

6.0 Technical Shortcomings and Portfolio Gap Engineering Plan for Continued Configuration Development

The N+2 time-frame allows approximately 8 years from today for technology, configuration, and design process development before committing to the available and near-term forecast levels. While any technology or configuration feature with a credible promise of reducing noise, reducing boom, raising fuel efficiency or lowering weight could help achieve the fuel efficiency, emissions and boom goals, a few stand out as critical.

Summary of key enablers:

- Aero- Propulso- Servo- Elastic (APSE) design and evolved fly-by-wire, multi-function surfaces, and multi-input/multi-output (MIMO) design.
- Configuration features that enable both low boom and low drag.
- Configuration optimization via CFD & FEM, MDA/O tools.
- Inlets & nozzles that are simple, efficient, and low noise.
- Durable engine materials, reduced SFC optimized engine cycles.
- Design for low speed performance, handling, field performance, noise.
- Credible & achievable certification requirements (boom, loads, emissions, etc.)

A more detailed compilation identifying specific technical shortcomings and portfolio gaps presently facing the N+2 configurations was prepared and categorized. They are in priority order under each Category.

Multi-Disciplinary Optimization and Trades: (In priority order)

- Outer-loop MDAO, especially between aero & structures, needs multiple cycles. N+2 aero-structural iteration not converged.
- Propulsion system sizing and technology selection.
- Overall thrust & wing area sizing along with technology selection.

Airframe/Structures (In priority order)

- Light weight detail design concepts to meet weight goals.
- Structure layout & materials systems needs more development.
- Further optimization work on the 076E structural configuration exploring whether global optimum has been reached.
- Certification i.e. loads criteria, rotor burst.
- Systems packaging and accessibility.
- Flight deck visibility and electronic supplemental vision.
- Certifiable fuel/CG management system.

Aero (In priority order)

- NASA 65 to 70 PLdB goal not achievable with current configuration & length.
- Non-linear boom optimization to achieve goal PLdB, i.e 100 vs 90 while maintaining L/D.
- Improved target wave forms compatible with configuration integration and certification.
- Low speed performance and handling qualities risks.
- Takeoff field performance margins with derated thrust.
- Propulsion system external flow aero interference & propulsion airframe integration.

Propulsion System (In priority order)

- Inlet/Diffuser technology opportunities
  - Fixed Ramp, Bleedless Inlet: Simplifies inlet by eliminating porous surfaces, bypassing & momentum loss. But may not provide adequate shock control to

satisfy traditional engine operability demands across flight envelope and power settings.
    - Flow Control Devices: (e.g., Micro Vanes) Will Reduce Potential for Shock Induced Separation and Energize Diffuser Flows. But may not satisfy performance and operability targets.
- Nozzle technology opportunities (in priority order):
    - Scarfed Nozzle Exit Plane: Facilitates engine integration, but results in suboptimal nozzle vector, impacting both performance and aircraft control.
    - Fixed External Nacelle Exit: Compromises off design nozzle performance.
    - Ultra Short Nozzle Duct: (Particularly on top) Provides little length to mix exhaust and turn flow axially, so performance and discharge characteristics may be compromised.
- N+2 Engine size optimization opportunity:
    - Engine / Nacelle Diameter Target vs Status, (66 vs 75 in.), High jet velocity at target diameter, aggravates inlet & nozzle length shortcomings.

The investigation of the propulsion system revealed several other specific technologies and opportunities for development that are relevant to any continued work on N+2-type airplanes. Areas recommended for continued development work include:

Propulsion System Roadmaps - Outline

- Upper Inlet - Compact Inlet designs with high pressure recovery and distortion tolerance
    - Establish key design requirements and objectives
    - Active and passive flow control techniques
    - Min L/D diffuser design studies
- High performance lightweight 2-D scarf nozzle designs
    - Establish key design requirements and objectives
    - Aero/mechanical design and analysis trades
- Reduced weight, high performance mixer / ejector nozzle
    - Establish target and status technology trends
    - Physical design constraints and features
- Higher fidelity engine sizing and cycle optimization
    - Improved component and subsystem performance models
    - Mixer/ejector trades and MDAO at the vehicle level

Engine Sizing and Optimization (Propulsion priority 1)

- Resize engine and optimize cycle with updated vehicle configuration
    - Use engine company proprietary parametric models with higher performance and additional N+2 engine technologies
    - Include additional cycle / architecture design variables

Mixer / Ejector Trade Studies / MDAO (Propulsion priority 2)

- Use parametric model with M/E performance logic
    - Establish M/E vs engine size and cycle design space
    - Development technology goals / targets required for M/E to buy its way onto the vehicle (weight, thrust loss, Vj reduction/ effectiveness)

Exetrnal Compressible Inlet (Propulsion priority 3)

- Compact inlet design with high pressure recovery and distortion tolerance
    - Passive and active control.
    - Minimum length diffuser design.

(Propulsion technology shortcomings & gaps, continued)

Upper Inlet Design Refinement (Propulsion priority 4)

- 3-D RANS Assessment of Main and Aux Inlet Performance at Critical Flight Points; Refine Lines to Achieve Target Performance

2-D Scarf Nozzle Design Refinement (Propulsion priority 5)

- Define Changes to Nozzle Envelope In Order to Close on Concept
- 3-D RANS Assessment of Low Speed Operation with Base Relief and Main Nozzle Performance at Critical Points in Flight Envelope
- Refine Nozzle Lines / Mechanical Concept of Operation and Verify Performance Targets Are Achievable

Acoustics—Jet Noise (Propulsion priority 6)

- Flyover – Develop and optimize a cutback procedure
- Flyover – Assess Program Lapse Rate (PLR) procedures to improve flyover altitude
- Flyover & Lateral – Consider nozzle noise suppression devices
- Approach - Improve low speed aerodynamic devices (increase L/D i.e. less thrust/rpm)

Georgia Insitute of Technology and Rolls Royce technology shortcomings and portfolio gaps are shown in Appendix 3.0.

7.0 Summary and Conclusions

7.1 Configuration Deliverables

Non-proprietary conceptual designs for supersonic airliners two technology generations into the future (N+2, 2020-2025 EIS) have been developed: the 100 passenger model 765-072B, and the 30 passenger model 765-076E. Both have the potential to achieve a trans-Atlantic range of 4000nm. Both of these "concept planes" are described in sufficient detail for them to serve as platforms for NASA technology assessments and as points of departure for other future work.
3D CAD lofts of the outer mold lines (OML) of these two configurations, along with selected sample geometries of other configurations considered, are available for use in future Multi-Disciplinary Analysis and Optimization (MDAO) studies.

7.2 Reference Vehicle Requirements

Aircraft concept development for the N+2 study was guided by first establishing a reference set of vehicle requirements appropriate for a commercial supersonic airliner hypothetically entering passenger service as early as the years 2020-2025. Important factors that could be expected to drive the design, certification, and economic viability of such an aircraft were identified. These factors included the long-standing supersonic airliner challenges of flight safety, low fuel-burn (for both operating economics and environmental acceptability), meeting ever more stringent takeoff and landing noise restrictions, minimizing sonic boom, low emissions engine combustion, engine and airframe durability, and fitting into any of the world's air traffic control regimes with minimal disruption. It was concluded that environmental concerns would be most critical in that regardless of vehicle payload, price, or performance, no future supersonic aircraft can be considered "viable" if it is perceived as an outlier raising environmental concerns disproportionate to any potential economic or social benefits. The combination of requirements was determined to be best satisfied by configurations flying slower than Concorde (Mach 1.6-1.8) at a maximum altitude of 55,000 feet, employing moderate bypass ratio mixed flow turbofan engines potentially having some variable cycle features, with variable area nozzles, and mixed composite-metallic airframe construction.

7.3 Design Space Exploration And Trades

Multiple aircraft general arrangements were investigated to meet the identified requirements at an initial conceptual design level. Initial TOGW and engine sizing were determined using proprietary engine definitions from previous Boeing internal studies, with appropriate scaling and technology assumption adjustments. A large design space was investigated around selected configuration "species" using several MDA/MDO approaches. Trade sensitivities for passenger payload, design range, cruise Mach, cruise altitude, and cabin shape constraints were conducted with low fuel burn or low sonic boom as alternate figures of merit.

A sophisticated non-proprietary parametric turbofan engine model was created for MDA/MDO studies, and was exercised extensively in a set of airframe-to-engine cycle matching trades and design space sensitivities. This engine model, based on the NPSS tool, was created using engine company inputs for engine architecture and stage efficiency assumptions and technology level setting for the N+2 time frame. This tool proved invaluable in optimizing the final configuration choices and provides propulsion modeling capabilities considerably more advanced than those available in previous supersonic studies (e.g. HSR's Design Optimization Synthesis System –DOSS).

7.4 Down-selected Configurations and Sonic Boom Considerations

Of various configurations studied, the first down-selected configuration, the -072B, was recommended by Boeing as the best representation of a low fuel burn, low emissions, higher passenger capacity configuration for the N+2 time frame. The -072B is intended to represent a design of challenging but

reasonable technical risk---a relatively straight-forward extension of experience obtained on the NASA HSR effort and the subsequent industry studies. The aircraft was configured to carry a number of passengers similar to Concorde at trans-Atlantic-plus ranges but at higher cabin comfort levels. The Mach 1.6-1.8 capable airplane would also have much more efficient subsonic cruise performance, would meet the same community noise standards as then-year subsonic aircraft, and could exceed the N+2 fuel mileage goal of 3 seat-nautical miles per pound of fuel burned. The airplane size and fuel use could potentially allow reasonable ticket surcharges when compared to premium subsonic fares or bizjet charter rates. The general arrangement, wing design, etc. for this configuration, have been biased toward meeting certification goals and fuel mileage performance with reasonable risk---it does not incorporate low-boom shaping. While still having an N-wave sonic boom and flying at altitudes lower than 55,000ft, the -072B would still keep maximum sonic boom levels below Concorde, meeting the minimum reduction proposed for future over-water supersonic flights. As with other "un-shaped" boom configurations, if future flight experiments and advances in real-time weather monitoring, flight management systems, and "free flight" routing enable reliable flight at "threshold Mach", then operation over land or in coastal regions might be allowable at up to Mach 1.15+/- without producing a boom at ground level.

The -076E, initially developed as an alternate concept to illustrate the impact of low-boom specifications on configurations, was down-selected by NASA for further development, additional definition and assessment due to its focus on low sonic boom shaping as a key long-lead enabling technology. It represents a higher risk configuration and presents larger "technology stretch" goals for performance, structures, and other elements. Sonic boom mitigation was highlighted in the N+2 vehicle requirements as a significant hurdle to environmental acceptability of any future supersonic civil aircraft. The economic productivity and practicality of supersonic business jets, a likely precursor to any future generation of airliners, may depend on the ability of operators to fly supersonically over land on a regular basis, at least in designated "boom corridors". Increased worldwide environmental awareness and concern over the impact of strong sonic booms will likely dictate that even an aircraft designed for supersonic operation only over water will need to incorporate some degree of boom "softening" to stay below the 2.2 psf overpressures generated by Concorde (substantially below the 3-3.5 psf forecast for the 300+ passenger HSCT's studied in the 1990's). Operation at maximum supersonic speed in remote over-land corridors and coastal areas maybe permitted at overpressures of 0.5-0.7 psf (PLdB's in the high 80's to low 90's), while operations over the continental U.S., even in corridors, will likely require PLdB levels in the low 80's.

In recent years, significant advances have been made in the ability to define specific target disturbance functions for "shaped" low-boom wave forms and to select aircraft general arrangements and features that greatly improve the likelihood of converging on the corresponding target using CFD-based optimization techniques. The use of shaped wave forms provides the minimization of the largest individual shocks in the signature and increases shock rise times---factors which dominate the perceived noise level decibels (PLdB). In spite of advances in low-boom design, the physics of sonic booms dictates that the boom noise level produced by a given signature shape is fundamentally related to vehicle length and gross weight. The theoretical minimum vehicle length required to produce a shaped signature is still given by the Seebass ("SEEB") formulation which is now several decades old. More sophisticated alternate disturbance functions or more extreme design features can produce lower PLdB levels for a given weight or provide added configuration integration freedom, but generally at a penalty in overall vehicle length, practicality, or loss of boom "robustness". These fundamental physical limitations make it increasingly difficult to achieve a given goal PLdB level as the size and payload of the configuration is increased or more constraints are placed on the design for integration, stability and control, or structural/APSE risk management. This means that a goal PLdB loudness level that is fairly easily achieved with a single seat "clean sheet" research aircraft becomes much more difficult to achieve with a modified existing aircraft, and is much more difficult to achieve with an airliner sized aircraft than with a small SSBJ type. High performing, multi-Mach optimized Boeing SSBJ concept planes that "close" from the integration and performance standpoint with reasonable technical and certification risk have been developed in recent years using Boeing proprietary design features and processes. Such designs could potentially meet all environmental and certification requirements in the N+1 time-frame (year 2020), while providing "shaped" sonic boom PLdB levels in the low 80's (at takeoff gross weights on the order of 100,000 lbs). Achieving a similar level of boom on an airliner of two or more times the weight while maintaining high performance levels is a formidable task, requiring the consideration of more unique general arrangements and the projection of

more advanced technologies which could be available in the years 2020-2025 and beyond. The same tools used to develop recent proprietary IR&D concept planes were used under the present NASA study to configure the -076E which is representative of such a future small low-boom airliner concept.

7.5 Assessment of the -076E and Development/ Technology Portfolio Gaps

Linear-based aerodynamics tools and "Quick-O" conceptual design weights were used to establish year 2025 "goal" performance levels for the -072B and -076E. Driven by the sonic boom requirement, the -076E used more aggressive initial integration assumptions, and higher effective percentage of supersonic L/D technology assumptions than would have been used in the HSR program or more recent industry SSBJ studies. Linear-based aerodynamics tools were also used to establish the "theoretically achievable" sonic boom potential of the -076E concept. An alternate "stretched" version (-076F) was investigated as part of a boom sensitivity to wing aft-loading and body length, but it was dropped after consultation with NASA due to concerns over very high structural /APSE risk levels this might introduced into the pending FEM analysis.

Because the -076E concept represents a much more aggressive "clean sheet" approach that does not relate well to configurations studied under HSR, nor to more recent industry proprietary studies, the status levels of performance, weights, internal loads, flutter risks, loadability, would be expected to be farther away from the configuration's eventual potential than with a more conventional concept. A single cycle CFD optimization for drag level, and "one and a half" cycles of Finite Element Method analysis were conducted to determine the existing shortfall between the "as-drawn" status and the goal levels projected for the concept assuming year 2025 technology. Results from the initial CFD optimization showed that the projected L/D levels should be quite achievable with today's industry tools. However it was concluded that retaining that performance level while simultaneously reshaping the vehicle's contours to capture the identified low-boom potential represents a significant technology challenge. Improvements will be needed in computational efficiency, optimization algorithms, CFD accuracy, and designer insights by 2025 if such goals are to be achieved with any certainty.

A partial FEM cycle was initially conducted based on a notional internal structural arrangement. This model was updated for the full FEM cycle with "first cut" design improvements and loads assumptions based on the initial results and observed behaviors that were similar to previous Boeing proprietary configurations. The FEM results gave important data on the running loads, load-paths, structural sizing challenges and identified key weight and loads-sensitive zones for this class of low-boom aircraft. These FEM results can be used to identify configuration concept improvements, and have highlighted the types of design development and technology gaps which would need to be filled by 2025 for such a concept to be viable. Such gaps would include improved structural arrangements, alternate materials mix, high strength/high modulus materials, and the need for rapid multi-cycle MDA/MDO iterations between aero and loads that include coupled internal and external topology changes. A number of specific candidate structural improvements and areas for trade-offs with aerodynamics were identified.

The reference vehicle requirements established for the N+2 study specified that any future supersonic airliner would need to meet then-year community noise levels. A projection was made that the likely noise restrictions in the 2020+ time frame will likely require a cumulative reduction of 15+ dB relative to "Stage 3" FAA/ICAO reference levels. The report contains a detailed discussion of the associated logic and requirements specific to each noise measuring point. The scope of the N+2 study and available propulsion system definitions precluded a detailed assessment of all of the source components of the -076E concept. However, as was done for the initial configuration selection studies and MDA/MDO trades and sensitivities, the assumption was made that jet noise would be the dominant source and engine mixed jet velocity (Vj) was evaluated as a surrogate for overall noise levels. A detailed analysis of the jet velocity noise of the -076E showed it would likely be capable of meeting the Stage 3 minus 15dB cumulative level with the NPSS-optimized engine cycle and a simple light weight nozzle. Turbo-machinery noise, inlet noise, and airframe noise components were not included, but neither was credit for optimized takeoff thrust lapse rate management (an advanced version of "PLR") or any potential noise shielding effects of the V-tail arrangement and over-wing engines. An example hypothetical low-noise inlet and variable area thrust reversing nozzle concept are shown as part of the configuration definition as "technology placeholders".

The development of high efficiency, distortion tolerant, compact inlet technology and integrated nozzle concepts with durable high-temperature seals were cited as additional "portfolio gaps" that would need to be filled to make such an airliner viable. It was further noted that if the actual then-year noise requirement calls for larger margins at sideline, or the net cumulative delta from Stage 3 needs to be 18-20dB ---a distinct possibility, then; a) other noise sources from the airframe, inlet and turbo-machinery will begin to intrude on the jet noise, and b) de-rate and some form of PLR may not be sufficient without some form or "low impact" suppressor nozzle technology.

8.0 References

1. S. L. Baughcum, I. C. Plumb, I. C., and P. F. Vohralik, "Stratospheric Ozone Sensitivity to Aircraft Cruise Altitudes and NOx Emissions", in *Proceedings of the European Conference on Aviation, Atmosphere and Climate*, R. Sausen and G.T. Amanatidis (Eds.), Air Pollution Research Report No. 83, Commission of the European Communities, 197-206, 2004.

2. D. J. Wuebbles, M. Dutta, K.O. Patten, and S. L. Baughcum, " Parametric Study of Potential Effects of Aircraft Emissions on Stratospheric Ozone", in *Proceedings of the European Conference on Aviation, Atmosphere and Climate*, R. Sausen and G.T. Amanatidis (Eds.), Air Pollution Research Report No. 83, Commission of the European Communities, 197-206, 2004.

3. S. R. Kawa, J. G. Anderson, S. L. Baughcum, C. A. Brock, W. H. Brune, R. C. Cohen, D. E. Kinnison, P. A. Newman, J. M. Rodriquez, R. S. Stolarski, D. Waugh, and S. C. Wofsy, *Assessment of the Effects of High-Speed Aircraft in the Stratosphere: 1998*, NASA Technical Report TP-1999-209237, 1999.

4. I Isaksen, C. Jackman, S. L. Baughcum, F. Dentener, W. Grose, P. Kasibhatla, D. Kinnison, M. Ko, J. McConnell, G. Pitari, and D. Wuebbles, "Modeling the Chemical Composition of the Future Atmosphere,", Chapter 4 in the Intergovernmental Panel on Climate Change (IPCC) Special Report on *Aviation and the Global Atmosphere*, [J. E. Penner, D. H. Lister, D. J. Griggs, D. J. Dokken, and M. McFarland (eds.)] Cambridge University Press, 1999.

Appendix 1 - Description of the 072B

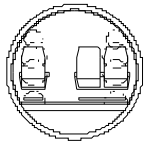

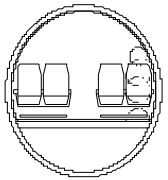

MINIMUM CROSS SECTIONS
1/50

	WING	CANARD	VERTICAL
AREA (sf)	4600	210	335
VOLUME	-	0.0327	0.0389
ASPECT RATIO	2.6	2.71	1.37
TAPER RATIO	0.045	0.275	0.281
LE SWEEP (deg)	68/40	40	39.4
TE SWEEP (deg)	-15/6	0	0
MAC (in)	1082	117	207
XREF (in)	1692	592.2	2509.8
SPAN (ft)	115	23	21

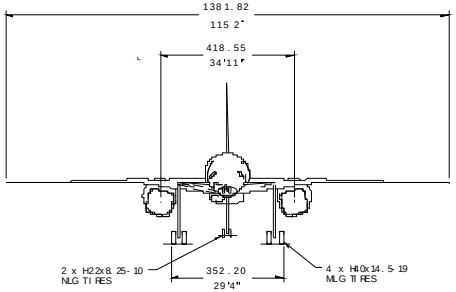

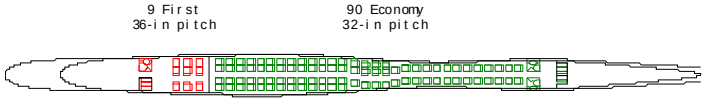

	Class (%)	Carts	Cart Ratio	Lavatory Ratio	Attendent Ratio
First	9.1	3	0.333	9	-
Economy	90.9	5	0.055	45	-
Total	-	8	0.081	33	25

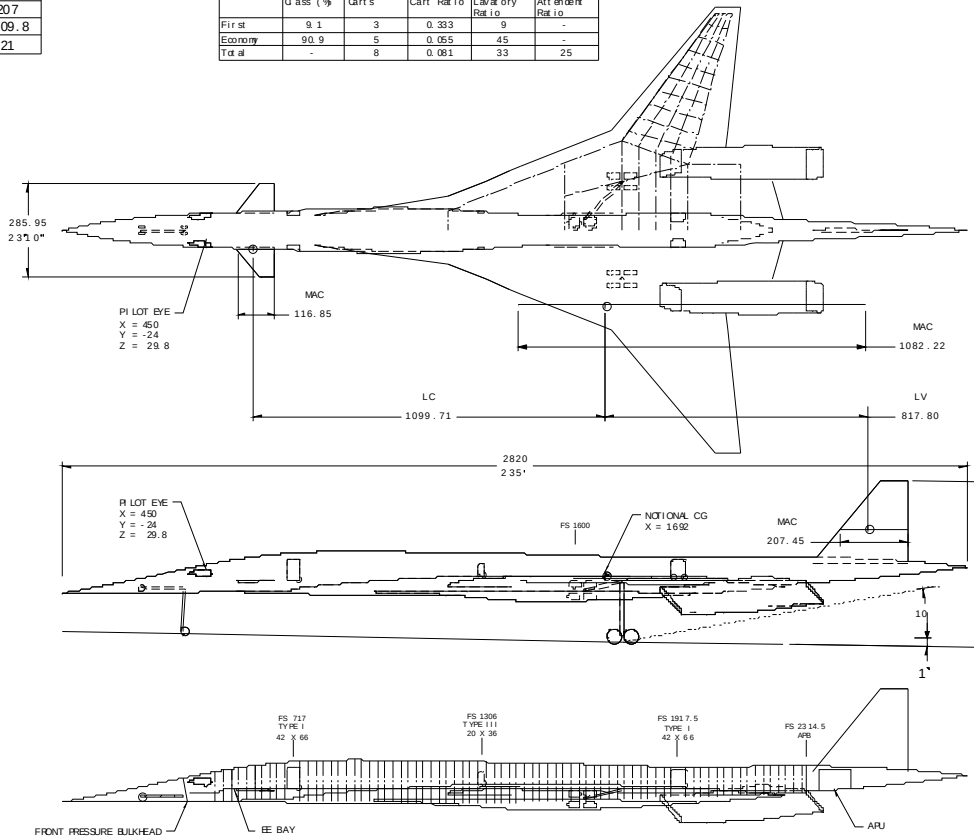

Figure A.1.1 072B General Arrangement

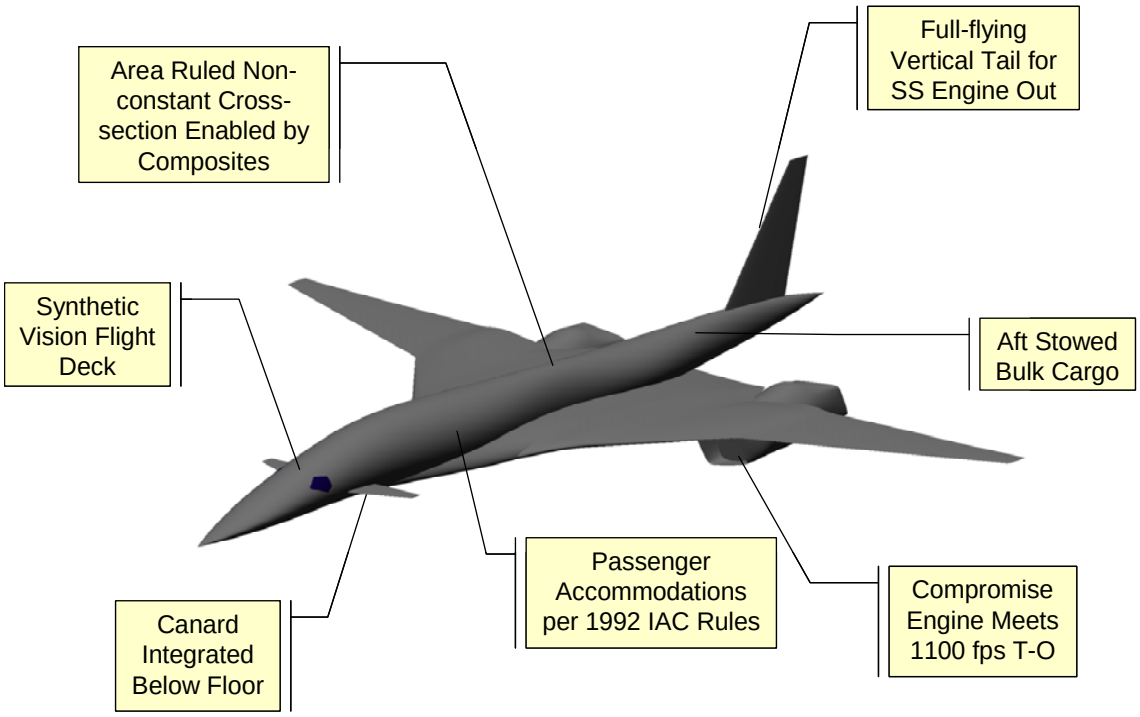

Figure A.1.2 072B Features

- Resheared inboard wing (to avoid passenger compartment)
  - Root airfoil likely too thick
- Reshaped fuselage for…
  - …non-circular section with flat floor
  - …integrated flight deck
  - …landing gear integration
- Lowered canard for integration with floor
- Shifted nacelle outboard for improved gear integration

Figure A.1.3 Modifications Made Post Analysis

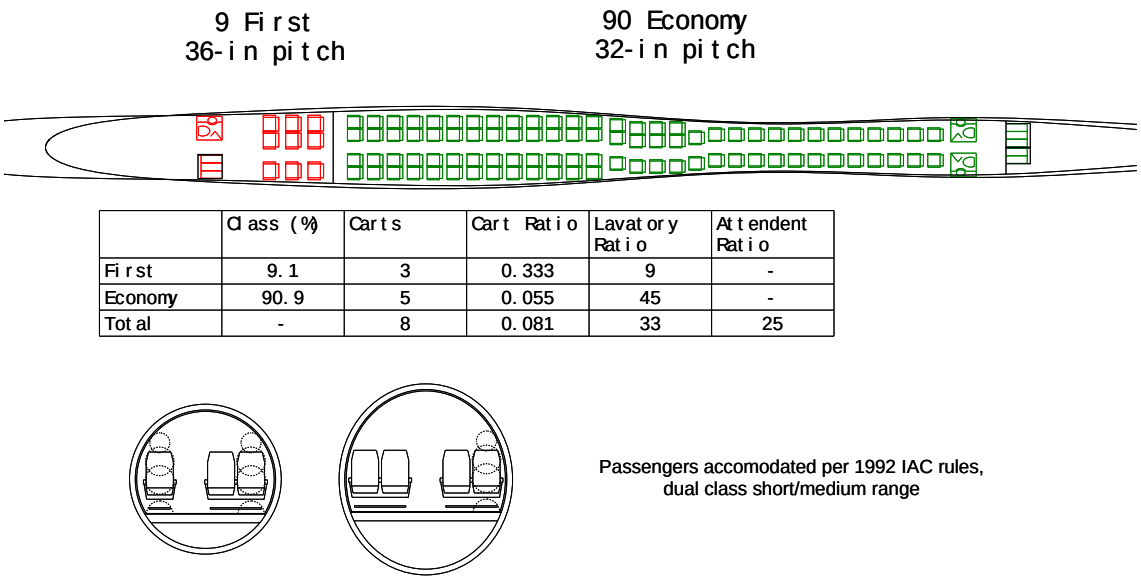

	Class (%)	Carts	Cart Ratio	Lavatory Ratio	Attendent Ratio
First	9.1	3	0.333	9	-
Economy	90.9	5	0.055	45	-
Total	-	8	0.081	33	25

Passengers accomodated per 1992 IAC rules, dual class short/medium range

Figure A.1.4 072B Interior Arrangement

- Main Landing Gear
  - Dual-tandem gear with 4 x H40x14.5-19
  - Fold forward and inboard
  - No unusual kinematics required
- Nose Landing Gear
  - Dual with 2 x H22x8.25-10
  - Fold forward
  - Cantilevered off front of pressure bulkhead (no doghouse)

Figure A.1.5 072B Landing Gear Integration

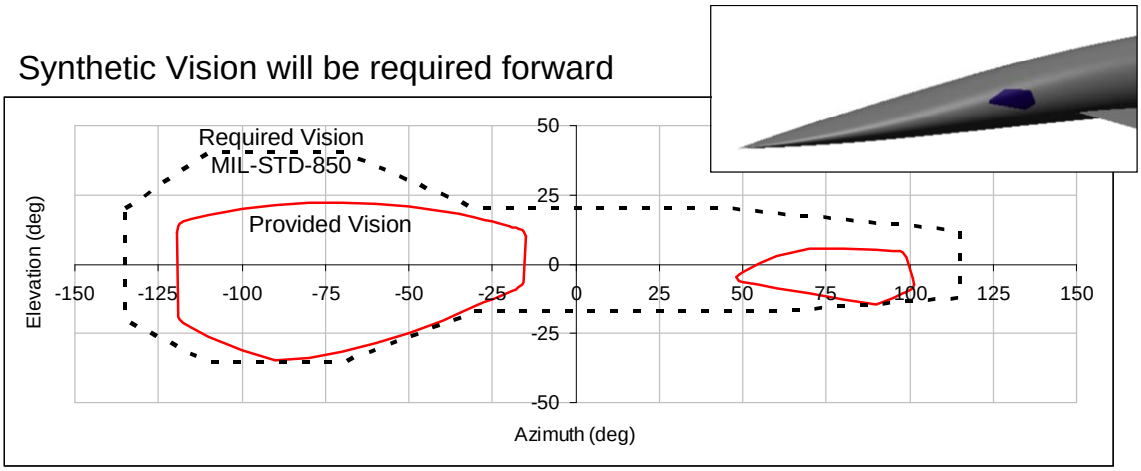

Figure A.1.6 072B Cockpit Vision

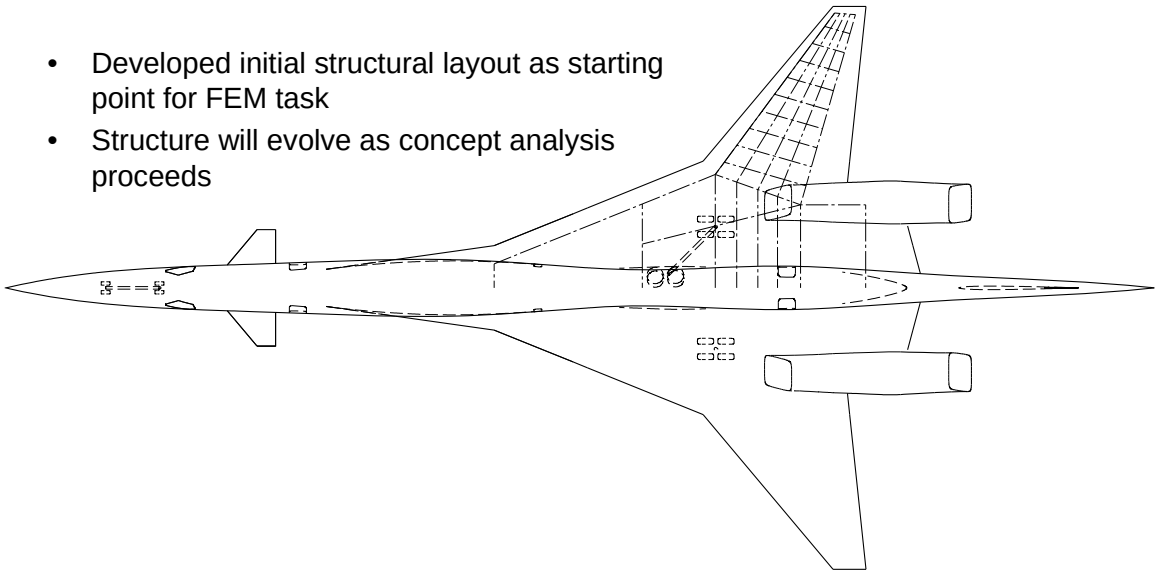

Figure A.1.7 072B Conceptual Structural Layout

Tank	Volume (cf)	X centroid
1	526	1438
2	526	1438
3	225	1651
4	225	1651
5	477	1816
6	477	1816
7	659	1991
8	659	1991

Total Volume	3,400	cf
Total Fuel Weight	160,000	lb

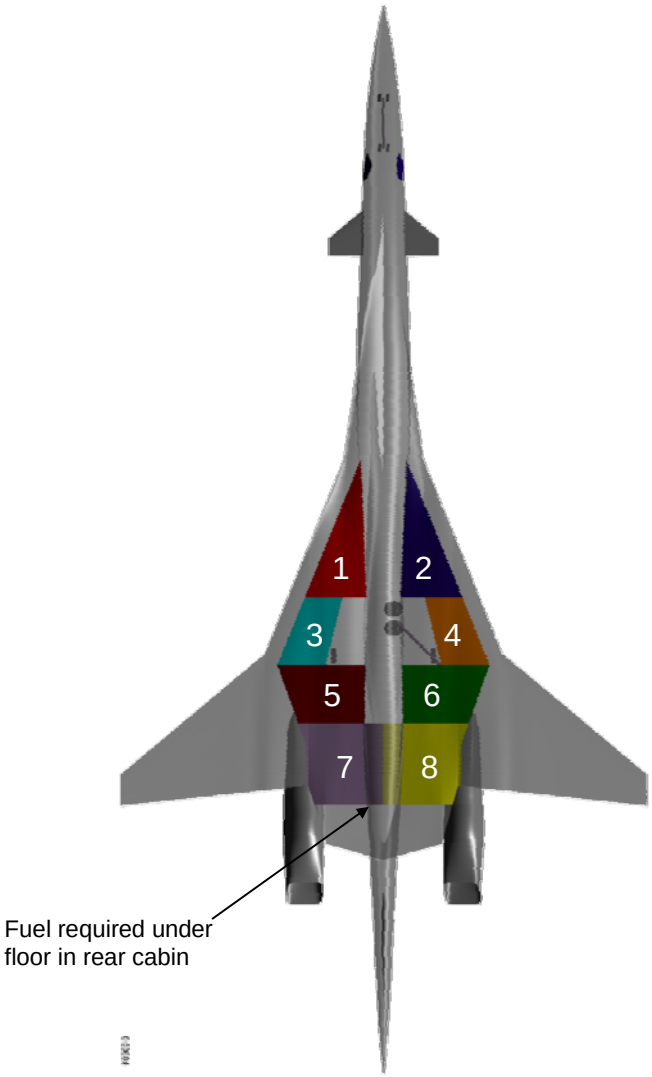

Figure A.1.8 072B Fuel Tank Layout

Appendix 2 - The Boeing In-House Multidisciplinary Design and Analysis Tool

Multi-Disciplinary Analysis (MDA) capability has been around since the dawn of airplane design embodied in the designer. Introduction of computers has enabled rapid analysis cycles in various engineering disciplines. Early implementation of a Multi-Disciplinary computer environment was introduced with CASES (Computer Analysis and Sizing Evaluation System) in 1985? Currently, Multi-Disciplinary Analysis has become highly integrated and automated due to faster processors, platform independent programming languages, and the speed of the internet.

Figure A.2.1 outlines the current Multi-Disciplinary Analysis used on the Supersonic NRA N+2 Contract. This BR&T developed capability addresses Advanced Design engineering disciplines associated in design and analysis of a supersonic air vehicle. In addition, Low Boom analysis capability was added to the process. Engineering disciplines representing Advanced Design are Configuration, Aerodynamics, Stability & Control, Propulsion, Mass Properties, Acoustics, and Performance.

Figure A.2.2 shows disciplinary modules and tools used in this process. Fidelity level of analysis is defined in methods used by each discipline. Disciplines shown in Figure A.2.3 are coordinated to ensure that the appropriate analysis match the intent of the study.

ModelCenter is used to integrate and automate required discipline modules. ModelCenter is licensed Phoenix Integration software intended for a modern Multi-Disciplinary environment. The ModelCenter model represents the fusion of inputs and analysis codes used in aircraft performance analysis and sizing. Amount of integration is set by engineering Subject Matter Experts (SME). This environment requires engineers to interact with results and ensure correct automation. In this context, automation is relative and requires engineering judgment.

Configuration is responsible for coordinating the flow of geometry information to engineering disciplines shown in Figure A.2.4. GeoDuck (Boeing parametric geometry program) was used to provide geometry inputs to the disciplines. Rules for generating geometry, inputs, and constraints are determined by SME using study requirements. Inputs on wing structure for Mass Properties, planform characteristics and airfoil definition for Aerodynamics are inputs needed by the analysis team. Another example of inputs is fuselage cross-sectional area constraints for minimum wave drag area-ruling by Aerodynamics as shown in Figure A.2.5. A brief description of GeoDuck is shown in Figure A.2.6.

Parametric geometry models representing attributes for Supersonic NRA N+2 were created for analysis shown in Figure A.2.7. GeoDuck output IGES files in ModelCenter enable the creation of analysis input datasets. Creating UDP (vortex lattice code) input datasets are examples shown on Figures A.2.8 & 9.

Aerodynamics is responsible for providing a starting linear design and Aerodynamic Characteristics for Performance. The aerodynamic module consists of low speed and high speed. Figure A.2.10 shows a description of the high speed module and associated tools for Aerodynamic buildups. Supersonic high speed drag buildups use Linear Theory plus nonlinear corrections from existing databases with provisions for technology projections. Aerodynamic codes wrapped in ModelCenter are TEA80 (wave drag), A389 (supersonic lift drag), and Dragj (high speed buildup). Example data release is shown as a Mach*Lift/Drag (ML/D) plot. The linear design uses camber definition obtained from A389 and area-ruled fuselage from TEA80.

Low speed aerodynamic module description is shown in Figure A.2.11. Similar to high speed the buildups use Linear Theory corrected by applicable databases. UDP is the vortex lattice code wrapped for low speed. Released aerodynamic data are shown as lift curves and drag polars for different high lift device deflections.

Stability and Control module is currently limited to tail volumes. Method activities have been initiated to incorporate static stability and time to double capabilities.

Propulsion module description is shown in Figure A.2.12. Initial capability allows engine decks to load automatically for Performance. Propulsion inputs are passed to the Propulsion module where scaling rules are invoked during Performance vehicle and engine sizing. Wrapping NPSS into the module under ModelCenter is a current BR&T method activity with preliminary implementation.

Mass Properties is responsible for Weights release to Performance. QWIKO (Supersonic Weights Estimation) shown in Figure A.2.13 was wrapped in ModelCenter. Mass Properties inputs are generated by GeoDuck and passed to QWIKO for weights buildup. Weights statement is automatically generated with appropriate outputs linked to Performance.

Performance module description is shown in Figure A.2.14. This module includes script wrappers to automate the flow of inputs required for Performance analysis. Takeoff and mission programs are operational with Landing in beta version. ModelCenter is setup for stand alone Performance run or Design of Experiments (DOE). DOE provides parametric results that could be reviewed in Data Explorer, exploring the design space with visualization tools.

In ModelCenter links are setup to iterate on Mission takeoff gross weight (TOGW) with the Weights module providing an initial guess. Scaling rules have been setup in the discipline modules to allow wing area and engine thrust scaling. Takeoff Performance noise constraint in terms of jet exit velocity, rate of climb at the transonic pinch point are all captured for design sensitivity trades. These trades are captured through DOE.

Low Boom configurations are enabling attributes for a viable supersonic aircraft. Supersonic NRA N+2 requires an exploration in design for Low Boom solutions. A Low Boom analysis module shown in Figure A.2.15 has been incorporated in the MDA ModelCenter model. This module does not have the same level of automation as the Performance modules. Difficulties in automation are due to the level of fidelity for Aerodynamic analysis. Addressing low boom design requires at least an Euler level solution for the initial pressure signature.

The low boom module incorporates MDBOOM (Boeing propagation code) in ModelCenter. GeoDuck IGES surface geometry shown in Figure A.2.16 is passed to MADCAP and ICEM for surface preparation and mesh generation shown in Figure A.2.17. Scripts are used to automate CART3D submits to obtain a solution at the cruise lift coefficient. CART3D pressure contours at the cruise lift coefficient are shown in Figure A.2.18. Lift and area distribution of the CFD solution shown in Figure A.2.19 are used to calculate the F Function shown in Figure A.2.20. The F Function is the final far-field signature that MDBOOM propagates through the atmosphere. Figure A.2.21 shows the sonic boom waveform at the ground and perceived loudness (noise metric).

Figure A.2.22 shows the summary and status of the MDA capability. The ModelCenter model has been demonstrated on the 765-072 Type Species with DOE. Sensitivity studies have been done at various level of automation. Low boom analysis has been exercised on converged Performance airplanes.

Further work needs to be done to mature models for robustness. It is difficult to have robust parametric geometries while producing high quality surfaces for CFD. Further work on low boom shaping is continuing for higher order analysis.

- Multi-Discipline Analysis Architecture
  - Configuration
  - Aerodynamics
  - Propulsion
  - Mass Properties
  - Performance
  - Acoustics (Vjet=1100 fps)
  - Stability and Control (Volumes)
- Low Boom Shaping
  - MDBOOM integration
  - Low boom design
- Summary and Status

Figure A.2.1 MDA Capability Outline.

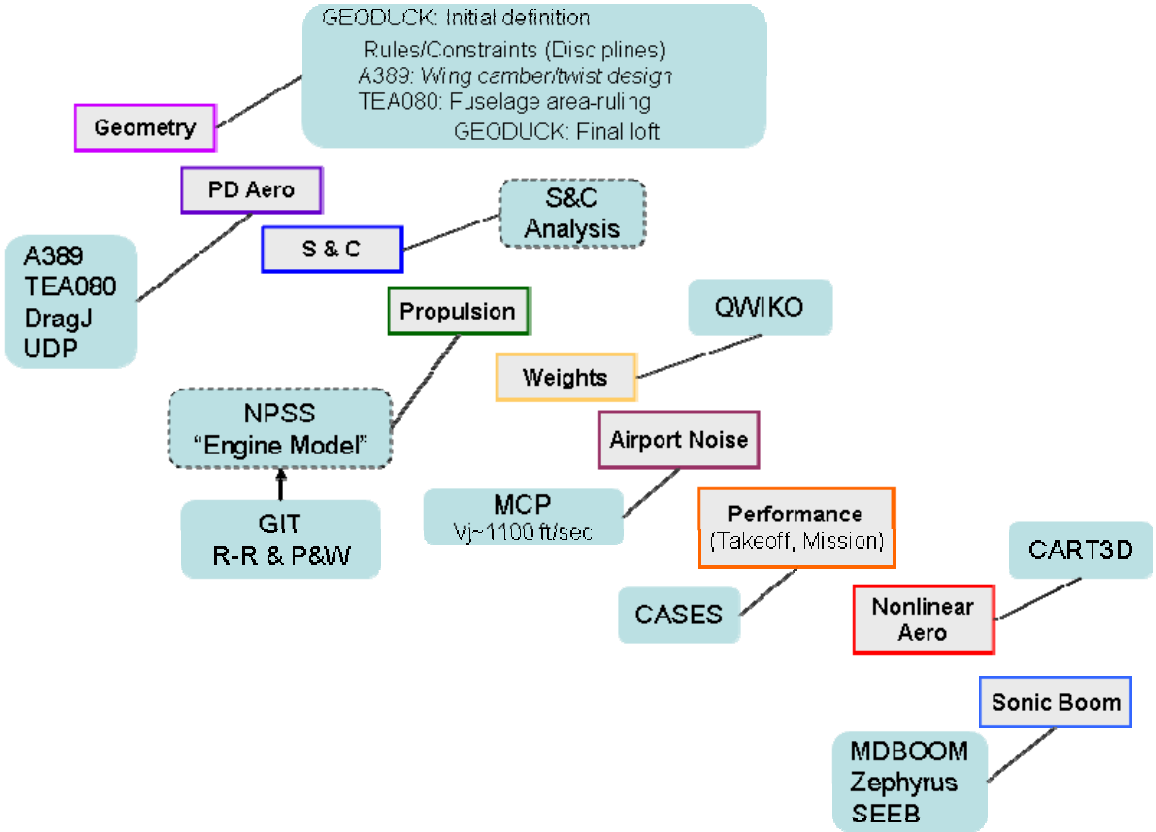

Figure A.2.2 MDA Tools Suite Components.

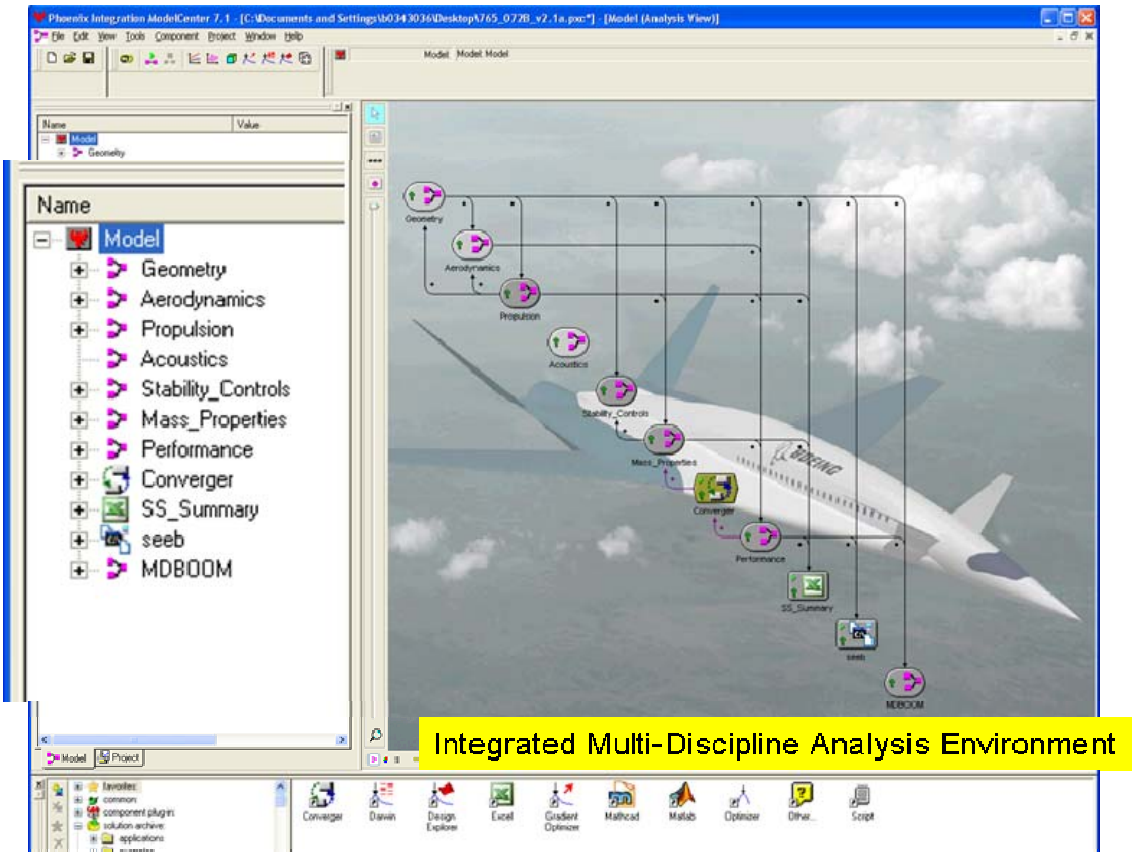

Figure A.2.3 Supersonic ModelCenter Model.

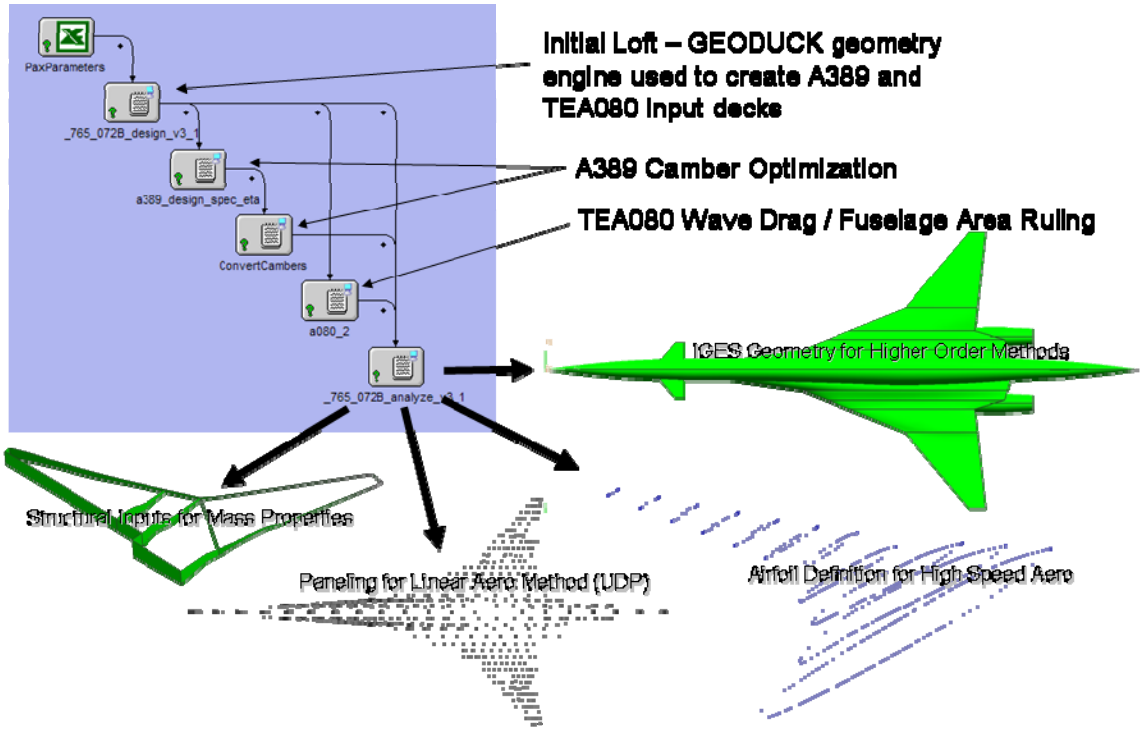

Figure A.2.4 Geometry Model Description.

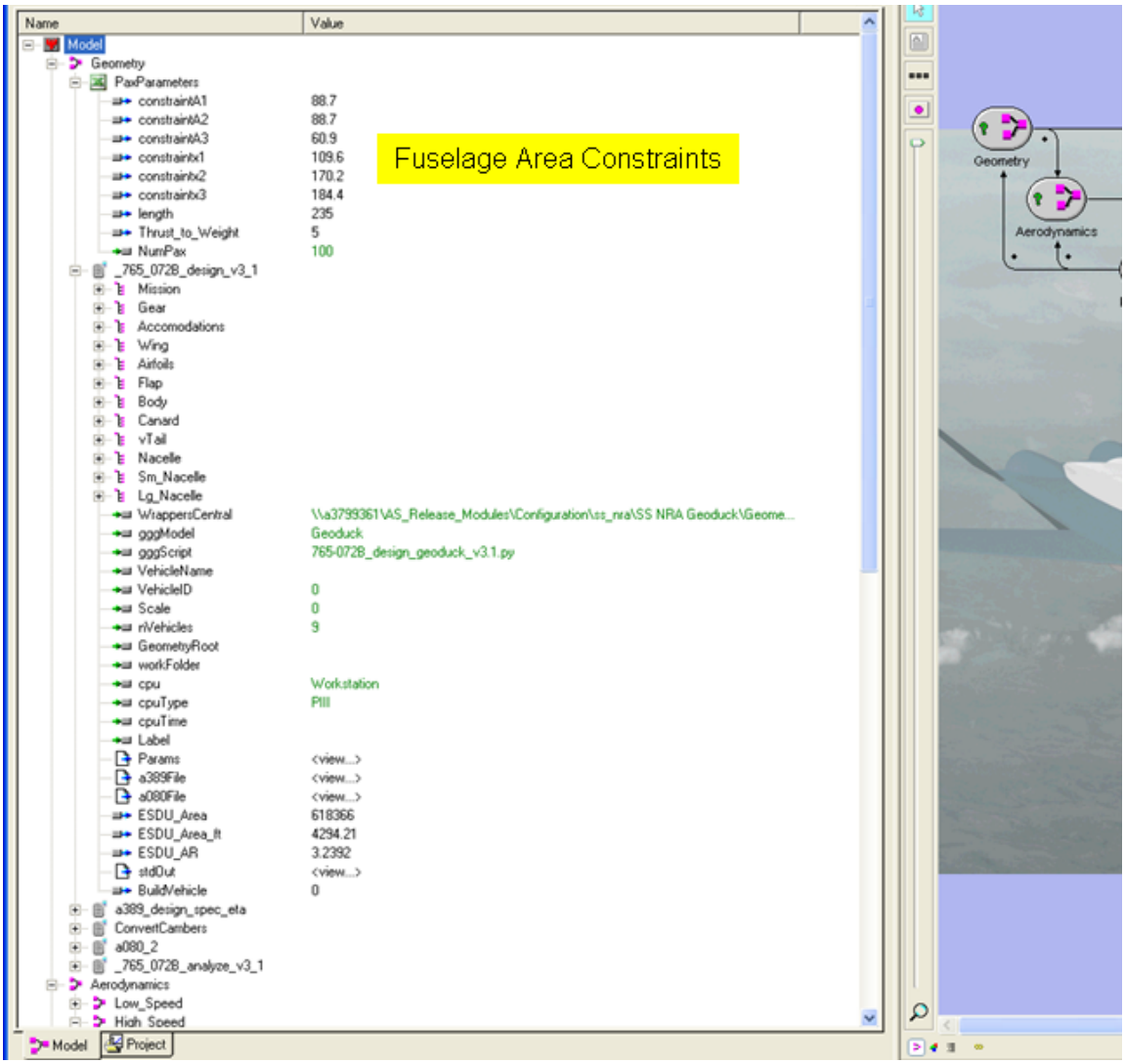

Figure A.2.5 Geometry Module Inputs.

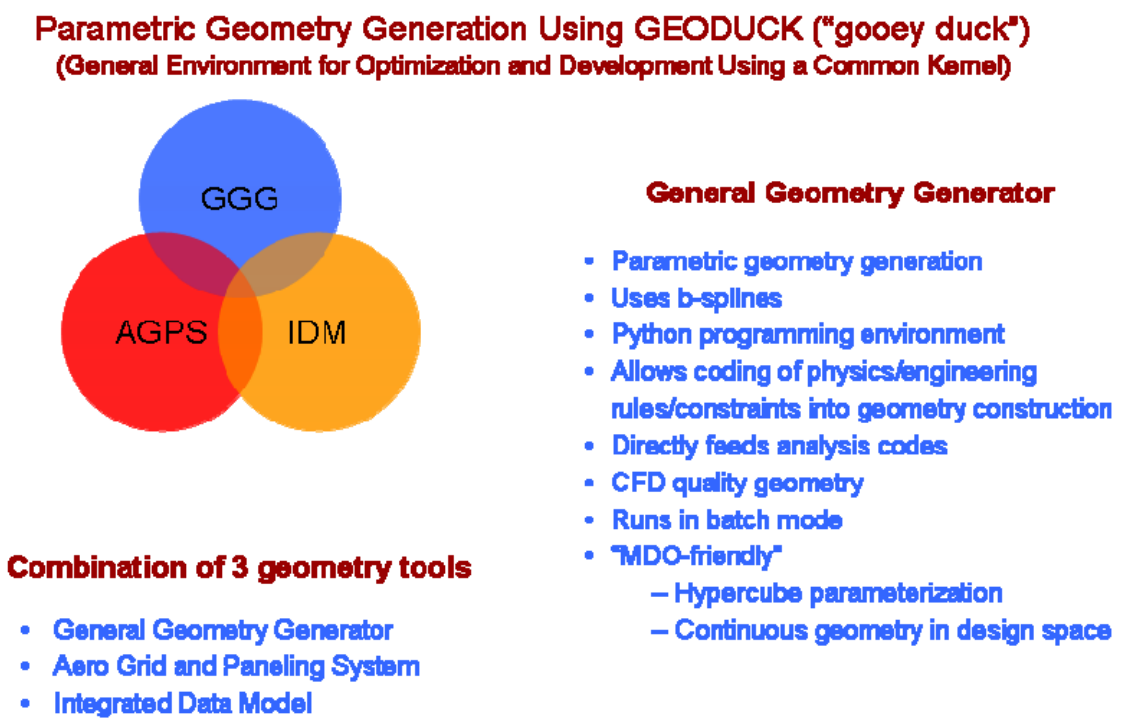

Figure A.2.6 GeoDuck Environment.

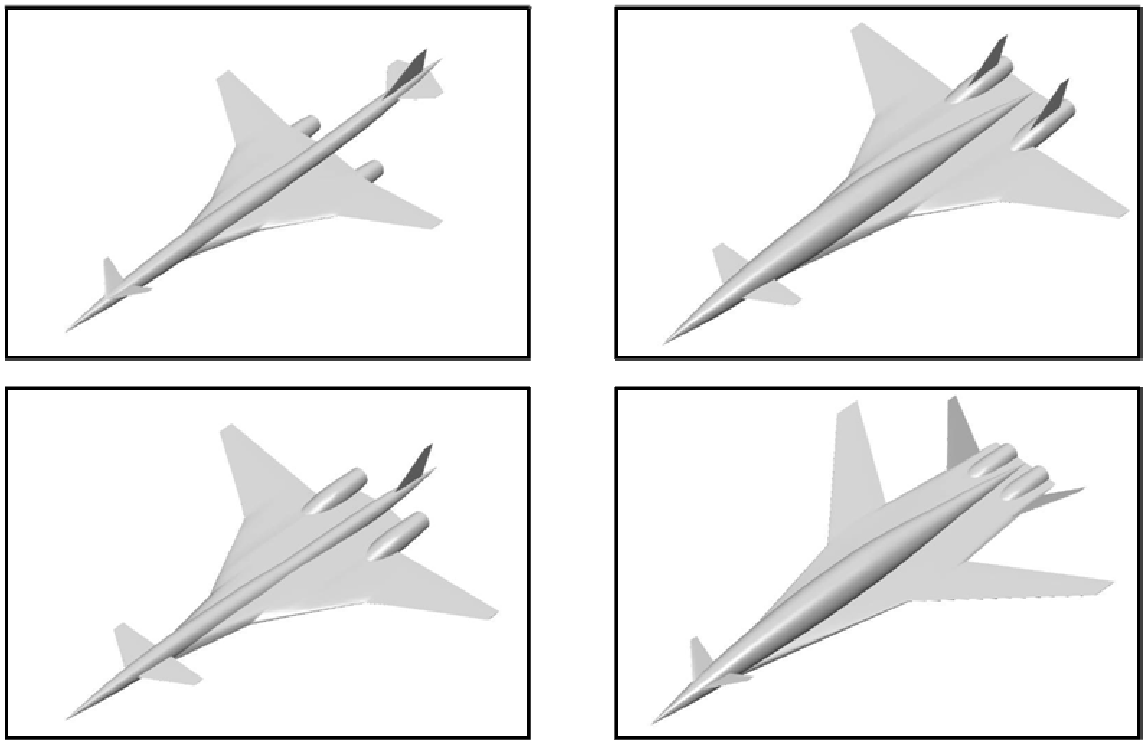

Figure A.2.7 Parametric Model Species.

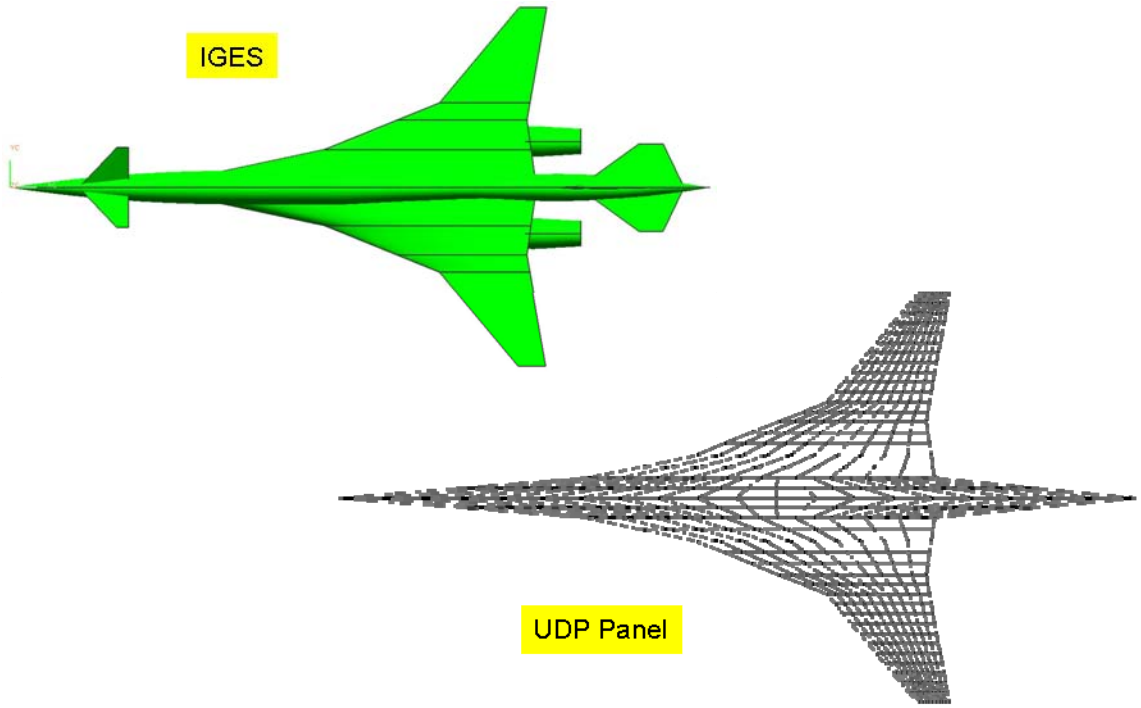

Figure A.2.8 765-070 Type Species UDP Modeling of Parametric Model IGES output.

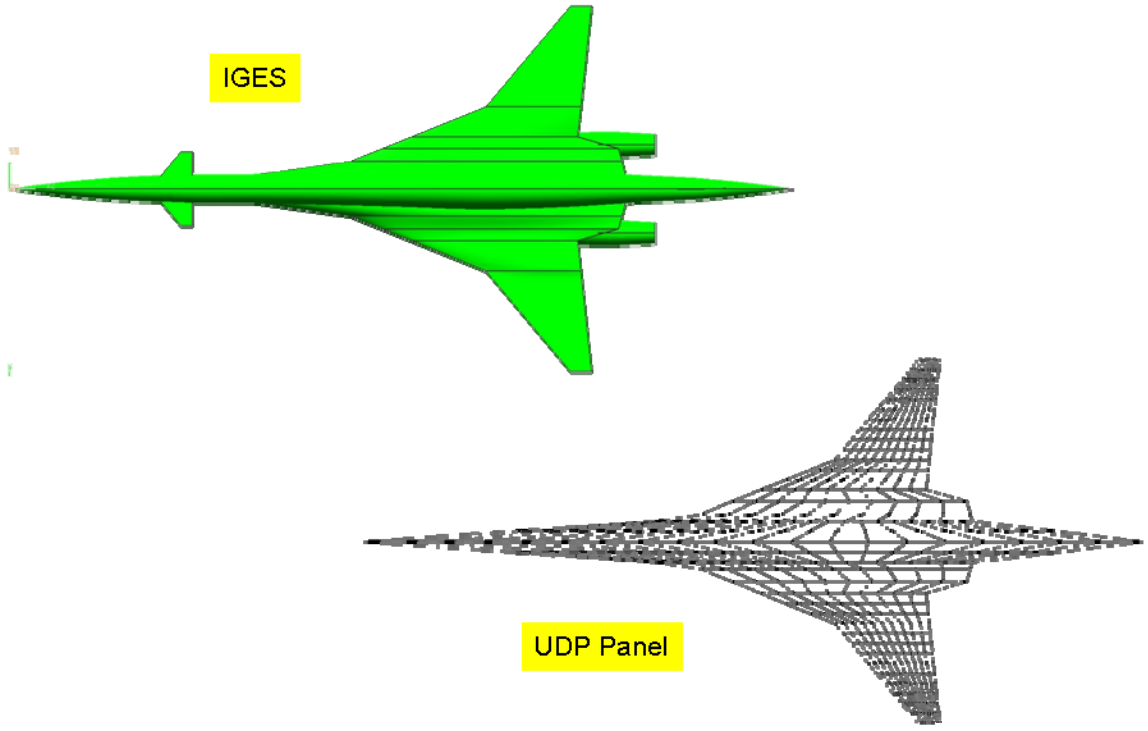

Figure A.2.9 765-072B Type Species UDP Modeling of Parametric Model IGES output.

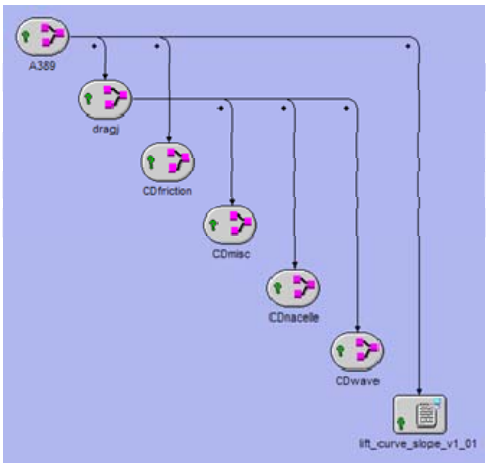

High Speed

TEA80 : Wave Drag
A389 : SS Drag
DragJ: HS Drag Buildup

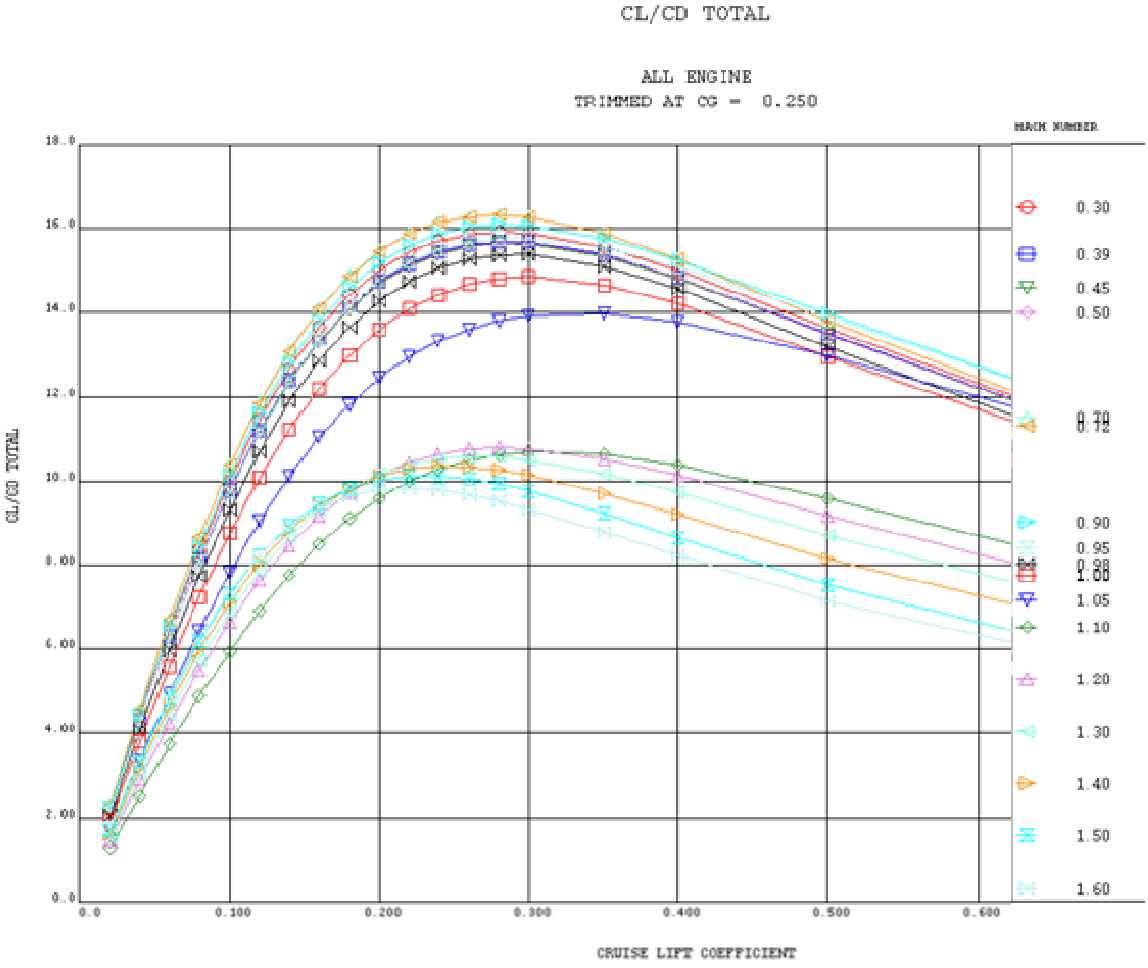

Figure A.2.10 High Speed Aerodynamic Module produces released data for Performance.

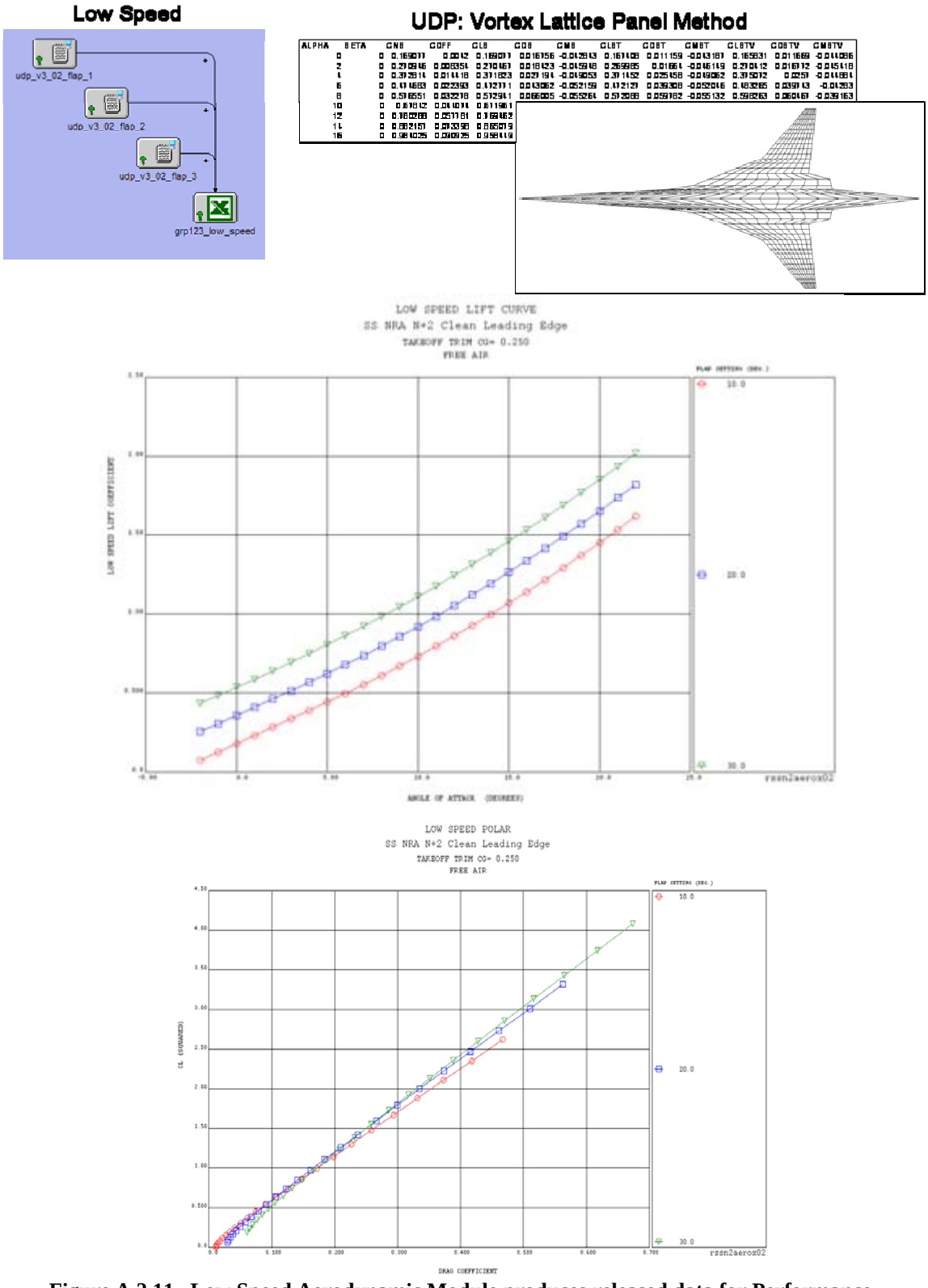

Figure A.2.11 Low Speed Aerodynamic Module produces released data for Performance.

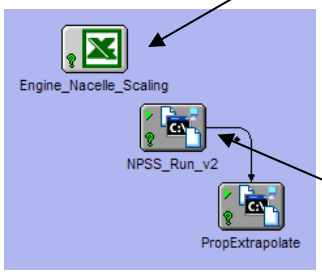

Engine/nacelle is scaled based on assumed trends. This information is passed to the GEODUCK geometry engine.

NPSS: Numerical Propulsion System Simulation
Given cycle parameters, NPSS produces an engine deck which can be read by performance codes.

Figure A.2.12 Propulsion Module Description.

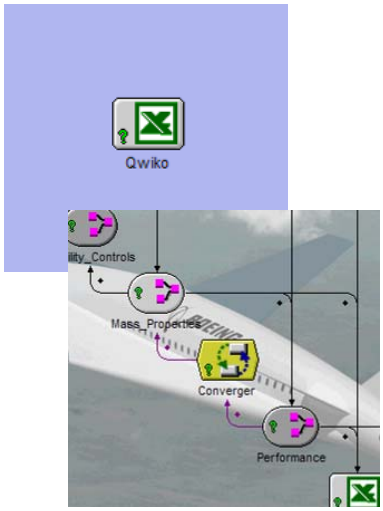

QWIKO is used for Mass Properties
Mass Properties inputs are generated by the GEODUCK model and are passed to QWIKO for weights buildup

Takeoff gross weight is cycled between QWIKO and mission codes until the two values converge

Figure A.2.13 Mass Properties Module Description.

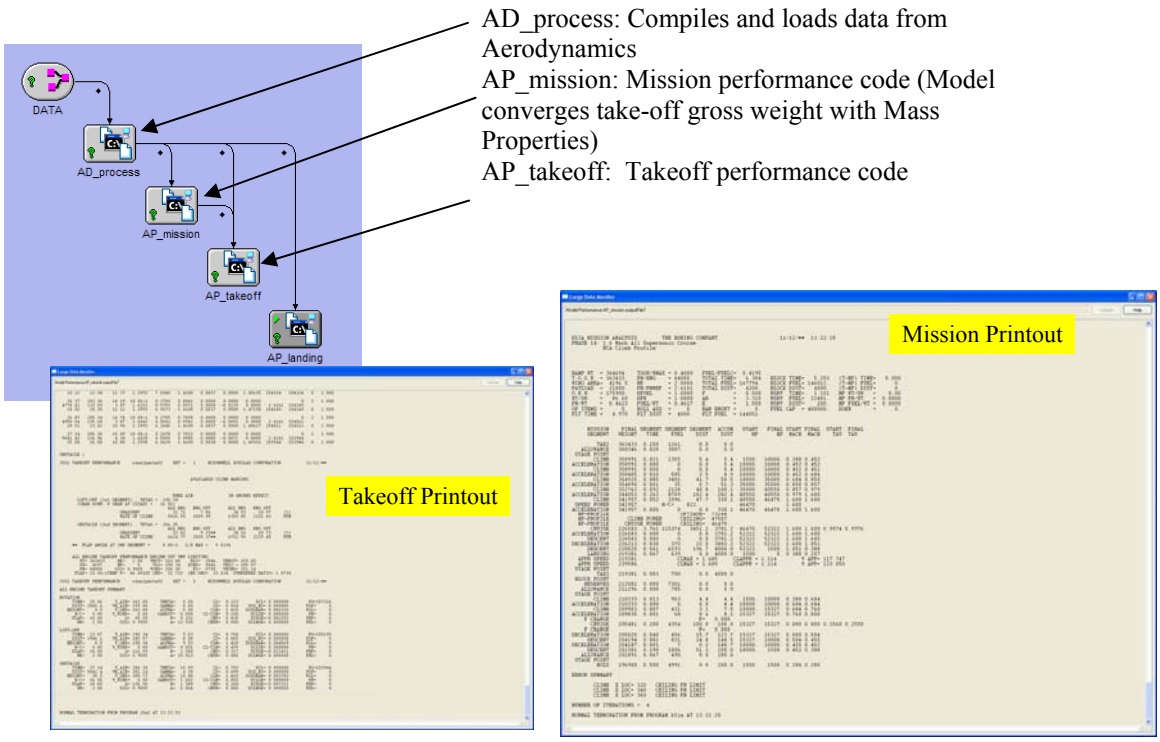

Figure A.2.14 Performance Module produce Takeoff and Mission results.

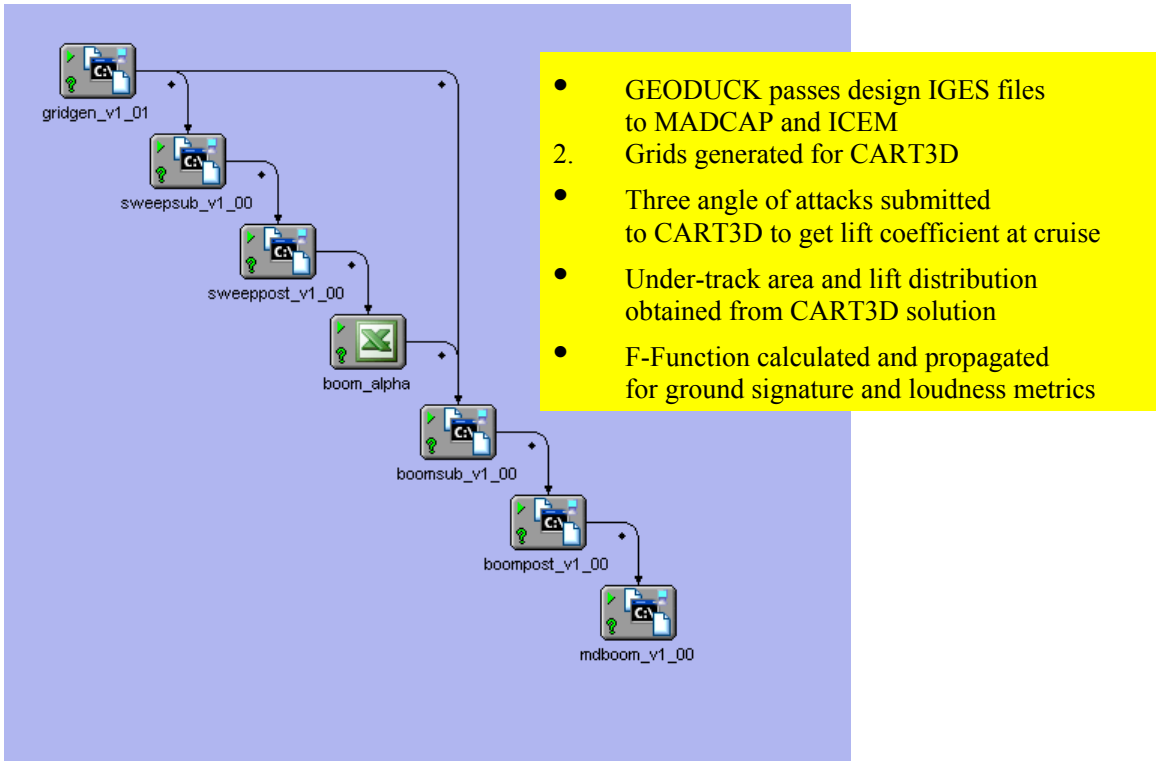

Figure A.2.15 Low Boom Module Description.

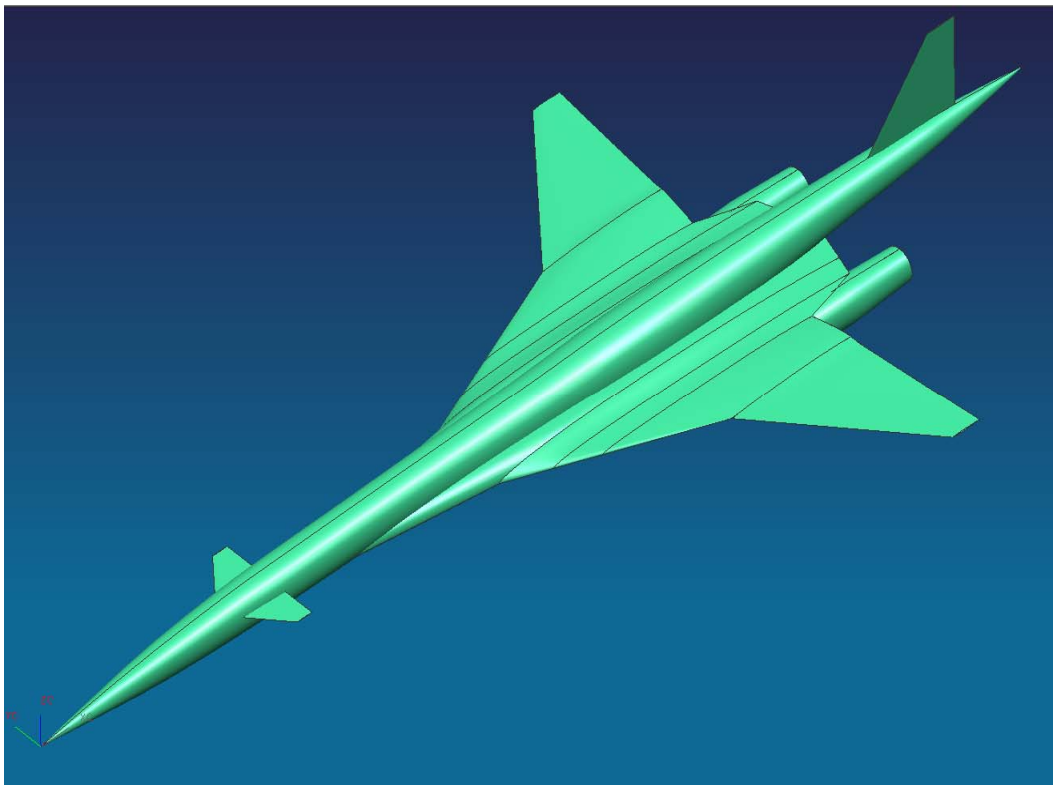

Figure A.2.16 Export IGES for Meshing.

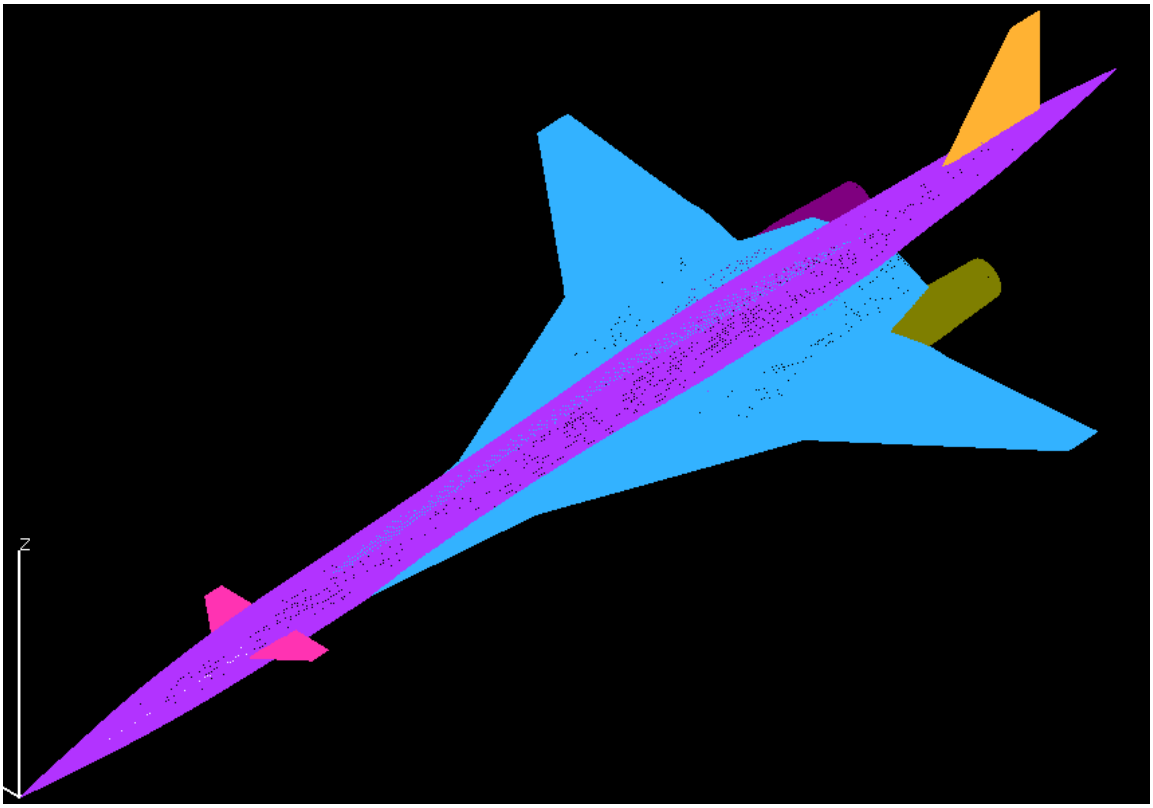

Figure A.2.17 Surface Mesh for CFD.

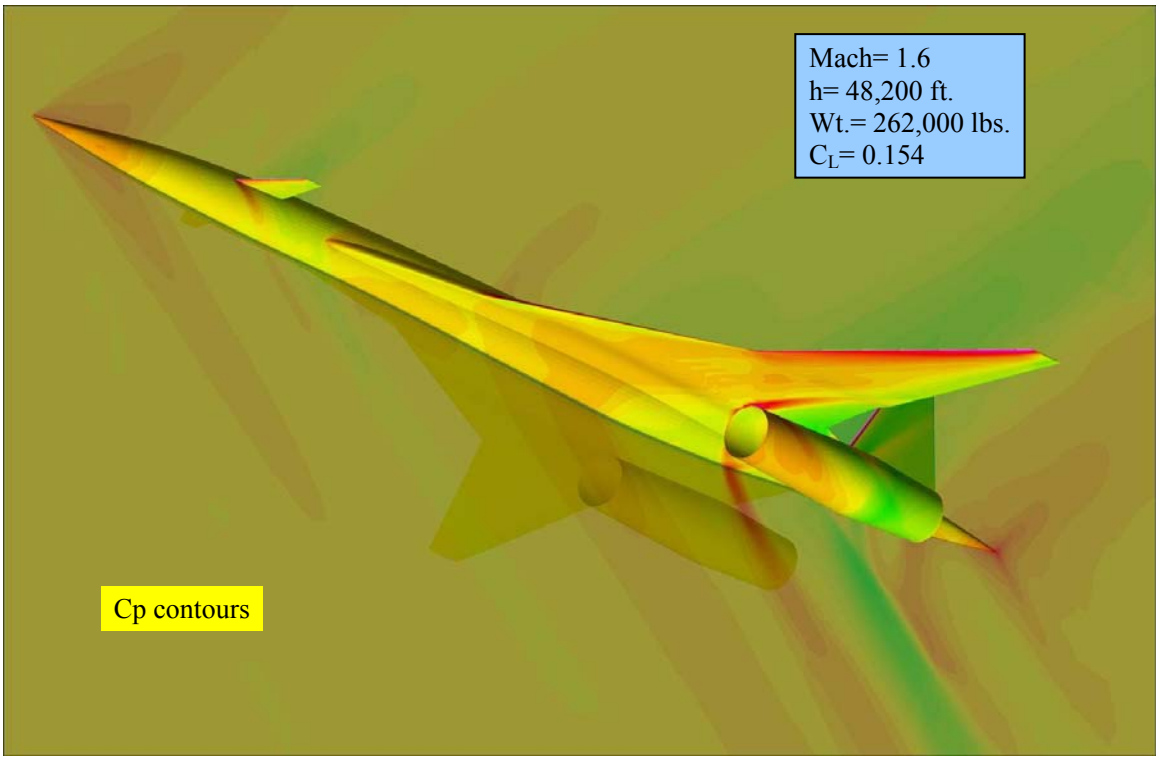

Figure A.2.18 CART3D (CFD) Solution for Sonic Boom Propagation.

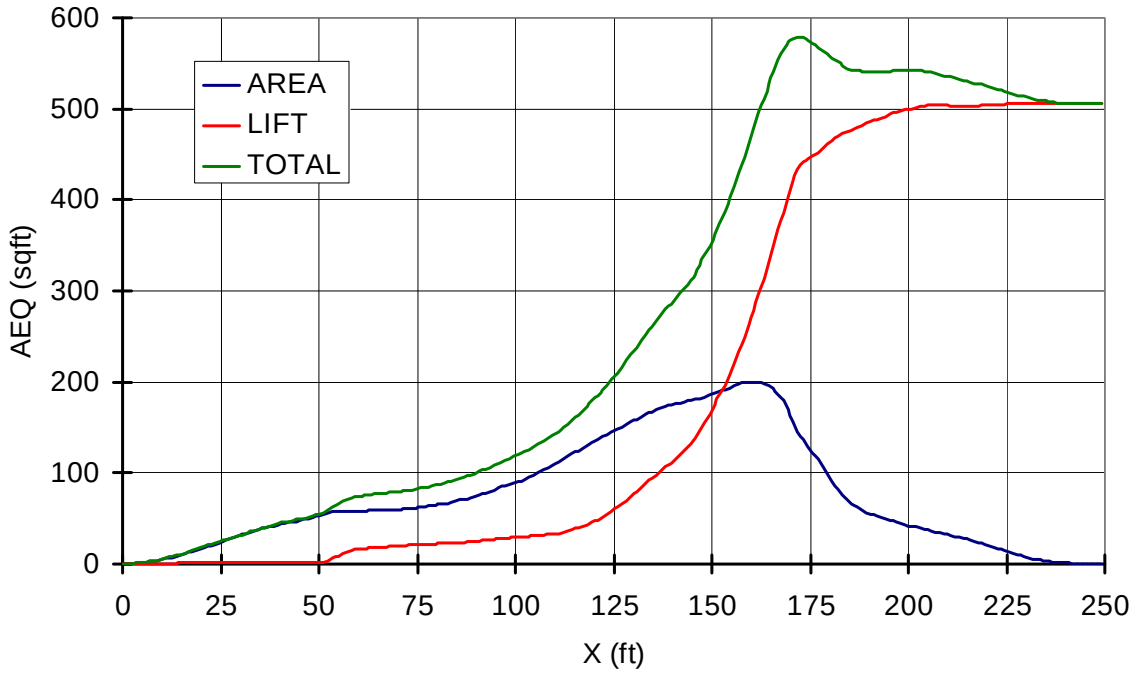

Figure A.2.19 Area and Lift Distribution for F Function analysis.

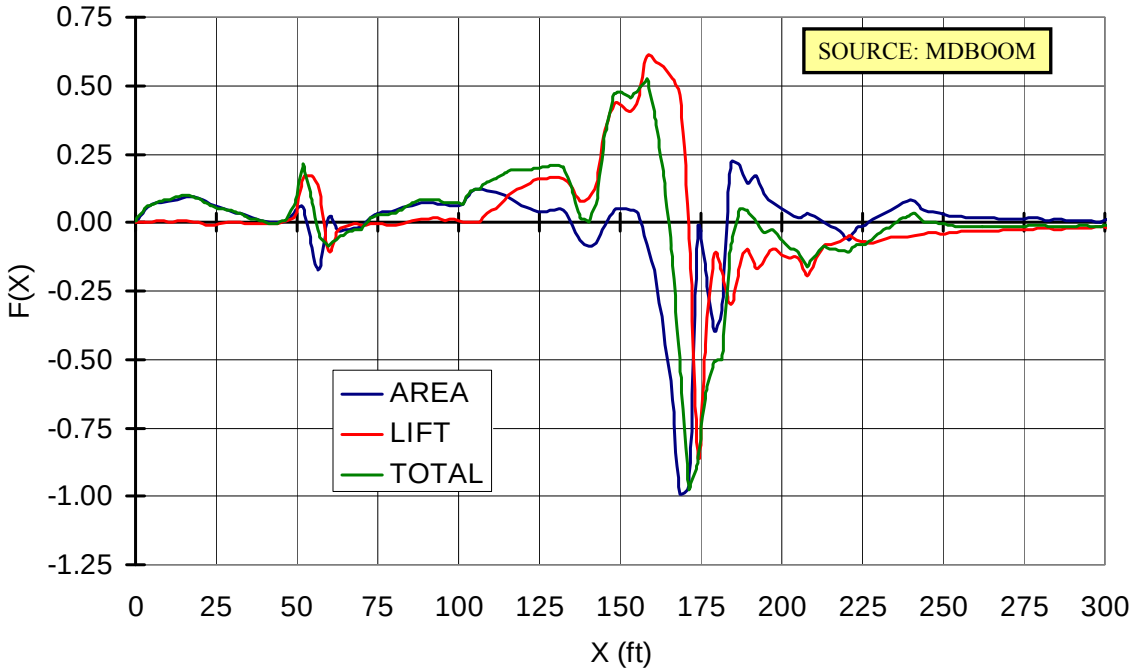

Figure A.2.20 Generated F Functions for Sonic Boom Propagation.

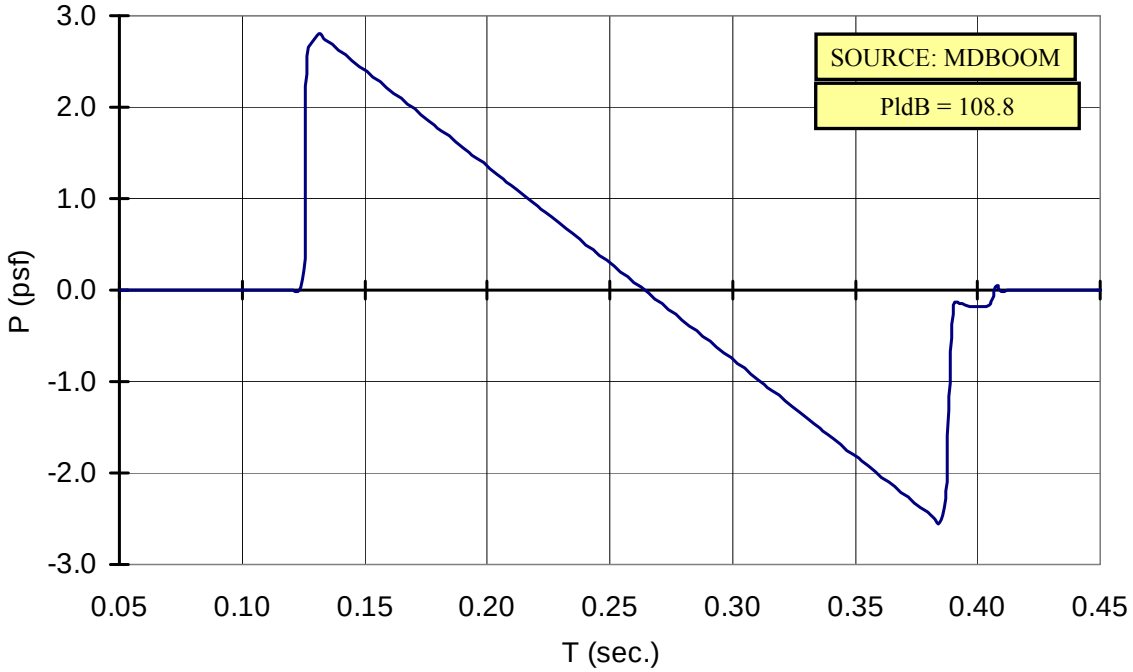

Figure A.2.21 Ground Signature and Loudness results.

- Multi-Discipline Analysis Architecture has been integrated in ModelCenter
  - Demonstrated in sensitivity studies
  - Beta version
- MDBOOM integration
  - IGES to CART3D completed
  - Area and lift distribution in checkout
  - F-Function, signature and loudness metrics in checkout
- Tasks to be completed
  - Model calibration
  - NPSS / WATE integration (option 2)
  - MDBOOM / Signature Shaping

Figure A.2.22 Summary and Status.

Appendix 3 - GIT and R-R Non-Proprietary Technology Roadmapping

The MFTF engine cycle selected by Boeing for the 076E configuration fails to meet the vehicle range requirement of 4000 nmi. In order to meet the range requirement Boeing determined that the vehicle fuel burn needed to be reduced by approximately four percent. Georgia Tech performed a technology gap analysis in order to determine what level of engine technology would be needed to meet mission goals. The process for the technology space exploration is shown in Figure A3.1. First the technology level is varied on the baseline cycle in order to determine the level of technology needed. After the technology level has been selected and implemented the engine cycle is re-selected to find the best solution.

Technology Space Exploration

The first step is to identify the technology level needed to achieve the mission goals. This was done by taking the engine cycle selected for the 076E, from now on referred to as the baseline cycle, adjusting the design point efficiencies and analyzing the results. Since the technology space exploration was performed without a vehicle mission analysis, TSFC at a constant mid cruise thrust was used as a surrogate for fuel burn. Mid cruise was defined as Mach 1.6 at approximately 51,800 feet for the purposes of this exploration. The NPSS MFTF model was modified to allow for "technology factors" to be applied. These technology factors are scalars on the design point efficiencies of the turbomachinery components. Technology effects on the inlet and nozzle were not investigated. A design of experiments was run to determine coefficients b_i and b_{ij} of the Response Surface Equations (RSE's) for the technology space. RSE's are a multivariate linear regression that assumes a Taylor series second-order approximation of the response, as follows:

$$R = b_o + \sum_{i=1}^{k} b_i x_i + \sum_{i=1}^{k} b_{ii} x_i^2 + \sum_{i=1}^{k-1} \sum_{j=i+1}^{k} b_{ij} x_i x_j + \varepsilon$$

Equation 1. Response surface equation (RSE).

A standard least squares regression is used to determine the coefficients in the RSE based on a given set of data generated intelligently through a Design of Experiments.

A DoE was executed using the ranges of technology scalars used are shown in Table A3.1. The baseline cycle was held constant during the DoE execution; however, thrust was allowed to vary so that the engine could scale to meet vehicle climb and cruise thrust requirements as the thrust lapse rate changed.

Once the DoE data was available RSE's were constructed and used to create a prediction profiler, as shown in Figure A3.2. The profiler allows the designer to easily obtain sensitivities, see potential tradeoffs, and rapidly explore the design space that allows instantaneous results without having to re-execute the entire NPSS model.

Several considerations went into selecting the resulting technology factors listed in Table A3.2. Technologies level increases for the various components were evenly distributed as much as possible. The purpose of this was to try to capture a gradual increase in all technology levels which is more a more feasible outcome than a drastic increase in one and no increase in the others. Also, since the HPC efficiency has such a large impact on the thrust lapse rate it was used not only to reduce SFC, but it's value was somewhat limited by the requirement to meet climb thrust requirements. Finally, since the technology needs to be ready for IOC in 2020, engineers at Georgia Tech decided to limit the maximum increase in component efficiency to 2%. The baseline cycle TSFC reduction was reduced by 2.2% using the selected technology level in Table A3.2. This does not meet the 4% requirement; however, the effect of higher component efficiency on engine performance is not independent of the cycle. For this reason the cycle needed to be reselected to attain the maximum possible performance increase.

Cycle Design Space Re-Exploration

Once the appropriate technology levels were selected another DoE was run. This time a Latin Hypercube type of DoE was executed. It maximizes the distance between DoE points in the multidimensional design space. The ranges used for the cycle design space exploration are the same as those used to originally select the baseline cycle. The cycle which met thrust requirements and had the best TSFC improvement was selected from the DoE results. This cycle, which represents a solution in the discrete design space, was then optimized for cruise TSFC using a gradient based optimizer. The HPC efficiency and CCA temperature drop were also allowed to vary in this gradient

optimization since they have a large correlation with the cycle parameters on thrust lapse. The resulting cycle and performance is shown in Table A3.3.

Non-Proprietary Technology Gap Analysis Conclusions

By increasing the technology level and re-optimizing the cycle a 3.6% reduction in TSFC was achieved relative to the baseline 076E cycle. If this same process were to be performed with a parametric vehicle in the loop then it may be possible to achieve the 4000 nmi mission range requirement. Also worth noting is that the resulting efficiencies listed in Table A3.3 are not excessively higher than today's levels. The HPC and HPT efficiencies are reasonable and since a multi-stage fan is assumed the low FPR means that two lower pressure ratio, more efficient, fan stages could be used.

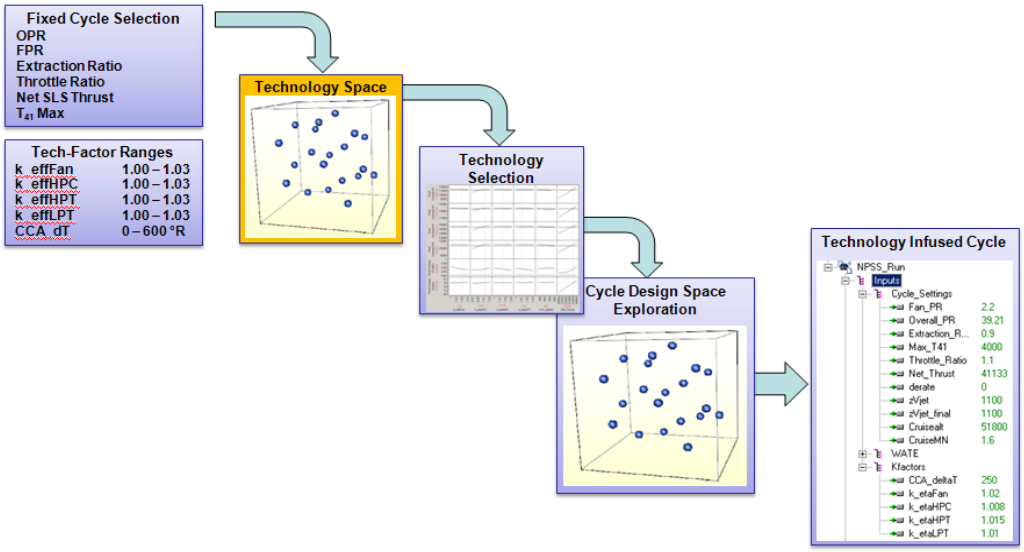

Figure A3.1 Process for Technology Selection

Table A3.1 Technology Factor Ranges for Technology Space Exploration

Inputs	Range
Fan poly eff scalar	1.00 – 1.03
HPC poly eff scalar	1.00 – 1.03
HPT adia eff scalar	1.00 – 1.03
LPT adia eff scalar	1.00 – 1.03

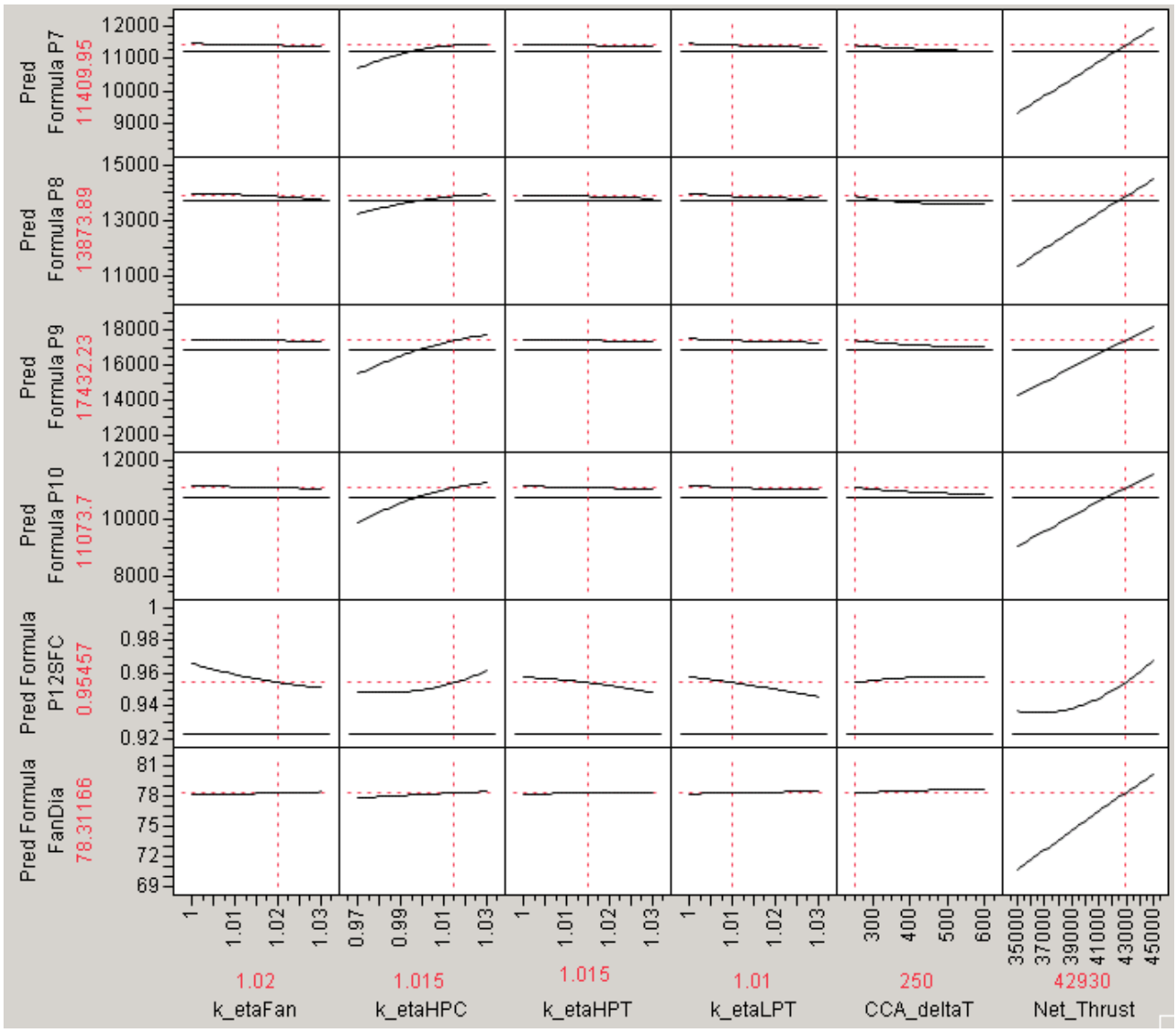

Figure A3.2 Technology Space Prediction Profiler

Table A3.2 Selected Technology Factors

Inputs	Value	Design Point Eff
Fan poly eff scalar	1.02	0.923 (polytropic)
HPC poly eff scalar	1.008	0.922 (polytropic)
HPT adia eff scalar	1.015	0.934 (adiabatic)
LPT adia eff scalar	1.01	0.939 (adiabatic)

Table A3.3 Results of Technology Gap Analysis

Engine Cycle and Technology-Factor Settings		
	Baseline	Technology Infused
FPR	2.21	2.20
OPR	39.21	37.60
Extraction Ratio	0.9	0.99
T_{41} Max (°R)	4,000	3,391
Throttle Ratio	1.100	1.087
SLS Net Thrust (lbf)	41,133	44,422
k_effFan	1.000	1.020
k_effHPC	1.000	1.015
k_effHPT	1.000	1.015
k_effLPT	1.000	1.010
CCA ΔT (°R)	0	125
Output from Engine Model		
Takeoff Thrust (lbf) (Mach 0.255 / 1000 ft)	39.826	42,605
Takeoff Exit Jet Velocity (ft/s)	1,516	1,448
Fan Spec Flow (lbm/s) @ SLS	40.0	42.75
Mid-Cruise TSFC lbm/(lbf*hr)	0.9611	0.9260
Fan Polytropic Efficiency	0.9050	0.9230
HPC Polytropic Efficiency	0.9150	0.9287
HPT Adiabatic Effciency	0.9200	0.9338
LPT Adiabatic Effciency	0.9300	0.9393

REPORT DOCUMENTATION PAGE

Form Approved
OMB No. 0704-0188

1. REPORT DATE *(DD-MM-YYYY)*	2. REPORT TYPE	3. DATES COVERED *(From - To)*
01- 08 - 2010	Contractor Report	03-2008 to 08-2009

4. TITLE AND SUBTITLE
N+2 Supersonic Concept Development and Systems Integration

5a. CONTRACT NUMBER
NNL08AA16B

5b. GRANT NUMBER

5c. PROGRAM ELEMENT NUMBER

6. AUTHOR(S)
Welge, Harry R.; Bonet, John; Magee, Todd; Chen, Daniel; Hollowell, Steve; Kutzmann, Aaron; Mortlock, Alan; Stengle, Josh; Nelson, Chet; Adamson, Eric; Baughcum, Steve; Britt, Robert T.; Miller, Gregory; Tai, Jimmy

5d. PROJECT NUMBER

5e. TASK NUMBER
NNL08AA35T

5f. WORK UNIT NUMBER
984754.02.07.07.12.05

7. PERFORMING ORGANIZATION NAME(S) AND ADDRESS(ES)
NASA Langley Research Center
Hampton, VA 23681-2199

The Boeing Company
5301 Bolsa Avenue
Huntington Beach, CA 92647-2048

8. PERFORMING ORGANIZATION REPORT NUMBER

9. SPONSORING/MONITORING AGENCY NAME(S) AND ADDRESS(ES)
National Aeronautics and Space Administration
Washington, DC 20546-0001

10. SPONSOR/MONITOR'S ACRONYM(S)
NASA

11. SPONSOR/MONITOR'S REPORT NUMBER(S)
NASA/CR-2010-216842

12. DISTRIBUTION/AVAILABILITY STATEMENT
Unclassified - Unlimited
Subject Category 05
Availability: NASA CASI (443) 757-5802

13. SUPPLEMENTARY NOTES
Langley Technical Monitor: Lori P. Ozoroski

14. ABSTRACT

Supersonic airplanes for two generations into the future (N+2, 2020-2025 EIS) were designed: the 100 passenger 765-072B, and the 30 passenger 765-076E. Both achieve a trans-Atlantic range of about 4000nm. The larger 765-072B meets fuel burn and emissions goals forecast for the 2025 time-frame, and the smaller 765-076E improves the boom and confidence in utilization that accompanies lower seat count. The boom level of both airplanes was reduced until balanced with performance. The final configuration product is two “realistic”, non-proprietary future airplane designs, described in sufficient detail for subsequent multi-disciplinary design and optimization, with emphasis on the smaller 765-076E because of its lower boom characteristics. In addition IGES CAD files of the OML lofts of the two example configurations, a non-proprietary parametric engine model, and a first-cycle Finite Element Model are also provided for use in future multi-disciplinary analysis, optimization, and technology evaluation studies.

15. SUBJECT TERMS
Advanced concepts; Conceptual Design; Supersonic; Systems Analysis

16. SECURITY CLASSIFICATION OF:			17. LIMITATION OF ABSTRACT	18. NUMBER OF PAGES	19a. NAME OF RESPONSIBLE PERSON
a. REPORT	b. ABSTRACT	c. THIS PAGE			STI Help Desk (email: help@sti.nasa.gov)
					19b. TELEPHONE NUMBER *(Include area code)*
U	U	U	UU	232	(443) 757-5802